Polymeric Nanofiber Conduits for Peripheral Nerve Regeneration

KOH HUI SHAN

(B. A. Sc., Honours, University of Toronto)

A THESIS SUBMITTED

FOR THE DEGREE OF DOCTOR OF PHILOSOPHY

Acknowledgements

I would like to express my sincere appreciation to those who have helped and contributed to this thesis. I would like to thank Professor Seeram Ramakrishna who has shown faith in me and given me tremendous encouragement and excellent supervision throughout this project.

My special appreciation to Dr Thomas Yong and Dr Susan Liao, who have provided unmatched guidance and support. Throughout the course of this project, they have given me invaluable advice, discussion, and suggestions. I would also like to thank Professor Casey Chan, Dr Mark E Puhaindran, Mr Dong Yixiang, Mr Teo Wee Eong, Mr Steffen Ng, all those who have helped me in one way or another, and Prof Seeram's lab members for their assistance on the completion of this project.

Also, I am grateful to NUS Graduate School for Integrative Sciences and Engineering for providing the funding for my studies at the National University of Singapore. My deepest appreciation to all the rats who were sacrificed for the experiments, without which this project would not have been successful.

Last, but not the least, I would like to thank my Dad and Mum for their love, and my Brother (Dr Koh Yaw Koon) who has provided me with excellent help. Special thanks to my husband (Mr Tay Chen Yu) who has accompanied and given me great support and encouragement throughout my studies.

TABLE OF CONTENTS

Chapter 4: Modification of PLLA nanofibers with extracellular matrix molecules

Chapter 5: Fabrication and characterisation of PLGA nanofiber intra-luminal guidance channels and modification with neurotrophins

Chapter 6: In vivo study of nanofiber nerve constructs in rat sciatic nerve injury model

Chapter 7: Conclusions and Recommendations

__Summary__

Traumatic injuries to the peripheral nerves can cause several functional deficiencies. The repair of peripheral nerve gap deficit remains a complex problem in clinical reconstructive surgery. Autologous nerve graft is used as the current approach to repair nerve gap injury, but there are several drawbacks that are accompanied with the use of patient's own tissue. A vast amount of research to produce bioengineered nerve bridging construct is being pursued that aim to replace the use of autologous nerve grafts. In this project, it is hypothesized that biodegradable bilayered nerve conduit containing aligned nanofibrous intra-luminal guidance channels produced by electrospinning can bridge and repair peripheral nerve gap. Moreover, this nerve construct can be modified with extracellular matrix molecules and neurotrophins to improve the outcome of nerve gap repair.

Synthetic poly(L-lactic acid) bilayered nanofiber conduit made up of nanofibers that mimic the extracellular matrix was fabricated using electrospinning to act as a guiding construct and a biomimetic environment for nerve repair. The conduit consisted of two layers of nanofibers membranes - inner layer of aligned nanofibers to guide neurite outgrowth; outer layer of randomly arranged nanofibers to provide mechanical integrity. Extracellular matrix proteins such as laminin were successfully incorporated into the nanofiber to improve the performance of the conduit. Intra-luminal guidance channels made from strands of aligned nanofibers were fabricated from poly(L-lactic-co-glycolic acid) using a novel electrospinning set-up. The aligned longitudinally nanofiber channels present a physical support for regenerating axons

and Schwann cells to adhere and extend to bridge up nerve gaps. The guidance channels closely imitated the intact nerve architecture of the basal laminae and bands of Büngner that allow the Schwann cells and axons to orientate along the axis of aligned nanofibers. Neurotrophins such as nerve growth factor had been coupled onto the guidance channels to provide sustained release of the growth factor to nerve regeneration.

This project has capitalized on the nano-scale architectures of nerve conduits to guide and increase the quality of nerve regeneration and functional recovery, and prevent scar tissue in-growth which acts as barrier to axonal outgrowth. Biomimetic conduit containing guidance channels was shown to support nerve regeneration across the nerve interstump gap effectively in 15 mm rat sciatic nerve transection injury model. The assessment mainly focused on post-operative function recovery and histological analysis: (1) nanofiber conduit with guidance channels supported axons and Schwann cells progression longitudinally along the nanofibers; (2) intra-luminal channels provided as guidance substrates and the conduit served to prevent scar formation and entrap biomolecules within the interstump gap to promote nerve regeneration *in vivo*; (3) laminin and nerve growth factor can be used to improve the performance of nanofiber construct. The capability of nanofiber nerve construct has been demonstrated to bridge nerve gaps with improved functional recovery suggests that this nanofiber construct can potentially be used in the clinical settings to reconstruct peripheral nerve gap.

List of Publications

Peer-reviewed papers

1. **Koh HS**, Yong T, Teo WE, Chan CK, Puhaindran ME, Tan TC, Lim AYT, Lim BH, Ramakrishna S. Nano-structured tubular grafts consisting of novel biomimetic intra-luminal guidance channels - synergism of physical and biochemical cues for nerve repair. Journal of Materials Chemistry (Submitted).

2. **Koh HS**, Tan TC, Puhaindran ME, Yong T, Teo WE, Chan CK, Ramakrishna S. Longitudinally aligned nanofiber guidance channels in biomimetic nerve conduit for peripheral nerve repair. Biomaterials (Submitted).

3. **Koh HS**, Yong T, Chan CK, Ramakrishna S. Fabrication and characterization of collagen coupled polymeric nanofibers for nerve tissue regeneration. Journal of Biomedical Materials Research Part A (Submitted).

4. **Koh HS**, Yong T, Chan CK, Ramakrishna S. Enhancement of neurite outgrowth using nano-structured scaffolds coupled with laminin. *Biomaterials* 29 (2008) 3574-82.

5. Yong T, Liao S, Wang K, **Koh HS**, Chan PX, Chan CK, Ramakrishna S. Engineered Nanofibers for Cell Therapy and Nanomedicine, *Locomotor System – Advances in Research, Diagnostics and Therapy* 14 (2007) 21 – 38.

Conferences

1. **Koh HS**, Puhaindran ME, Tan TC, Chan CK, Lim BH, Lim AYT, Ramakrishna S. 2008 "Biomimetic nerve guidance grafts: Synergism of physical nano-topography and biochemical guidance cues" International Symposium on Nanotoxicology Assessment, Biomedical, Environmental Application of Fine Particles and Nanotubes, Sapporo, Japan (Oral) *Awarded Young Researcher Travel Award*

2. **Koh HS**, Chan CK, Ramakrishna S. 2008 "Nanofibers for nerve regeneration" 3rd MRS-S Conference on Advanced Materials, Singapore (Poster).

3. **Koh HS**, Yong T, Chan CK, Tan TC, Lim BH, Lim A, Ramakrishna S. 2007 "Modification of polymeric nanofibrous scaffolds with ECM bioactive molecules to improve nerve regeneration" 3rd World Congress on Regenerative Medicine, Leipzig, Germany (Oral).

4. **Koh HS**, Yong T, Chan CK, Tan TC, Lim BH, Lim A, Ramakrishna S. 2007 "Modification of poly(L-lactic acid) nanofibers with Type I collagen for enhancement of nerve regeneration" SBE's 3rd International Conference on Bioengineering and Nanotechnology, Singapore (Poster).

Provisional Patent

US provisional application no. 61/084,306. Title: BIOMIMETIC FIBROUS IMPLANT DEVICES FOR NERVE REPAIR Inventors: **Hui Shan Koh**, Wee Eong Teo, Casey Chan, Seeram Ramakrishna, Ter Chyan Tan, Mark E Puhaindran.

LIST OF TABLES

LIST OF FIGURES

XIX

LIST OF ABBREVIATIONS

AFM	atomic force microscopy
BDNF	brain-derived neurotrophic factor
CNS	central nervous system
ECM	extracellular matrix
EDC	1-ethyl-3-(3-dimethylaminopropyl) carbodiimide hydrochloride
FDA	United States Food and Drug Administration
FITC	fluorescein isothiocyanate
GDNF	Glial-derived growth factor
HFP	1,1,1,3,3,3-hexafluoro-2-propanol
kDa	unit of 1000 Dalton
LSCM	laser scanning confocal microscopy
MES	2-(N-morpholino)ethanesulfonic acid
NGF	nerve growth factor
NHS	N-hydroxysuccinimide
PBS	phosphate buffered saline
PCL	poly(ε-caprolactone)
PCL-LA	poly(ε-caprolactone)-co-poly(lactic acid)
PLGA	poly(lactic acid)-co-poly(glycolic acid)
PLLA	poly(L-lactic acid)
PNS	peripheral nervous system
RBITC	rhodamine B isothiocyanate
TEM	transmission electron microscopy
SEM	scanning electron microscopy
w	weight
v	volume
XPS	x-ray photoelectron spectrometry
avg	average

LIST OF APPENDICES

Chapter 1

Introduction

1.1   Background

It is estimated that approximately 360,000 patients suffered from health problems related to upper extremity paralytic syndromes annually in the United States, and over 300,000 people suffer peripheral nerve injuries in Europe yearly [1]. Mechanical, chemical, thermal, and/or pathological etiologies can cause peripheral nerve injuries in humans. If there are no interventions to repair the damaged nerves, loss of function with impaired sensation and painful neuropathies will occur that affect the patients adversely. Because mature neurons do not regenerate effectively, it is a challenge to obtain successful and good rehabilitation for peripheral nerve repair. And no patients make a complete recovery following transection injuries to the nerves. However, axonal outgrowth of the peripheral nerves and outcome of nerve repair can be optimized if appropriate nerve repair techniques and/or nerve implant devices are used, thus reconnecting the proximal and the distal nerve stumps to obtain satisfactory functional recovery.

The current clinical gold standards for the treatment of injured peripheral nerves are direct tension free end-to-end anastomosis for the transected nerve stumps. Frequently, tension free repair is not possible due to too large of a gap, and in this

situation the gold standard is to use autologous nerve grafts to bridge these gaps. Even then, recovery of sensory, motor and autonomic functions are never complete and at best, a clinical function recovery rate of about 80% is achieved [2]. Other disadvantages of autologous nerve grafts include: 1) donor site morbidity, 2) multiple surgical procedures, 3) insufficient donor nerves, 4) possible formation of painful neuroma, and 5) donor and recipient size mismatch with poor alignment of fascicles [3]. Other biological nerve scaffolds such as veins and skeletal muscles are alternatives that have been used to repair nerve gaps [2, 4], but these scaffolds have not produce optimum nerve regeneration results.

Bioengineered nerve construct is an attractive alternative substitute for clinicians to use for the repair peripheral nerve injuries because they can overcome certain disadvantages of using autologous grafts like donor site morbidity, insufficient donor nerves and size mismatches. Although FDA-approved nerve constructs are already available, these devices are reserved for small gaps in humans (several millimeters or up to 30 mm) that do not address the repair of larger peripheral nerve gaps commonly found in the clinical situations [2, 5]. The main challenge is to bioengineer artificial nerve constructs that are capable of bridging large nerve gaps that are currently not achievable with the non-biological nerve substitutes, and to provide improved rate of recovery and better clinical return to functions than autologous nerve grafts [2]. Recent advances in tissue engineering techniques have sparked interests in making scaffolds with natural materials and/or biodegradable synthetic polymer nanofibers [6]. However most often, the current non-biological nerve implant devices do not

possess the physical topography that recapitulates the hierarchical organization and biological functions of peripheral nerve natural extracellular matrix (ECM) that consists of submicron fibers and fibrils. The rationale for using nano-scale fibers is based on the theory that cells attach and organize well around fibers with diameters smaller than the diameter of the cells and axons [7]. The non-woven polymeric meshwork is a mimic to the nano-scale protein fiber meshwork in native ECM. Therefore it will be advantages to create a nerve construct that possesses the physical topographical of nerve ECM to bridge nerve gaps for repair.

Another important aspect to consider when designing the nerve construct is the use of intra-luminal guidance channels in the lumen of a bridging conduit. One of the reasons why the autologous nerve graft is an excellent scaffold for nerve repair is because it provides the basal lamina structure with biochemical signals (e.g. laminin and collagen) that promote efficient axonal extensions [8]. For transected nerve repair, a fibrin matrix will initially form in the lumen of an empty conduit that is used to bridge the nerve gap [8]. Subsequently capillaries, axons and non-neuronal cells such as Schwann cells, macrophages, and fibroblasts invade this matrix. However if the fibrin matrix is not formed appropriately or infiltrated with the cellular components, it will disintegrate and nerve regeneration might fail, especially in large nerve gaps [8]. Intra-luminal guidance channels can thus be incorporated in the conduit to support the formation of the fibrin matrix and act as the initiate substrates for cellular infiltration that will aid in bridging large nerve gaps [9]. Hence, the use of

novel longitudinally aligned nanofibrous intra-luminal guidance channels could potentially improve the outcome of nerve repair.

1.2   Motivation

Topographical presentation of the nerve scaffold is important for promoting nerve regeneration. Recent studies have shown the potential and importance of nano-texture scaffolds for nerve tissue engineering applications [10]. It has been proposed that since peripheral nerve trunk is structurally made up of ECM [11] and electrospinning is an enabling technology to fabricate nano- and micro- size fibers that mimic the structural ECM of the body. By controlling the processing parameters, fibrous scaffolds with controllable fiber diameter ranging from nano to micro-meter scale can be achieved to fabricate scaffolding architectures that promote peripheral nerve regeneration. Nerve construct made up of nanofibers may be beneficial for nerve regeneration.

Furthermore recent studies have shown that with the use of aligned nanofibers, the cells orientate along the alignment of the nanofibers with neurites extending along the direction of the nanofibers, and aligned nanofibers promote the longest neurite extension when compared to random nanofibers, and aligned and random microfibers [12]. Studies illustrated that the orientation of the nanofibers has a marked effect on the morphology and alignment of the attached cells. Human coronary artery smooth muscle cells and mouse neuronal cells when cultured on aligned scaffolds orientate

along the direction of the nanofibers [12, 13]. The cytoskeletal proteins were also observed to follow the orientation of these cells when cultured on aligned nanofibers. In addition, neurite extensions of mouse neuronal cells were also found to follow the orientation of the nanofibers. The use of aligned nanofibers to prepare both the outer tubular scaffold and the intra-luminal guidance channels of the nerve conduits will guide as well as potentially promote the rate of axonal elongation.

In addition, natural ECM materials can be electrospun with polymer nanofibers or incorporated into the nerve conduits. Growth factors which are more labile that need to remain biologically active and slowly release to support axonal growth, can be incorporated into electrospun fibers to enhance nerve regeneration. In this project, we utilized electrospinning to fabricate a nanofibrous conduit that contained novel longitudinally aligned nanofibrous strands (termed intra-luminal strands or guidance channels) (Fig. 1.1) and studied its effectiveness to promote nerve regeneration in a 15 mm rat sciatic nerve model.

1.3   Hypothesis and Objectives

Hypothesis

Nerve conduit containing aligned nanofibrous intra-luminal guidance channels with nerve enhancing biomolecules promote peripheral nerve regeneration.

a) Nano-scale architectured nerve conduit with aligned nanofibrous intra-luminal guidance channels could be fabricated.

b) Incorporation of ECM bioactive molecules such as laminin and collagen (which promote neurite growth) into nerve conduit enhance axonal outgrowth.

c) Sustained release of incorporated neurotrophins such as nerve growth factor (NGF) that are essential for neuronal growth and survival, in the design nerve construct.

d) Nerve conduit with aligned intra-luminal nanofibrous guidance channels enhance nerve regeneration to aid peripheral nerve regeneration.

Objectives

- Utilize electrospinning technology to fabricate three-dimensional nanofibrous nerve conduit with aligned intra-luminal guidance channels;

- Capitalize on the nano-scale architectures of nerve construct to guide nerve regeneration, and prevent scar tissue in-growth which acts as barrier to axonal outgrowth;

- Incorporate ECM bioactive molecules and provide sustained release of neurotrophins to enhance nerve regenerative ability of the nerve construct;

- Demonstrate the capability of the nanofibrous nerve construct to bridge nerve deficits larger than 10 mm in rat sciatic nerve model.

The strategy and scheme of nanofibrous nerve guide is depicted in Figure 1.1. Bioengineered nerve construct consists of an outer nerve conduit that was fabricated using PLLA and aligned PLGA nanofibrous intra-luminal guidance channels. ECM bioactive molecules such as laminin were coupled into the outer conduit fabrication and neurotrophins such as NGF was incorporated into the intra-luminal guidance channels for sustained release to enhance nerve regeneration.
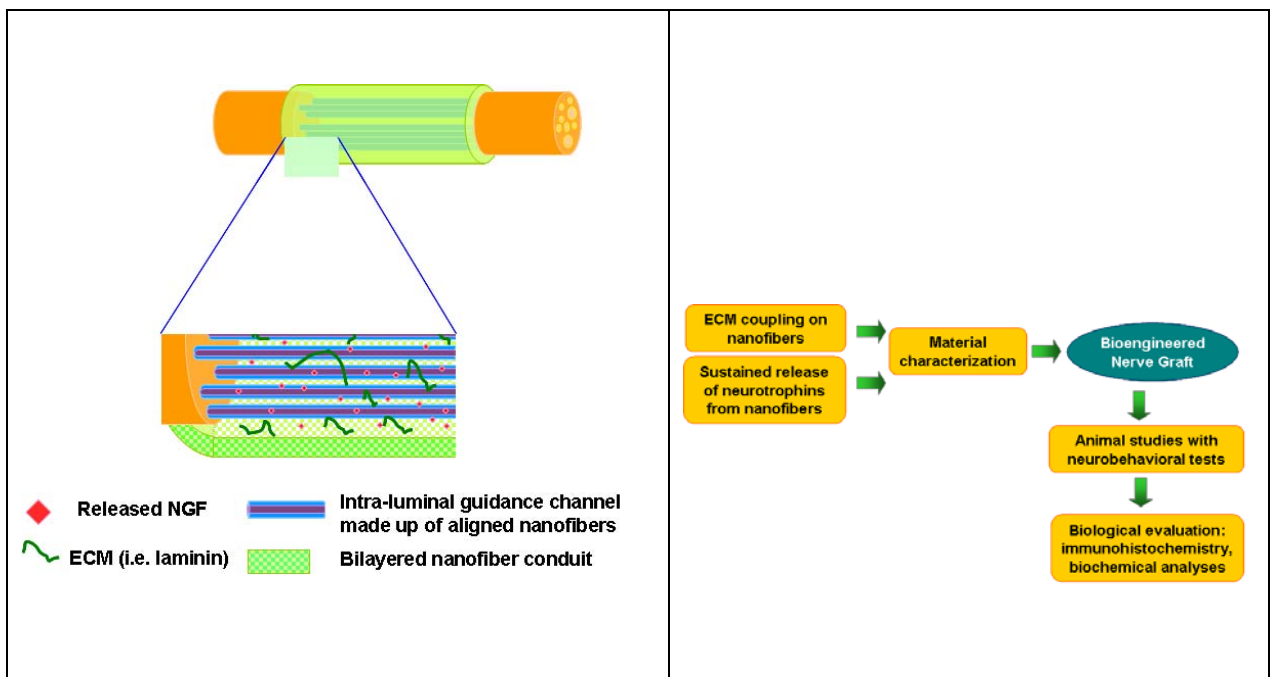
Figure 1.1. Peripheral nerve construct strategy (Figure not drawn to scale).

1.4 Overview of work scope

In this dissertation, a detailed literature review is presented in Chapter 2 that includes the fabrication of various nanofibrous scaffolds by electrospinning and the different aspect of peripheral nerve engineering. Conclusions for this thesis and recommendations for future work are described in Chapter 7.

Table 1.1. Overview of project scope.

Hypothesis	Objective	Descriptions	Thesis
Nano-scale architectured nerve conduit with aligned nanofibrous intra-luminal guidance channels could be fabricated.	Utilize electrospinning technology to fabricate three-dimensional nanofibrous nerve conduit with aligned intra-luminal guidance channels.	Bilayered nanofibrous nerve conduit and aligned nanofibrous intra-luminal guidance channels were successfully fabricated using electrospinning.	Chapter 3 and Chapter 5
Incorporation of ECM bioactive molecules such as laminin and collagen (which	Incorporate ECM bioactive molecules and provide sustained release of neurotrophins to	Study on collagen and laminin coupling onto nanofiber were done. The *in vitro* results showed that blending of laminin was the optimum	Chapter 4

promote neurite growth) into nerve conduit enhance axonal outgrowth.	enhance nerve regenerative ability of the nerve construct.	method to produce the nerve construct that can be used to enhance nerve regeneration in rat sciatic nerve repair.	
Sustained release of incorporated neurotrophins such as nerve growth factor (NGF) that are essential for neuronal growth and survival, in the design nerve construct.		Bioactive NGF was incorporated into the nanofiber by blending electrospinning to fabricate protein coupled intra-luminal guidance channels for sustained release of neurotrophins.	Chapter 5
Nerve conduit with aligned intra-luminal nanofibrous guidance channels enhance nerve regeneration to aid peripheral nerve regeneration.	Demonstrate the capability of the nanofibrous nerve construct to bridge nerve deficits larger than 10 mm in rat sciatic nerve model.	(1) nanofibrous conduit with longitudinally aligned nanofibrous intra-luminal guidance channels supported Schwann cell migration and axon extensions *in vivo*; (2) nerve enhancing biomolecules such as laminin could aid in nerve regeneration for bridging peripheral nerve gaps.	Chapter 6

Chapter 2

Literature Review

2.1   Introduction

Tissue engineering is a multi-disciplinary field of research that involves the use of cells, biological molecules, mechanical stimuli, and biomaterials to facilitate the repair of damaged/diseased tissue or to regenerate functional tissue [14-16]. Diverse and complex integration of various technologies such as the combination of material science research, scaffold technologies and the study of molecular and cell biology are essential to produce a fully-functional tissue [16-18]. Although tissue engineering research has progressed significantly over the years and yielded many invaluable results, there remain challenges for tissue engineers to translate the laboratory research to practical clinical use. The importance of enhancing interactions and bridging developmental biology and tissue engineering is judiciously identified because this can be a key to realize the potential of applying tissue engineering strategies in clinics to improve human health [19].

We need to understand how the cells and tissues construct themselves during development, remodeling, and repair and regeneration after injury to form the distinct three-dimensional structures with specific positions and arrangements [19]. After which we can bioengineer the appropriate structural physiochemical micro-

environment for specific damaged tissue to promote and aid in the healing and remodeling of the damaged tissues.

2.2   Tissue Engineering

2.2.1   Biomimetic scaffolds for tissue engineering

Every tissue type has its unique structure, morphology, chemical gradients, hydrodynamic and electrical forces, and mechanical properties [19]. Design of tissue engineering systems is a challenging task because the design criteria is required to address the general and tissue-specific needs to create a viable environment for each damaged tissue [19]. A key principle in tissue engineering is based upon that the cells surrounding the damaged tissue or the cells that are involved in the spontaneous repair of the damaged tissue have the capacity to reorganize into structures that resemble the original tissue [20]. Cells lives in native ECM consisting of nano- to micro- structured fibers (proteins and proteoglycans). This hierarchical organization presents a defined environment with nano-scale intermolecular binding interactions that will affect the morphological and functional development of the cells. Recent studies have shown the importance of nano-texture scaffolds for tissue engineering applications [10]. Cells that were cultured on micro-size fibrous scaffolds were flattened and the cells spread as if they were cultured on flat surfaces (Figure 2.1) [21]. Scaffolds with nano-scale architectures have larger surface area to adsorb proteins and present many more binding sites to cell membrane receptors would be more biomimetic to support better cell-matrix interactions [21]. Thus the presentation

of suitable topographical cues is an important aspect to consider when designing tissue engineered scaffolds.
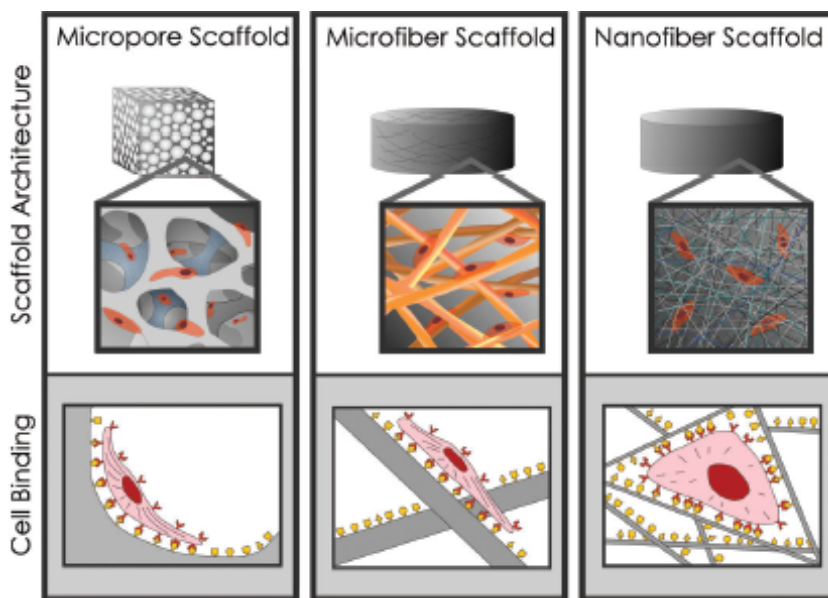
Figure 2.1. Scaffold architecture affects cell binding and spreading [21].

Bioengineered scaffolds or creation of biomimetic environments that have similarities to the natural ECM can be achieved using various techniques such as self-assembly, phase separation, and electrospinning processing methods (Table 2.1). The table compares the three methods that can be used to produce submicron scaffolds that structurally resemble the natural ECM. Self-assembly of nanofibers has been elegantly studied to produce scaffolds that biomimic the micro-environment of the tissue [22, 23]. Peptide nanofiber scaffolds were prepared by self-assembly for the nerve regeneration with accompanied functional return of vision in animals [23]. However self-assembled peptide scaffolds are mechanically weak to act as a supporting substrates. Phase separation is a technique to produce controllable nano-

structured porous scaffolds that can allow cell in-growth for tissue engineering applications. Nanofibrous matrices that were fabricated by phase separation were shown to support nerve cells growth and differentiation [24]. A limitation of phase separation process is that it is unable to produce long and continuous fibers. Electrospinning is a simple and scalable fabrication method to produce nanofibrous scaffolds that have been shown in several studies to support tissue repair [25, 26]. An advantage of electrospinning over the other two techniques are that it is a simple process that is able to produce long and continuous fibers with control over fiber orientation. However one could also consider that electrospinning is limited to some polymer.

Table 2.1. Comparison of various nanofibrous scaffold processing methods [23, 24, 26].

Scaffold processing method	General descriptions	Advantages	Disadvantages
Self-assembly	A process in which atoms, molecules, and supramolecular aggregates organize and arrange themselves into an ordered structure through weak and noncovalent bonds; typically involves a	Mimic the biological process in certain circumstances.	Complex process, limited to a few polymers, unable to produce long and continuous fibers with control over fiber orientation.

	bottom-up approach.		
Phase separation	A process that involves various steps, typically raw material dissolution, gelation, solvent extraction, freezing and drying, leading to the formation of nanofibrous foam-like structure.	Simple process, tailorable mechanical properties.	Limited to a few polymers, longer processing time, unable to produce long and continuous fibers with control over fiber orientation.
Electrospinning	A process that essentially employs electrostatic forces for the production of polymer nanofibrous scaffolds, typically involves top-down approach.	Simple and cost-effective process, capable to produce long and continuous fibers with control over fiber orientation, versatile to many polymers.	Use of high-voltage apparatus.

2.2.2   Nano-structured scaffolds by electrospinning

One of the basic premise of tissue engineering is to design and fabricate suitable structural scaffolds using biomaterials that are able to support cell adhesion, migration, proliferation and differentiation [27]. It can also involves the provision of an appropriate cocktail of bioactive molecules and/or cells that can induce the

formation of functional healthy tissue [28, 29]. Electrospinning is a simple and versatile technique that can produce non-woven ECM-like nanofiber scaffolds with nano-topographical cues to interact with the cells. This process was first patented by Formhals in 1934 [30] and until 1990s electrospinning has attracted more attention. Electrospun polymer fibers can be easily tailored and manipulated for desirable assembly structures, mechanical properties, and degradation time. These submicron fibrous scaffolds have large surface to volume ratio, well-interconnected pores, and high porosity that are suitable for different application purposes. Synthetic polymeric nanofibers such as poly(ε-caprolactone) (PCL) [31], poly(L-lactic acid) (PLLA) [12], poly(glycolic acid) (PGA) [32] and poly(lactic-*co*-glycolic acid) (PLGA) [33], and natural-occurring polymeric nanofibers such as collagen [34] and gelatin [35] have been electrospun. Electrospun nanofibers have been actively explored for applications in the different areas of tissue engineering such as skin [36], cartilage [37], bone [31], blood vessel [38], heart [39], and nerve [40].

Briefly, this technique utilizes an electric field generated by an applied voltage that subsequently introduces surface charges on the polymer solution. This thus induces the formation of a Taylor cone polymeric droplet at the tip of the spinneret. As the electric potential that is created at the droplet surface exceeds a critical value, the electrostatic forces will overcome the solution surface tension to initiate polymer jet stream. The charged jet is accelerated towards the grounded collector and undergoes bending instability, elongation, and solvent evaporation or jet solidification which leads to rapid thinning of the jet and deposition of dry fibers in a random manner onto

the collector [33, 41, 42]. Several factors can affect the electrospinning process and fiber morphology (Table 2.2). We can therefore change various conditions to obtain suitable fibers for specific applications.

Table 2.2. Effect of changing electrospinning process parameters on the resultant fiber morphology [26].

Process Parameter	Effect on fiber morphology
Viscosity/concentration	▪ Low concentrations/viscosities yielded defects in the form of beads and unction; increasing concentration/viscosity reduced the defects; ▪ Fiber diameters increased with increasing concentration/viscosity.
Conductivity/solution charge density	▪ Increasing the conductivity aided in the production of uniform bead-free fibers; ▪ Higher conductivities yielded smaller fibers in general (except PAA and polyamide-6).
Surface tension	▪ No conclusive link established between surface tension and fiber morphology.
Polymer molecular weight	▪ Increasing molecular weight reduced the number of beads and droplets.
Dipole moment and dielectric constant	▪ Successful spinning occurred in solvents with a high dielectric constant.
Flow rate	▪ Lower flow rates yielded fibers with smaller diameters; ▪ High flow rates produced fibers that were not dry upon

reaching the collector.

Field strength/voltage	▪ At too high voltage, beading was observed; ▪ Correlation between voltage and fiber diameter was ambiguous.
Distance between tip and collector	▪ A minimum distance was required to obtain dried fibers; ▪ At distance either too close or too far, beading was observed.
Needle tip design	▪ Using a co-axial, 2-capillary spinneret, hollow fibers were produced.
Collector composition	▪ Smooth fibers resulted from metal collectors; ▪ Aligned fibers were obtained using a conductive frame, rotating drum, or a wheel-like bobbin collector; ▪ Yarns and braided fibers were also obtained.
Ambient parameters	▪ Increased temperature caused a decrease in solution viscosity, resulting in smaller fibers; ▪ Increasing humidity resulted in the appearance of circular pores on the fibers.

Electrospinning can facilely produce nanofibrous scaffolds with different assemblies and architectures by slight modification or changing of the set-ups. Randomly arranged nanofibers is the most commonly electrospun substrates. This form of nanofiber orientation presents a network of interconnected pores, high porosity and anisotropic mechanical properties. Although randomly arranged nanofibers are useful in tissue engineered scaffolds, defined and orderly aligned fiber arrangement seem to

be more beneficial for most of the natural occurring tissues [26]. Aligned nanofibers

play a significant role in the influence of morphology and cytoskeleton of many cell

types. Endothelial cells, smooth muscle cells, osteoblasts, fibroblasts, and neural stem

cells displayed alignment and actin organization dictated by the prevailing nanofiber

orientation [10]. Aligned fibers were shown to guide oriented *in vitro* neurite

outgrowth and glial cells migration from dorsal root ganglia [43]. Also, enhanced

Schwann cell orientation and maturation was observed when they were cultured on

aligned nanofibers [44]. Therefore novel electrospinning set-ups have been developed

over the years to generate bioengineered nanofibrous scaffolds with diverse nanofiber

arrangements and structures (Fig. 2.2), especially for aligned fibers substrates

production.
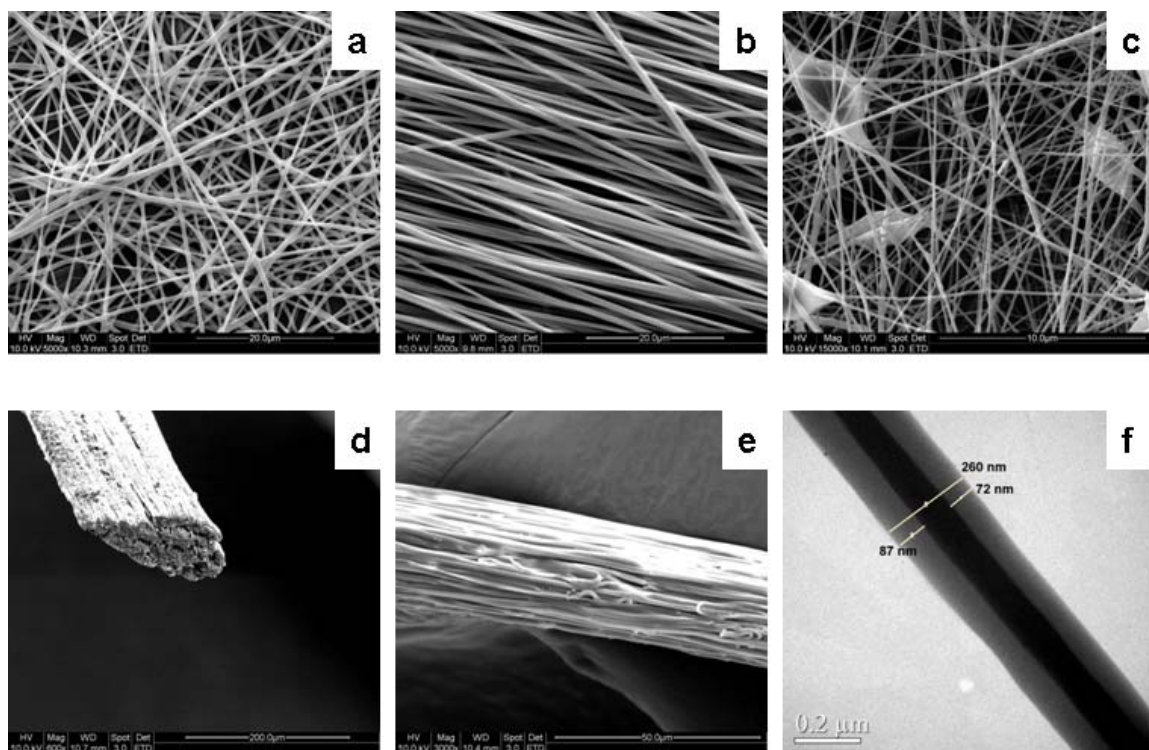
Figure 2.2. Various architectures of electrospun nanofibers or scaffolds: (a) random nanofibers, (b) aligned nanofibers, (c) beaded nanofibers, (d) nanofibrous yarn scaffolds, (e) nanofiber bundle, and (f) core-shell nanofibers.

Fabrication set-up for randomly oriented nanofibers

Figure 2.3 shows a typical electrospinning set-up for the production of randomly arranged nanofibers. The collector described herein is a planar plate that is conventionally used to assemble randomly oriented nanofibers.
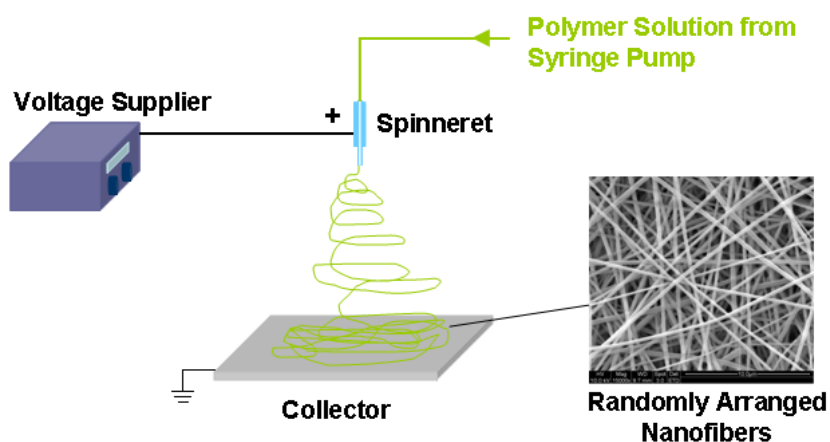
Figure 2.3. Schematic diagram of simple electrospinning set-up for production of random nanofibers.

Variations of the set-up to fabricate multi-layered nanofibrous mats and mixed polymer mats where the nanofibers are randomly arranged can also be achieved (Fig. 2.4). Multi-layering electrospinning allows the flexibility to produce stacks of

nanofibers comprising of different materials, while mixing electrospinning that use two or more spinnerets enables the production of scaffolds with blended nanofibers.

(a) Multi-layering electrospinning   (b) Mixing electrospinning
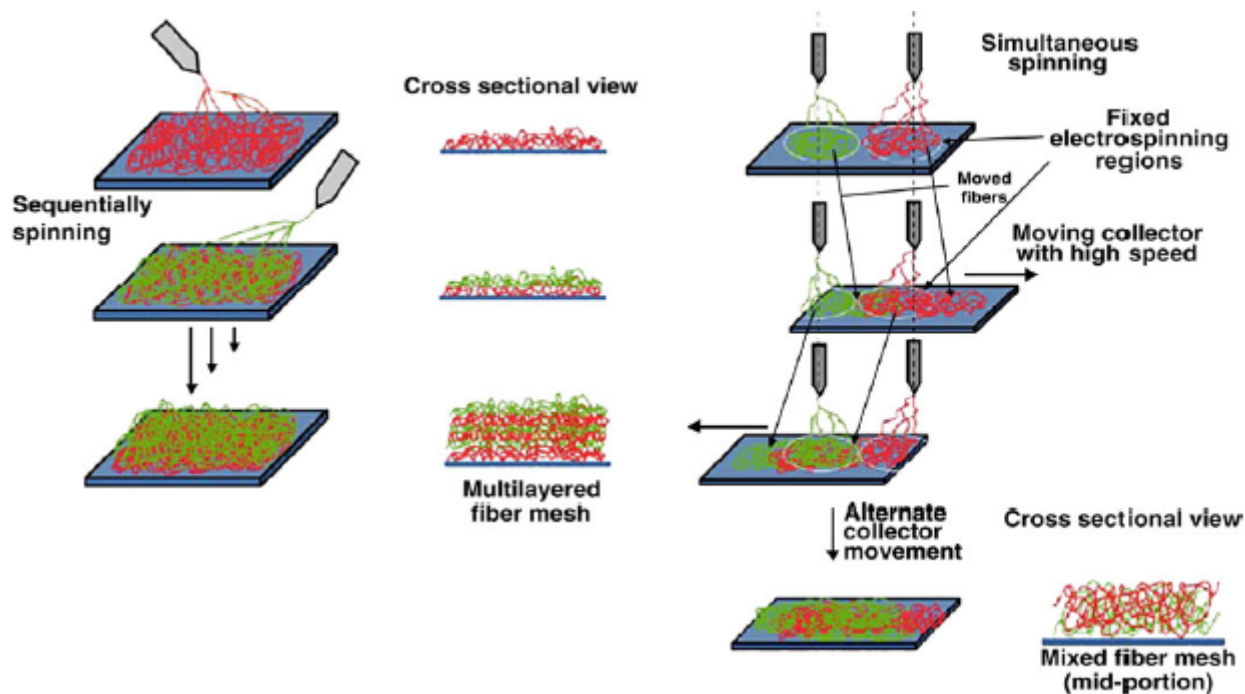
Figure 2.4. Electrospinning set-ups (a) Multi-layering electrospinning, and (b) Mixing electrospinning [45].

Fabrication set-ups for aligned nanofibers

Considerable efforts have been used to explore the fabrication of bioengineered scaffolds with highly controllable fiber orientations. Usually, aligned nanofibers are electrospun onto rotating drums at relatively high rotational speeds (e.g. several

thousands rpm). However there is a maximum limit for the rotating speed of the collectors that can be used because continuous fibers will not be formed if the critical speed is exceeded that break the polymer jet [26]. Tables 2.3 and 2.4 illustrate the various electrospinning set-ups that are used to produce aligned nanofibers.

Table 2.3. Descriptions of electrospinning set-ups using rotating drums for collection of aligned nanofibers [26].
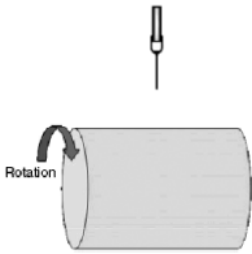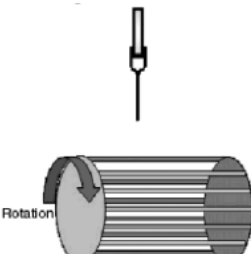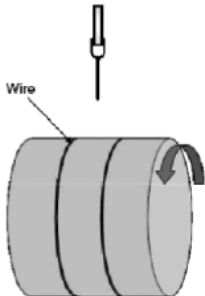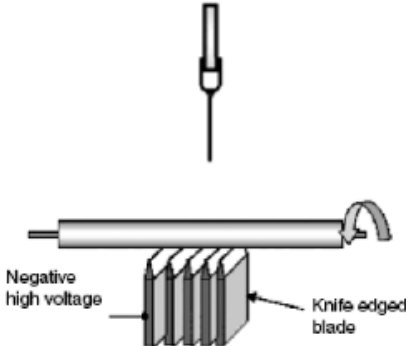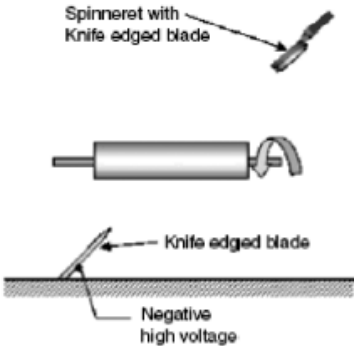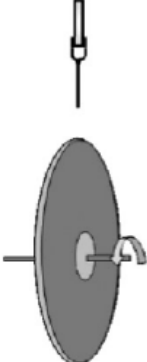
Rotating Drum Collectors		
Simple drum	Wire drum	Wire wound around the drum
Large are of aligned fibers can be fabricated; precise orderly aligned fibers are difficult to achieve.	Highly aligned nanofibers can be electrospun; thick layer of aligned fibers are not possible.	Highly aligned fibers are achievable and area of aligned fibers on the wire is adjustable by varying wire thickness; aligned fibers are concentrated on the wire only.

Table 2.4. Descriptions of electrospinning set-ups using rotating mandrels for collection of aligned nanofibers [26].

Rotating Mandrel Collectors		
Knife-edge electrodes below drum (tube) collector	Knife-edge electrodes to control electrospinning jet	Disc collector
Highly aligned fibers can be fabricated and thick layer of fibers can be collected; only possible with small diameter tube and set-up requires a negative electrode.	Thick layer of highly aligned fibers can be produced; set-up requires a negative electrode and applicable only with small diameter tube.	Highly aligned fibers can be collected; small area of collection and retaining high fiber alignment at same rotating speed when the deposited fibers become thicker is difficult.

Another electrospinning set-up that can produced aligned nanofibers involves the use of two parallel blades as the collector (Table 2.5). In this set-up, the fibers are suspended across a gap created by the parallel blades due to the electrostatic interactions that stretch the fibers across the space [46].

Table 2.5. Descriptions of electrospinning set-ups using blades for collection of aligned nanofibers [26].

Other forms of collectors

Parallel electrodes
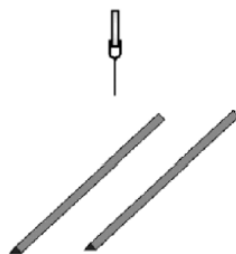
Highly aligned fibers can be obtained easily and fibers are easily transferable to another substrate; thick layer of aligned fibers are not possible and limitation of length of aligned fibers is present.

Fabrication set-up for co-axial electrospinning

Co-axial electrospinning has been designed to create core-shell structured nanofibers (Fig. 2.5). Two polymer solutions can concurrently be ejected through the two co-axial capillaries into the electrostatic field created by the high voltage supplied to the set-up. Zhang *et al.* electrospun core-shell nanofibers where gelatin and PCL formed the core and shell components, respectively [47]. Similarly, the same electrospinning set-up was used to fabricate individually collagen-coated PCL nanofibers and demonstrated their enhanced effect in promoting dermal fibroblasts proliferation and migration [48]. In fact, an advantage of using such set-up allows the fabrication of materials that are not easily electrospun. Solutions that are not electrospinnable can still be electrospun into the core component as long as the shell fluid is electrospinnable [49]. In the literature, Jiang *et al.* [50], Huang *et al.* [51], and Zhang *et al.* [52] have used coaxial electrospinning to produce protein- and/or drug-

encapsulating core-shell fibers and investigated their release behaviors. Interestingly, this type of device can be used to encapsulate living cells in the nanofibers for various applications that enable significant advances in tissue engineering and regenerative medicine [53].
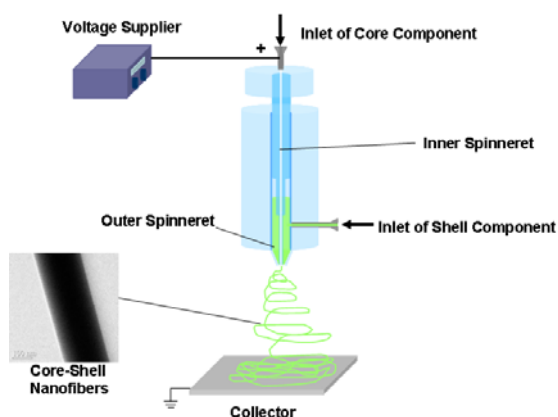
(a) Co-axial electrospinning set-up   (b) Co-axial cell spinning device
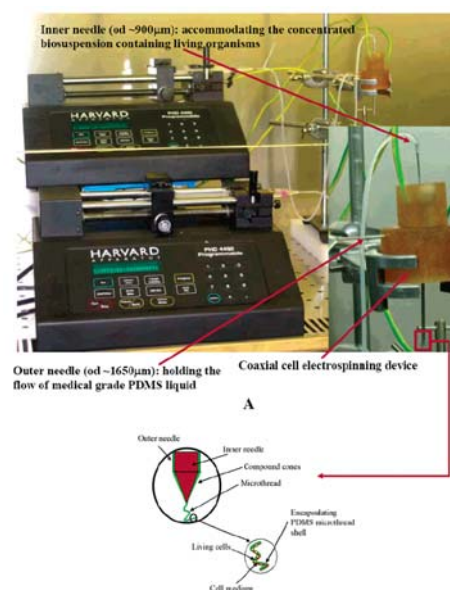
Figure 2.5. Core-shell fiber electrospinning set-ups. (a) Co-axial electrospinning, and (b) co-axial cell spinning device [53].

Fabrication set-ups for three-dimensional nanofibrous scaffolds

Besides producing nanofibrous substrates that are mainly in the form of mats or membranes, electrospinning can be used to fabricate scaffolds in the forms of tubular, yarn and mesh architectural constructs.

(a) Nanofibrous conduit

Figure 2.6 shows the electrospinning set-up used to fabricate nanofibrous conduits. Briefly, nanofibers are electrospun and collected on a rod that is attached to a rotating mandrel. This easily forms a tubular conduit made up of electrospun nanofibers. The nanofibrous conduits have been studied in vascular graft [54], nerve conduit [40] applications.
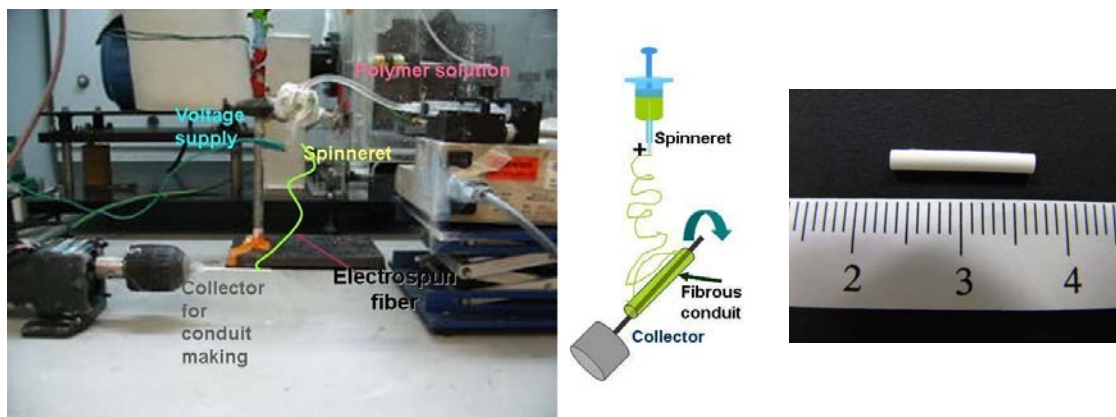
Figure 2.6. Schematic diagram of tubular construct electrospinning set-up.

(b) Nanofibrous yarn

The electrospinning set-up (Fig. 2.7) [55] is a novel and unique method that has been developed to fabricate nanofibrous strands of a few microns that are made up of

longitudinally aligned nanofibers bundle. Briefly, a high voltage is delivered to the spinneret and the nanofibers are drawn towards a basin of flowing water. The vortex created by the flowing water will coalesce the nanofibers into a bundle to form the nanofibrous yarn to be drawn onto a rotating mandrel for the collection of individual strands. The yarn is made up of several highly aligned nanofibers that can provide excellent supporting structures for growth and maintenance of cells.
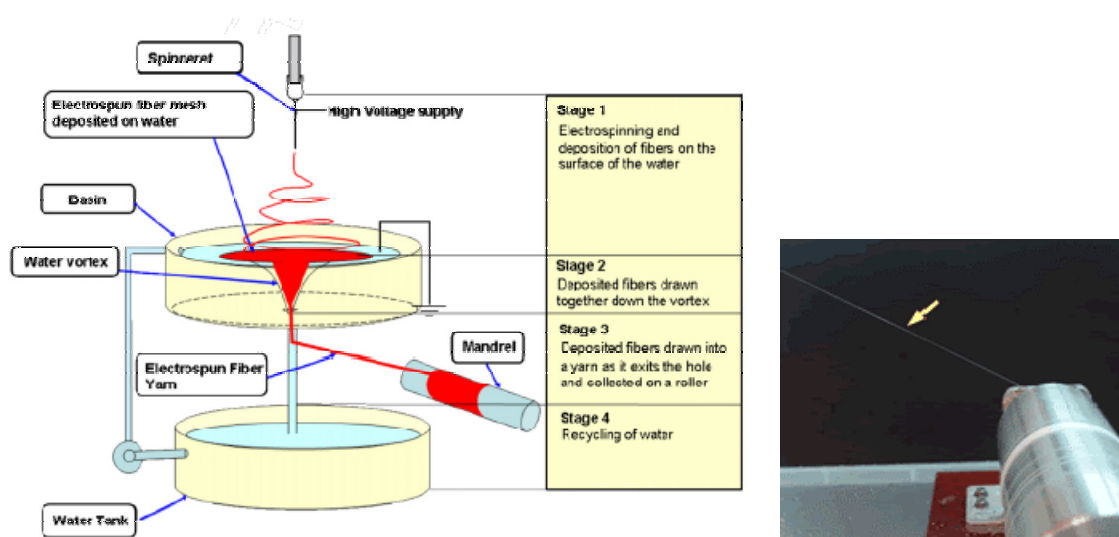
Figure 2.7. Schematic of the electrospinning set-up to fabricate nanofibrous yarn [55].

(c) Nanofibrous three-dimensional mesh

Generally, it is difficult to fabricate three-dimensional scaffolds through electrospinning because individual nanofibers are too fragile to be physically manipulated using standard apparatus. Residual charges on the deposited fibers generally divert subsequent incoming fibers to the side that prevent fibers to form a

bulk substrate efficiently. Although nanofibers can be stacked to form a membrane substrate, there is the presence of limitations. The stacked nanofibrous substrates will consist of pore sizes that are relatively too small to allow cell penetration through the scaffold. Hence, Teo *et al.* modified the set up shown in Figure 2.7 to fabricate a three-dimensional nanofibrous mesh made up of nanofibrous yarn as shown in Figure 2.8. The nanofiber yarns were not drawn onto a rotating mandrel for individual strand collection, but simply gathering at the bottom of the set-up shown. This scaffold has relatively good mechanical properties, porosity, and pore-size that can allow cell penetration. Scaffolds made up of PGA, PLGA, PLLA, or blended collagen-polymers have been successfully fabricated using this unique set-up.
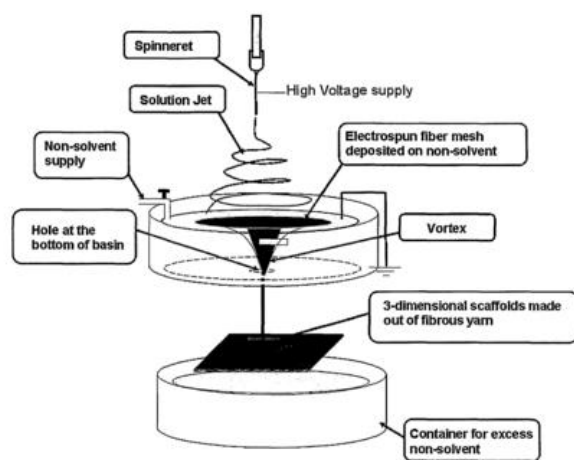
Figure 2.8. Schematic of the electrospinning set-up to fabricate nanofibrous 3-D mesh [56].

(d) Nanofiber bundle

Manageable three-dimensional bundle made up of highly ordered aligned nanofiber can be created using electrospinning through the use of steel blades to control the electric field (Fig. 2.9). Similar to the set-up shown in Table 2.5, the blades are placed in the direction shown in Figure 2.9. Nanofibers are first collected along the two-fixed steel blades and by dipping the electrospun nanofiber bundle in water and drying the bundle, robust micro-size bundle that is made up of highly aligned nanofibers are produced.
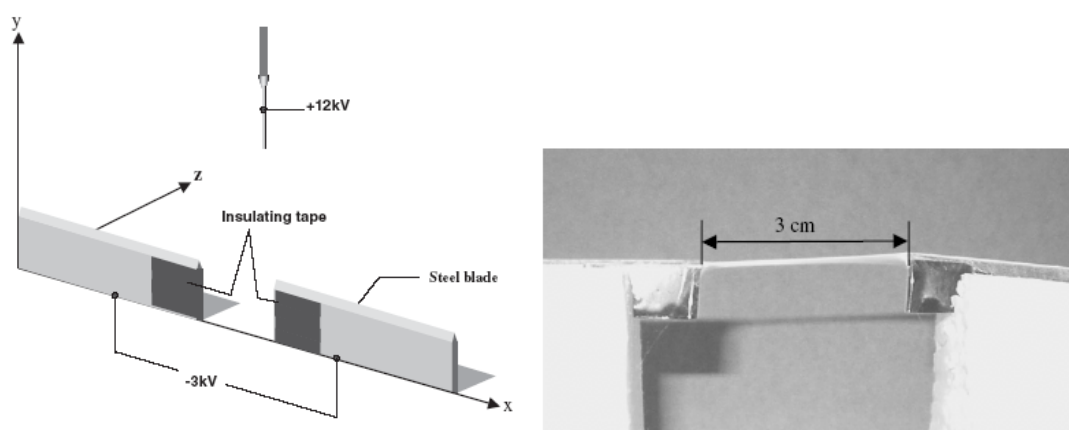
Figure 2.9. Schematic of the electrospinning set-up to fabricate nanofibrous 3-D bundle [57].

In general, electrospinning allows researchers to fabricate nanofibrous scaffolds that mimic the natural ECM with reproducible structures. Extensive amount of research has been done to produce electrospun nanofibers for its use in tissue engineering applications.

2.2.3 Modifications of nano-structured scaffolds for tissue engineering applications

Most commonly used biodegradable synthetic polymer materials such as PLLA, PGA, PCL, and co-polymers have been electrospun due to the easy dissolution of these polymers in electrospinning solvent. Besides synthetic materials, natural occurring polymers like collagen [18-23], and gelatin can also be electrospun into fibrous scaffolds. Although natural occurring materials present a more conducive environment for cell-matrix interactions, these nanofibers are seldom used as tissue engineered scaffolds because they do not possess adequate mechanical properties upon contacting with water. Although synthetic polymeric nanofibers possess adequate mechanical integrity for handling and implantation, they do not provide a biochemical-like environment to interact with the damaged tissues that require repair. Interactions between cells and their environments are usually mediated by bio-recognition signals [58]. In native tissues, ECM presents their adhesion proteins such as laminin, collagen, fibronectin, and vitronectin to affect cell attachment through the binding between integrin receptors on the cell surfaces. Therefore much work is done to enhance the biocompatibility of polymeric tissue engineered scaffolds to create a biochemical-like environment on the biomaterial surfaces [10].

Biomolecules such as adhesive proteins like collagen, RGD peptides, fibronectin and growth factors like basic fibroblast growth factor, epidermal growth factor and insulin that can be easily recognized by the cells can be coupled onto the biomaterials to induce bio-recognition mechanisms of the interaction of cells and polymeric

biomaterial scaffolds. These modifications can preserve the mechanical integrity of polymeric scaffolds while creating an ECM-like environment to the scaffolds. Common methods used to modify nanofibers include physical adsorption of biomolecules onto the polymer surface or blending biomolecules into the bulk polymer for electrospinning [42, 59]. These two methods are the most straightforward techniques to enhance the surface of the materials, but possibility of easily losing the biomolecules by physical coating and loss of bioactivity of biomolecules by blended electrospinning should be considered. Covalent binding of biomolecules onto nanofibers is an alternative way to introduce cell recognition signals onto the biomaterial surface [60]. This method is useful because covalent attachment of the biomolecules onto the nanofibers can ensure long-term chemical stability until the polymer degrades. However this chemical method is tedious that involves several steps and several chemicals are needed to carry out the procedures and the bioactivity of the biomolecules may be compromised. Generally, nanofibrous scaffolds can be modified with bioactive molecules for use in tissue engineering applications.

2.3 Peripheral Nerve Tissue Engineering

2.3.1 Peripheral nerve injuries

Nerve injuries are generally quite common and their causes are very diverse which include external compression, direct intraneural injection of steroid or anesthetic agents, metabolic or neoplastic diseases, and physical injuries. Failure to restore these damaged nerves can lead to the loss of muscle function, impaired sensation, and painful neuropathies. The response of the nerve tissue to injury is stereotypical, i.e. it

depends on the degree of injury sustained and the types of cells that are involved in recovery. Nerve injuries were first classified into three categories by Seddon in 1943. They were neurapraxia, axonotmesis and neurotmesis. Sunderland [61] expanded this classification further in 1951 (Table 2.6).

Table 2.6. Classification of nerve injuries [62].

Seddon's classification	Sunderland's classification	Injury
Neurapraxia	I	A local area of nerve conduction block.
Axonotmesis	II	Loss of the relative continuity to the axon such that Wallerian degeneration occurs distal to the injury.
	III	Axon injury and scarring within the endoneurium.
	IV	Nerve regeneration across the area of injury blocked by a functional scar at the level of the nerve injury.
Neurotmesis	V	Nerve is completely transected, no functional recovery anticipated.
	VI	Individual responses of axons, end organs, and nerve connective tissue to the particular injury.

2.3.1.1 Peripheral nerve anatomy

Peripheral nerve consists of sensory and/or motor axons that are the extensions of the nerve cell bodies. These nerve cell bodies are located in the dorsal root ganglia (sensory neurons), autonomic ganglia (autonomic neurons) and the ventral horn of the spinal cord or brain stem (motor neurons) of the nervous system [63]. In general terms, peripheral nerves can be simply divided anatomically in three layers – namely endoneurium, perineurium and epineurium (Fig. 2.10 and Table 2.7 [63]). Axons are arranged in bundles and found in the endoneurium layer [61]. In the endoneurium compartment (En), a single Schwann cell envelops several unmyelinated axons, and another Schwann cell provides multiple wrappings of the plasma membrane forming the myelin sheath of a myelinated axon. Schwann cells associated with both unmyelinated and myelinated axons are covered with a continuous basal lamina [54]. Capillaries (Cap) are present within the endoneurial compartment and collagen fibers [64] run primary longitudinally between axons. Axons, Schwann cells, collagen, and endoneurial fluid are bundled into a fascicle by the perineurium (Pe). The perineurium consists of several layers of flattened perineurium cells that are covered internally and externally by a basal lamina. Several nerve fascicles are bundled together by the epineurium [65] as shown in Figure 2.10 to form a single peripheral nerve.
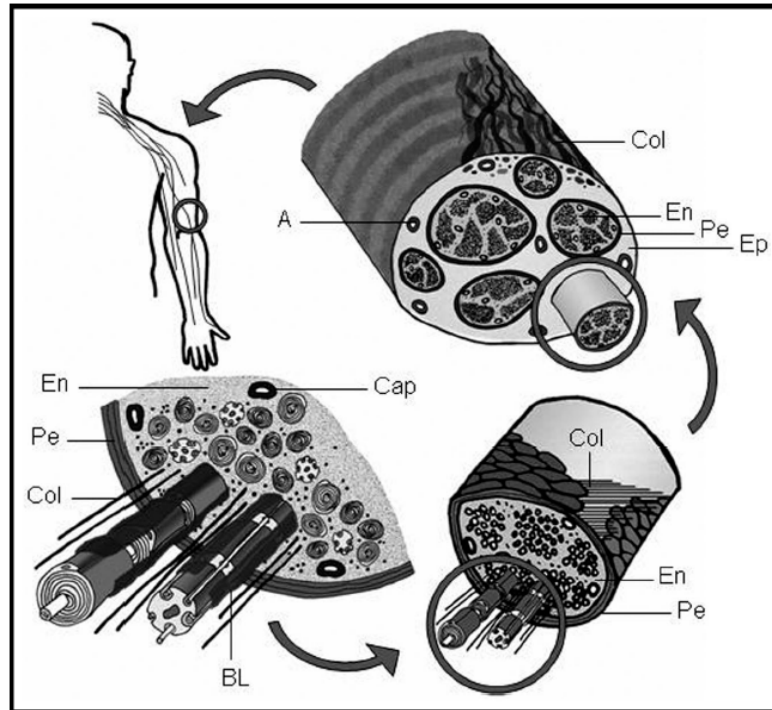
Figure 2.10. Structural components of peripheral nerve. Artery (A), basal lamina

(BL), capillary (Cap), endonerium (En), epineurium (Ep), and perineurium (Pe).

Adapted from [63].

Table 2.7. Anatomical layers of the peripheral nerve [63].

Layer	Primary Component
Endoneurium	Basal lamina of type IV collagen, fibronectin and heparin sulfate proteoglycan.
	Loose connective tissue of type I and type II collagen fibrils arranged longitudinally.
	Fibroblasts, mast cells, macrophages and endoneurial fluid.
Perineurium	Layers of type I and type II collagen fibrils.
	Elastic fibers arranged circumferentially oblique and longitudinally.
	Basal lamina with laminin, heparin sulfate proteoglycan and

fibronectin.

Epineurium   Bundles of type I and type III collagen fibrils.

Elastic fibers, fibroblasts, mast cells and fat cells.

2.3.1.2 Nerve injury: the process of degeneration and regeneration

After complete transection of the nerve cable, the cell bodies, axons and Schwann cells immediately undergo changes that prepare the injured nerve for regeneration (Fig. 2.11) [61, 66-69]. Neuronal cell bodies would swell that is accompanied by a significant increase in cellular metabolism and production of proteins that would subsequently be transported down the axon for nerve outgrowth [67]. Axonal degeneration, termed Wallerian degeneration, occurs at the distal site of injury that is characterized by neurofilbrillar, microtubular and myelin sheath fragmentations that form granular and amorphous debris. At the same time macrophages secrete a variety of cytokines which promote Schwann cells division. This thus increases the number of Schwann cells available for axons to interact. Macrophages also secrete interleukin 1, which stimulates the Schwann cells to produce nerve growth factor, thereby enhancing the nerve regeneration process [70]. Within 24 hours, most of the distal axons would have been degenerated [71]. Degradation also occurs at the proximal site, but to a limited degree as the initiation of the nerve regeneration would halt the degeneration process [2, 61].

Random sproutings of the axon, either myelinated or unmyelinated, occurs at the intact node of Ranvier [72]. Subsequently, the random sprouting would be replaced by a permanent filopodia containing cytoskeleton that is known as the growth cone and would appear at the proximal broken nerve cable [67, 72]. Removal of the degraded axonal tissue by the resident or circulating-recruited macrophages and adjacent Schwann cells also facilitate the preparation of the injured nerve environment for reinnervation process [72]. By 48 hours, myelin sheath would be degraded into segments of ovoids; the myelin debris and macrophage-derived cytokines would initiate the mitosis of Schwann cells by 96 hours after injury [73]. At 21 days, the Schwann cells would have formed dense Schwann cell tubes (i.e. Büngner bands) that would guide the regeneration of axons [71]. Figure 2.12 shows the simplified process of nerve regeneration in an empty nerve bridging conduit.
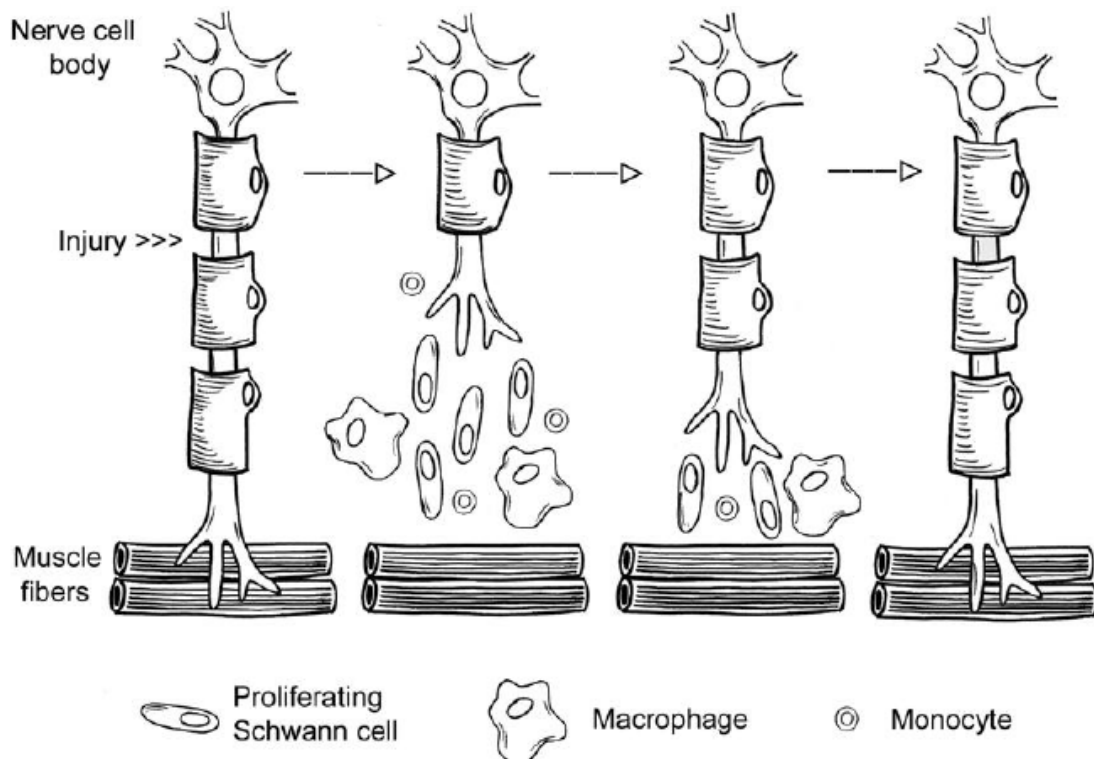
Figure 2.11. Simple schematic of nerve process after peripheral nerve injury [2].

During nerve regeneration, axons regenerate and elongate at a rate of approximately 1 mm/day *in vivo* [74]. But the suggested rate varies according to the length of the deficit, position of the nerve injury, and the time between the onset of injury [61]. Growth cones would innervate an end tissue by the formation of synapses [61]. Although axon extends and reaches end targets such as muscle and skin, functional impairment is still very common due to the random and unspecific innervations of axons to the end organs that are not identical to those that existed prior to injury [75, 76]. There are a number of molecular interactions taking place in nerve regeneration. This involves a variety of molecules in the environment that interact with axons, examples of such molecules are present on the surface of axons and Schwann cells (L1 and N-cadherin), in the ECM and axon's surroundings as soluble secreted molecules. The surface molecules of the axon growth cones have to interact with molecules of neighboring cells, and also the interaction of substrate adhesion molecules with ligands in the ECM have to take place in order to exert tension on the growth axons and make regenerative progresses [70].

Axon regeneration can often be inhibited by factors such as the presence of scar tissue in the nerve. Sometimes, axons fail to regenerate across nerve injuries and grow into a fibroblastic scar tissue at the site of damage. The axons at this region will not be able to grow further and the scar will develop into a swollen club ending. This scar tissue

creates a barrier against axonal regeneration in the peripheral nerve because fibroblasts do not secrete neurotrophic factors that axons require they are trying to grow through the scar tissue. In addition, fibroblasts associated with peripheral nerve produces a large amount of highly inhibitory proteoglycan (NG2 chondroitin sulfate proteoglycan) that will prevent axonal regeneration [77]. In certain cases whereby long stretches of the nerve are traumatized by contusion or by stretch injuries, scarring occur though the whole length of the injury and axons in these regions will not be able to regenerate.
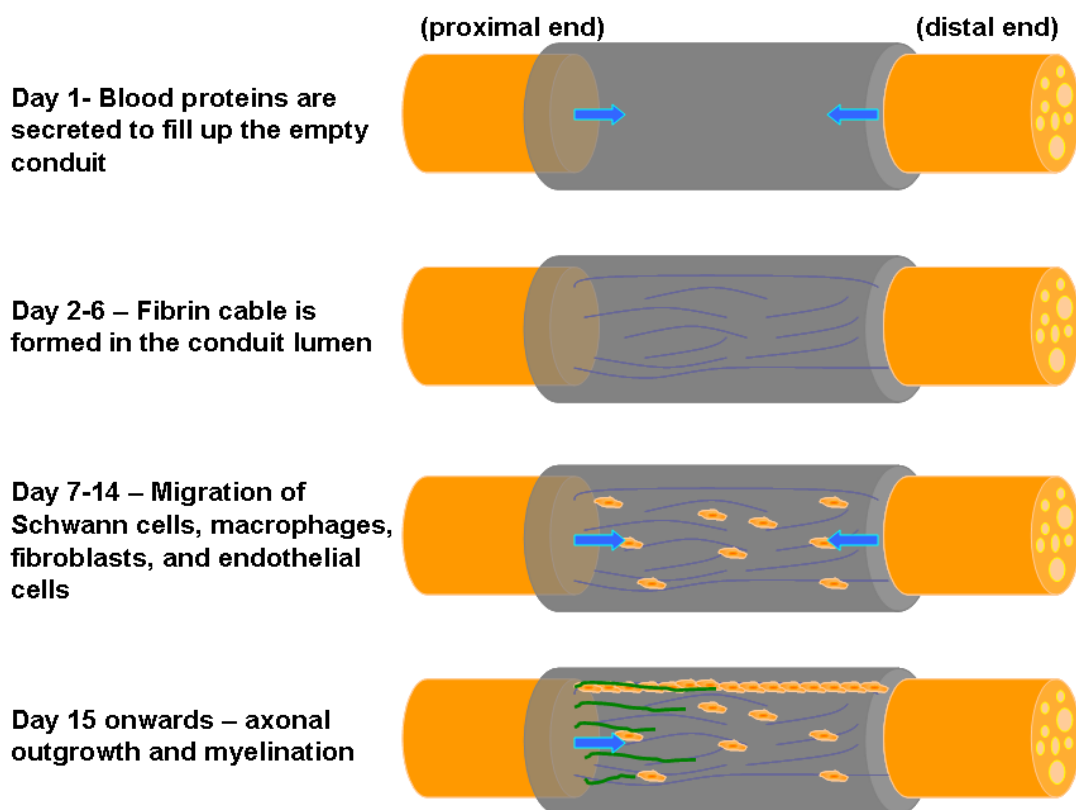
Figure 2.12. Timeline process of nerve regeneration in a bioengineered conduit.

2.3.2   Peripheral nerve repair in clinical situations
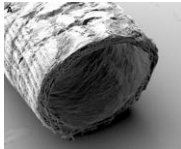
Peripheral nerve injury management has improved greatly in the past decades. The knowledge in basic science research is increasingly becoming important as it helps refine nerve surgical procedures, offering the promise of near-anatomic restoration of nerve structure and function. At the same time, a good understanding of intra-neural topography and anatomy of the peripheral nerve is also required to ensure better chances of functional recovery.

Autologous nerve transplantation is the gold standard to repair peripheral nerve injuries that result in gaps that cannot be repaired by simply suturing to reconnect the proximal and distal stumps. The sural nerve is the most common nerve graft used because this nerve is easy to harvest that can provide approximately 25-30 cm nerve tissue, leaving minor sensory deficits [78]. However, clinical reconstruction usually encompasses repairing of mixed or motor nerve deficits with sensory nerve graft that might present inappropriate nerve alignment and size disparity [3]. Other biological bridging conduits such as vein grafts presents limitations that involved the penetration of regenerated fibers through the vessel wall to entangle with the scar tissue, and also the collapsing of the veins due to their thin walls [79].
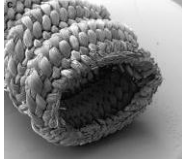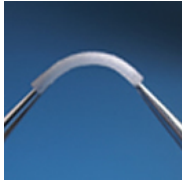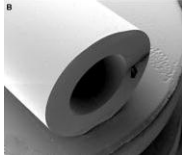
Bioengineered nerve construct is an alternative to bridge up nerve deficit to achieve functional recovery of the damaged nerve. These non-biological nerve guide implants can replace autologous nerve graft transplantations that are frequently limited by

tissue availability, secondary deformities, and second surgical step to obtain the donor nerves that result in loss of functions at the donor-site nerve. Although FDA-approved tissue engineered nerve devices (Table 2.8) are already available, these devices are reserved for small defects (several millimeters or up to 30 mm) that do not address larger peripheral nerve gap injuries commonly found in the clinics [2, 5]. Tissue engineered construct to facilitate axonal growth and glial cell proliferation, which include a scaffold, support cells, growth factors, ECM molecules have been previously studied. Results in the past with these constructs have failed to equal the nerve regeneration achieved with autologous nerve grafts [2]. Recent advances and contributions in the field of tissue engineering, in particular advances in tissue scaffolds preparation, and better understanding of the biology of nerve regeneration, have focused research on the combination of materials and desired biomolecules to create new composite materials that can actively stimulate the rate of nerve regeneration, increase the gap distance that the nerve construct can successfully bridge, target motor and sensory nerves reinnervation to their respective organs, and minimize inflammation.

Table 2.8. List of commercially available artificial nerve grafts [64, 78, 80].

Nerve Guide (Company)	Material	Nerve Guide Image
NeuraGen® (Integra)	Collagen Type I	

NeuroTube® (Synovis Micro)	Poly(glycolic acid)	
Salubridge^{TM} [80]	Polyvinyl alcohol hydrogel	
Avance^{TM} (Axogen Inc.)	Acellular nerve graft	-
Neuroflex™ (Collagen Matrix Inc.)	Collagen Type I	
Neurolac® (Polyganics)	Poly(ε-caprolactone)-co-(DL-lactic acid) (50:50)	

2.3.3 Designing biomimetic synthetic peripheral nerve construct

Repairing nerve transection injury is a unique process whereby the injured nerve cells do not heal by proliferation to increase the numbers. The repair of individual nerve cell and its axon takes place in an environment of intense cellular (e.g. Schwann cells, fibroblasts, endothelial cells) proliferation [81]. Growth cone explores its surrounding environment as it advances and they are guided to their targets by a combination of contact mediated and diffusible chemoattraction cues that are either attractive or repulsive (Fig. 2.13) [82]. Bioactive molecules that can aid in nerve regeneration for

attracting advancing growth cone to extend towards the distal stumps are actively examined. Axons can be guided at short-range by contact mediated mechanisms involving cell surface and ECM molecules and long range chemoattraction involves the secretion of diffusible chemoattractant substances by target cells to guide axon towards the target organs [82] as shown in Figure 2.13.
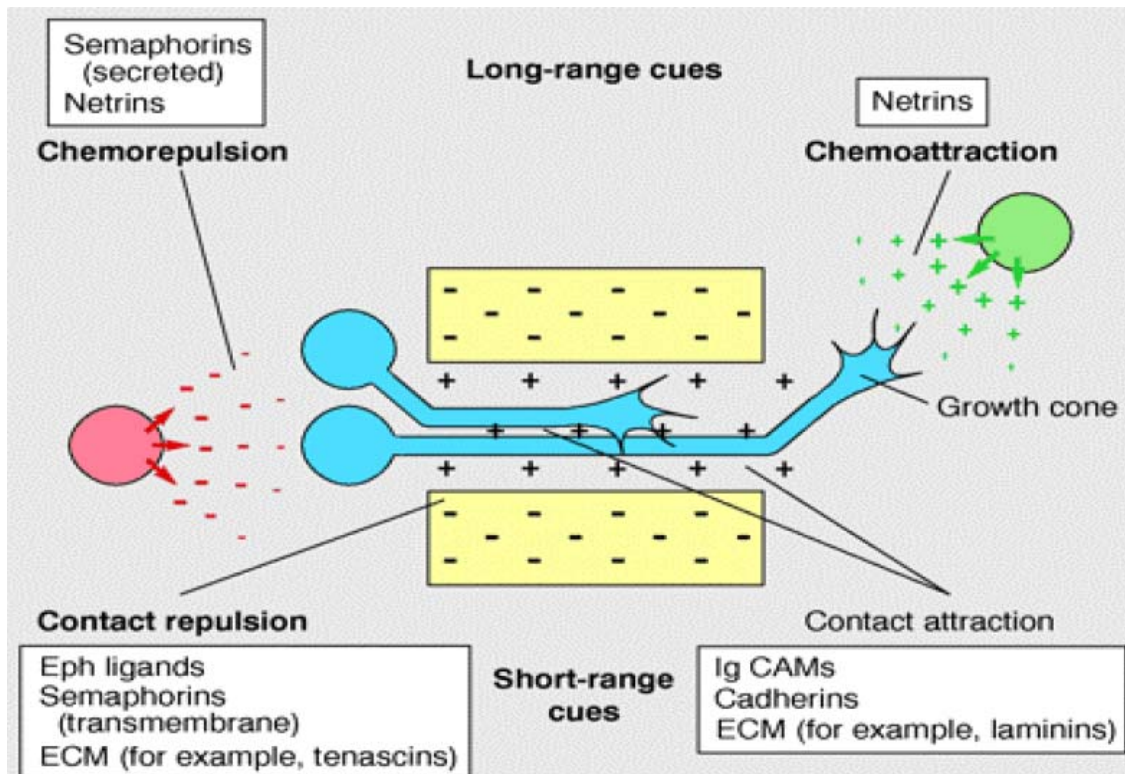
Figure 2.13. The molecular biology of axon guidance [82].

The ideal nerve construct must be easily available, biodegradable, readily vascularized, and porous for oxygen and nutrients diffusion. It should have low antigenicity and can avoid long-term compression. Current approaches of nerve

conduit research include the use of biodegradable polymer scaffolds, and incorporation of supporting cells such as Schwann cells, growth factors, and ECM molecules. A excellent review by Yannas *et al.* [83] described existing theories on nerve regeneration (Table 2.9) that occurred in a artificial conduit. The same paper suggested that an ideal tubular configuration for good nerve regeneration support ought to involve the ability to block myofibroblasts from forming contractile capsule while facilitating formation of microtubes (e.g. bands of Büngner).

Table 2.9. Descriptions of nerve regeneration theories [83].

Description	Postulation of mechanism
Neurotrophic theory	Axon elongation from the proximal stump is controlled by diffusion of growth-promoting soluble factors produced at the distal stump.
Contact guidance theory	Elongation of axons requires contact guidance with appropriate substrate(s). Enhanced Schwann cells and fibroblasts proliferation and migration occur in the presence of insoluble substrates.
Pressure cuff theory	For large nerve gap regeneration, axon growth is mechanically blocked by the circumferential forces that are exerted by the contractile fibroblasts (myofibroblasts). Closure of the wound might result. If myofibroblast capsule is allowed to develop fully, formation of neuroma would occur that effectively block elongation of axons across the gap.

Basement membrane microtube theory	Axons regrowth into preformed microtubes (i.e. linear columns form by the Schwann cells after nerve transection). This provides a linear path for axon elongation and myelination.

Pressure cuff theory and microtube theory appeared to play dominant role in peripheral nervous system (PNS) regeneration. Although neurotrophic theory and contact guidance theory are not thought to greatly influence the quality of regeneration, their importance is not ruled out. Figures 2.14 and 2.15 depict the flowchart of the various features of a tubular conduit that would affect nerve regeneration and the mechanisms of nerve regeneration, respectively. We have to carefully study the configurations of the conduit, the fillings for the conduit, the soluble factors, and the cells that enhance nerve regeneration.
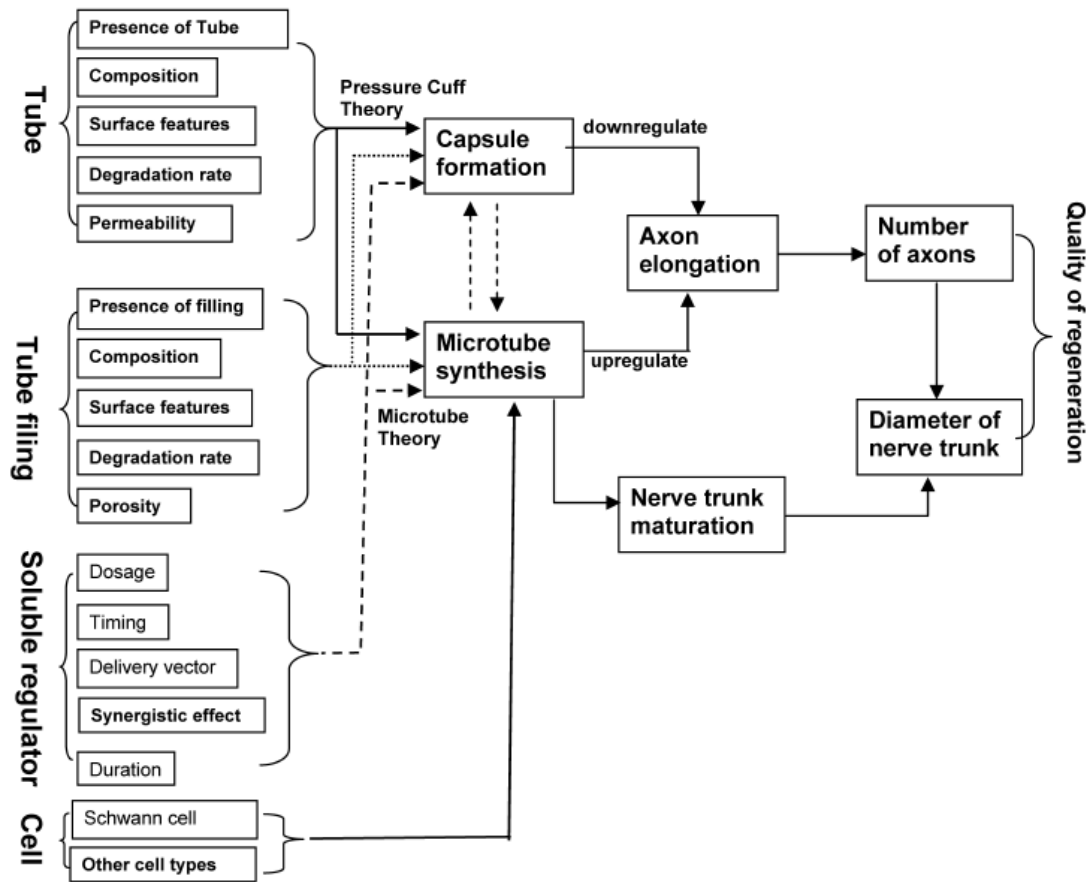
Figure 2.14. Effects of chamber parameters on quality of regeneration through regulation of the synthesis of two types of tissues: contractile cell capsule and microtubes [83].
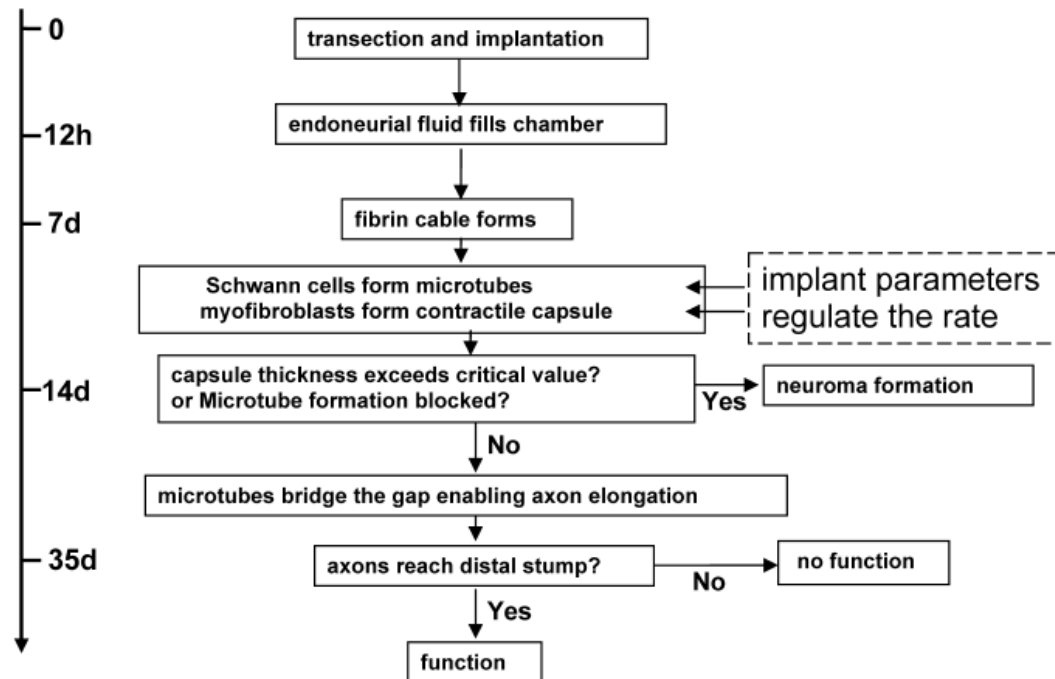
Figure 2.15. Hypothesized mechanisms of peripheral nerve regeneration: outcome of regeneration depends on both up-regulation by synthesis of microtubes and down-regulation by formation of contractile cells capsule [83].

The schematic model of a synthetic nerve construct design strategy (Fig. 2.16) that provides a defined microenvironment consisting of culture cells, growth factors, ECM molecules, and physical substrates in the lumen of the conduit is illustrated.

Nerve Related Growth Factors ▬▬▬ Intra-Luminal Guidance Channels

Biomolecules   Cells   ECM (e.g. Collagen, Laminin)
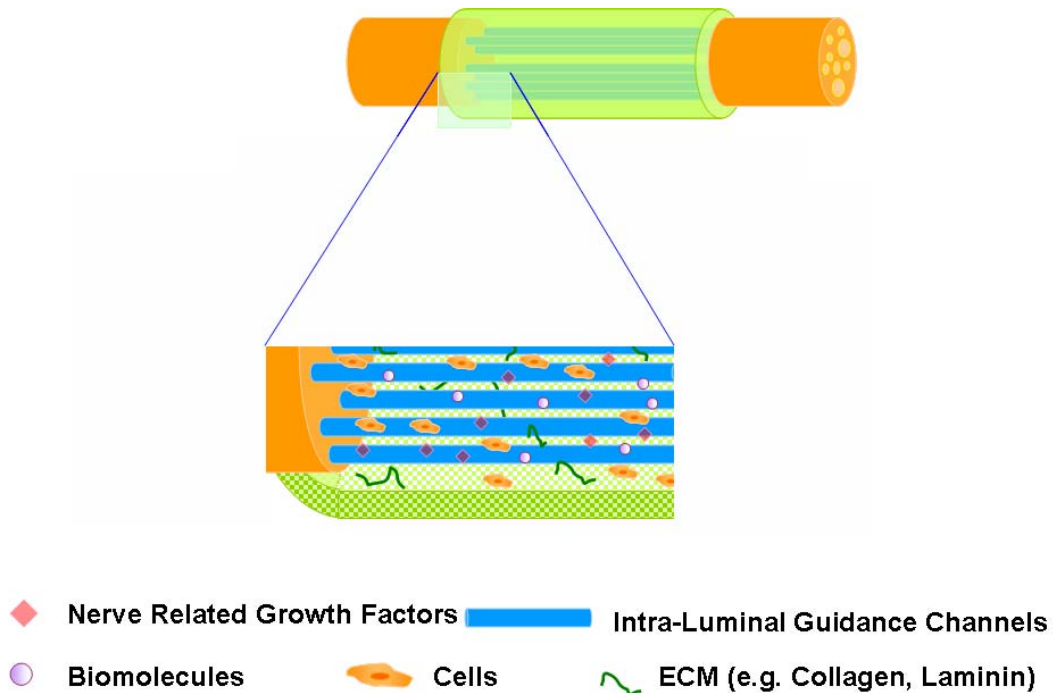
Figure 2.16. Schematic representation of the designed features of a synthetic nerve construct.

2.3.3.1 Materials

Lungborg is one of the pioneers to evaluate use of non-biological conduits for nerve repair. Non-biodegradable tubes such as silicone or polytetrafluoroethylene conduits were initially used to reconstruct the nerve after transection injuries that have shown promising results. However these non-biodegradable conduits pose long term complications such as fibrosis and chronic nerve compression that eventually require surgical removal of the conduits. Conduits made from bioabsorbable polymers (synthetic and naturally occurring) are promising alternatives to non-degradable

tubes. Table 2.10 lists some of the common biodegradable materials used to construct

tubular conduit that have been used in *in vivo* studies.

Table 2.10. Some common materials used to fabricate conduit that have been used in

in vivo studies.

Materials	General Properties (e.g. degradation[+])	Fabrication technique	Surface properties	Permeability	References
Synthetic					
PGA*	Aliphatic polyester, Crystalline, degradation in 6-12 months	Woven mesh fabrication technique	-	Semi-permeable	[78]
PLLA	Aliphatic polyester, crystalline, slow degradation (e.g. > 24 months)	Solvent casting, extrusion, and particulate leaching	Rough-looking due to the open-pore structure	Porous, mean pore size of 12.1 μm	[84-86]
PLGA		Electrospinning	Randomly arranged nanofibers provide relative smooth	Semi-permeable	[40]

			surface		
PCL-LA*	Amorphous, degradation within year(s)	Dip-coating	Inner layer is dense to prevent in-growth of fibroblast, outer layer is porous	Semi-permeable	[4], [87]

Natural

Collagen*	Degradation between one and 9 months	Spinning of collagen fibers around a central mold to form tubular geometry	Interconnected pores with laminated appearance; inner layer consisting of densely packed fibers that are intertwined with multi-layered structure	Semi-permeable (e.g. permeable to molecules the size of BSA)	[88]
Alginate		Freeze-drying of hydrogel		Porous	

[+] Degradation rate is dependent on the fabrication methods

* Commercially available nerve conduit

The advantages of using natural biomaterials for nerve construct production are the presence of biological recognition to provide a better environment for tissue regeneration. However, natural biomaterials may exhibit inflammatory and antigenic responses though collagen exhibits these immunological responses minimally. In contrast, synthetic polymers can be produced reproducibly in large scale that have controlled properties of strength, degradation rate, and microstructure. A drawback of synthetic polymers is the lack of biological recognition but this can be circumvented through the incorporation of cell-recognition molecules or domains such as laminin or tripeptide RGD into these materials. In fact, mixing of natural materials such as collagen and synthetic polymers such as PGA were performed to fabricate tubes to bridge up nerve gaps, and this combination of materials shows excellent nerve regeneration over large nerve gaps [89]. The many key characteristics possessed by synthetic polymers such as high porosity and surface area, structural strength, and specific three-dimensional shapes outweigh the lack of biological recognition in their use in tissue engineering or other bioengineering applications, especially in nervous tissue repair.

2.3.3.2 Cells

Glial cells, Schwann cells, are identified to be essential for successful peripheral nerve regeneration. During development, Schwann cells actively deposit ECM comprising of basal lamina sheets that surround individual axon-Schwann cell units. Following injuries, denervated Schwann cells will produce a number of neurotrophic

factors to support the survival of injured neurons, promote macrophage infiltration to the injured nerve, and provide substrate for axonal regeneration. Another important role of the Schwann cells involves the ensheathing and remyelination of regenerating axons. Although it is not exactly known about the mechanisms between axon and Schwann cell partnership during nerve regeneration, experiments have shown that a close relationship is present [90, 91] and regenerating axons could be misdirected by atypical Schwann cells processes [91]. Guidance of Schwann cells migration, adhesion, and maturation have been observed when cultured on various substrates [92, 93]. Incorporation of Schwann cells in the nerve conduits achieved good regeneration in the sciatic nerve repair compared with the nerve conduits without Schwann cells [94, 95]. Coupling Schwann cells [90, 96] in artificial nerve conduits is a potential strategy to improve peripheral nerve regeneration. However, Schwann cells application in the clinics remains controversial because *in vitro* expansion of culture Schwann cells is limited and the potential rejection of non-autologous donor Schwann cells has to be addressed.

Stem cells may be an alternative source for Schwann cells. Neural stem cells [97] and trans-differentiated bone marrow stromal cells [98-100] that express glial phenotype show potential use of stem cell therapy for peripheral nerve tissue engineering. Grafting of glial-differentiated bone marrow stromal cells into peripheral nerve repair showed a beneficial effect on Schwann cell growth within the nerves, thus indirectly promoting axonal regeneration [100]. However trans-differentiation of stem cells into neuronal or glial-like cells for use in clinical settings would require considerable

evaluation to justify the use in the design of artificial nerve conduits. Besides stem cells, research to use olfactory ensheathing cells [101], and genetic modified cells that over-express neurotrophins [2, 102-106] for nerve regeneration have also been described. Olfactory ensheathing cells that could be derived centrally from the olfactory bulb or derived peripherally from the olfactory epithelium possess similar phenotypes as Schwann cells and astrocytes [2]. It is however suggested that in order to warrant the use of olfactory ensheathing cells in peripheral nerve regeneration, distinct advantages of these cells over Schwann cells would have to be shown [2].

2.3.3.3 Extracellular matrix molecules

Schwann cells ensheathing the axons actively deposit sheets of ECM. The molecular constituents found in the peripheral nerve ECM are listed in Table 2.11. ECM mechanically stabilized cells and is critical for myelination of axons [107]. There are two major components: basal lamina surrounding the Schwann cells and axons, and endoneurial collagen that are both formed during embryonic development. Basal lamina contains collagen type IV and V, laminin, fibronectin, entactin, and heparan sulfate proteoglycan [107]. Endoneurial collagen contains longitudinally arranged collagen fibrils that are mainly collagen type I, II, IV, and V [107]. Since ECM plays important role for supporting the axons and Schwann cells, it may be advantageous to mimic the structure and biochemical signals found in the PNS ECM to enhance the performance of synthetic nerve constructs to bridge nerve deficits.

Table 2.11. Description of ECM molecules of the peripheral nervous system [11].

Extracellular matrix molecules	Active peptide sequence	Distribution in ECM of nervous system	Major Function
Laminin	IKVAV, YIGSR, RGD	Perhaps all basement membranes including those of Schwann cells and skeletal muscle, appears prior to development of intact basement membranes, on astrocytes in culture	Interact and influence with Schwann cells activities. Supports nerve fiber growth, stimulates aggregation of acetylcholine receptors on culture myotubes
Collagen	RGD	Synthesized by Schwann cells, Schwann cell basement membrane	Major structural protein of lamina densa, stimulates ensheathment of neurons by Schwann cells
Fibronectin	RGD	Radial glia in developing cerebellum, skeletal muscle and Schwann cell basement membranes, ECM of neural crest	Guidance of migrating neuroblasts, and growing nerve fibers, Schwann cell mitogen
Entactin	-	Basal lamina of Schwann cells	Cell attachment
Heparan sulfate	-	Basement membrane of Schwann cells	Myoneural synaptogenesis, adhesion of culture

neural cells to substrates, associated with a neurotrophic factor

Haptotactic cues for nerve regeneration include the incorporation of contact-mediated signals such as ECM proteins or short sequences of the "functional" nucleotides of the ECM to guide axons to extend to the synaptic targets [82]. It is well recognized that ECM components like collagen, laminin, and fibronectin can improve the results of nerve repair.

Collagen, a major component of the peripheral nerve's ECM, consists of different isoforms that display different functions for the PNS [11]. For example, collagen type I supports Schwann cells attachment and proliferation through interaction with the cell surface integrins, and collagen type IV is the main structural component of the basal densa [11]. Collagen type I is minimally antigenic that limits fibrotic and foreign body reaction [108], and can be broken down by collagenase possessed by fibroblast, macrophages and polymorphonuclear leukocytes [109]. Numerous studies have evaluated collagen for nerve tissue engineering applications. Incorporation of collagen gel or collagen sponge in the lumen of nerve guides were shown to improve nerve regeneration [110-112]. Collagen type I filaments were found to enhance nerve regeneration in a 30 mm rat sciatic nerve deficit [113]. Collagen-based nerve guides have also been produced commercially for clinical use [78].

Laminin, a major component of the basal lamina, is one of a series of structural proteins that activate the β1-integrin receptor. It plays a crucial role in cell migration, differentiation of Schwann cells and axonal growth [114-116]. *In vitro* experiments have shown that neurite outgrowth can be enhanced on scaffolds that have been coupled with laminin [96, 117-119]. In addition, short bioactive oligopeptides sequences of laminin (e.g. IKVAV and YIGSR) that can be recognized by specific receptors have been shown to improve neurite outgrowth [120, 121]. Fibronectin has been reported to affect the motility of Schwann cells. Fibronectin has been shown to influence axonal elongation, Schwann cell attachment and proliferation [122]. In addition, fibronectin-containing matrices were formed in the lumen of synthetic conduits used to bridge the nerve gaps [66]. Experiments demonstrated the effectiveness of fibronectin mesh as a delivery vector of chemotactic cues to promote nerve regeneration [123, 124], while providing support as a basal lamina scaffold.

2.3.3.4 Neurotrophic proteins

In normal nerve state, cellular and molecular activities are dependent on the influence of neurotrophic factors secreted by the peripheral target cells. Neurotrophic factors mediate chemotaxis processes that are required for successful re-establishment of functional synaptic connections. Actions of neurotrophic factors are influenced by the neurotrophic receptors such that the binding of each individual neurotrophin with their specific receptor(s) will initiate a cascade of reactions. During nerve regeneration, axons can respond to specific neurotrophic proteins and grow back

preferentially towards the original target organs to form functional synaptic innervations. Researchers have applied exogenous neurotrophic factors at the injury sites to promote better nerve regeneration and functional recovery [125, 126]. Biodegradable polymers are usually used to produce the delivery vectors to provide sustained release of bioactive neurotrophic proteins. Since neurotrophins usually have short plasma half-life, considerations have to be taken when encapsulating growth factors into the design of the nerve conduit. Encapsulation of proteins for drug release surrounds several concerns that include maximizing therapeutic activity, maintaining the protein stability, and minimizing toxic side effects [20]. Table 2.12 shows the various neurotrophic growth factors that have been studied for their potential use in peripheral nerve repair.

Table 2.12. Neurotrophic factors for peripheral nerve regeneration.

Growth factor	Abbreviation	Major Target	Delivery Vector(s)	References
Nerve growth factor	NGF	Sensory neurons, small axons	Microspheres, hydrogel, nanofibers	[126-128]
Neurotrophin-3	NT-3	Sensory neurons, small and medium size axons	Fibronectin scaffolds	[124]
Brain-derived neurotrophic	BDNF	Sensory neurons, large axons	Collagen gel	[129]

factor				
Glial-derived neurotrophic factor	GDNF	Motor neurons	Synthetic polymeric nanofiber conduit	[130]
Fibroblast growth factor 2	FGF-2	Vascular endothelial cells	Synthetic polymer conduit	[131]
Ciliary neurotrophic factor	CNTF	Schwann cells (injury factor)	Protein solution	[125]
Vascular endothelial growth factor	VEGF	Vascular endothelia cells	Protein solution	[132]
Insulin-like growth factor I	IGF-I	Inflammatory cells (anti-inflammatory)	Covalently bound to conduit	[133]
Glial growth factor	GGF	Schwann cells	Alginate hydrogel	[134]

NGF, the first identified neurotrophic factor, is essential for the survival and maintenance sensory and sympathetic neurons [135]. It binds to the p75 neurotrophin receptor and the trk-A receptor. Another growth factor that is closely related to NGF is the brain-derived growth factor (BDNF). BDNF is expressed by skeletal muscle that primarily binds to the trk-B receptor and is important for the regulation of

neuromuscular synapse development [136, 137]. Evidence obtained from *in vitro* experiment has shown that BDNF is an important biomolecule for the survival and differentiation of motor neurons and could assist to prevent neuron death after nerve injury [136]. *In vitro* and *in vivo* studies have shown that neurotrophins-3 (NT-3) and -4 (NT-4) and ciliary neurotrophic factor (CNTF) bind to the trk receptors and the glycosyl-phosphatidylinostiol-linked CNTF receptor, respectively, that are required for the survival of certain motor neurons [137, 138] as well. Glial cell line-derived neurotrophic factor (GDNF) that binds to the tyrosine kinase receptor (RET) and the GDNF receptor-alpha is distantly related to transforming growth factor beta family [29] and has the ability to promote survival of both motor and sensory neurons [137].

Many studies have introduced neurotrophic factors in the peripheral nerve tissue engineering strategies to evaluate the extent of nerve regeneration. Release of neurotrophic factors such as nerve growth factor that were encapsulated in microspheres [139], matrices [140], scaffolds [128, 141, 142] or covalently bound to scaffolds [143] have demonstrated improved neurite outgrowth. The presence of exogenous nerve-related bioactive molecules such as NT-3 and BDNF has demonstrated enhanced nerve regeneration [2, 144]. Also, concentration gradients of NGF and NT-3 have been immobilized on hydrogel to promote neurite outgrowth [145, 146].

Usually, protein release profiles are characterized by a marked initial burst release that results in subsequent low amount of neurotrophic factors delivered to the injury

sites [147]. Efforts are made to minimize this problem to achieve controllable and continuous delivery of proteins using different biodegradable polymers or vectors such as microspheres or hydrogel. Increasing interests to use nano-scale delivery vectors such as nanoparticles, nanotubes, and nanofibers to provide improved sustained release of drug are underway [20]. Among those, the nanofibers are promising as a dual functional scaffold that not only provides controlled drug delivery but also supports cell and tissue growth as the nano-scale topography closely mimics the natural ECM.

2.3.3.5 Intra-luminal guidance channels and scaffolds

An important process in nerve regeneration to repair transected nerve involves the migration of Schwann cells into the synthetic nerve grafts from the proximal and distal nerve stumps [148], subsequently forming cellular bridges across the interstump gap that are termed bands of Büngner (Fig. 2.17). These physical structures play a significant function in nerve regeneration as they act as guiding cues and substrates for growth cone adherence and axon outgrowth towards the distal end. The longitudinally oriented cell matrix organize axon extension such that if regenerating axons accidentally leave the supporting matrix, axonal elongation usually terminates that can result in the formation of neuroma [149]. The molecular driving force for Schwann cells to form these cellular bridges are not known, but this could likely be due to the polarized expression of adhesion proteins along the proximal-distal axis of the Schwann cells [149].
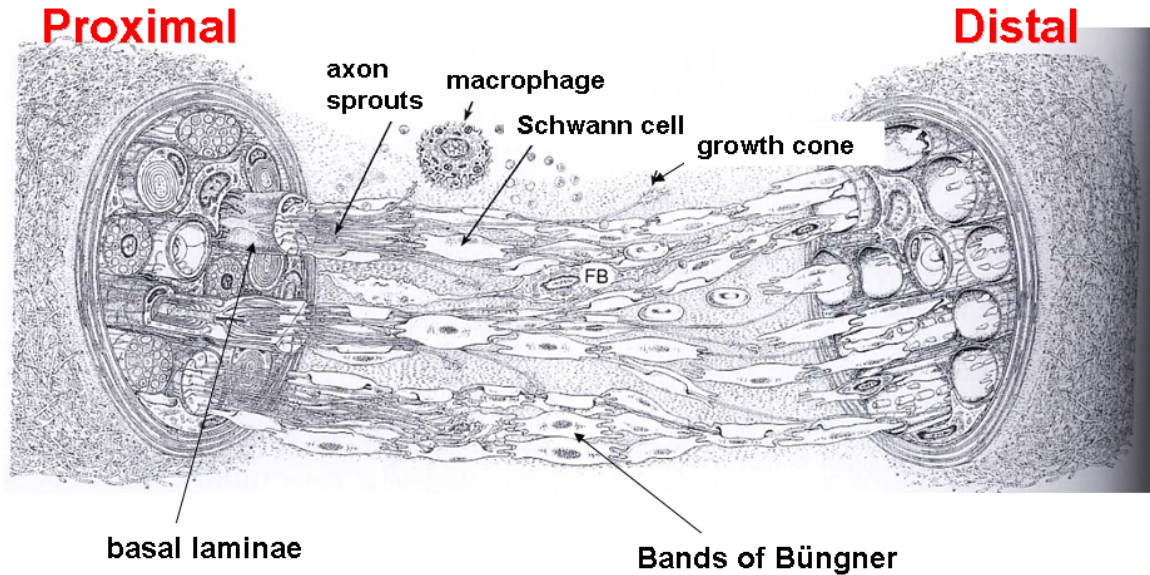
Figure 2.17. Formation of bands of Büngner by the Schwann cells during nerve regeneration [81].

Tubulation devices that utilize hollow conduits provide a physical substrate to guide sprouting axonal elongation towards the distal stumps, thus preventing aberrant outgrowth of axons and formation of scar tissue that impede nerve repair. In a hollow conduit, formation of fibrin matrix occurs that is subsequently infiltrated with Schwann cells and non-neuronal cells. Formation of physical cellular bridges (i.e. bands of Büngner) will be created by the proliferated Schwann cells that are shown to influence nerve regeneration and can act as scaffolds for advancing axons (Fig. 2.17). If the nerve gap deficits are too great, formation of fibrin matrix and bands of Büngner might be compromised, thus affecting nerve regeneration and functional recovery. Researchers have thus introduced physical scaffolds within the lumen of the conduits to potentially enhance axonal regeneration (Table 2.13).

Table 2.13. Fillings and scaffolds in the lumen of nerve conduit.

Fillings	Materials	Features	References
Denatured muscle scaffolds	allogenic and acellular	Presents longitudinally oriented basal lamina of muscle that also contains ECM molecules such as laminin and collagen type IV.	[150, 151]
Hydrogel	Natural occurring materials such as collagen, Matrigel, hyaluronic acid, etc.	Highly porous. Can be coupled with neurite-promoting biomolecules	[119]
Magnetically aligned fibrils hydrogel	Collagen	Fibers that mimic the natural ECM. Can be coupled with neurite-promoting biomolecules	[112]
Synthetic or natural-occurring polymeric filaments (intra-luminal guidance channels)	Collagen and synthetic polymer (e.g. PLLA, PGA)	Micro-sized fibers (5 μm – 150 μm). Can be coupled with neurite-promoting biomolecules.	[9, 113, 118, 152]

Incorporation of fillings in the conduits are aimed to create a permissive regenerative environment that can regulate appropriate axonal growth and promote excellent functional activities of the nonneuronal cells essential for nerve regeneration. The use of denatured muscles have been shown to effectively direct outgrowing axons as the presence of longitudinally oriented basal lamina of the muscle tissue that contains biochemical molecules [150] was considered as beneficial. Longitudinally aligned guidance scaffolds have been described to provide excellent guiding function for regenerating axons. A study has shown that aligned collagen fibrils in collagen conduits enhance the regeneration in the mice's sciatic nerves compared to conduits containing unaligned collagen gel [111]. Micro-grooved polymer filaments inside nerve conduits allowed nerve regeneration to occur with highly oriented axon growth without meandering [149]. Incorporation of intra-luminal guidance channels can thus potentially improve nerve regeneration [2, 9, 118, 152, 153] to repair large nerve defect injuries since they can mimic the bands of Büngner. For a 18 mm and 30 mm nerve lesion gap, Cai *et al*. [152] and Yoshii *et al*. [113] have reported that conduits containing physical filaments could enhance axonal regeneration in the animal studies. This thus assists to recreate an environment that resembles more like the native nerve tissue organization architecture.

2.3.4   Electrospun nano-scale scaffolds for peripheral nerve regeneration

Current interests for using electrospun nanofibers in tissue engineering strategy can be attributed to the nano- and micro- hierarchical architecture of the scaffolds easily

fabricated by electrospinning [154]. Scaffolds possessing nano-texture surface had been previously shown to allow adhesion and proliferation of neural stem cells [155].

Poly(L-lactide-co-glycolide) (PLGA) biodegradable polymer conduit made up of random nanofibers has been fabricated and this conduit demonstrated nerve regeneration after one-month implantation as evidenced by neurofilament immuno-staining and histomorphometrical analyses (Figs. 2.18 and 2.19). *In vitro* study also showed that neural cells were able to extend their neurites well on synthetic poly(L-lactide) (PLLA) nanofibers (Fig. 2.20) [12].
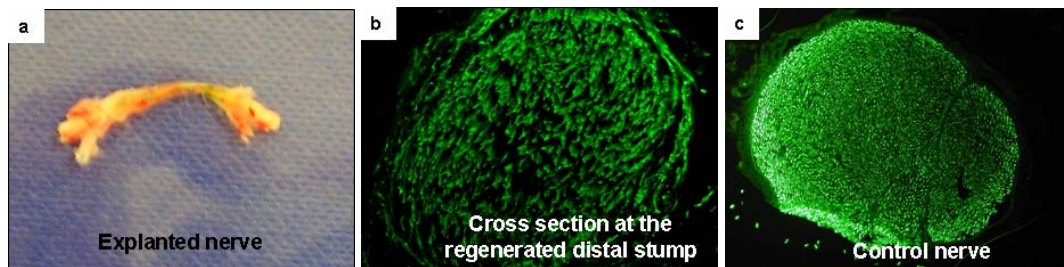
Figure 2.18. Immunostaining for the neurofilament protein (NF68) confirmed axonal distribution of the regenerated nerves in the nanofiber conduits. (a) Explanted nerve regenerated nerve cable after a month of implantation, (b) Cross-sectional view of the conduit regenerated distal stump, and (c) Cross-sectional view of the control rat sciatic nerve [40].
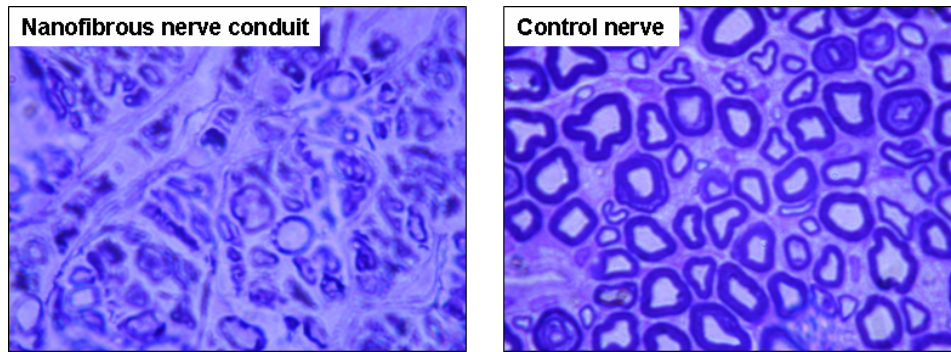
Figure 2.19. Histology analysis of the varying degrees of myelinated axons in regenerated rat sciatic nerves in the nanofiber conduit [40].

Fiber orientation plays a significant role in the influence of morphology and cytoskeleton of many cell types. Aligned PLLA nanofibers were able to promote longest neurite extension when compared to the random PLLA nanofibers. It has been reported that more than 80% of cells have been induced to elongate neurite parallel to the fiber axis of the aligned nanofibrous scaffolds through the contact guidance effect [12]. In the same study, differentiation rate of the neural cells was observed to be better on nanofibrous scaffolds compared to that of the microfibrous scaffolds [12]. Aligned fibers were shown to guide oriented neurite outgrowth and glial migration from dorsal root ganglia [43].
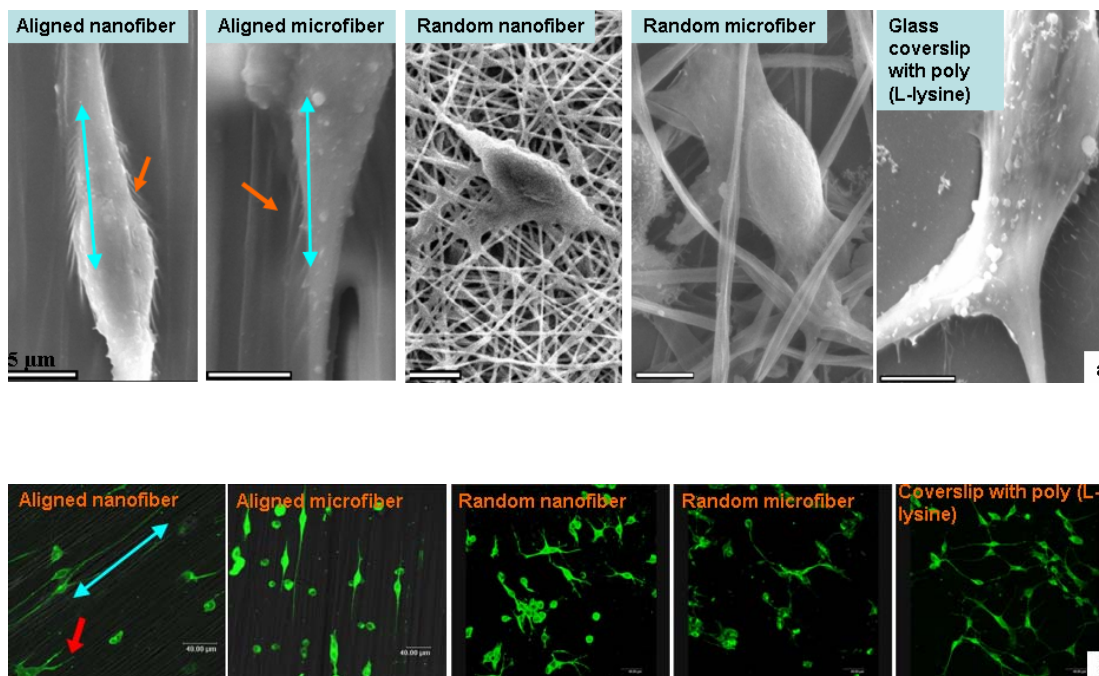
Figure 2.20. (a) Phase contrast micrographs and (b) Confocal laser scanning micrographs (antibody staining of neurofilament 200 kDa) of neural cells interactions with nanofibers on day 2 after cell seeding. The fiber alignment may have effects on mediating the interaction between the neural cells and the scaffolds. The preferred growing direction of the neural cells is parallel to the fiber axis and the process is dynamically directed over time [12].

In addition, fiber arrangement (i.e. aligned vs. random) may have mediation effects on the interaction of the nerve supporting cells with the scaffolds. It has been reported that when dorsal root ganglia were cultured on random nanofibers, neurite outgrowth were modest and Schwann cell migration (Fig. 2.21) were not as directed. However when ganglia were cultured on aligned nanofibers, axons were directed to extend

along the axis of the fibers. In addition, Schwann cell migrations were prominent along the axis of the nanofibers orientation indicating that the aligned nanofibers acted as physical substrates to direct movement and subsequently affect Schwann cell maturation.
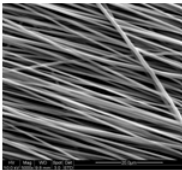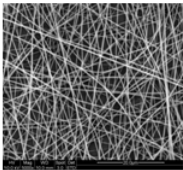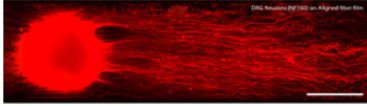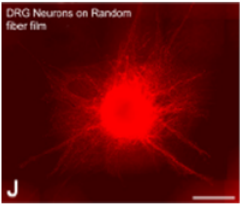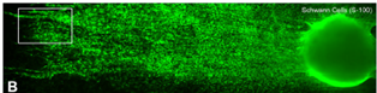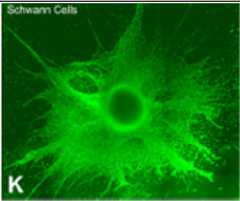
Fibers	Aligned	Randomly Oriented
Arrangement		
Neurofilament Staining of Dorsal Root Ganglia (DRG)		
Schwann Cell Protein, S-100, Staining of DRG		

Figure 2.21. Comparison of aligned and randomly oriented nanofibers on cell morphology [156].

In another study, enhanced Schwann cell orientation and maturation was observed when cultured on aligned nanofibers (Fig. 2.22) [44].

Schwann Cell Culture	Aligned	Randomly Oriented
Day 3		
Day 7		
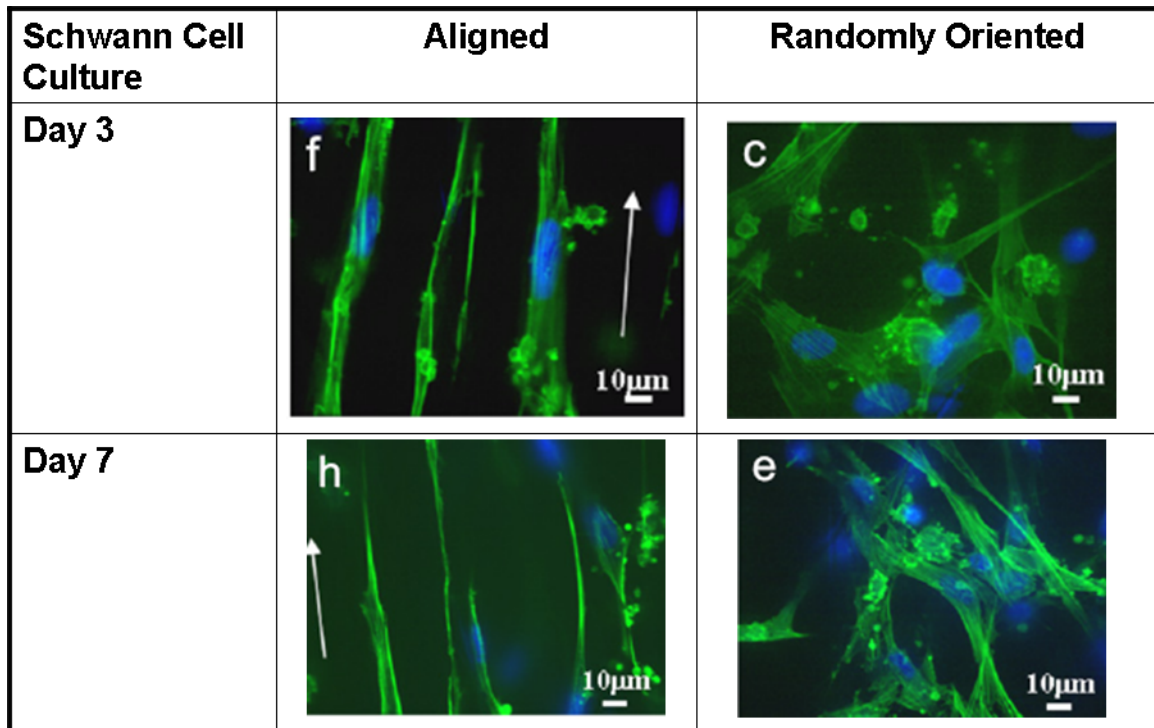
Figure 2.22. Schwann cell cultured on aligned and randomly oriented nanofibers [44].

2.3.5   Summary

In an effort to regenerate peripheral nerve to bridge nerve gap of clinically relevant critical lengths, several major advances have been made in the recent years in the field of peripheral nerve engineering. Despite these improvements in the field, there remains no adequate substitute for autologous nerve grafts, the present gold standard for bridging peripheral nerve gap injuries. Current research focuses mainly on the creation and development of an ideal nerve construct that will most probably encompass several strategies such as the use of different biodegradable materials, cellular components, ECM molecules, neurotrophins, and lumen fillings, which have been described in this chapter. In the present study, a biomimetic nanofibrous nerve

Chapter 2

construct will be designed and discussed on its effectiveness to repair nerve injury and potentially replace the use of autologous nerve grafts. An acellular approach is to fabricate the nanofibrous nerve construct consisting of intra-luminal guidance channels that is coupled with ECM protein (laminin or collagen) and neurotrophic factor (NGF). The strategy aims to provide an advanced nerve repair implant device to bridge up nerve gap that will bring about better clinical outcomes.

Chapter 3

Fabrication of PLLA nanofiber membrane and nanofiber nerve conduit

3.1   Introduction

Enhancing cell interactions with bioengineered biomaterial is crucial for successful applications of scaffolds for repairing and regenerating damaged tissue. The scaffolds can be designed to mimic complex biological structures, and/or provide the mechanical support to allow the cells of the damaged tissue to remodel and repair to form distinct three-dimensional tissue structures that resembles the original tissue [19, 20]. In recent years, electrospinning has been extensively used to construct bioengineered scaffolds because it is a simple fabrication process that can easily produce nano- and micro- size synthetic polymeric fibers. Synthetic polymeric nanofibers such as PCL [31], PLLA [12], PGA [32] and PLGA [33], and natural-occurring polymeric nanofibers such as collagen [34] and gelatin [35] have been electrospun for studies in bone [31], vascular [59], nerve [12, 157], and other bioengineered grafts.

PLLA, an FDA approved biomaterial, is a widely-used for scaffold fabrication because it is biodegradable and generally shows good biocompatibility. In one study, PLLA has been shown to maintain its structural shape and size that display minimum swelling or shrinking issue when immersed in PBS up to 42 days, and presented

sound fibrous architecture throughout the 28-day cell culture period [32]. In neural tissue engineering, PLLA possesses sufficient mechanical integrity to be used as the scaffold material for nerve scaffolds [12, 43, 158] or guidance channels fabrication [86]. Porous PLLA conduits [84, 85] and PLLA filaments [9, 118] were evaluated in rat sciatic nerve model that yielded some promising results for applications in peripheral nerve repair. Recently, nano-textured PLLA scaffolds made up of nano-fibrils have been shown to allow adhesion and proliferation of neural cells [12, 43, 158].

Additionally, upon seeding onto polymeric biomaterial, cell attachment to polymer is the first cellular event to occur. After the cells are securely adhered, other events such as cell migration, proliferation and differentiation will then subsequently take place [32]. Therefore, optimal cell adhesion is critical for favorable cellular response. Li *et al.* described that PLLA nanofibers were found to perform better than PCL, PGA and PLGA nanofibers, in terms of supporting cell-matrix interaction and cellular proliferation in certain cell types [32]. A preliminary study was performed in this project to evaluate the various electrospun nanofibrous scaffolds that were fabricated from the biodegradable polymers for nerve cell culturing. Neural cell viability assay showed that PLLA provided better substrates for nerve cell growth that have been compared with PLLA, PLGA, P(DL)LA, PGA, PCL and PCL-LA (Appendix A).

3.2   Materials and Methods

All chemicals were obtained from Sigma-Aldrich (St Louis, MO) and were used as received, unless otherwise stated. PLLA was bought from Polysciences, Inc. (Warrington, PA) at molecular weight of 100 kDa. All the parameters of electrospinning process had been optimized.

3.2.1   Fabrication of random and aligned PLLA nanofibers

Random and aligned PLLA nanofibrous membranes were fabricated by electrospinning as shown in Figure 3.1a and 3.1b, respectively. PLLA solution was prepared by dissolving PLLA in 1,1,1,3,3,3-hexafluoro-2-propanol (HFP) at a concentration of 10% w/v. The polymer solution was fed using a 27-G spinneret at a rate of 0.5 mL/h using a syringe pump (KDS100, KD Scientific Inc., USA). The distance between the spinneret tip and the collector was set at 12 cm. Electrospinning voltages were applied using a high-voltage power supply (AU-301P1Matsusada Precision Inc., Japan) at 10 and 21 kV for random and aligned PLLA nanofibers, respectively. Aligned nanofibers were electrospun at disk rotation speed of 1000 rpm, corresponding to take-up velocity of 630 m/min. All the experiments were performed in a humidity of less than 65% and a temperature of 24-26 ^{o}C.
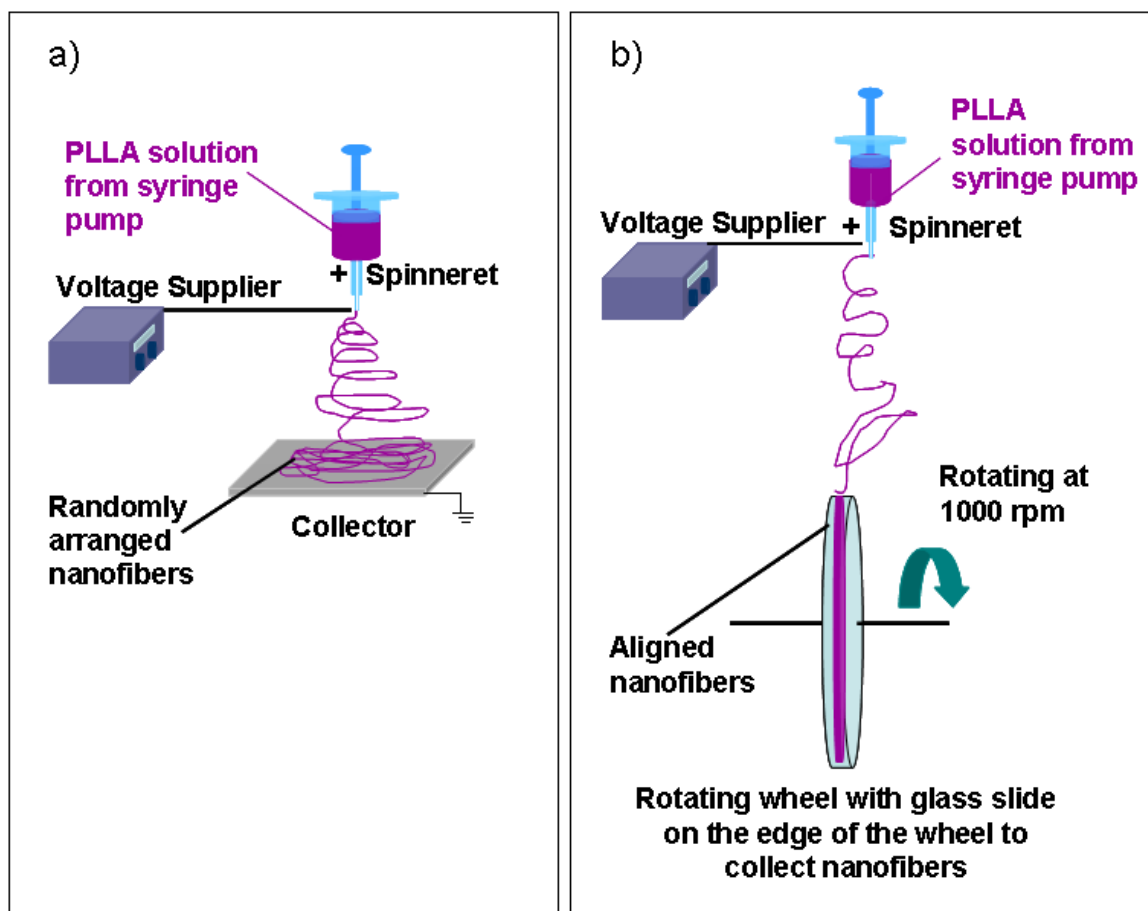
Figure 3.1. Electrospinning of nanofibers. (a) random nanofibers membrane, and (b) aligned nanofibers membrane.

3.2.2   Fabrication of PLLA nanofibrous nerve conduit

Nanofibrous nerve conduit was made up of two layers of nanofiber membranes as shown in Fig. 3.2. Aligned PLLA nanofibers membrane was produced by using the electrospinning set up shown in Fig. 3.3a. PLLA solution at 10% w/v was pumped at a rate of 1 mL/h to the spinneret that was set at 10 cm from the rotating drum collector. The rotating drum collector (diameter = 6 cm) was set at 3000 rpm and the electrospinning voltage was at 10 kV (high-voltage power supply, AU-301P1Matsusada Precision Inc., Japan). Aligned nanofiber membrane was removed

from the collector and wrapped around a 1.5 mm diameter metallic rod (for nerve repair in a rat sciatic nerve injury model). Subsequently, PLLA solution at 10% w/v was pumped at a rate of 1 mL/h to the spinneret that was set at 10 cm from the rotating mandrel (Fig. 3.3b) to produce randomly arranged nanofibers that enclosed the aligned nanofibers membrane that had been wrapped around the metallic rod. Randomly oriented nanofibers were electrospun and collected on the rod attached onto a rotating mandrel (revolving at approximately 100 rpm). Finally the fabricated bilayered nanofibrous conduit was removed from the rod. All the experiments were performed in a humidity of less than 60% and a temperature of 24-27 ^{o}C.
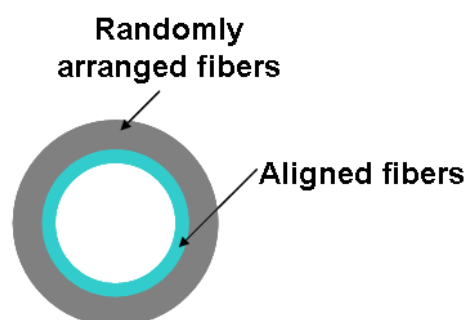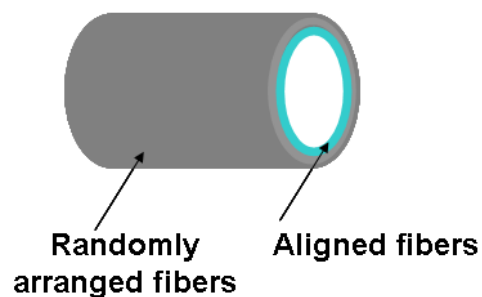
Figure. 3.2. Schematic of bilayered nanofibrous conduit.
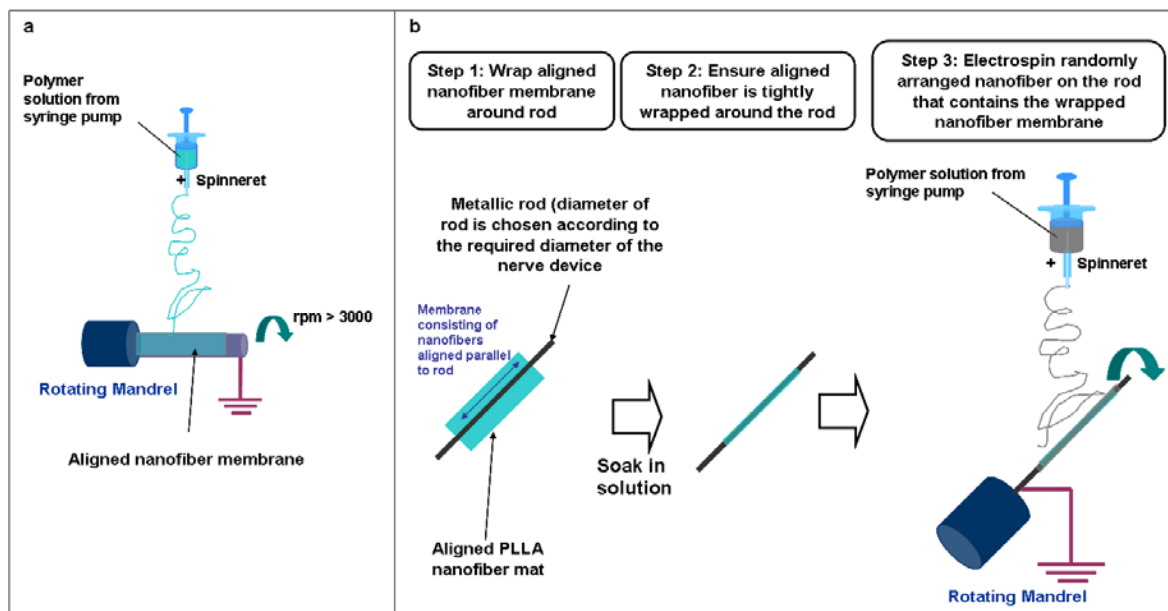
Figure. 3.3. Fabrication technique of bilayered nerve conduit (a) aligned nanofiber membrane, and (b) randomly oriented nanofiber membrane.

3.2.3 Characterization of PLLA nanofibers

Atomic force microscopy (Dimension 2100; Digital Instruments Nanoscope, USA) in "dynamic force mode" was used to examine the topography of the nanofibrous substrate. Silicon nanoprobe tips (Nanosensors, Switzerland) with resonant frequencies near 270 kHz were used.

Transmission electron microscopy (TEM) (JEM-2010F FasTEM, JEOL) was used to study the electrospun nanofibers. Nanofibers for TEM samples were prepared by direct depositing of the as-spun nanofibers on copper grids (Structural Probe, SPI Supplies Division, West Chester, PA) and observations were made a voltage of 100 kV.

Morphology of electrospun nanofibers was studied using a scanning electron microscopy (SEM) (JSM-5800LV, JEOL, Tokyo Japan). The nanofibers were sputter-coated with gold up to 90 s in a JEOL JFC-1200 fine coated and an accelerating voltage of 10 kV of the SEM was used to examine the morphology of the electrospun scaffolds. Range of nanofiber diameters were determined based on SEM micrographs with the use of image analysis software (ImageJ; National Institutes of Health, Bethesda, MD).

3.2.4 *In vitro* degradation of PLLA nanofibers with cultured cells

Degradation study of PLLA nanofibers was conducted for 4 months. Randomly arranged nanofiber membranes were cut and glued (Implant-grade silicone adhesive, Silbione, MED ADH 4300 RTV, Rhodia, France) onto glass slides. Samples were sterilized overnight in 70% ethanol and rinsed with PBS prior to cell seeding. Rat pheochromocytoma cell line, PC12 cells, was obtained from American Type Culture Collection (ATCC). Undifferentiated PC12 cells were seeded at a density of 10,000 cells/cm^2 and cultured for the predetermined time-points. At every fortnight, samples were trypsinized at 37 $^{\circ}$C and washed thoroughly to remove the cells from the nanofibers. Nanofibers were dried at room temperature and kept in vacuum for subsequent mechanical tensile test. Standard tensile test for fabric materials were performed with a micromechanical tester (Instron 5848 microtester, USA) at a stroke rate of 5 mm/min on 10 mm x 20 mm electrospun nanofiber sheet. The thickness of

the nanofiber sheet was determined by a micrometer (Mitutoyo, Japan). SEM was used to observe the morphologies of the degraded fibers.

3.2.5 Characterization of PLLA conduits

SEM was used to examine the morphology of PLLA nanofibrous conduit. The nanofiber conduits were placed in PBS pH 7.4 at 37 °C. After a month, the conduits were removed from the solution and blotted dry with an absorbent Kimwipe tissue. Macroscopic images were then taken using a bright-field microscope and camera (Leica, Germany). Swelling test was also analyzed by measuring the changes of wall thickness and tube diameter of the conduit using a bright-field microscope and ImageJ (National Institutes of Health, Bethesda, MD). Shrinkage percentage was expressed as follows:

$$\% \text{ in shrinkage} = \left(1 - \frac{\text{wall thickness }(\mu\text{m}) \text{ after one month}}{\text{initial wall thickness }(\mu\text{m})}\right) \times 100\%$$

Apparent density and porosity of nanofiber membranes were calculated based on the following equations:

$$\text{Membrane apparent density (g/cm}^3) = \frac{\text{mass of membrane (g)}}{\text{membrane thickness (cm)} \times \text{membrane area (cm}^2)}$$

$$\text{Membrane porosity} = \left(1 - \frac{\text{membrane apparent density (g/cm}^3)}{\text{bulk density of PLLA (g/cm}^3)}\right) \times 100\%$$

where bulk density of PLLA = 1.2-1.3 g/cm^3

Structural pore properties was assessed using a capillary flow porometer (1200-AEHXL, Porous Media Inc., Ithaca, NY). Briefly, pore size distribution was determined by allowing a non-reacting gas to flow through the dry nanofiber membrane, and subsequently the flowing gas streamed through the same membrane that had been wetted by a liquid of known surface tension. The difference in flow rate is thus measured as a function of pressure for both dry and wet processes. The pore size was determined using the software provided by Porous Media Inc.

3.2.6 Statistical analysis

Mechanical tensile testing were performed using 5 samples. The results are averaged and expressed as mean ± standard deviation (SD). Variance analysis using an ANOVA Single Factor test, with 95% confidence was used for statistical analysis. A p-value of less than 0.05 was considered as statistically significant.

3.3   Results

3.3.1   Characterization of PLLA randomly arranged and aligned nanofiber membranes

3.3.1.1 Atomic force microscopy and transmission electron microscopy

PLLA nanofibers were successfully electrospun to form fibrous membranes. Figure 3.4 illustrates the various images of the nanofibers. The electrospun nanofiber had smooth morphological appearance.

a)   b)
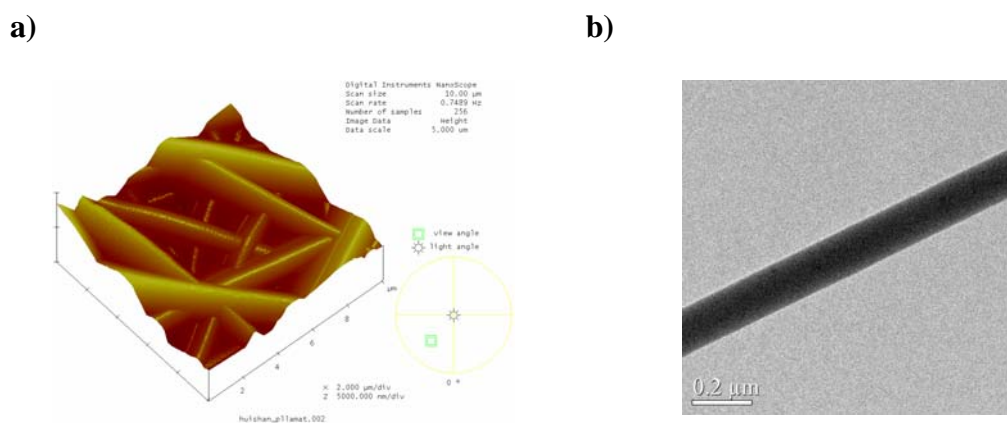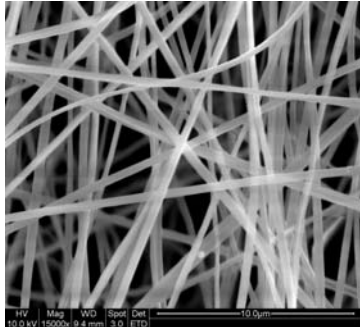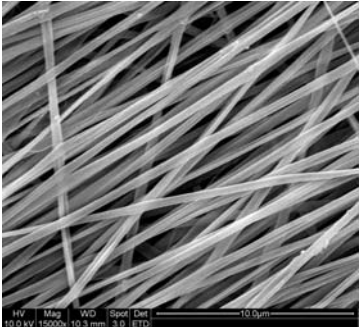
Figure 3.4. PLLA nanofibers (a) Atomic force micrograph, and (b) transmission electron micrograph.

3.3.1.2 Scanning electron microscopy

Electrospinning parameters were optimized to obtain morphologically smooth PLLA nanofibers. Diameter ranges of the nanofibers (Table 3.1) were determined by direct measurement of the nanofiber images from the scanning electron micrographs.

Table 3.1. SEM images of randomly oriented and aligned PLLA nanofiber membranes.

Nanofiber orientation	Random	Aligned
Scanning electron micrograph		
Nanofiber diameter (nm)	312 ± 67	265 ± 61

3.3.2 Mechanical and morphology of PLLA nanofibers after *in vitro* degradation

In vitro biodegradation was performed by culturing undifferentiated PC12 neuronal cells on PLLA randomly arranged nanofiber membranes for 4 months and mechanical tensile test was performed to evaluate the degree of degradation of the polymers. There was no significant decrease in ultimate tensile strength (Fig. 3.5a) and ultimate

tensile strain (Fig. 3.5b) of PLLA nanofibers cultured with PC12 cells. The variable

data obtained could be due to the tendency of PC12 cells to aggregate that might not

be uniformly distributed on the cultured membranes, thus leading to the observed

large standard deviations of the mechanical properties. However, there was a gradual

decrease in of the Young's Modulus (Fig. 3.5c) of the nanofibrous sheets. In general,

the degradation results showed that *in vitro* tests did not degrade the mechanical

properties of the nanofiber sheets to any statistically significantly extent. From this

degradation study, the mechanical properties of PLLA nanofibrous sheets were

maintained and the degradation rate was slow when cultured with cells.
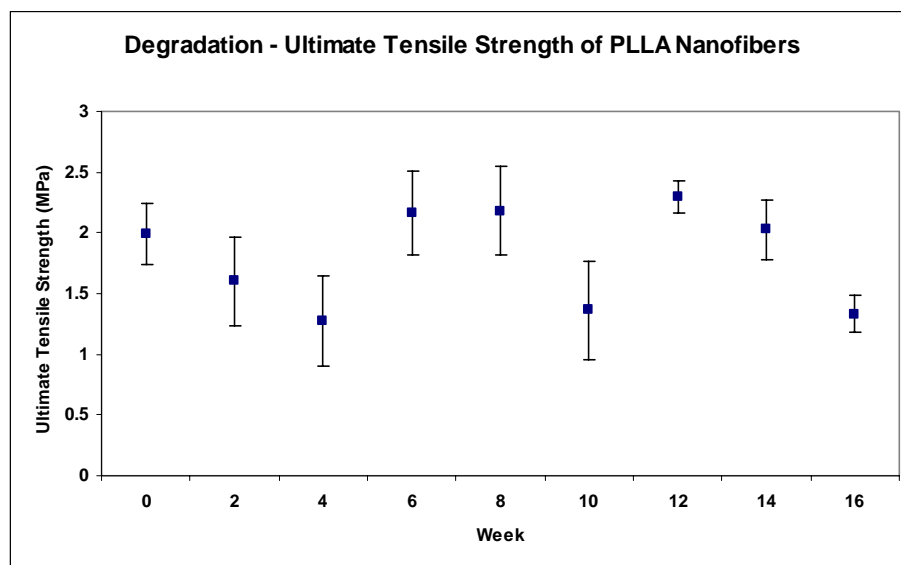
(a)
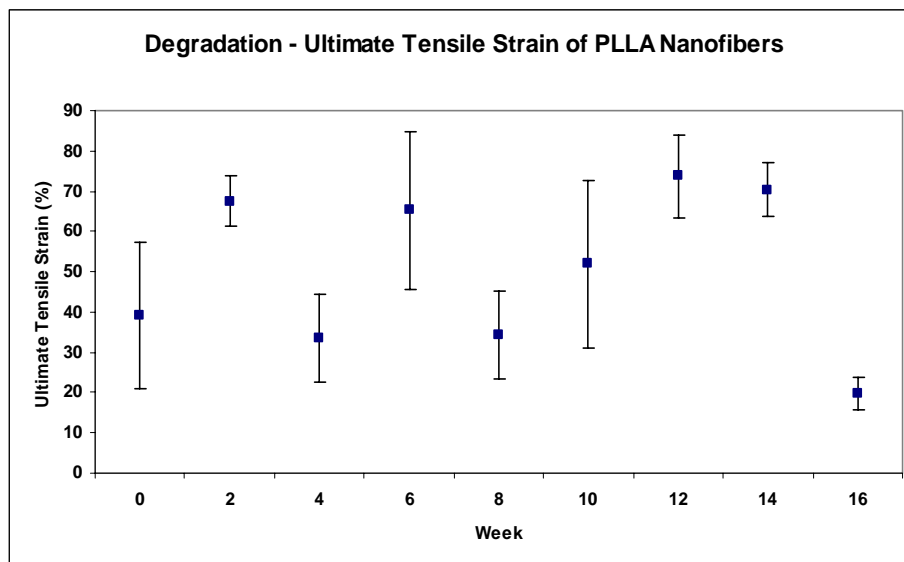
(b)
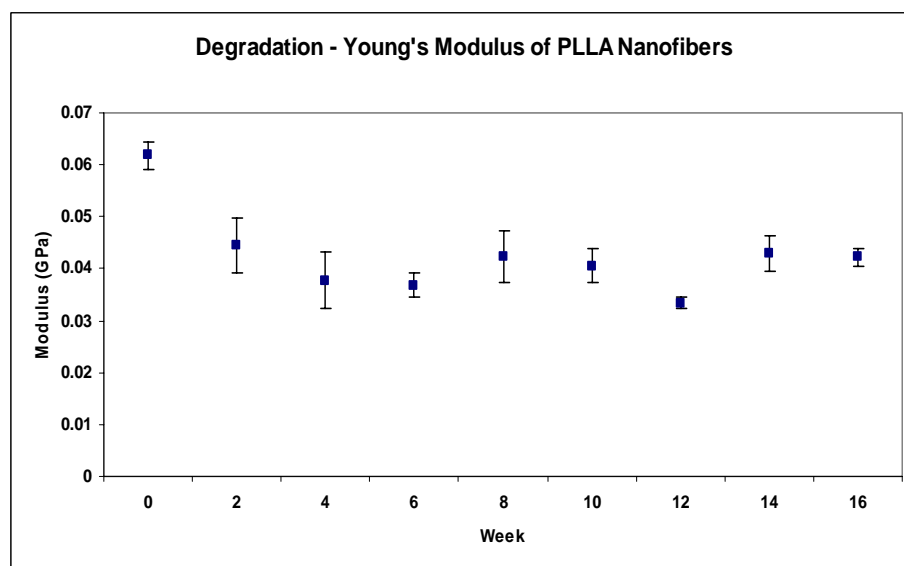
(c)

Figure 3.5. Mechanical tensile test of PLLA nanofibrous sheets cultured with PC12 cells (a) ultimate tensile strength, (b) ultimate tensile strain, and (c) Young's Modulus.

Figure 3.6 illustrates the scanning electron micrographs of PLLA nanofibers that were degraded for four months. The nanofibers maintained its morphology, without any signs of breakage of the nanofibers. In another *in vitro* study, PLLA nanofibers did not show significant changes in weight loss and crystallinity after 45 days of experiment [159].
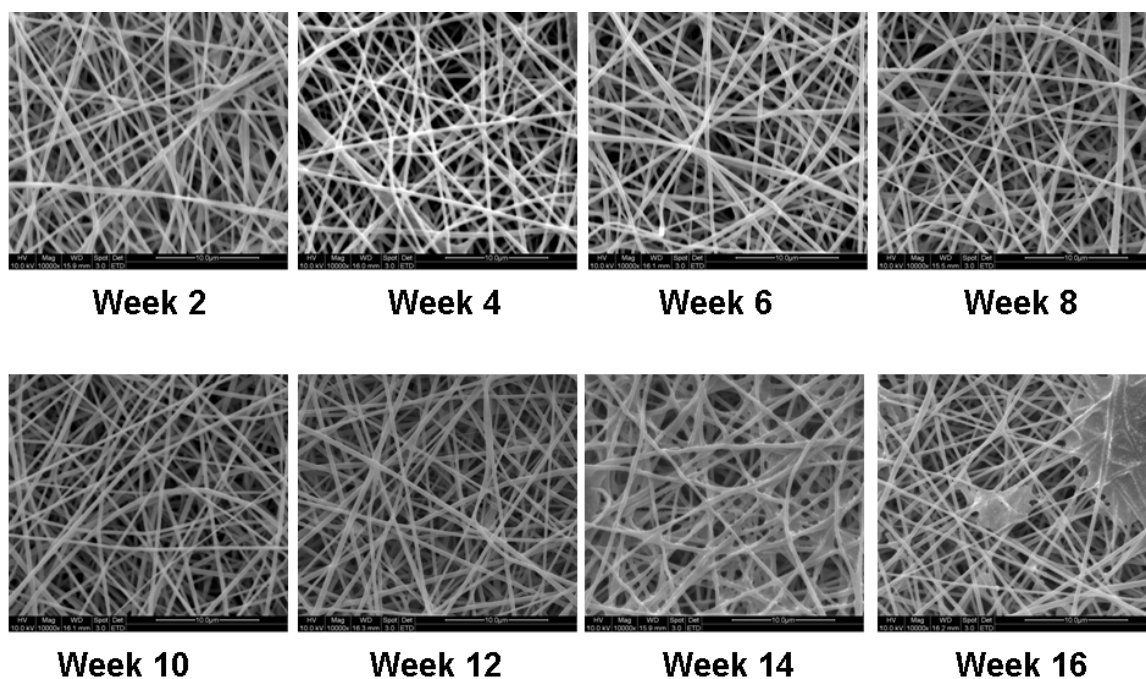
Figure 3.6. SEM images of degraded PLLA nanofibers over four months *in vitro*.

3.3.3   Characterization of bilayered nanofiber conduit

3.3.3.1 Scanning electron microscopy

Bilayered nanofibrous conduit was electrospun using the set-up shown in Figure 3.3. Figure 3.7 shows the scanning electron micrographs of the fabricated nerve conduit. The conduit was made up of two layers of electrospun membranes: inner membrane was made up of longitudinally aligned nanofibers to guide axonal extensions and

Schwann cells migration, while the outer membrane were formed by randomly oriented nanofibers to minimize collapse of conduit along the axis of the aligned fibers found in the inner layer. Electrospinning of nanofiber conduit using the described method provides the flexibility to obtain the conduit with various inner diameters (results not shown) for application in the repair of nerves with different dimensions. The conduit was fabricated to have an inner diameter of 1.5 mm measurement that can be used to repair rat sciatic nerve. If the conduit possessed too small or too large inner diameter, quality of nerve regeneration will be compromised [160].
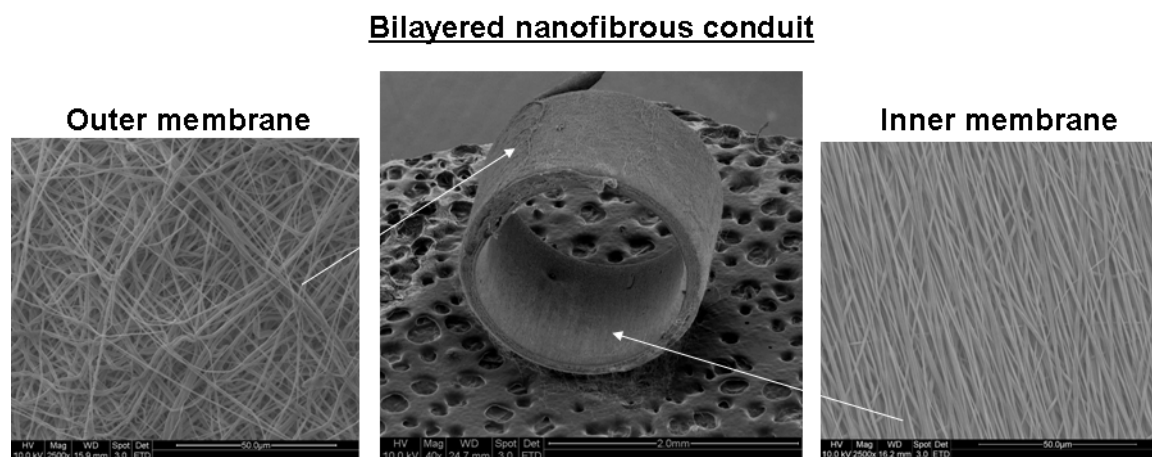
Figure 3.7. SEM images of bilayered nerve conduit. Inner and outer layers consisted of longitudinally aligned nanofibers and randomly arranged nanofibers, respectively.

3.3.3.2 Porosity and pore size of nanofiber conduit

Nanofibrous conduit consisted of fibers that were in a diameter range of 250-1000 nm. The pore size of conduit was 1.19 ± 0.50 μm, and Table 3.2 describes the

thickness and porosity of the nerve conduit. Since the nerve conduit will be implanted

into the rat sciatic nerve, a 1.5 mm diameter nerve conduit was fabricated as shown in

Figure 3.8.

Table 3.2. Description of nanofiber conduit.

Nanofiber membrane (orientation)	Inner (Aligned)	Outer (Random)
Thickness of membrane (μm)	53 ± 4	102 ± 11
Apparent density (g/cm^3)	0.24 ± 0.02	0.23 ± 0.01
Porosity (%)	81.0 ± 1.2	82.0 ± 0.7
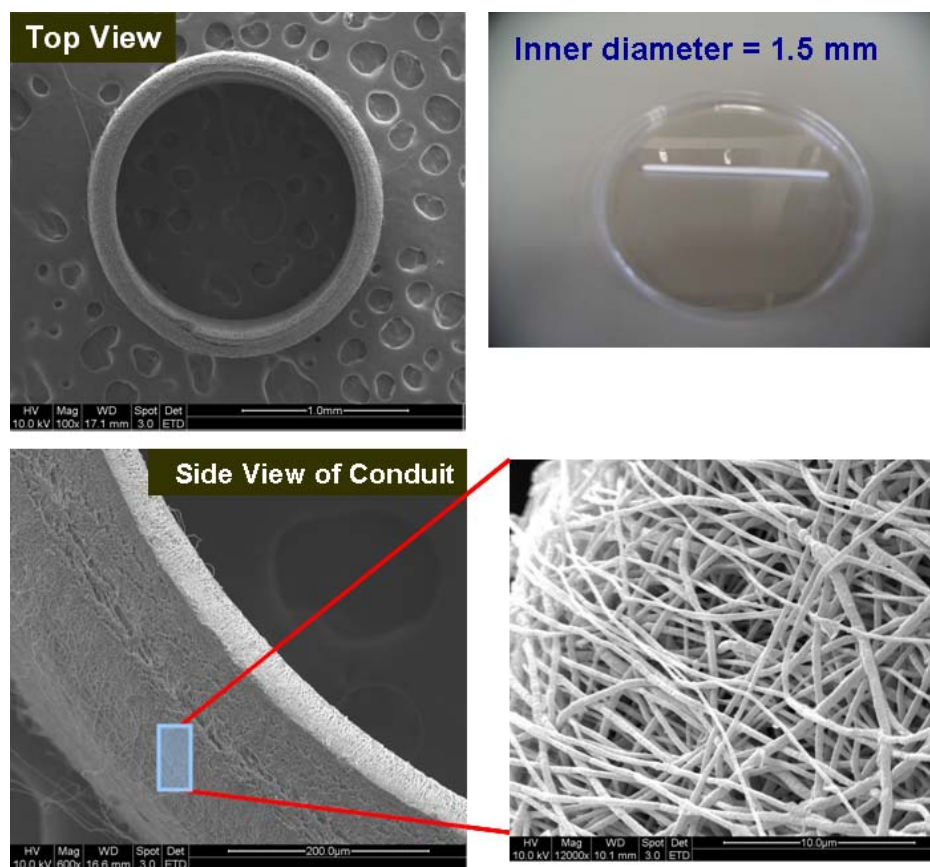
Figure 3.8. Illustrations of electrospun PLLA nerve conduit for nerve repair.

3.3.3.3 Swelling property of PLLA nanofiber conduit

Swelling or shrinking of polymer nerve conduit in physiological fluid may pose problems in nerve repair because they may compress the regenerating axons [160]. The shrinkage percentage of the conduit wall was 6 ± 2 %. PLLA nanofibrous conduit did not show significant swelling or shrinking after immersion in PBS for one month.

3.4   Discussion

In tissue engineering and regenerative medicine of damaged tissue, it is desired that the cells will reorganize into structures that resemble the original tissue for spontaneous repair. A defined environment can influence adhesion, proliferation, migration and differentiation of cells surrounding or involved in the repair of the damaged tissue [19]. Nanotopographic patterns have been shown to influence cell shape, gene expression, neurite outgrowth, and cell migration in a positive manner [158]. The mechanisms of the effects of nano- and micro-topographies on neural cells adhesion and differentiation had not been extensively reported. However, as nerve cells and their axons live in native ECM consisting of hierarchical organization of nano-scaled fibers and intermolecular binding interactions, scaffolds with nano-topography could have positive effects on the morphological and functional development of neural cells and nerve supporting cells. Also, synthetic polymers interact with the cellular components through the serum and/or ECM proteins that have been adsorbed on the polymer surface. Comparing to micro-scale scaffolds,

electrospun nanofibrous scaffolds have higher surface to volume ratio that allowed adsorption of more biomolecules for cell adhesion [32] that would be suitably used as bioengineered substrates. In addition, polymeric nanofibers are usually strong in mechanical properties, so the scaffold can have good tensile strength and excellent flexibility. Electrospinning was successfully used to fabricate PLLA nanofibers for nerve regeneration applications [12, 43, 158].

In vitro study showed that aligned nanofibers provided superior contact guidance such that the ganglia neurites extended along the nanofibers upon contact and the neurites never left the nanofibers to grow on the cover-slip substrates that was not covered with nanofibers [43]. It was hypothesized that axons preferred to grow along the path of minimal principal curvature due to their inherent stiffness of the cytoskeletal structure that rendered better neurite extensions on aligned fibers [152]. *In vitro* culture of Schwann cells on aligned fibers showed cell cytoskeleton and nuclei aligning along the fibers with narrow morphology that resembled the bands of Büngner [43, 44]. Therefore, the incorporation of aligned nanofibers in nerve conduit design would potentially benefit the outcome of nerve repair of transection injury.

Bilayered nanofibrous conduit made up of two layers of nanofibers membranes: (1) hierarchically placed in the inside were longitudinally aligned nanofibers that aimed to provide contact guidance for regenerating axon and proliferating Schwann cells, and (2) hierarchically located on the outside were randomly oriented nanofibers to provide mechanical strength, enable the transport of diffusible biochemical molecules

has been fabricated by electrospinning and prevent scar tissue formation. Several studies reported enhanced *in vivo* nerve regeneration using aligned nanofibrous conduits. However, it has been postulated that nanofibrous conduit that was made up of only aligned nanofibers might collapse easily along the axis of the aligned fibers. Hence, a bilayered nanofibrous conduits made up of aligned and randomly arranged nanofibers that could potentially improve the mechanical integrity of the nanofibrous nerve conduit was successfully fabricated.

Biodegradation of biological scaffold to repair damaged tissue is generally necessary because long term presence of the non-degradable scaffold will cause chronic foreign body reaction. Depending on the type of tissue to be repaired, different degradation rate of the scaffold to support the repair and regeneration process will be required. The rate of synthetic polymer degradation depends on several factors such as crystallinity, molecular weight, and morphological structures. PLLA was chosen as the nerve conduit material because it has a relatively slow degradation rate that will not rapidly present acidic byproducts at the site of nerve repair. The collapse of conduit would also occur if the conduit degraded too fast and lost its mechanical integrity, hence a slower degrading polymer was used to fabricate nanofibrous nerve scaffold. Additionally, PLLA has been shown to support good neurite outgrowth in PC12 cell culture studies (Appendix A).

The nanofiber conduit fabricated in this study possessed sufficient wall thickness to maintain the mechanical integrity and provide conduit flexibility to allow movement

of joints and associated motion as well. It was designed to provide tension-free repair site, and guide nerve regeneration across the nerve gap to prevent axonal escape at the repair site. Thin walled conduit was described to be beneficial for nerve repair strategy because less neuroma formation has been observed when nerve was bridged as compared to thicker walled conduit. Furthermore, less amount of the biomaterial used for a thin walled conduit will minimize the amount of degradation byproducts over time.

The pore size of the nerve conduit was in the micro-scale region (1-10 μm) that was described to be beneficial for nerve regeneration. Vleggeert-Lankamp *et al.* [161] reported that the small pores were effective for nerve regeneration. Scaffolds that possess a thickness (e.g. wall thickness of a tube or membrane thickness) of 100-200 μm were described to provide sufficient diffusion [162] for nerve repair. Hence nanofibrous conduit described herein possessed appropriate wall thickness (approximately 150 μm) for efficient diffusion of nutrient exchange and waste transport. In addition, the availability of endogenous neurotrophic factors and nutrient exchange in conduits with a porosity ranging from semi-permeable to macroporous were shown to influence nerve regeneration [141].

Electrospinning has been shown to lower the glass transition temperature of synthetic polymer that could retard the crystallization behaviour of polymers especially in semicrystalline polymers. This in turn will cause a large shrinkage in polymer scaffolds that can be undesirable in several medical applications. It has also been

shown that electrospun PLLA conduit retained its wall thickness and internal diameter after incubation in PBS for a month well that will not negatively affect nerve repair after implantation in the body. Shrinking (or swelling) of nerve conduit can have negative effect on the speed and quality of nerve repair as the conduit will compress and exert pressure on the regenerating axons. Negligible shrinkage in electrospun PLLA nanofibers scaffold has been observed due to the significant increase in crystallinity of the polymer.

A latency period of three weeks is usually observed in nerve regeneration of transected nerve injury in humans. The nerve will subsequently regenerate at a rate of 1 mm/day. Maturation of nerves will occur thereafter while the conduit should stay intact to support the nerve regeneration process. Therefore, the nanofiber conduit was designed to prevent scar formation and provide the mechanical and physical support for regenerating nerves across the interstump gap.

3.5   Conclusion

In this chapter, PLLA nanofibrous membranes and bilayered nanofibrous nerve conduit were successfully fabricated using electrospinning. The nanofibrous membrane had smooth nanofiber morphology and maintained its mechanical properties after 16 weeks of *in vitro* degradation evaluation under cell culture conditions.

Chapter 4

Modification of PLLA nanofibers with extracellular matrix molecules

4.1   Introduction

During development of the PNS, haptotactic factors are known to influence and stimulate axon guidance and neurite extension. In this chapter, collagen and laminin will be studied as the contact guidance biochemical cues for axonal outgrowth.

Collagen is one of the most commonly used natural materials tested for its use in scaffolds design. Peripheral nerve ECM comprises mainly of collagen that acts as structural protein. Additionally, collagen has specific amino acid motifs can bind to cell-surface receptors that can aid in nerve regeneration process. Nanofibers had been modified with collagen using coating technique [59] or blending collagen in polymer solution for electrospinning [42] to enhance cell attachment and viability. These studies showed that nanofibers can be easily modified with ECM bioactive proteins to enhance interactions of the scaffolds with cultured cells.

Laminin is one of the ECM component that is continuously synthesized after nerve injury [68] and it plays a crucial role in cell migration, differentiation and axonal growth [114-116]. For example, myelination in the PNS is affected by laminin.

Studies have described that even as Schwann cells could proliferate and migrate along axons, differentiation of myelinating phenotype was not observed without the presence of laminin [163, 164]. Furthermore, *in vitro* experiments have shown that neurite outgrowth is enhanced on scaffolds that were covalently bound with laminin [117]. Physical adsorption of laminin onto substrates with microgrooves [96] or microfilaments that acted as intra-luminal support matrices [118] have also been evaluated. These studies showed that *in vitro* directional guidance of the neurite outgrowth was achieved and enhanced using scaffolds that were physically adsorbed with laminin. Improved axonal outgrowth has also been observed in nerve guides filled with laminin gel as well [119]. Therefore, the incorporation of laminin onto nanofibers can potentially improve the rate of nerve regeneration.

In Chapter 3, PLLA was used to fabricate nanofibrous membranes and conduits. Although PLLA is generally biocompatible, PLLA does not have biological recognition sites that can interact with the cells. It is therefore desirable to modify PLLA nanofibers using simple methods to improve the biocompatibility of PLLA to enhance cell-matrix interaction. Also, PLLA is generally hydrophobic due to the non-polar groups along its backbone and synthetic polymer nanofibers are relatively hydrophobic as the decrease in fiber diameter will correspond to an increase in effective contact angle [25]. Improving the hydrophilic property of electrospun and incorporation of cell-recognition domains such as RGD onto nanofibers can be done to enhance cell-scaffold interactions. In a previous study [60], air plasma treatment was used to improve the hydrophilic property of electrospun nanofibers.

In this chapter, the aim was to investigate and compare the chemical composition of modified PLLA nanofibers through the addition of collagen or laminin by covalently binding, physical adsorption, and blending bioactive ECM molecules with PLLA polymer solution during electrospinning. In addition, neural cell viability and differentiation were analyzed to determine the suitability of using collagen and laminin modified PLLA nanofibers and compare the efficiency of the modification methods for peripheral nerve regeneration applications.

4.2 Materials and Methods

All chemicals were obtained from Sigma-Aldrich (St Louis, MO) and were used as received, unless otherwise stated. Rat pheochromocytoma cell line, PC12 cells, was obtained from American Type Culture Collection (ATCC). PLLA of 100 kDa was bought from Polysciences, Inc. (Warrington, PA). Collagen type I was purchased from Koken Co., Ltd (Japan). Mouse 2.5S NGF and laminin were purchased from Invitrogen Corporation, USA. Cell Titer 96 A_{queous} One Solution assay (MTS assay) was acquired from Promega (Madison, WI). BCA Protein Assay kit and MicroBCA protein assay were bought from Pierce (USA).

4.2.1 Fabrication of PLLA nanofibers

PLLA nanofibers were fabricated by electrospinning technique. Polymer solution was prepared by dissolving PLLA in HFP at a concentration of 10% w/v. Using a syringe

pump (KDS100, KD Scientific Inc., USA), PLLA solution was fed at a rate of 1mL/h through a 27-G spinneret placed 11 cm from the grounded collector. A high-voltage power supply (AU-301P1Matsusada Precision Inc., Japan) was used to apply an electrospinning voltage of 10 kV DC to produce PLLA nanofibers. Electrospinning was conducted in a humidity of less than 60% and a temperature of 22-24 ^{o}C.

4.2.2 Modifications of PLLA nanofibers with ECM molecules

4.2.2.1 Covalent binding

Method 1: Covalent binding of ECM molecules onto nanofibers

PLLA nanofibers were plasma-treated in air using an electrode-less, inductively coupled radio-frequency glow discharge plasma cleaner (Harrick Plasma PDC-001, Ithaca, NY) for 5 min at a radio-frequency power of 30 W to increase the hydrophilic property of the nanofibers. Subsequently, the nanofiber mats were immersed in 2-(N-morpholino)ethanesulfonic acid (MES) buffered solution (0.1 M, pH 5.0) of 5 mg/mL of 1-ethyl-3-(3-dimethylaminopropyl) carbodiimide hydrochloride (EDC) and 5 mg/mL of *N*-hydroxysuccinimide (NHS) for 1 h at room temperature. The nanofibers were then rinsed with MES buffer and immersed in collagen solution (300 μg/mL in 0.01 N HCl) or laminin solution (10 μg/mL) for 24 h at 4 ^{o}C with gentle shaking (Fig. 4.1). Covalently bound collagen-PLLA and laminin-PLLA nanofibers were then immersed in 70% ethanol overnight and subsequently rinsed thoroughly with sterile 0.01 M PBS. The samples were kept sterile for cell culture studies or dried completely for characterization.

4.2.2.2 Physical adsorption

Method 2: Physical adsorption of ECM molecules onto nanofibers

Similarly, PLLA nanofibers were plasma-treated in air for 5 min using an electro-less, inductively coupled radio-frequency glow discharge plasma cleaner. PLLA nanofiber mats were then immersed in collagen solution (300 µg/mL in 0.01 N HCl) or laminin solution (10 µg/mL) for overnight at 4 ^{o}C with gentle shaking (Fig. 4.1). Physically adsorbed collagen-PLLA and laminin-PLLA nanofibers were then immersed in 70% ethanol overnight and subsequently rinsed thoroughly with sterile 0.01 M PBS. The samples were kept sterile for cell culture studies or dried completely for characterization.

4.2.2.3 Blended electrospinning

Method 3: Electrospinning of blended collagen-PLLA and laminin-PLLA nanofibers

Blended collagen-PLLA nanofibers were fabricated by electrospinning as shown in Fig. 4.1. Blended collagen-PLLA solution (10% w/v) at ratio of 10:1 (weight of PLLA : weight of collagen) was prepared by uniformly mixing PLLA and collagen in HFP at room temperature. Blended laminin-PLLA nanofibers were fabricated by electrospinning as shown in Figure 4.1. Blended laminin-PLLA solution (10% w/v) at a ratio of 250:1 (weight of PLLA : weight of laminin) was prepared by uniformly mixing PLLA and laminin in HFP at room temperature. The ECM-polymer solutions were fed through a 27-G spinneret at a rate of 1mL/h using a syringe pump (KDS100, KD Scientific Inc., USA). The distance between the spinneret tip and the grounded collector was set at 11 cm. Electrospinning voltage was applied using a high-voltage

power supply (AU-301P1Matsusada Precision Inc., Japan) at 10 kV DC for the fabrication of blended collagen-PLLA and laminin-PLLA nanofibers. All experiments were performed in a humidity of less than 60% and a temperature of 22-24 °C.

Blended collagen-PLLA and laminin-PLLA nanofibers were sterilized overnight with 70% ethanol, followed with thorough rinsing in 0.01 M PBS for cell culturing or dried completely for characterization. The amount of collagen used for covalent binding or physical adsorption was equivalent to the amount of collagen used for blended electrospinning (i.e. 100 μg collagen per mg PLLA nanofibers). Similarly, the amount of laminin used for covalent binding or physical adsorption was equivalent to the amount of laminin used for blended electrospinning (i.e. 4 μg laminin per mg PLLA nanofibers).
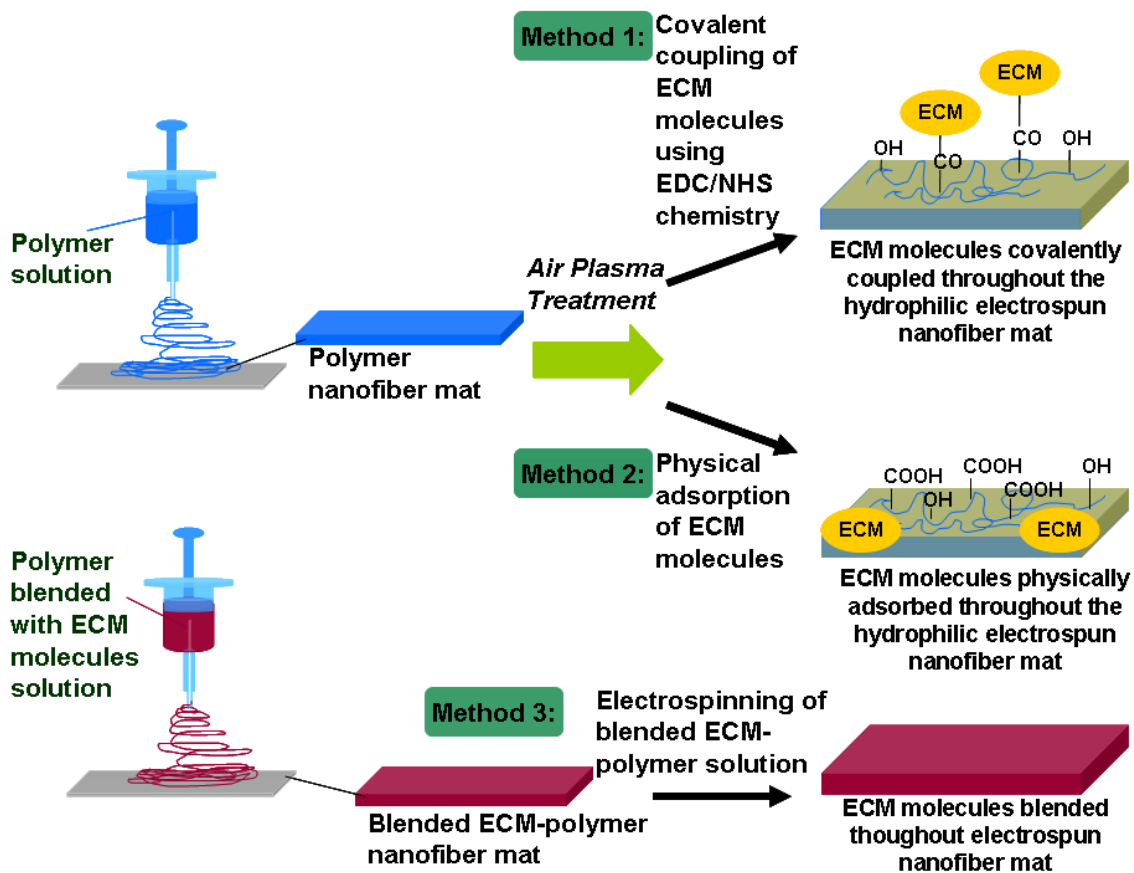
Figure 4.1. Schematic of modification of nanofibers with collagen or laminin: Method 1 – Covalent immobilization, Method 2 – Physical adsorption, and Method 3 – Electrospun blended ECM-polymer solution.

4.2.3 Characterization of laminin-modified PLLA nanofibers

4.2.3.1 Scanning electron microscopy

Morphology of electrospun nanofibers was studied using a SEM (JSM-5800LV, JEOL, Tokyo, Japan). Ranges of nanofiber diameters were measured based on the SEM micrographs by using an image analysis software (ImageJ; National Institutes of Health, Bethesda, MD).

4.2.3.2 Visualization of RBITC-collagen and FITC-laminin on nanofibers

Collagen was conjugated to rhodamine B isothiocyanate (RBITC) for detection and examination of the modification methods. Collagen was mixed with sodium carbonate buffer (0.1 M, pH = 9.0) and RBITC (Sigma, USA) in dimethylsulfoxide. The reaction was performed at 4 ^{o}C for 10 h. Subsequently, the unreacted RBITC was removed by centrifuging the mixture in size exclusion chromatography columns that had exclusion limit of 6 kDa (Biorad, Hercules, CA).

Laminin was conjugated to fluorescein for detection and examination of the modification methods. Laminin was mixed with sodium carbonate buffer (0.1 M, pH = 9.0) and fluorescein isothiocynate (FITC, Molecular Probes, Carlsbad, CA) in dimethylsulfoxide. The reaction was performed at 4 ^{o}C for 10 h. Subsequently, the unreacted FITC was removed by centrifuging the mixture in size exclusion chromatography columns that had exclusion limit of 6 kDa (Biorad, Hercules, CA).

RBITC-collagen and FITC-laminin were then used for modification of PLLA nanofibers as described in the above nanofiber modification section. RBITC-collagen and FITC-laminin modified nanofibers were mounted using FluorSave[TM] reagent (Calbiochem, Germany) onto coverslips and viewed under laser scanning confocal microscope (LSCM, Fluoview FV300, Olympus).

4.2.3.3 X-ray photoelectron spectrometry

X-ray photoelectron spectra of collagen-PLLA and laminin-PLLA nanofibers were taken on a Kratos XPS AXIS His System (Shimadzu, Japan) with a takeoff angle of 90° and binding energy referenced to C1S of saturated hydrocarbon at 284.5 eV.

4.2.3.4 Protein analysis: BCA assay

BCA protein assay was used to quantify the amount of collagen coupled onto the nanofibers according to the RT (room temperature) Test Tube Protocol provided by the manufacturer. Collagen concentration was calculated from collagen standard curve. MicroBCA protein assay (Promega, Madison, WI) was used according to manufacturer's test tube protocol for analysis of the amount of laminin coupled onto the laminin-PLLA nanofibers. Laminin concentration was calculated from laminin standard curve.

4.2.4   *In vitro* PC12 cell culture

Rat PC12 cells were used to study the effect of collagen-PLLA and laminin-PLLA nanofibers on neurite extensions. The cell-line was used because PC12 cells undergo differentiation when they are exposed to nerve growth factor. Thus it serves as a useful model system to study neuronal differentiation. Also, it has been extensively used to evaluate biomaterials for nerve regeneration applications [165-167]. PC12 cells were cultured in high glucose DMEM supplemented with 10% heat-inactivated horse serum, 5% fetal bovine serum and 1% antibiotic/antimycotic solution (Gibco USA) (complete medium). Nanofiber mats were placed in 24-well plate for cell

culture study. PC12 cells were seeded at a density of 5000 cells/cm^2 for MTS cell viability assay. Similarly, cells were seeded at a density of 5000 cells/cm^2 to minimize contact inhibition of neuritogenesis and cultured in differentiation medium (high-glucose DMEM, 1% horse serum, 0.5% fetal bovine serum and 1% antibiotic/antimycotic solution) supplemented with 50 ng/mL NGF. For differentiation studies, PC12 cells were primed by the addition of 50 ng/mL NGF at least 48 h prior to seeding for neurite outgrowth study. The cells were cultured in a humidified incubator at 37 $^{\circ}$C with 5% CO$_2$.

Glass coverslips were coated with 100 µg/mL poly L-lysine (Sigma, St Louis, MO) overnight at 4 $^{\circ}$C with gentle shaking. The coated glass coverslips were then immersed in 70% ethanol overnight and subsequently rinsed thoroughly with sterile 0.01 M PBS for cell culture study.

4.2.5   PC12 cell viability study

Cell viability of the materials was analysed using MTS assay (Promega, Madison, WI) after day 1, 3 and 5 of cell culture. Briefly, the cell-nanofiber complex was incubated with assay reagent in complete medium for 4 h, and aliquots were pipetted into the wells of a 96-well plate to be analyzed with a spectrophotometric plate reader (FLUOstar OPTIMA; BMG Labtech, Offenburg, Germany). The absorbance at 490 nm for each well was recorded.

4.2.6 Immunoctyochemistry and neurite length analysis

After day 1, 3 and 5 of cell culture, immunostaining for neurofilament 160/200 kDa (NF160/200) was performed to observe and compare phenotypes and neurite outgrowth of the differentiated PC12 cells seeded on the nanofibrous scaffolds. Briefly, the scaffolds were rinsed with PBS and fixed in 4% paraformaldehyde for 15 min at room temperature followed by permeation with 0.1% TritonX-100 for 5 min. Non-specific labeling was blocked with incubating in 2% BSA. The samples were immersed in mouse anti-NF160/200 (diluted at 1:200, Sigma) overnight. Subsequently the samples were washed and incubated in FITC conjugated rabbit anti-mouse secondary antibody (diluted at 1:50, Chemicon, USA) for 1 h at 37 $^{\circ}$C. Counterstaining with propidium iodide (2.5μg/mL) for 1 min at 37 $^{\circ}$C was conducted. The immunostained samples were mounted onto glass slides with FluorSave^{TM} reagent and viewed under laser scanning confocal microscope (LSCM, Fluoview FV300, Olympus). Ten random, separate fields per well were recorded at 20 x lens objective and neurite outgrowth analysis was determined with image analysis software (ImageJ; National Institutes of Health, Bethesda, MD).

4.2.7 Scanning electron microscopy of nanofibers cultured with cells

Proliferating and differentiating cell morphology on nanofiber mats were studied using SEM. Samples were fixed in 4% paraformaldehyde for 15 min and dehydrated with graded concentration (50%-100% v/v) of ethanol. Subsequently, hexamethyldisilanze (HMDS) were added to the samples and kept in a fume hood for air drying and used for SEM observation.

4.2.8   Statistical analysis

All data presented are expressed as mean ± standard deviation (SD). ANOVA Single Factor analysis was conducted and the level of statistical significance is defined as $p < 0.05$. Each parameter was conducted with three samples (n = 3). MTS cell viability assay results showed the values consisted of three samples of triplicate readings.

4.3   Results

4.3.1   Morphology and chemical composition of electrospun PLLA and ECM-PLLA nanofibers

4.3.1.1 Scanning electron microscopy

Electrospinning was employed to produce and functionalize polymeric nanofibers. Functionalization of nanofibers was achieved using covalent binding, physical adsorption, or blending ECM bioactive molecules (i.e. collagen and laminin) with PLLA solution for electrospinning. SEM revealed that PLLA and functionalized collagen-PLLA and laminin-PLLA nanofibers had smooth morphology that consisted of nanofibers in the diameter range of 100-500 nm (Table 4.1 and Fig. 4.2).

Table 4.1. Diameter range of nanofibers (nm).

Nanofibers	Collagen	Laminin
Covalently bound	312 ± 68	312 ± 68
Physically adsorbed	312 ± 68	312 ± 68

Blended	238 ± 114	272 ± 80
PLLA	312 ± 68	312 ± 68
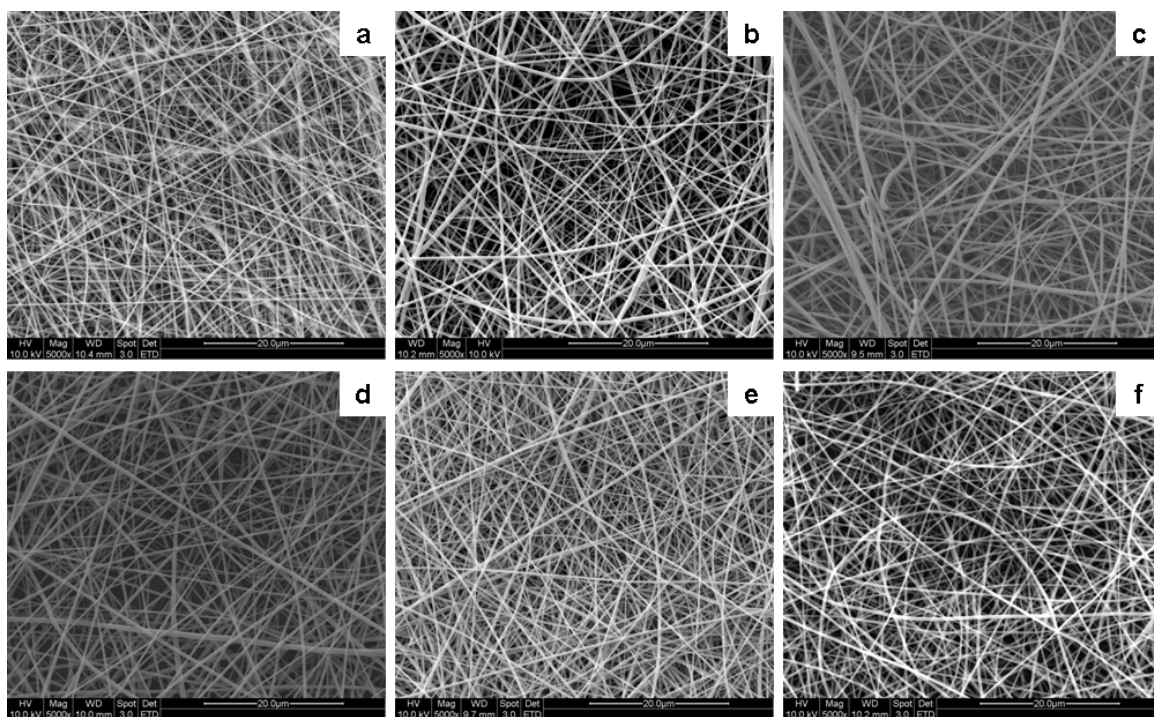
Figure 4.2. Scanning electron micrographs of electrospun nanofibers (a) covalently bound collagen-PLLA, (b) physically adsorbed collagen-PLLA, (c) blended collagen-PLLA, (d) covalently bound laminin-PLLA, (e) physically adsorbed laminin-PLLA, and (f) blended laminin-PLLA.

4.3.1.2 RBITC-collagen and FITC-laminin on nanofibers

Confocal scanning laser micrographs (Figs. 4.3 and 4.4) showed the uniform distribution of collagen and laminin coupled onto the nanofibers (RBITC conjugated collagen-PLLA and FITC conjugated laminin-PLLA nanofibers).
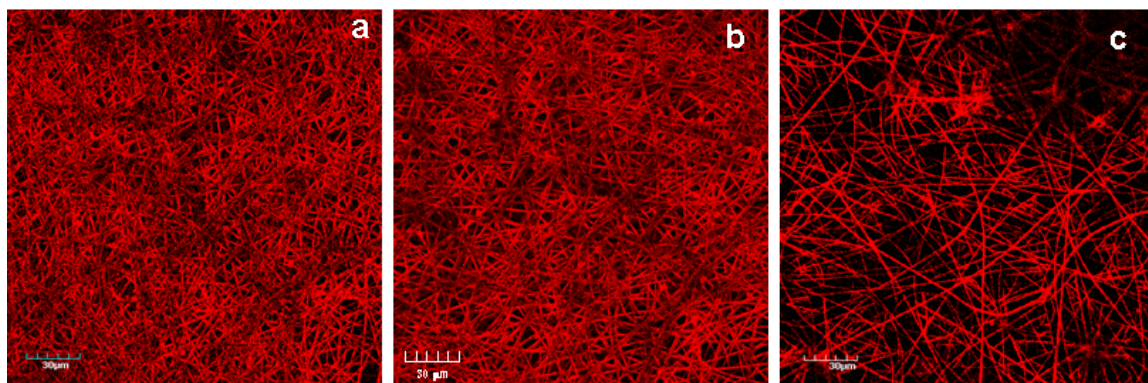
Figure 4.3. LSCM micrographs of PLLA nanofibers modified with RBITC-collagen (a) covalently bound collagen-PLLA, (b) physically adsorbed collagen-PLLA, and (c) blended collagen-PLLA.
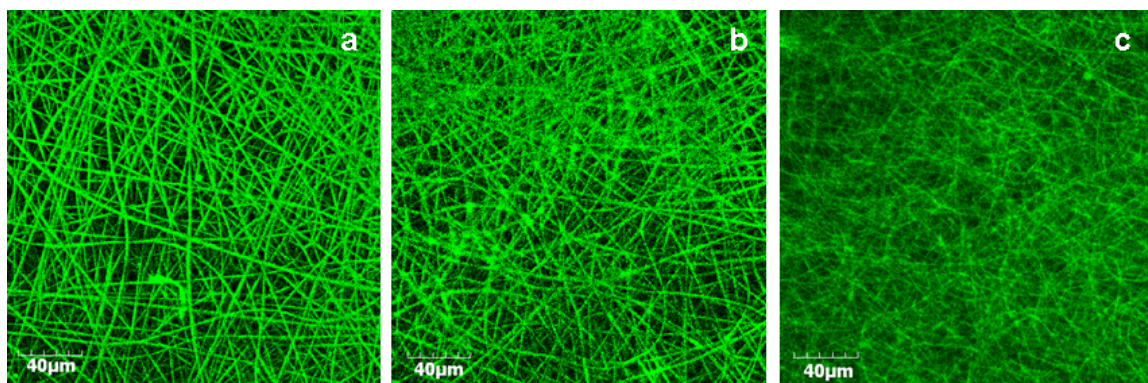
Figure 4.4. LSCM micrographs of PLLA nanofibers modified with FITC-laminin (a) covalently bound laminin-PLLA, (b) physically adsorbed laminin-PLLA, and (c) blended laminin-PLLA.

4.3.2 Chemical composition of electrospun PLLA, collagen-PLLA, and laminin-PLLA nanofibers

4.3.2.1 X-ray photoelectron spectrometry

Chemical composition of collagen and laminin coupled onto PLLA nanofibers were shown and verified using X-ray photoelectron spectrometry (XPS). Tables 4.2 and 4.3 show that collagen and laminin were successfully added onto the surface of the nanofibers as indicated by the presence of N1S peaks in the spectra, respectively. Since XPS only examined the surface of the functionalized nanofibers, quantification of collagen and laminin coupled onto the nanofibers was achieved using protein assay described below.

Table 4.2. Atomic ratios of carbon, oxygen, and nitrogen on the surface of PLLA and collagen-PLLA nanofibers as determined by X-ray photoelectron spectrometry.

Nanofiber mat	C atomic concentration %	N atomic concentration %	O atomic concentration %
Covalently bound collagen-PLLA	53.58	5.28	41.14
Physically adsorbed collagen-PLLA	56.67	5.03	38.30
Blended collagen-PLLA	53.51	2.56	43.93
PLLA	54.49	0	45.51

Table 4.3. Atomic ratios of carbon, oxygen, and nitrogen on the surface of PLLA and laminin-PLLA nanofibers as determined by X-ray photoelectron spectrometry.

Nanofiber mat	C atomic concentration %	N atomic concentration %	O atomic concentration %
Covalently bound laminin-PLLA	64.49	4.65	30.85
Physically adsorbed laminin-PLLA	67.67	0.99	31.34
Blended laminin-PLLA	63.50	0.37	36.13
PLLA	60.85	0	39.15

4.3.2.2 BCA assay for protein quantification

The presence and quantity of collagen and laminin coupled onto the nanofibers were evaluated using BCA protein assays. Analysis showed that more collagen had been coupled onto PLLA nanofibers via the blended electrospinning method (Table 4.4). Similarly, significantly more laminin were found throughout the nanofibrous membranes (Table 4.5) in blended laminin-PLLA nanofibers than on covalently bound and physically absorbed laminin-PLLA nanofibers.

Table 4.4. Pierce's BCA^{TM} protein assay for collagen-PLLA nanofibers.

Nanofiber mat	Covalently Bound	Physical Adsorption	Blended
Quantity of collagen	$42 \pm 17 \, \mu g$	$22 \pm 10 \, \mu g$	$58 \pm 19 \, \mu g$

coupled per mg of PLLA

Table 4.5. Pierce's MicroBCA^{TM} protein assay for laminin-PLLA nanofibers.

Nanofiber mat	Covalently Bound	Physical Adsorption	Blended
Quantity of laminin coupled per mg of PLLA	1.75 ± 0.41 μg	1.50 ± 0.54 μg	3.12 ± 0.63 μg

4.3.3 Effect of collagen-PLLA and laminin-PLLA nanofibers on PC12 cell viability

Incorporation of ECM proteins has been shown to enhance nerve regeneration in several studies [117, 118]. In this study, PLLA nanofibers were modified by the addition of collagen or laminin through covalent binding, physical adsorption or blending with PLLA polymer solution during electrospinning to determine the effects of ECM modification methods of nanofibers on neurite outgrowth. MTS assay was used to study the viability of PC12 cells cultured on collagen-PLLA and laminin-PLLA nanofibers.

In general, coupling of collagen onto nanofibers improved cell viability as compared to PLLA nanofibers that were not modified with collagen. In this study, covalently bound collagen-PLLA nanofibers were found to support better cell viability (Fig. 4.5). Figure 4.6 shows the SEM micrographs of cell proliferation on collagen-PLLA

nanofibers. It has been shown that collagen modified PLLA nanofibers were able to support cell proliferation, as compared to unmodified PLLA nanofibers.

It was observed that laminin-PLLA nanofibers supported better cell viability compared to the unmodified PLLA nanofibers and control samples (glass coated with poly(L-lysine)) as shown in Figure 4.5. Laminin modified scaffolds also supported the attachment and proliferation of PC12 cells (Fig. 4.7) for subsequent neurite outgrowth when nerve growth factor was introduced. It has been shown that nanofibers that were coupled with laminin could enhance PC12 cell viability and adhesion, and can serve as effective substrates to enhance nerve regeneration.
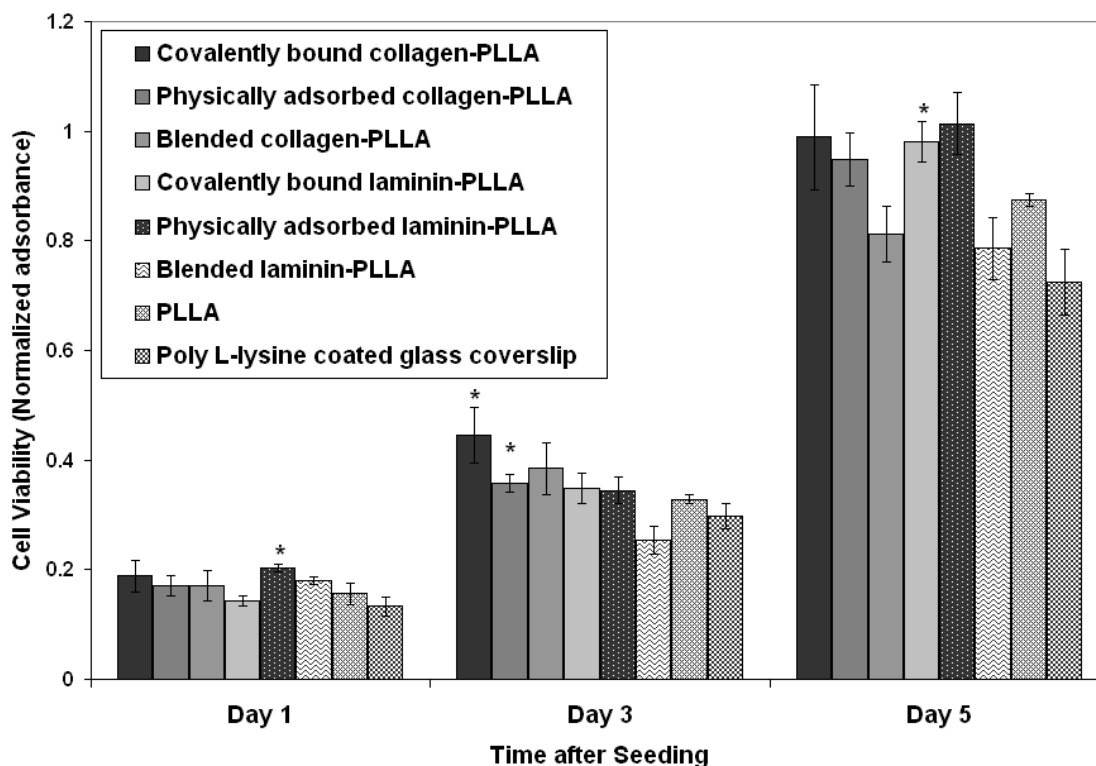
Figure 4.5. Viability of PC12 cells cultured on collagen and laminin-PLLA nanofibers. Data are expressed as mean ± SD (n = 3, triplicate) (* $p < 0.05$, compared to the PLLA nanofibers group).

Covalently bound collagen-PLLA nanofibers	Physically adsorbed collagen-PLLA nanofibers	Blended collagen-PLLA nanofibers	PLLA nanofibers	Poly L-lysine coated glass coverslip
Day 1				
Day 3				
Day 5				
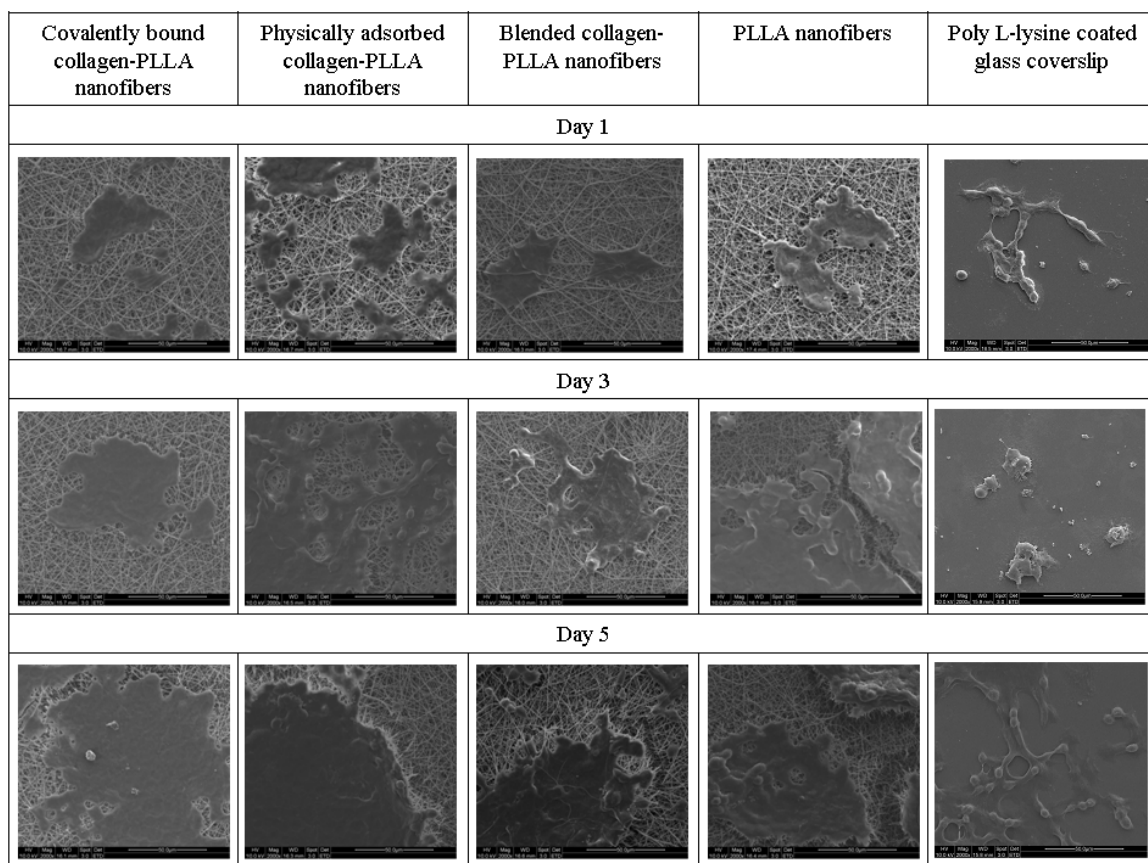
Figure 4.6. Representative scanning electron micrographs of PC12 cell proliferation on collagen-PLLA nanofibers.

Covalently bound laminin-PLLA nanofibers	Physically adsorbed laminin-PLLA nanofibers	Blended laminin-PLLA nanofibers	PLLA nanofibers	Poly L-lysine coated glass coverslip
Day 1				
Day 3				
Day 5				
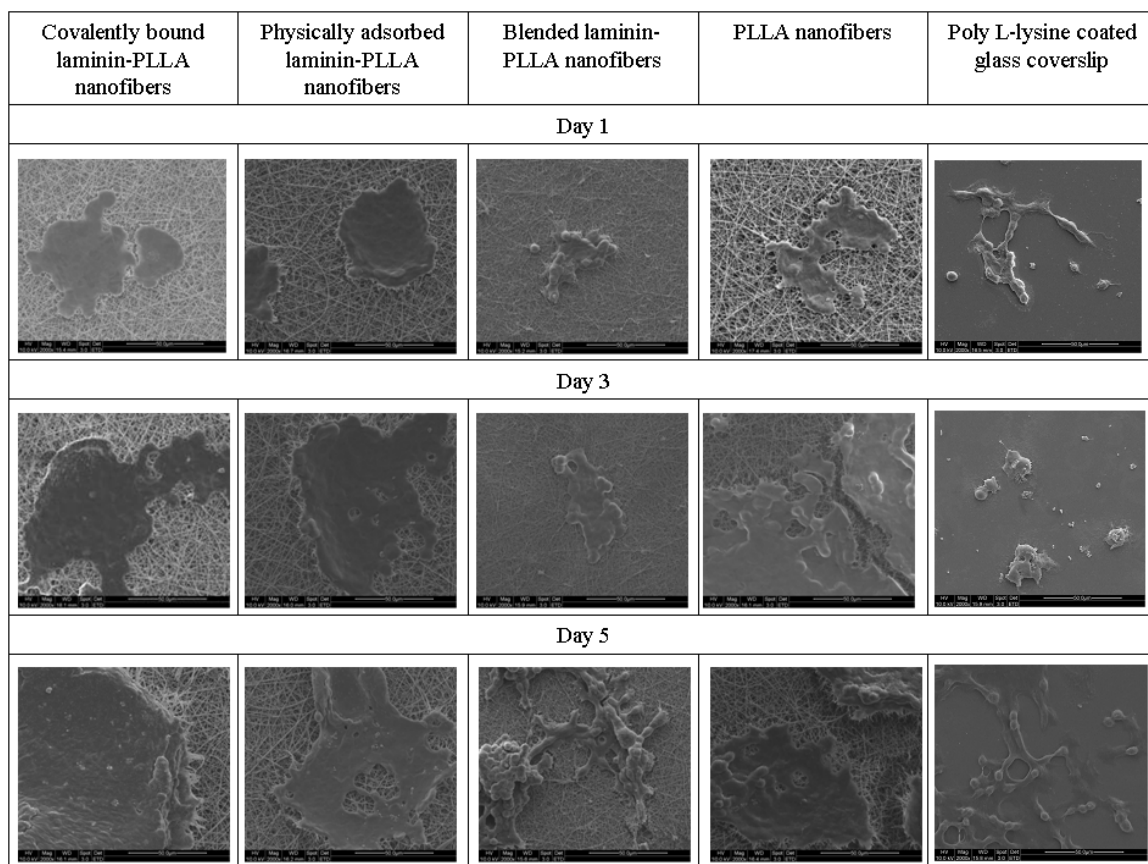
Figure 4.7. Representative scanning electron micrographs of PC12 cell proliferation on laminin-PLLA nanofibers.

4.3.4 Effect of collagen-PLLA and laminin-PLLA nanofibers on PC12 cell differentiation

PC12 cell differentiation on collagen-PLLA and laminin-PLLA nanofibers was studied by analysing the neurite outgrowth observed on the nanofiber scaffolds. PLLA nanofibers that were modified with collagen and laminin could promote neurite extension more significantly than on the unmodified PLLA nanofibers (Fig. 4.8).

The results showed that covalently bound collagen-PLLA nanofibers enhanced neurite outgrowth of PC12 cells when compared to physically adsorbed or blended collagen-PLLA nanofibers (Fig. 4.8). This correlates to the better viability of PC12 cells cultured on covalently bound collagen-PLLA nanofibers (Fig. 4.5), indicating that covalent coupling of collagen on PLLA nanofibers could be a potential method to improve PLLA nanofibers for nerve regeneration applications. Scanning electron micrographs of neurite extensions of PC12 cells on nanofibers are shown in Figure 4.9. Immuno-staining of neurofilament 160/200 kDa of cultured PC12 cells on collagen-PLLA nanofibers are shown in Figure 4.10. As the culture progressed, more neurite outgrowth was observed on covalently bound collagen-PLLA nanofibers as compared to the other modified collagen-PLLA nanofibers.

Figure 4.8 illustrates that more neurite outgrowth of PC12 cells were observed on blended laminin-PLLA nanofibers as compared to the other two modification methods. This observation may be attributed to more laminin were coupled onto the blended laminin-PLLA nanofibers. Although blended laminin-PLLA nanofibers were found to be better substrates to provide enhanced neurite outgrowth (Fig. 4.8, 4.11 and 4.12) but this result did not correlate to better PC12 cell viability on blended laminin-PLLA nanofibers (Fig. 4.5). This may be attributed to the tendency of laminin to promote neurite outgrowth than to enhance viability of nerve cells [115]. In general, blended electrospinning is thus an effective modification technique to

introduce biochemical cues onto synthetic polymer nanofibers for creating biomimetic peripheral nerve scaffolds.
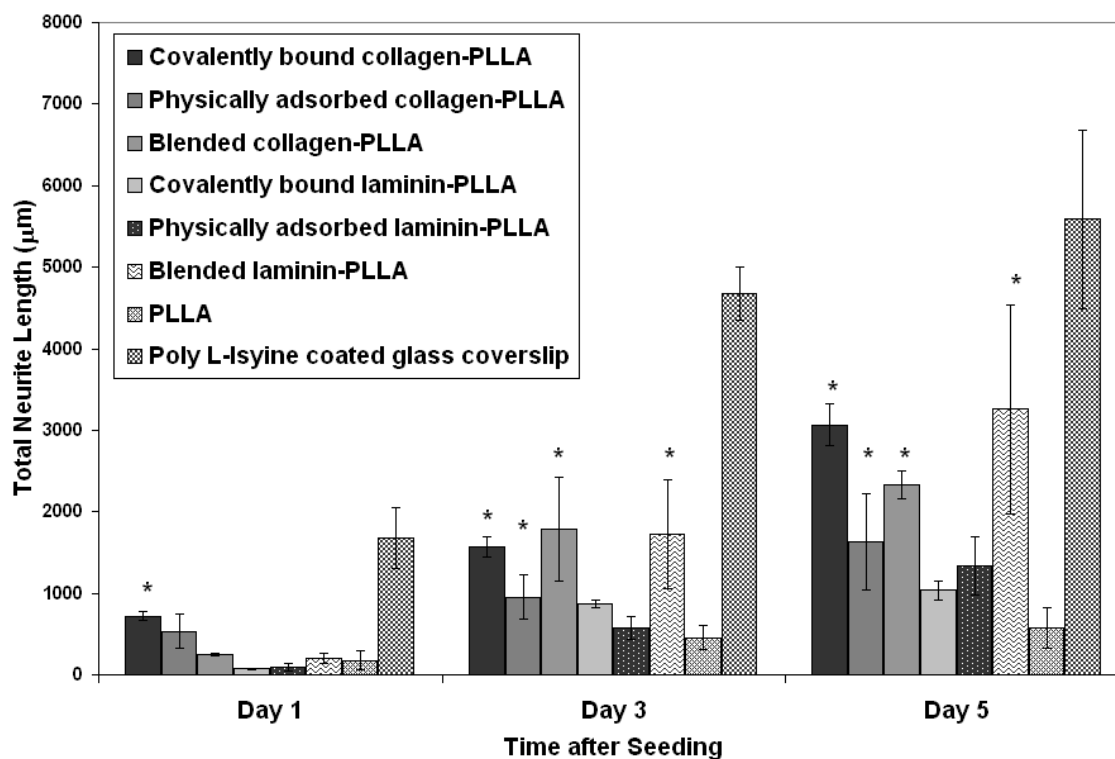
Figure 4.8. Neurite extension of PC12 cells cultured on collagen-PLLA and laminin-PLLA nanofibers. Data are expressed as mean ± SD (n = 3) (* $p < 0.05$, compared to the PLLA nanofibers group).

Covalently bound collagen-PLLA nanofibers	Physically adsorbed collagen-PLLA nanofibers	Blended collagen-PLLA nanofibers	PLLA nanofibers	Poly L-lysine coated glass coverslip
Day 1				
Day 3				
Day 5				
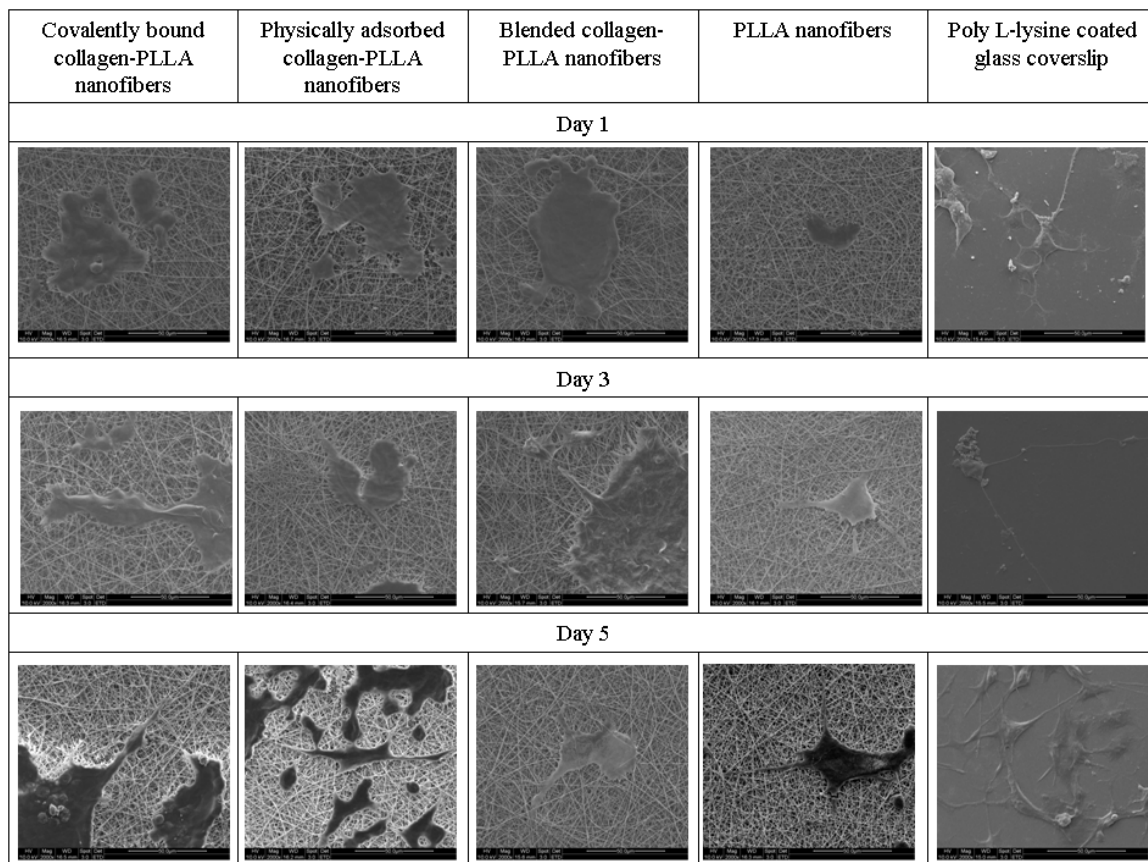
Figure 4.9. Representative scanning electron micrographs of PC12 cell differentiation on collagen-PLLA nanofibers.

Covalently bound collagen-PLLA nanofibers	Physically adsorbed collagen-PLLA nanofibers	Blended collagen-PLLA nanofibers	PLLA nanofibers	Poly L-lysine coated glass coverslip
Day 1				
Day 3				
Day 5				
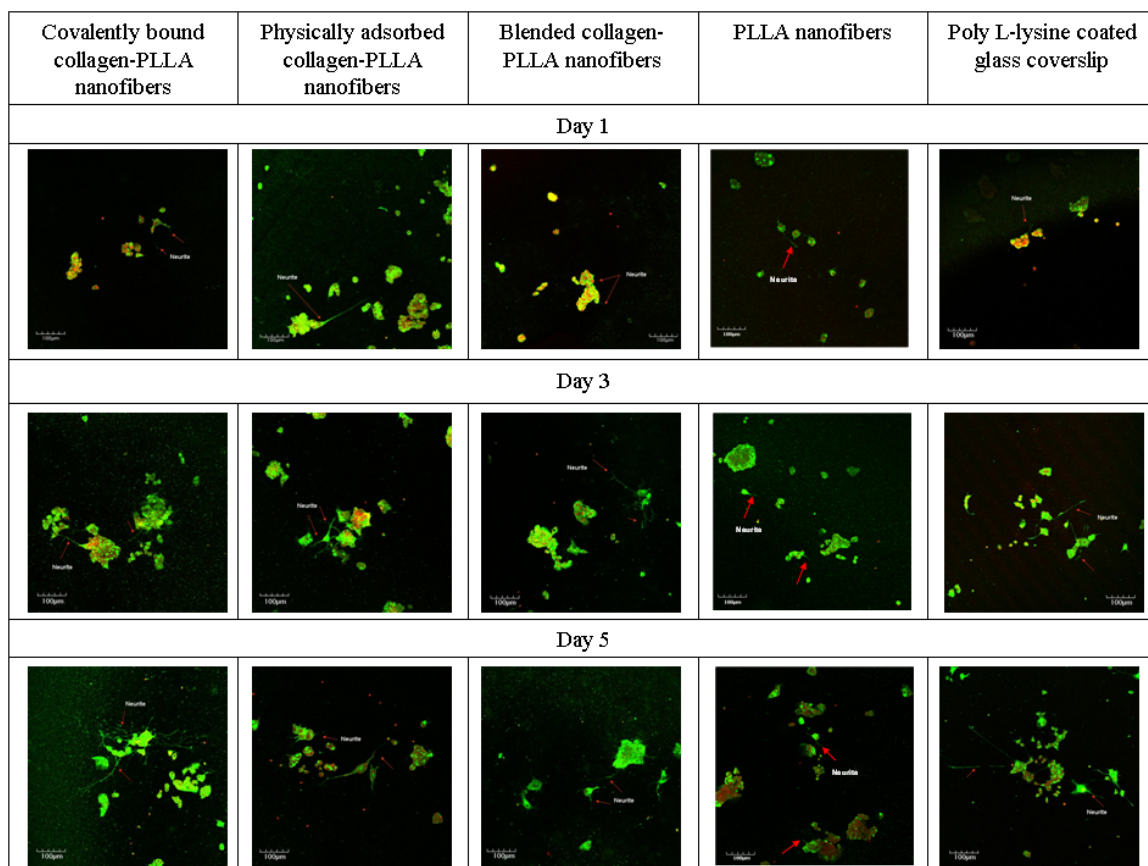
Figure 4.10. Representative LSCM of cells cultured on collagen-PLLA nanofibers. Neurite was stained for neurofilament 160/200 kDa (green) and nuclei of the cells were stained with propidium iodide.

Covalently bound laminin-PLLA nanofibers	Physically adsorbed laminin-PLLA nanofibers	Blended laminin-PLLA nanofibers	PLLA nanofibers	Poly L-lysine coated glass coverslip
Day 1				
Day 3				
Day 5				
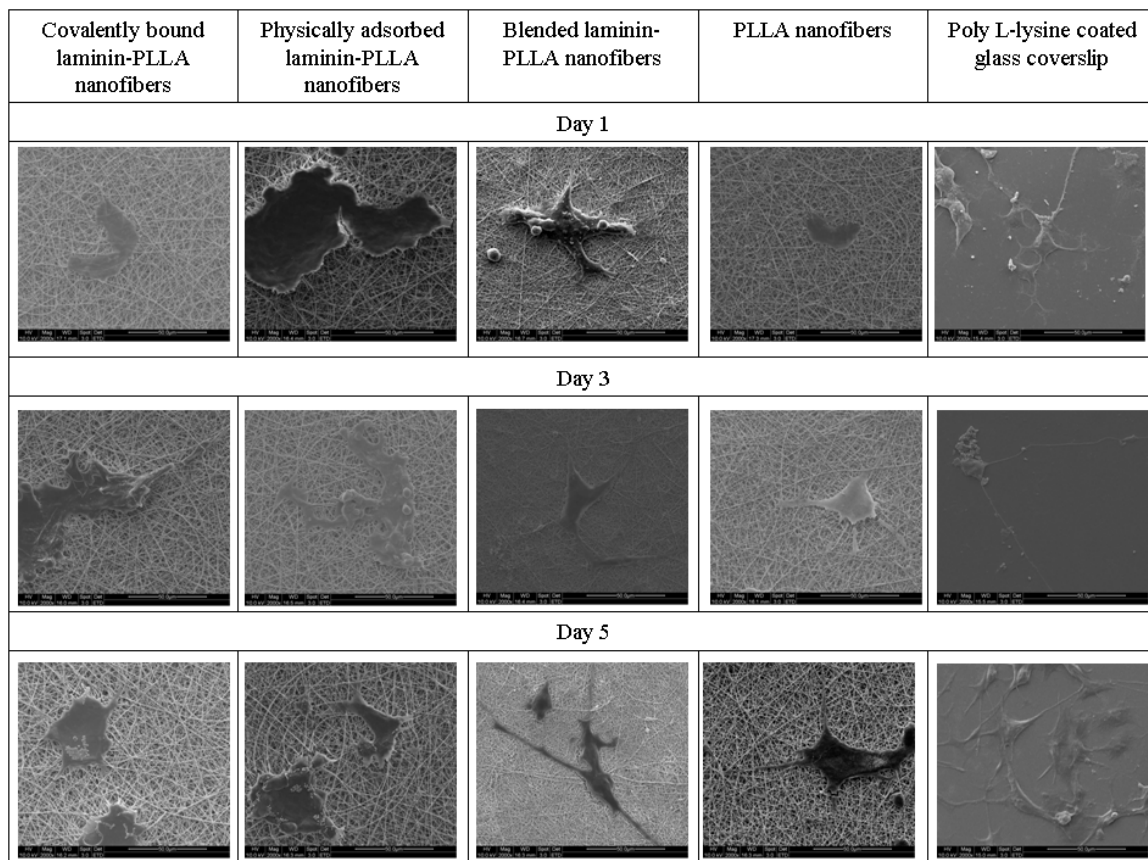
Figure 4.11. Representative scanning electron micrographs of PC12 cell differentiation on laminin-PLLA nanofibers.

Covalently bound laminin-PLLA nanofibers	Physically adsorbed laminin-PLLA nanofibers	Blended laminin-PLLA nanofibers	PLLA nanofibers	Poly L-lysine coated glass coverslip
Day 1				
Day 3				
Day 5				
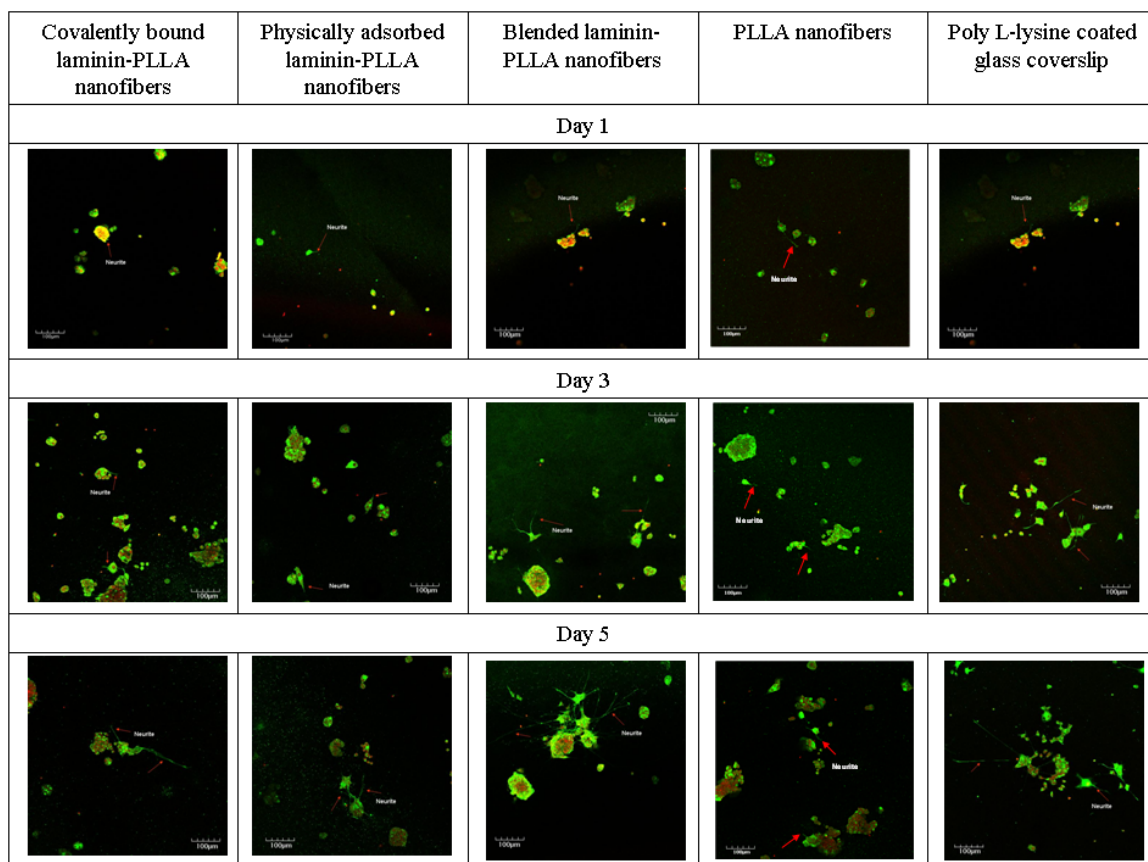
Figure 4.12. Representative LSCM of cells cultured on laminin-PLLA nanofibers. Neurite was stained for neurofilament 160/200 kDa (green) and nuclei of the cells were stained with propidium iodide.

4.4   Discussion

Although synthetic polymers such as PLLA and PLGA nanofibers possess biodegradation capacity and good mechanical properties, many do not possess cell recognition signals. In this chapter, collagen and laminin were introduced into the nanofibers to improve cell-matrix interactions. Collagen and laminin were successfully coupled onto PLLA nanofibers using three methods 1) covalent binding

using water-soluble carbodiimide and *N*-hydroxysuccinimide as the coupling reagents, 2) physical adsorption, or 3) physical blending of collagen or laminin together with PLLA solution for electrospinning procedure (blended electrospinning). Careful steps were taken to ensure that the collagen or laminin added to the scaffolds were consistent for the modification methods to compare the efficiency of attaching ECM molecules throughout the scaffolds.

Covalently immobilized collagen on polymer can improve material-tissue interface by promoting ingrowth of soft tissue and tissue adhesion [168]. Physical adsorption of collagen is a simple technique employed to alter the surface chemistries of the biomaterials to enhance cell attachment and proliferation [59]. Study has described that fibrotic foreign-body reactions were minimized using collagen coated synthetic implants that promoted integration of implant and host tissue [108]. Also, luminal epithelium of the jugular vein that was coated with collagen greatly improved nerve regeneration [169]. Blending of collagen with polymer solution for electrospinning allowed the refining of the composition of polymeric nanofibers for improved biocompatibility [42]. Our results showed that covalently bound collagen-PLLA nanofibers supported better cell viability even when there was more collagen coupled on the blended collagen-PLLA nanofibers. It is suggested that physically adsorbed collagen-PLLA nanofibers provided the least favorable substrate for neurite outgrowth as compared to covalently bound collagen-PLLA and blended collagen-PLLA nanofibers because physically adsorbed collagen was less biologically stable due to the easy desorption of adhesive molecules when cells were cultured [170].

Enhanced neurite outgrowth was observed on covalently bound collagen-PLLA nanofibers as compared to the other two types of collagen modified nanofibers. The reason may be due to the preference of axonal outgrowth on smooth surfaces [2]. Pure collagen nanofibers were found to swell into hydrogel-like structure in cell culture medium [42], thus blended collagen-PLLA nanofibers that consisted of blended collagen-PLLA nanofibers would also swell to affect neural cell attachment and viability.

Laminin is well-characterized to induce cell attachment and neurite outgrowth and its involvement in nerve regeneration *in vivo* [116, 118] and is a major component of the basal lamina and is potent in promoting neurite outgrowth [11]. Laminin interacts with surface receptors, such as Schwann cell surface integrin receptors $\alpha 1\beta 1$, $\alpha 6\beta 1$, $\alpha 6\beta 4$, to activate signaling pathways that influence cell viability and functions [164]. It also presumably activates myelination which is essential for successful nerve regeneration [107]. Laminin had been cross-linked onto PLLA nanofibers to provide a bioactive scaffold possessing both physical and biochemical cues for the induction, enhancement and guidance of neurite outgrowth of neural cells [158]. Blended electrospinning were found to be an efficient technique to introduce laminin into the scaffolds (on the surface and in the interior of the nanofibers) as more laminin were found to couple onto the scaffolds as compared to the other two methods (Table 4.5). Blended electrospinning is considered a rapid and simple modification technique as compared to the other two modification methods. Covalent immobilization and physical adsorption involved several steps to achieve modification of the nanofibrous

scaffold that did not achieve similar laminin coupling efficiency. In addition, the presence of laminin molecules on the surface and in the interior of the blended nanofibers can provide the necessary signals for cell interaction as the synthetic polymer degrades.

PC12 cells extended their neurite well on blended laminin-PLLA nanofibers. Especially, extensive neurite outgrowth was observed on blended laminin-PLLA nanofibers that highly suggest that electrospinning of laminin at high voltage had not adversely affected the bioactivity of the ECM protein. Many studies have shown successful electrospinning of collagen nanofibrous scaffolds using HFP as the solvent [42, 92]. Electrospun nanofibrous collagen-blended PCL-LA nanofibers were shown to support the attachment, viability and preserve phenotype of the cultured endothelial cells [42]. Collagen-PCL nanofibers produced by blended electrospinning also supported glial cell migration and axonal outgrowth [92]. Thus, it is postulated that laminin that had been blended in the polymer and HFP solution will remain viable bioactive molecule to promote neurite outgrowth. In addition, it is well known that laminin contains bioactive neurite binding sites for neural cell attachment and differentiation (namely YIGSR and IKVAV, respectively), and studies had shown enhanced neurite extensions on substrates that were modified with laminin peptides [120, 121, 171]. If these peptide sequences are not adversely influenced by the solvent used for blended electrospinning, the bioactivity of the ECM proteins found in the blended electrospun nanofibers could remain bioactive after treatment with the electrospinning solvent.

In vitro neurite extension of neural cells is a good indirect measure of the ability of ECM molecules to promote nerve regeneration [92, 122, 172]. In this chapter, it is observed that collagen and laminin modified PLLA nanofibers were found to support neurite extension. More importantly, better encapsulation efficiency of ECM molecules in the nanofibers was obtained using blended electrospinning (Fig. 4.8). Comparing collagen and laminin, laminin is a more potent biomolecule that support better neurite outgrowth and activities of Schwann cells for nerve regeneration (Figs. 4.10 and 4.12). Additionally, laminin has been found to encourage better attachment and proliferation of Schwann cells when compared to collagen and fibronectin [122]. *In vivo* studies have shown that laminin performed better than collagen in the improvement of outcome of nerve regeneration [119]. It had been reported previously [2] that neurites grew well on smooth surfaces and it is interesting to observe that the positive control samples in this study(i.e. coverslips coated with poly(L-lysine) supported excellent neurite outgrowth (Fig. 4.8). Hence the good neurite extensions observed on coverslips coated with poly (L-lysine) could be due to the smooth surface that had been presented by the coverslips to the extending neurites to effect better neurite outgrowth.

Successful fabrication of nanofibers using electrospinning depends on the characteristics such as solubility in suitable solvents and their molecular weight, of the material to be electrospun. Blended electrospinning can be used to fabricate scaffolds from materials that cannot be easily electrospun alone (e.g. low molecular

weight polymer or bioactive molecules such as laminin) because these materials can be blended with polymers that are well-suited for electrospinning (e.g. PLLA and PLGA) which can further act as a good mechanical support. In this study, three modification methods were studied that shows blended electrospinning as a facile and efficient method to fabricate bioactive nanofibrous scaffolds that contain both synergistic topographical and biochemical cues for enhancement of nerve regeneration.

4.5   Conclusion

This chapter demonstrates that nanofibrous scaffolds can be fabricated by electrospinning to produce nano-scale architectured scaffolds and can be easily functionalized with biochemical cues (e.g. collagen and laminin) to further enhance neurite outgrowth for potential applications in neural tissue repair. Importantly, blending laminin for electrospinning is a useful and easy method to modify scaffolds that have both topographical and biochemical cues.

Chapter 5

Fabrication and characterisation of PLGA nanofiber intra-luminal guidance channels and modification with neurotrophins

5.1 Introduction

Bridging developmental biology, tissue engineering and regenerative medicine has been identified as an important key to realize the potentials of applying bioengineered scaffolds in the clinics [19]. It is essential to understand how cells construct themselves during development to form the distinct three-dimensional tissue structures; and how cells of damaged tissue remodel, repair and regenerate after injury to form desirable structures that resemble the original tissue [20]. Appropriate designs of bioengineered nerve constructs are therefore crucial to encourage better tissue regeneration to replace damaged tissue. For nerve regenerative medicine, the presence of endoneurium layer in which the axons are arranged in nerve bundles is an important feature of the autologous nerve graft. Autologous nerve grafts contain these longitudinal endoneurial tubes of the basal lamina for nerve growth cones or non-neuronal cells to adhere and attach for elongation, migration and maturation. Especially for large peripheral nerve gaps repair, this important architecture found in

the autologous nerve graft may render the better nerve regeneration and functional recovery observed in autograft repair [152].

Previous study has shown that without inner filament bundles in peripheral nerve gap repair, Schwann cell cables were formed in a discontinuous manner [152] to present an unfavorable environment that affected nerve regeneration. Therefore, the lack of intra-luminal guidance channels in synthetic nerve conduits might limit the rate or degree of peripheral nerve regeneration. Comparison of empty nerve conduits and conduits containing microfilaments has previously been examined. The results demonstrated that the presence of microfilaments enhanced axonal regeneration in rats that were subjected to a 18 mm nerve lesion injury [152]. Also, bundles of collagen filaments that were used to bridge 30 mm rat sciatic nerve gaps had been shown to provide contact guidance for the regenerating axons [113]. Therefore bioengineering conduits that resemble the hierarchical levels of the native nerve, for example to incorporate intra-luminal guidance scaffolds that mimic the endoneurial tubes, might improve the capacity of synthetic nerve constructs to enhance nerve regeneration and obtain better functional recovery.

Besides providing physical structures to allow axons and non-neuronal cells to regenerate across a nerve gap, it is advantageous to provide further biochemical cues to enhance nerve regeneration. Nerve growth cone is influenced and elongated by chemotactic soluble guidance molecules that can be cell-cell (short-range) interactions or diffusion gradient (long-range) mediation by possibly signal

transduction mechanisms [173]. Besides directing and attracting the growth cones, neurotrophic factors are also known to regulate the maturation of axons [173, 174]. Soluble biomolecules may possess attractive or repulsive capabilities that could be classified and applied accordingly [173] for the purpose of peripheral nerve engineering. NGF is a critical guidance molecule that is actively involved in nerve regeneration. NGF binds to specific receptors at the nerve growth cone that are then internalized and retrogradely transported to the soma [175]. This interaction influences neurons on many levels, including gene expression and apoptosis. Controlled and sustained delivery of neurotrophic factors can be achieved by several methods, such as the use of biodegradable microspheres, genetically modified cells that produce NGF, immobilizing growth factors on biomaterials, or mini pumps [2, 126, 140]. Recently growth factors have been encapsulated in biodegradable nanofibers to provide sustained release to encourage better nerve regeneration [128, 130]. In this chapter, NGF was incorporated onto the nanofibers as a model therapeutic drug to provide continuous release of the biomolecules for promoting nerve regeneration.

PLGA is one of the most commonly used biomaterial for designing delivery vector for the releasing drug. It is co-polymer of PLLA and PGA that are both approved by FDA use in implant devices. It is an extremely versatile material as its properties such as mechanical strength, degradation rate, and degree of crystallinity can be adjusted by varying the ratio content of the two components or molecular weight to achieve desired drug release pattern. Numerous studies have used PLGA microspheres to

deliver proteins for various applications. Protein release from microspheres is usually characterized by an initial diffusion-controlled burst release phase that is followed by little or incomplete protein release [176]. In addition, the instability of protein released from microspheres has been attributed to the local pH drop due to the acidic PLGA degradation products trapped in the environment [176]. In this study, NGF has been designed to be encapsulated in nanofibrous intra-luminal guidance channels that can provide protein delivery capacity. The sustained release of NGF could potentially improve the performance of synthetic nerve constructs to repair peripheral nerve injuries.

5.2   Materials and Methods

All chemicals were obtained from Sigma-Aldrich (St Louis, MO) and were used as received, unless otherwise stated. Poly(L-lactic acid)-*co*-poly(glycolic acid) [70:30] (PLGA) was bought from Polysciences, Inc. (Warrington, PA) at an of molecular weight of ~ 10,000-20,000. Rat pheochromocytoma cell line, PC12, was obtained from American Type Culture Collection (ATCC). Mouse NGF was purchased from Invitrogen (USA). Rat 2.5S NGF and ELISA kit were obtained from R&D Systems (USA). Cell Titer 96 A_{queous} One Solution assay was purchased from Promega (Madison, WI).

5.2.1 Fabrication of PLGA and NGF-PLGA nanofiber membranes

PLGA nanofibrous membranes were fabricated by electrospinning. PLGA solution was prepared by dissolving the polymer in HFP at a concentration of 35%. The polymer solution was fed using a 27-G spinneret at a rate of 1 mL/h using a syringe pump (KDS100, KD Scientific Inc., USA). The distance between the spinneret tip and the collector was set at 12 cm. Electrospinning voltages were applied using a high-voltage power supply (AU-301P1Matsusada Precision Inc., Japan) at 10 kV. Blended NGF-PLGA solution was prepared by mixing 25 µL of NGF solution (100 µg/mL) with 1 mL of PLGA solution (35% w/v in HFP). Blended NGF-PLGA nanofibers were prepared by electrospinning NGF-PLGA solution at a voltage of 12 kV with a flow rate of 1 mL/h. The distance between the spinneret and the collector was set at 10 cm apart. Nanofibers were collected on 15 mm glass coverslips that were used for morphology observation and NGF bioactivity study.

5.2.2 Characterization of PLGA and NGF-PLGA nanofiber membranes

5.2.2.1 Scanning electron microscopy

Morphology of electrospun nanofibers was studied using SEM (JSM-5800LV, JEOL, Tokyo Japan). The nanofibers were sputter-coated with gold up to 90 s in a JEOL JFC-1200 fine coated and an accelerating voltage of 10 kV of the SEM was used to examine the morphology of the electrospun scaffolds. Range of nanofiber diameters were determined based on SEM micrographs with the use of image analysis software (ImageJ; National Institutes of Health, Bethesda, MD).

5.2.2.2 Release of NGF from nanofiber membrane

Analysis of released NGF from the nanofibers was performed by placing the nanofiber membrane that was collected on glass coverslip in a 24-well plate. The nanofibers were soaked in the DMEM medium that contained antibiotic-antimycotic (Invitrogen, USA) solution at a dilution of 1:200. Under static conditions, the fibers were incubated at 37 ^{o}C in the presence of 5% CO_2. At various time points, 500 mL of supernatant was collected and an equal amount of fresh medium was replaced.

5.2.2.3 Viability of PC12 cells

Rat PC12 cells were used to study the effects of the addition of NGF onto nanofibers on cellular components. PC12 cells were cultured in high glucose DMEM supplemented with 10% heat-inactivated horse serum, 5% fetal bovine serum and 1% antibiotic/antimycotic solution (Gibco USA) (complete medium). PC12 cells were seeded at a density of 5000 cells/cm^2 in a 96-well plate for MTS cell viability assay (Promega, Madison, WI). PC12 cells seeded onto the 96-well cell culture plate for one day in a humidified incubator at 37 ^{o}C with 5% CO_2. The culture medium was completely removed and replaced with medium containing released NGF from the nanofibers. In one of the control groups, an addition of 50 ng/mL exogenous NGF was added to the medium to serve as the positive control group. The negative control group consisted of cells that were cultured in medium that did not contain the addition of exogenous NGF. The cells were then cultured for another two days for MTS assay analysis. The medium was removed and replaced with assay reagent in complete

medium for 4 h, and aliquots were pipetted into the wells of a 96-well plate to be analyzed with a spectrophotometric plate reader (FLUOstar OPTIMA; BMG Labtech, Offenburg, Germany). The absorbance at 490 nm for each well was recorded.

5.2.2.4 Bioactivity of NGF released using PC12 cells

Cells were seeded at a density of 5000 cells/cm^2 in a 96-well plate to minimize contact inhibition of neuritogenesis and cultured for one day (high-glucose DMEM, 1% horse serum, 0.5% fetal bovine serum). Bioactivity of released NGF from the nanofibers was studied by analyzing the differentiation of PC12 cells cultured in release medium. Similar to cell viability assay, after two days of culture, immunostaining for neurofilament 160/200 kDa was carried out on the cultured cells to evaluate the maintenance of NGF bioactivity.

5.2.3   Fabrication of PLGA intra-luminal guidance channels

Intra-luminal guidance channels made up of bundles of nanofibers were fabricated using electrospinning set-up shown in Fig. 5.1. PLGA solution were prepared by dissolving PLGA in HFP at a weight concentration of 35% w/v. The polymer solution was fed using a 27-G spinneret at a various flow rates (i.e. 4, 5, and 7 mL/h) using a syringe pump (KDS100, KD Scientific Inc., USA). The distance between the spinneret tip and the collector was set at 12 cm. Electrospinning voltages were applied using a high-voltage power supply (AU-301P1Matsusada Precision Inc., Japan) at 12 kV DC for PLGA nanofibrous channels. All the experiments were performed in a humidity of less than 60% and a temperature of 24-26 $^{\circ}$C. Briefly, PLGA solution (35%, w/v in HFP) was delivered to the spinneret and nanofibers were

electrospun and deposited on a surface of distilled water. The deposited nanofibers were then drawn down a funnel by a vortex created by the flowing water in the basin and coalesced into a nanofibrous strand. Drawn nanofibrous strand bundle were then collected on the rotating mandrel to produce intra-luminal guidance strands as shown in Figure 5.1. This bundle was collected on a rotating mandrel and was cut to appropriate length for use as the intra-luminal guidance channel
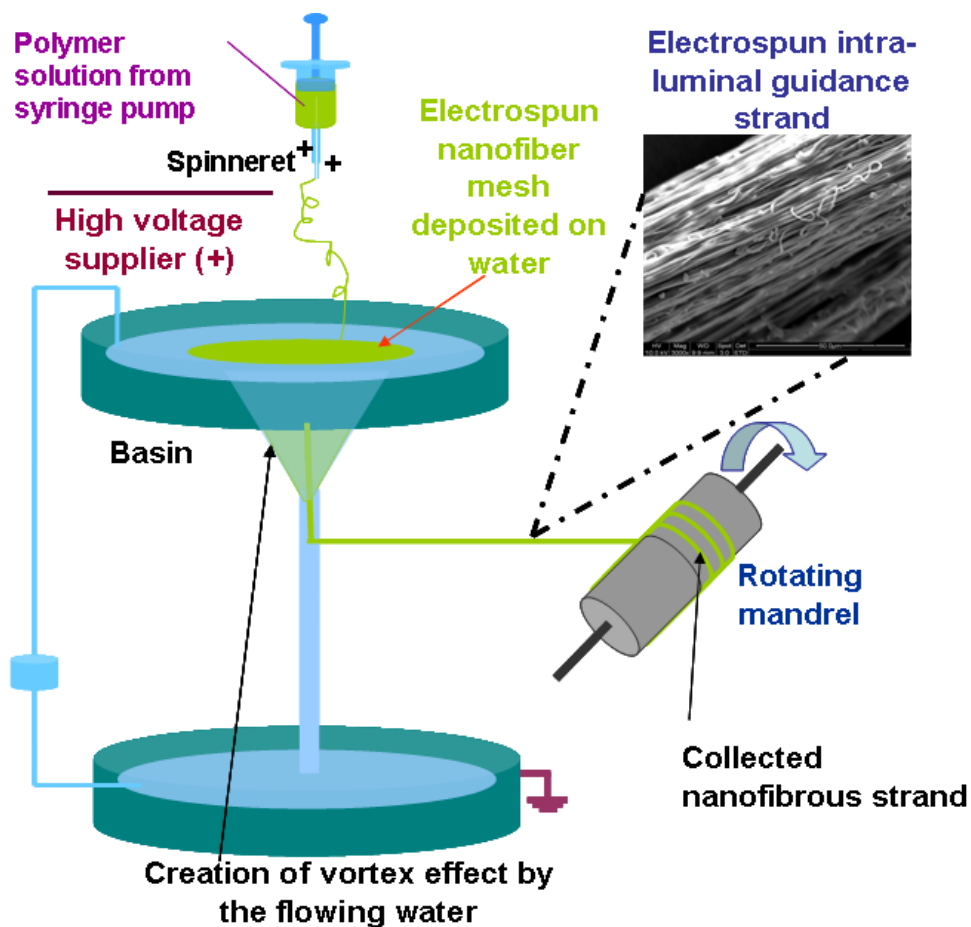
Figure 5.1. Schematic representation of electrospinning set-up to fabricate intra-luminal guidance channels.

5.2.4   Fabrication of PLGA intra-luminal guidance channels containing NGF

NGF-PLGA solution was prepared by dissolving PLGA in HFP at a concentration of 35% w/v. An amount of 50 μg rat 2.5S NGF (R&D Systems, USA) and 3 mg bovine serum albumin (BSA, Sigma) were added to 1 g PLGA solution (35% w/v in HFP) to form blended NGF-PLGA solution. Briefly, protein-polymer solution was delivered using a 27-G spinneret at feeding rate of 3-5 mL/h using a syringe pump (KDS100, KD Scientific Inc., USA). Electrospinning voltage was applied using a high-voltage power supply (AU-301P1Matsusada Precision Inc., Japan) at 12-15 kV DC. The distance between the spinneret tip and the collector (e.g. surface of the distilled water) was set at 7-10 cm.

5.2.5   Characterization of PLGA nanofiber guidance channels

Morphology of electrospun nanofibers was studied using a scanning electron microscopy (SEM) (JSM-5800LV, JEOL, Tokyo Japan) using similar protocol for observation of PLGA nanofibers.

5.2.6   Characterization of NGF-PLGA nanofiber guidance channels

5.2.6.1 NGF ELISA assay

NGF-PLGA intra-luminal guidance channels mesh (n = 3), each weighing 40 ± 7 mg, were each soaked in a 6-well plates filled with 3.0 mL of serum-free medium. The medium contained antibiotic-antimycotic (Invitrogen, USA) solution at a dilution of 1:200. Under static conditions, the fibers were incubated at 37 ^{o}C in the presence of 5% CO_2. At various time points, 1 mL of supernatant was collected and an equal amount of fresh medium was replaced. Using a standard ELISA kit (R&D Systems, USA) for rat NGF, released NGF that had diffused from the nanofibrous guidance channels was analyzed. Release kinetics of NGF released over time from the channels was thus calculated using the NGF ELISA data.

5.3   Results
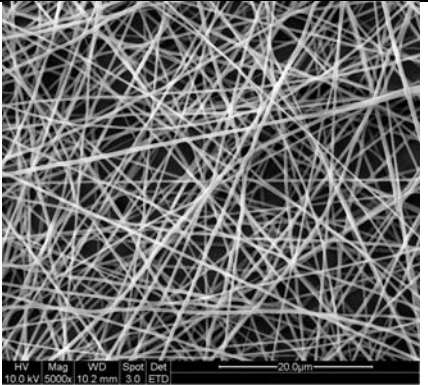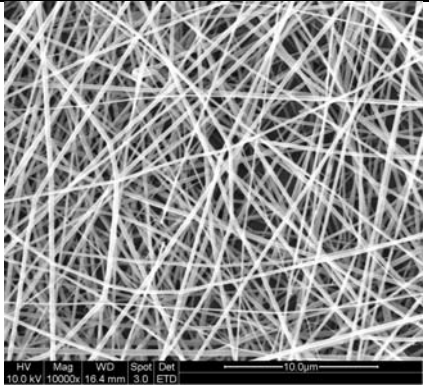
5.3.1   PLGA and NGF-PLGA nanofiber membranes

5.3.1.1 Scanning electron microscopy of nanofiber membrane

SEM images of PLGA and NGF-PLGA membranes (Table 5.1) showed smooth morphological presentation of the nanofibers.

Table 5.1. SEM images of PLGA and NGF-PLGA nanofiber membranes.

Nanofiber	PLGA	NGF-PLGA
Scanning electron		

micrograph		
Diameter (nm)	330 ± 29	240 ± 110

5.3.1.2 Released NGF maintained bioactivity

Since neurotrophins are essential for neurons growth and survival, NGF was blended with PLGA solution during the electrospinning process to fabricate NGF-PLGA nanofibers. Cell viability was assessed using PC12 cells with release medium of day 20. Figure 5.2 shows that release of NGF from the nanofibers supported cell viability indicating that the some of the released NGF retained its bioactivity.
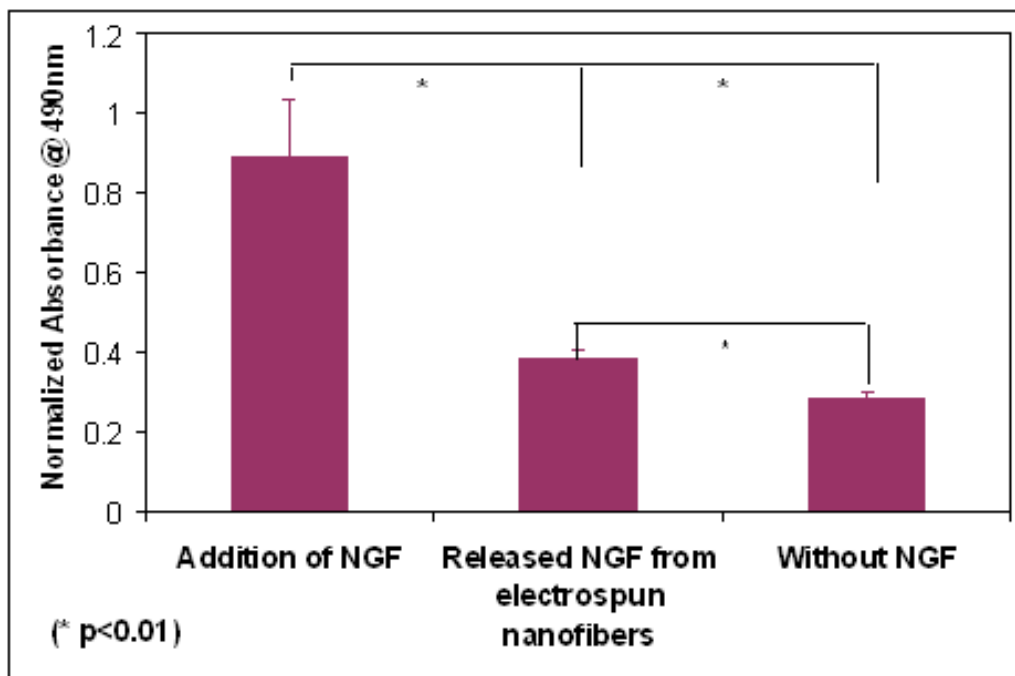
Figure 5.2. PC12 cell viability analysis on released NGF from nanofibers.

The bioactivity of NGF in the nanofibers was evaluated by incubating the cells in release medium for two days and using the medium to evaluate PC12 cell differentiation (Fig. 5.3). The NGF released from the electrospun NGF-PLGA nanofibers was found to induce PC12 cell differentiation, illustrating the maintenance of NGF bioactivity.

(a)   (b)   (c)
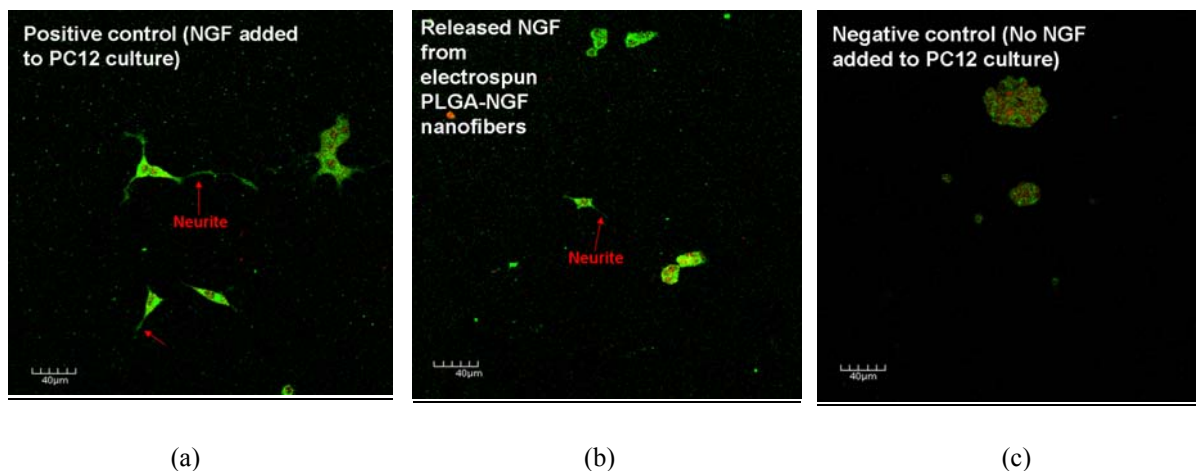
Figure 5.3. Maintenance of the bioactivity of NGF released from electrospun NGF-PLGA nanofibers (a) LSCM of positive control PC12 culture with NGF, (b) LSCM of experimental PC12 culture with released NGF from electrospun blended NGF-PLGA nanofibers, and (c) LSCM of negative control PC12 culture without NGF.

5.3.2   PLGA and NGF-PLGA nanofiber membranes

5.3.2.1 Scanning electron microscopy of PLGA guidance channels

Morphology of the electrospun nanofibrous guidance channels is shown in Figures 5.4 and 5.5. Figure 5.5 shows the electrospun bundles of intra-luminal guidance channels.
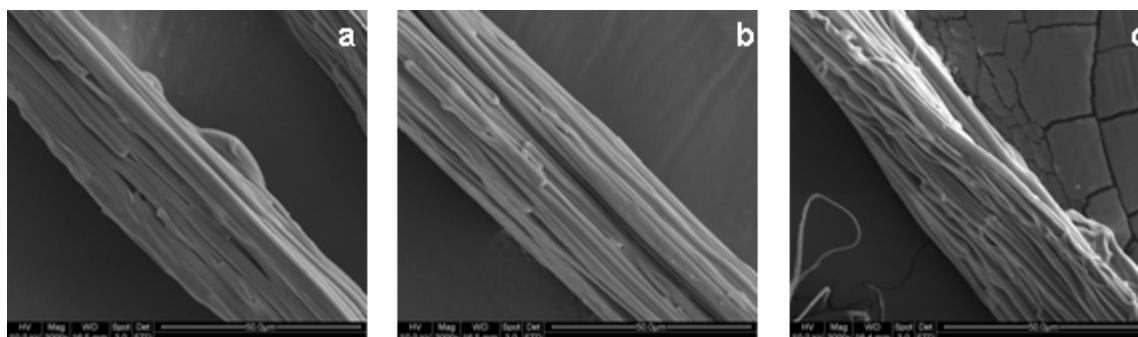
Figure 5.4. SEM micrographs of PLGA guidance channels (a) 4 mL/h, (b) 5 mL/h, and (c) 7 mL/h.

Intra-luminal guidance channels made up of nanofibrous yarns
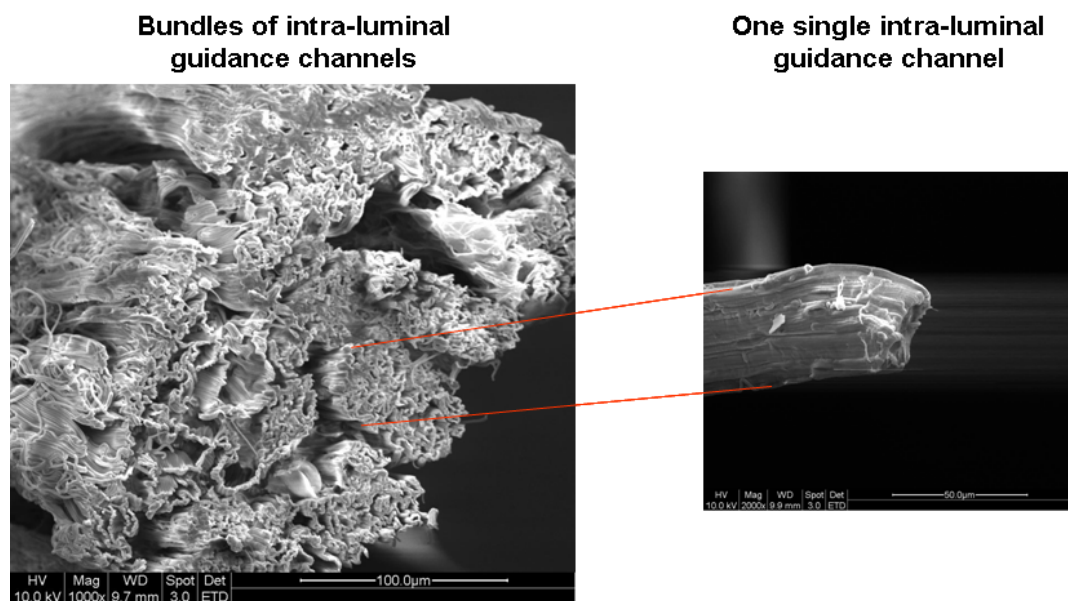
Figure 5.5. Scanning electron micrographs of intra-luminal guidance channels made up of longitudinally aligned nanofibers.

5.3.2.2 Dimensions of intra-luminal guidance channels using different flowing rates

Figures 5.6 and 5.7 depict the analysis of the guidance channel (yarn) diameters and nanofiber diameters with respect to the change in the feed rate of the polymer solution, respectively. Consistent with results reported by Teo *et al.* [55], the diameters of the channel and nanofiber increased as the flowing rate of the polymer solution is increased used for electrospinning.
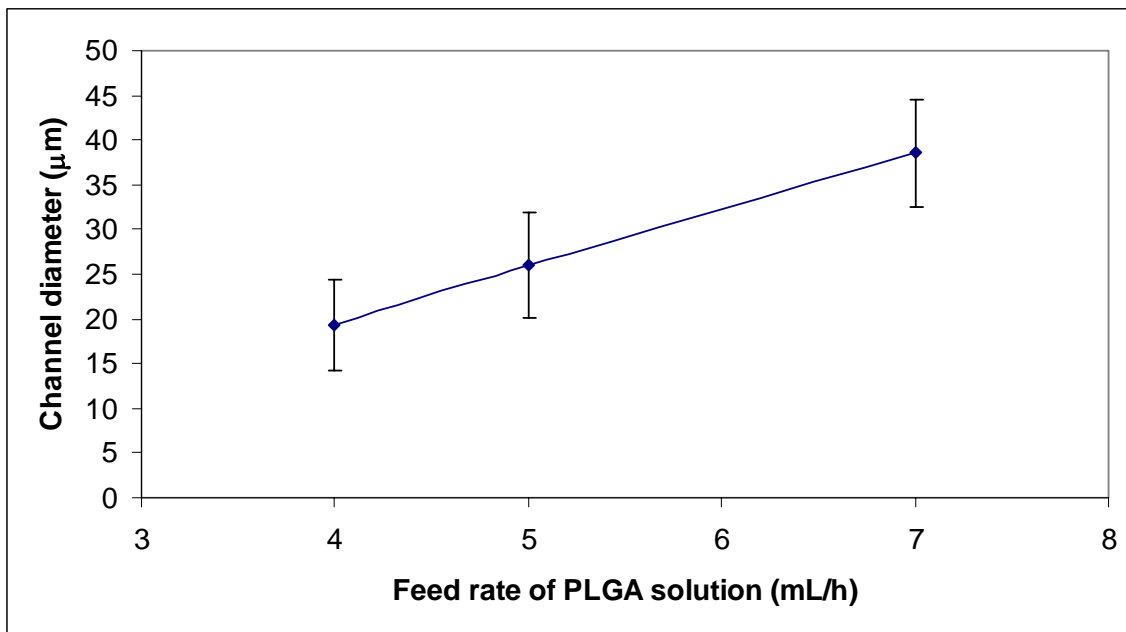
Figure 5.6. Analysis of electrospun nanofibrous guidance channels – diameter
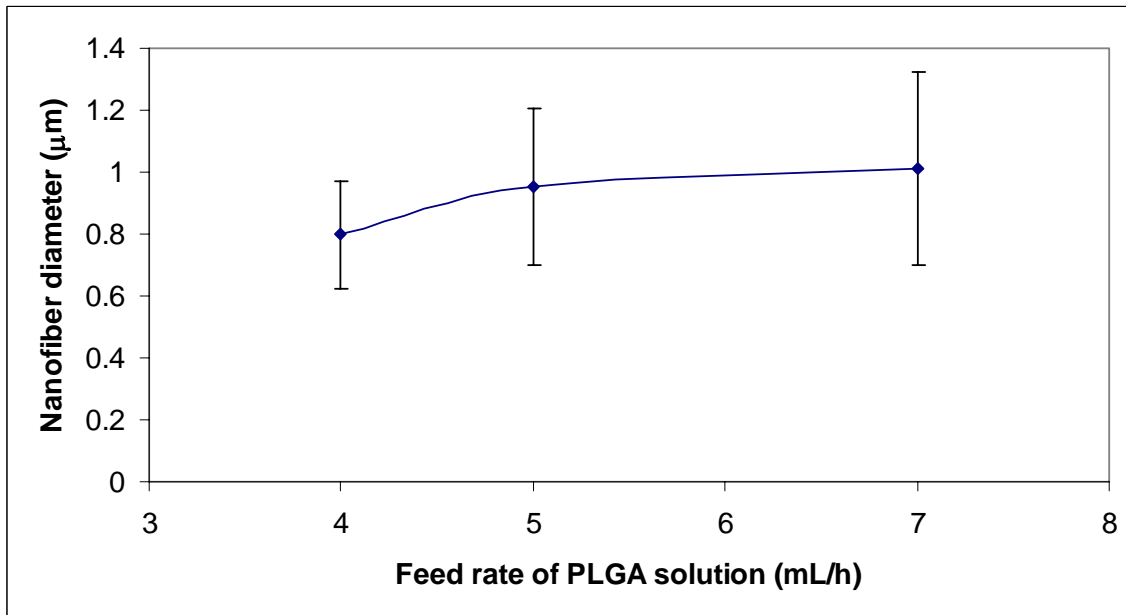
Figure 5.7. Analysis of electrospun nanofibrous guidance channels - nanofiber

diameter

5.3.3   NGF-PLGA nanofiber intra-luminal guidance channels

5.3.3.1 ELISA analysis of released NGF from intra-luminal guidance channels

To verify the presence of NGF in the intra-luminal channels, protein release kinetics was performed. Figure 5.8 shows the cumulative mass of NGF released per milligram of intra-luminal channels that was determined by NGF ELISA. Similar to previous studies that have used electrospinning to produce proteins-polymer nanofibers [128, 130], a continuous release of partially bioactive nerve growth factor was achieved for at least two months.
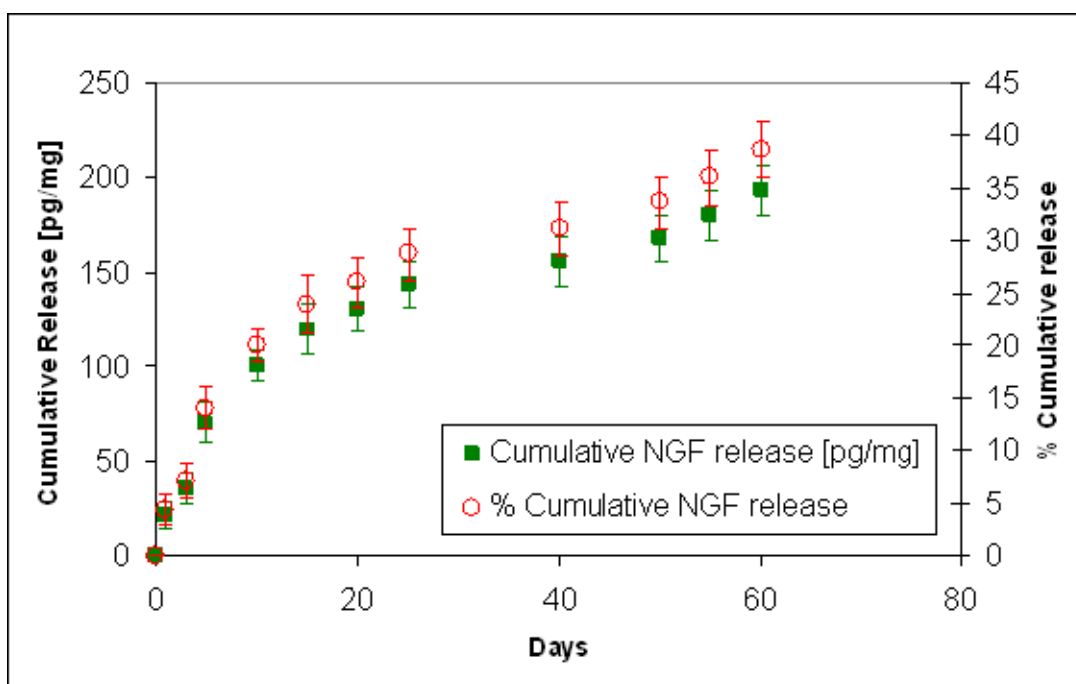
Figure 5.8. Cumulative release profile of NGF from PLGA intra-luminal guidance channels. The concentration of NGF was determined by using NGF ELISA.

5.4   Discussion

Empty bridging conduit for nerve gap repair provides limited tissue-level guidance because of the lack of tissue or artificial structures to guide the growing axons across the site of the injury. This can thus cause axon misdirection and suboptimal functional recovery [9]. To effectively design scaffolds for nerve repair, it is essential to understand the biological events that follow after nerve transection. After injury, the distal axons will degenerate and associated Schwann cells will break down their myelin sheath after nerve injury. During Wallerian degeneration, axons and myelin debris will be removed by the denervated Schwann cells and infiltrating macrophages through phagocytosis. Schwann cells start to proliferate 3 to 4 days after injury [177]. As Schwann cells lose contact with the axon, they will proliferate and subsequently form the bands of Büngner which are oriented columns of cells and laminin [122]. The bands of Büngner are critical physical substrates that support and allow the regenerating axons to cross the nerve gap. If the nerve gap is too large, formation of these biological structures would be compromised [9]. Therefore it may be advantageous to produce and bioengineer intra-luminal guidance channels that can act as exogenous support for axons to advance towards the distal stump.

In this chapter, poly(L-lactic acid)-*co*-poly(glycolic acid) was used to fabricate nanofiber membranes and intra-luminal guidance channels. In the preliminary study, poly(D,L-lactic acid)-*co*-poly(glycolic acid) nanofibrous membrane, another commonly used biomaterial used to fabricate scaffolds for medical applications, was observed to shrink extensively in PBS that rendered it to be unsuitable for producing

the guidance channels. Another report has also shown that poly(D,L-lactic acid)-*co*-poly(glycolic acid) nanofibrous membranes could shrink up to 84% from its original size [178]. Because extensive shrinking of the nanofibrous intra-luminal guidance channels will block the lumen of the conduit that will impede the extension of axons and migration of Schwann cells, careful selection of polymer to fabricate guidance channels in this project was made. In a preliminary study, minimal shrinking was observed when poly(L-lactic acid)-*co*-poly(glycolic acid) nanofibrous membrane were incubated in PBS and ethanol, it was suitably used to fabricate guidance channels by electrospinning.

The formation of cellular cable by the Schwann cells to provide a bridge that direct and organize the axonal extension as the nerve regenerates across the conduit. However for relative large nerve gaps, formation of this cellular guidance cable may not be completed in a timely manner for the advancing growth cone to adhere and extend. To enhance the guidance environment in the nerve conduit, bioabsorbable PLGA nanofibrous intra-luminal channels were introduced into the conduit lumen to act as an initial substrate for the migration of Schwann cells and extension of axons. At the polymer solution feed rate of 3-5 mL/h, diameter of PLGA and NGF-PLGA guidance channels measured 25 ± 5 μm, with nanofiber diameters of 200-600 nm. Although the incorporation of intra-luminal guidance strands had been studied previously, these strands were made up of single fiber with diameter of 5 μm or more [152, 153]. They did not take advantage of the nano-scale topography that has the potential to enhance and promote nerve regeneration significantly. In this chapter,

three-dimensional nanofibrous intra-luminal guidance channels were successfully fabricated such that each guidance channel was made up of several aligned nanofibers that had sufficient mechanical properties to be implanted *in vivo*. The nanofiber bundle could provide excellent supporting substrates for advancing growth cone due to a larger surface area to volume ratio, and the longitudinally aligned nanofibers resembled the endoneurial tubes that served to guide the advancing axons linearly towards the distal nerve stumps.

Electrospinning has been shown to be useful in encapsulating neurotrophic factors for sustained release applications. The ease of production of nanofibers and incorporation of various therapeutic molecules into nanofibers has made electrospinning a versatile technique in fabrication of nanoscaffolds. PLGA nanofibers can be electrospun with proteins that allow us to incorporate neurotrophins for sustained release at the nerve repair site. PLGA and NGF-PLGA nanofibers were electrospun and shown to support neural cell attachment, proliferation and differentiation. Several polymer-protein scaffolds were studied for repair of spinal cord and peripheral nerve injuries [130, 179]. The released of NGF from the nanofiber membrane was shown to induce neurite extensions on cultured undifferentiated PC12 cells. A previous study that used a cellular assay has shown that bioactivity of NGF released from electrospun nanofibers was demonstrated for 85 days [128]. Hence the described results suggested that bioactive NGF was successfully incorporated into electrospun fibers to act as a drug-delivery vehicle for supporting nerve regeneration.

Continuous release of neurotrophic factors from the nano-topograhical intra-luminal channels can potentially provide a sustained amount of biochemical signals to guide axonal extension for nerve tissue engineering. NGF was incorporated into the intra-luminal guidance channels. The fabricated fibers had an average loading of 0.002% as determined by NGF ELISA, despite the theoretical NGF loading efficiency that was calculated at 0.005%. The lower NGF encapsulation efficiency observed possibly suggested that some growth factor was denatured by the organic solvent and electrical potential during preparation and fabrication procedures. In this study, encapsulation efficiency of NGF in electrospun fibers was satisfactory albeit the low encapsulation efficiency. Delivery rates of 2.78 and 44.8 ng/mL/day were reportedly required to maintain a two-month NGF concentration of 1 ng/mL (minimum concentration to maintain survival of dorsal root ganglion neurite outgrowth) for human median nerve and rat sciatic nerve repairs [126]. Based on the ELISA study, it was calculated that the intra-luminal channels that were used in the animal study (described in Chapter 6) had a NGF release rate (bioactive and/or non-bioactive) of approximately 7 ng/mL/day. NGF was successfully incorporated into the nanofibers for therapeutic release. Electrospinning technique used in this chapter provided flexibility for the use of different polymer or polymer-protein blend to fabricate the membranes and intra-luminal guidance channels. This also allows the moderation of the biodegradation rate that can be optimized for nerve regeneration.

Superior performance of autologous nerve grafts can be attributed to the presence of Schwann cells that produce adhesion molecules and neurotrophic factors. Although

Schwann cells produce several growth factors such as NGF and BDNF [180], providing exogenous Schwann cells need to be further analyzed for optimal seeding density despite their importance for essential for successful nerve regeneration [181]. Additionally, the implantation of foreign cells in medical applications would likely cause immunological problems, it is aimed to design a cell-free nerve construct that can promote Schwann cell migration and maturation [92]. There are no known studies that evaluated the use of intra-luminal guidance channels made up of longitudinally aligned nanofibers in the lumen of nerve conduits to repair nerve transection injury. In this chapter, novel intra-luminal channels of longitudinally aligned nanofibers were electrospun to support Schwann cells migration and axonal extension that can be placed in a nerve conduit to study its effectiveness to aid nerve regeneration *in vivo*.

5.5   Conclusion

Presently, intra-luminal guidance channels that have been reported in literature were mainly made up of single fibers in the micro-scale dimensions. The intra-luminal channels made up of aligned nanofibers were successfully fabricated using electrospinning. Nerve growth factor was successfully coupled onto the nanofibers to fabricate NGF-PLGA intra-luminal guidance channels that provided sustained release of the biomolecules.

Chapter 6

In vivo study of nanofiber nerve constructs in rat sciatic nerve injury model

6.1   Introduction

Nerves can be injured by physical trauma, external compression, thermal, chemical, or pathological etiologies. Unlike neurons in the central nervous system, peripheral nerve and its neurons can repair spontaneously when injured although varying degree of functional recovery will be obtained. The current clinical gold standard practice to bridge up transected peripheral nerve gap is the use of autologous nerve graft such as the sural nerve or the lateral antebrachial cutaneous nerve [79]. However repair using autologous nerve grafts presents problems such as donor site mobility, potential formation of painful neuroma at the donor site, or shortage of donor nerves. In nerve tissue engineering, synthetic nerve devices have been designed to replace the use of autologous nerve grafts. They are typically tubular conduits made from natural or synthetic biodegradable polymers [2] to bridge up nerve gaps of several millimeters. Introducing intra-luminal guidance channels in the lumen of a conduit may also improve the result of nerve repair. In this chapter, bilayered nanofibrous conduit containing novel intra-luminal guidance channels that were made up of longitudinally aligned nanofibers (Fig. 6.1) was evaluated to determine if the nerve construct was beneficial for nerve repair and regeneration.
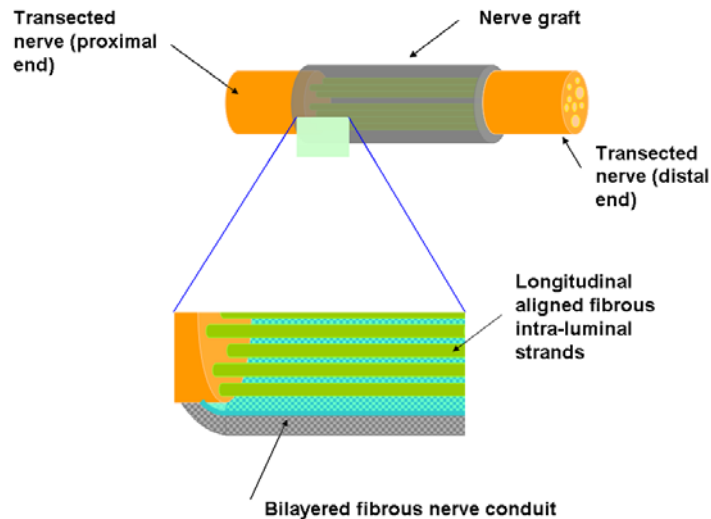
Figure 6.1. Schematic of nanofibrous nerve implant device for peripheral nerve repair. Bilayered nerve conduit was made up of longitudinal aligned nanofiber inner membrane and randomly arranged nanofiber outer membrane. Intra-luminal guidance channels (strands or yarns) were made up of several longitudinally aligned nanofibers.

Biochemical signals that are beneficial for nerve regeneration include haptotactic and chemotactic cues. Haptotactic cues that involves the use of ECM proteins such as collagen, fibronectin, and laminin have considerable positive effects on nerve regeneration [11, 122]. Chemotactic cues involve using neurotropic and neurotrophic factors to regulate the survival, maintenance, and functions of the neurons. Hence it would be valuable to incorporate haptotactic and chemotactic signals in the design of bioengineered nerve constructs. This chapter aimed to evaluate the nanofibrous nerve implant device consisting of a bridging conduit and intra-luminal guidance channels

(Fig. 1.1) that combined synergistic effects of physical topographical and biochemical cues to repair and bridge up transected sciatic nerve in rats.

6.2   Materials and Methods

All chemicals were obtained from Sigma-Aldrich (St Louis, MO) and were used as received, unless otherwise stated. Poly(L-lactic acid) (PLLA) that had an inherent viscosity of 1.09 dL was bought from Lactel Absorbable Polymers (Pelham, AL). Poly(L-lactic acid)-co-(glycolic acid) (PLGA) (70:30) was bought from Polysciences, Inc. (Warrington, PA). Rat 2.5S NGF was obtained from R&D Systems (USA) and mouse laminin was purchased from Invitrogen Corporation, USA.

6.2.1   Fabrication of nanofibrous nerve construct

PLLA solution was prepared by dissolving PLLA in HFP at a concentration of 15% w/v. Blended laminin-PLLA solution (15% w/v) at ratio of 250:1 (weight of PLLA : weight of laminin) was prepared by uniformly mixing PLLA and laminin in HFP at room temperature. Bilayered nanofibrous conduit was fabricated using the electrospinning set-up and procedures described in Chapter 3.

PLGA solution were prepared by dissolving PLGA in HFP at a weight concentration of 35% w/v. NGF-PLGA solution was prepared by dissolving PLGA in HFP at a concentration of 35% w/v. An amount of 50 μg rat 2.5S NGF (R&D Systems, USA) and 3 mg bovine serum albumin (BSA, Sigma) were added to 1 g PLAGA solution (35% w/v in HFP) to form blended NGF-PLGA solution. PLGA and NGF-PLGA

intra-luminal guidance channels were fabricated by the electrospinning set-up and procedures described in Chapter 5.
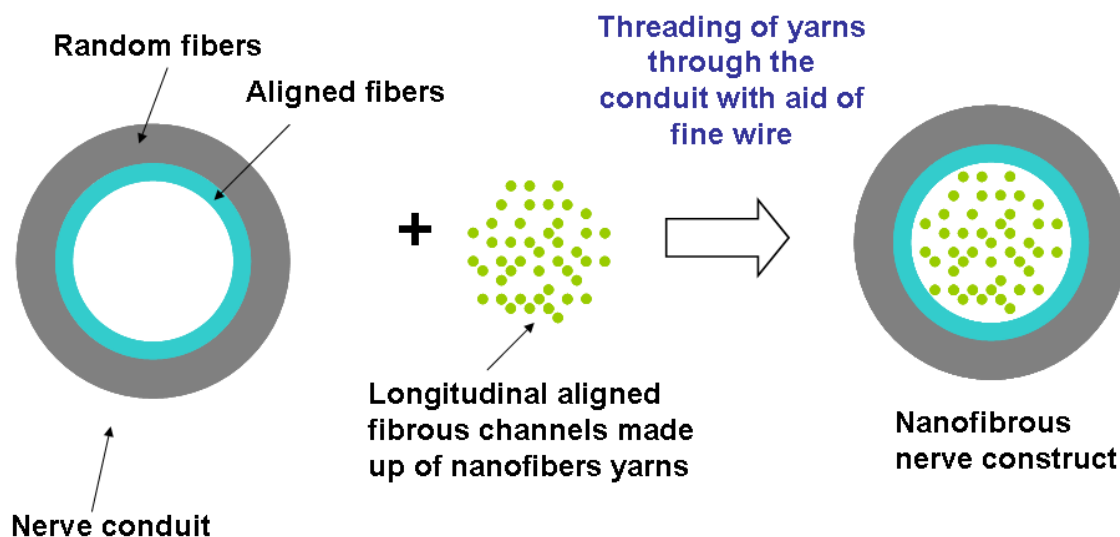
Figure 6.2. General fabrication scheme of nanofiber nerve construct.

Bilayered nerve conduit was packed with intra-luminal channels at a density that occupied approximately 10% of the entire conduit lumen area to minimize hindrance of nerve tissue growth in the bilayered conduit. Briefly, 1.5 mm conduit had lumen area of 1.8 mm^2 and 10% of intra-luminal guidance channels would occupy 0.18 mm^2. Guidance channels of 25 mm in length were weighed that covered approximately 0.02 mm^2 (assuming each channel was 25 μm in diameter). Subsequently, mass of intra-luminal guidance channels that occupied 0.18 mm^2 (i.e. 10% of the lumen area) were weighed and incorporated into the conduit.

6.2.2 Characterization of nanofibrous nerve construct

Morphology of electrospun nanofibers was studied using SEM (JSM-5800LV, JEOL, Tokyo, Japan). The nanofibers were sputter-coated with gold up to 100 s in a JEOL JFC-1200 fine coater. An accelerating voltage of 10 kV was used to examine the morphology of the electrospun scaffolds. Ranges of nanofiber diameters were determined based on the SEM images with the use of an image analysis software (ImageJ; National Institutes of Health, Bethesda, MD).

6.3 Animal implantation study

6.3.1 Experimental groups

Nanofibrous nerve constructs were evaluated for their efficacy to promote nerve regeneration. Experimental groups include (a) nerve conduit only (Group A, n = 10), (b) nerve conduit + intra-luminal guidance channels (Group B, n = 10), (c) nerve conduit coupled with laminin + intra-luminal guidance channels (Group C, n = 10), (d) nerve conduit + intra-luminal guidance channels encapsulated with NGF (Group D, n = 9), (e) nerve conduit coupled with laminin + intra-luminal guidance channels encapsulated with NGF (Group E, n = 10), and (f) autologous nerve graft as the positive control group (Group F, n = 7). Prior to implantation, the excess intra-luminal guidance channels that were protruding the conduit were trimmed with sterile surgical scissors.

6.3.2   Implantation

Operations were performed on male Wistar rats (weighing 200-250 g). All procedures strictly adhered to the guidelines of the University Institutional Animal Care and Use Committee that has been approved. The rats were anesthetized subcutaneously with xylazine and ketamine hydrochloride mixture. Surgical sites were shaved and prepared with iodine. A skin incision was made and the muscles were exposed and retracted. Sciatic nerve was exposed and a 10 mm nerve segment was resected in each animal, and resulted in a gap of approximately 15 mm (Fig. 6.3). The nerve construct was sutured into the resulting gap using non-absorbable 10-0 suture ethilon (Ethicon, USA) on each end and muscle and skin incisions were closed with absorbable 4-0 Vicryl suture (Ethicon, USA). The closed wound was further treated with Opsite spray dressing (Smith & Nephew, UK). The rats were monitored for a duration of 3-month.
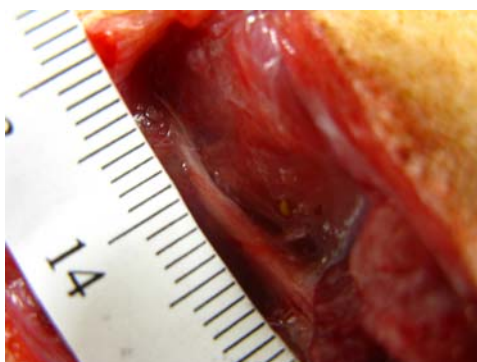
Autologous nerve graft   Nanofibrous nerve construct

Figure 6.3. Implantation of nerve constructs in sciatic nerve.

6.3.3 Neurobehavioral tests

6.3.3.1 Sensory function recovery analysis

Sensory functional recovery was evaluated by positioning the rats to stand with affected hind foot on a hotplate at 56 ^{o}C (Fig. 6.4). The time was measured for the rat to withdraw the affected hind foot from the hotplate, and the test was terminated when no withdrawal occurred within 12 s to prevent any injury. A positive sensory recovery was considered when the rat was able to remove its hind limb within 12 s as placed on the hotplate. The animal was tested at week 0, and fortnightly until week 12 post-implantation.

Figure 6.4. Sensory recovery test using hot plate at 56 ^{o}C.

6.3.4 Neurophysiological test

Nerve conduction studies were performed prior to tissue harvesting at the 12 week end-point using a 2 channel nerve conduction machine (Medelec Synergy Oxford Instrument). Nerve action potential (NAP) conduction velocity and NAP amplitude of the reinnervated gastrocnemius muscle were measured to analyze axonal regeneration (Fig. 6.5). Stimulating electrode was placed at the distal stump (to repair) of the repaired sciatic nerve, while recording electrode (TECA Accessories; Oxford Instruments, UK) was placed in the right gastrocnemius muscle. A ground electrode was placed at the skin. Evaluation of the test was performed when the rats were under general deep anesthesia. Conduction velocities were calculated from the measured latencies and distances.
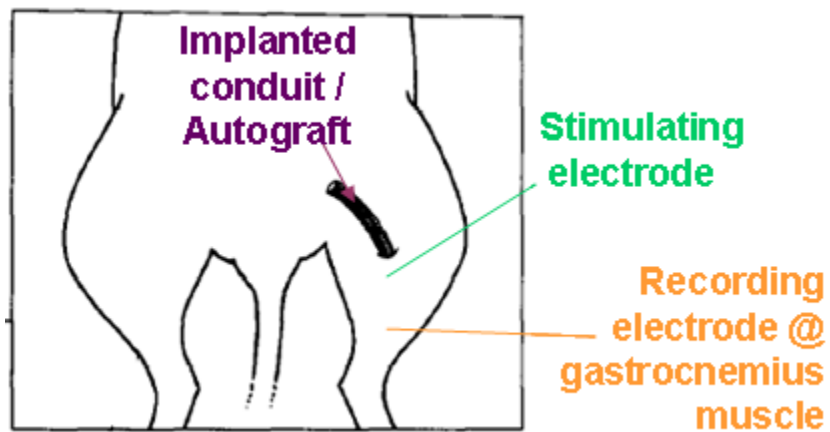
Figure 6.5. Schematic representation of nerve conduction test performed on regenerated sciatic nerve.

6.3.5   Explant of tissue

6.3.5.1 Regenerated Nerves

A skin incision was made and the muscles were exposed and retracted in the anesthetized rats at the study end-point (week 12 post implantation). The implant device was exposed and the surrounding tissues were carefully dissected from the device. The repaired sciatic nerve was excised, including several millimeters proximal and distal to the implanted device.

6.3.5.2 Muscles

Muscle wasting is normally observed after nerve transection injury. The degree of long-term recovery of muscle reinnervation was assessed by weighing the gastrocnemius muscles [65]. At the study end-point (week 12 post implantation), the muscles were harvested and weighed from the experimental and normal sides while the animals were under deep anesthesia. If muscle reinnervation occurred as nerve repair progressed, muscle atrophy at the experimental side would be minimized. Hence, indirect measurement of muscle reinnervation was evaluated by analyzing the calculated ratio of experimental muscle and contralateral intact muscle mass [65].

6.3.6   Biological examinations

6.3.6.1 Neurofilament and S-100 Schwann cell protein immunostaining

The repaired sciatic nerve was carefully dissected from surrounding tissues and excised, including several millimeters proximal and distal to the implanted device. The specimen was fixed by immersion in 4% paraformaldehyde cacodylate-buffered solution overnight at 4 ^{o}C. Subsequently, the segments were cryopreserved in 30% sucrose solution overnight at 4 ^{o}C and frozen in tissue embedding OCT compound in a -80 ^{o}C freezer (Tissue-Tek, Sakura). The tissue was sectioned at 10 μm and processed for double immuno-staining of neurofilament 200 kDa (NF200, Sigma) and S-100 (S-100, Dako) proteins. Non-specific antibody adhesion was blocked by incubation in 20% goat serum for 2 hours and then incubated with mouse anti-NF200 and rabbit anti-S-100 antibodies overnight at 4 ^{o}C. Subsequently, secondary goat anti-mouse FITC and goat anti-rabbit TRIBC antibodies were incubated with the tissue sections and processed for confocal scanning laser microscope observation.

6.3.6.2 Quantification of regenerated axons

Axon density and axon diameter distribution were quantified from the confocal scanning laser micrographs using image analysis software (ImageJ, NIH). Random and separate cross sections of every experimental animal's mid-graft nerve tissue sections (20 x lens objective) were taken for evaluation.

6.3.6.3 Scanning electron microscopy of nerve implant and regenerated tissue

Regenerated nerve tissue and conduit were fixed in 4% paraformaldehyde cacodylate-buffered solution overnight at 4 $^{\circ}$C and cryo-protected in OCT (optimum cutting temperature) embedding medium in -80 $^{\circ}$C freezer. The tissue was sectioned at 10 μm and was thoroughly with PBS. The tissue section was subjected to a graded series of ethanol dehydration and dried completely before observation under the scanning electron microscope. SEM (JSM-5800LV, JEOL, Tokyo Japan) was used to visualize the tissue and the nerve construct after 3 months of implantation. The nanofibers and regenerated tissue were sputter-coated with gold up to 90 s in a JEOL JFC-1200 fine coated and an accelerating voltage of 10 kV of the SEM was used to examine the morphology of the electrospun scaffolds. Range of nanofiber diameters were determined based on SEM micrographs with the use of image analysis software (ImageJ; National Institutes of Health, Bethesda, MD).

6.3.7 Statistical analysis

All data presented are expressed as mean ± standard deviation (SD). Each of the dependent variables from muscle mass, neurophysiological and histochemical data was analyzed separately. Mean values from each variable were compared using ANOVA Single Factor analysis to compare 2 groups using a 95% confidence interval. ANOVAs analysis was conducted and the level of statistical significance is defined as $p < 0.05$.

6.4   Results

6.4.1   Nanofibrous nerve construct

Bilayered nanofibrous conduit and longitudinally aligned nanofibrous intra-luminal guidance channels were fabricated by electrospinning. PLLA and laminin-PLLA nanofibrous conduits were fabricated to exploit the physical nano-topographical morphology and the ECM to present a more natural interface and biochemical motifs for cell-matrix interactions. Intra-luminal guidance channels were fabricated to mimic the basal laminae of peripheral nerve that could act as substrates for axonal outgrowth and Schwann cells migration for nerve repair. Figures 6.6 and 6.7 illustrate the macrographs and scanning electron micrographs of the nerve construct, respectively.

Figure 6.6. Macrographs of nanofibrous nerve construct. (a) bilayered nanofibers nerve conduit, (b) intra-luminal guidance channels, and (c) nerve conduit containing intra-luminal channels.
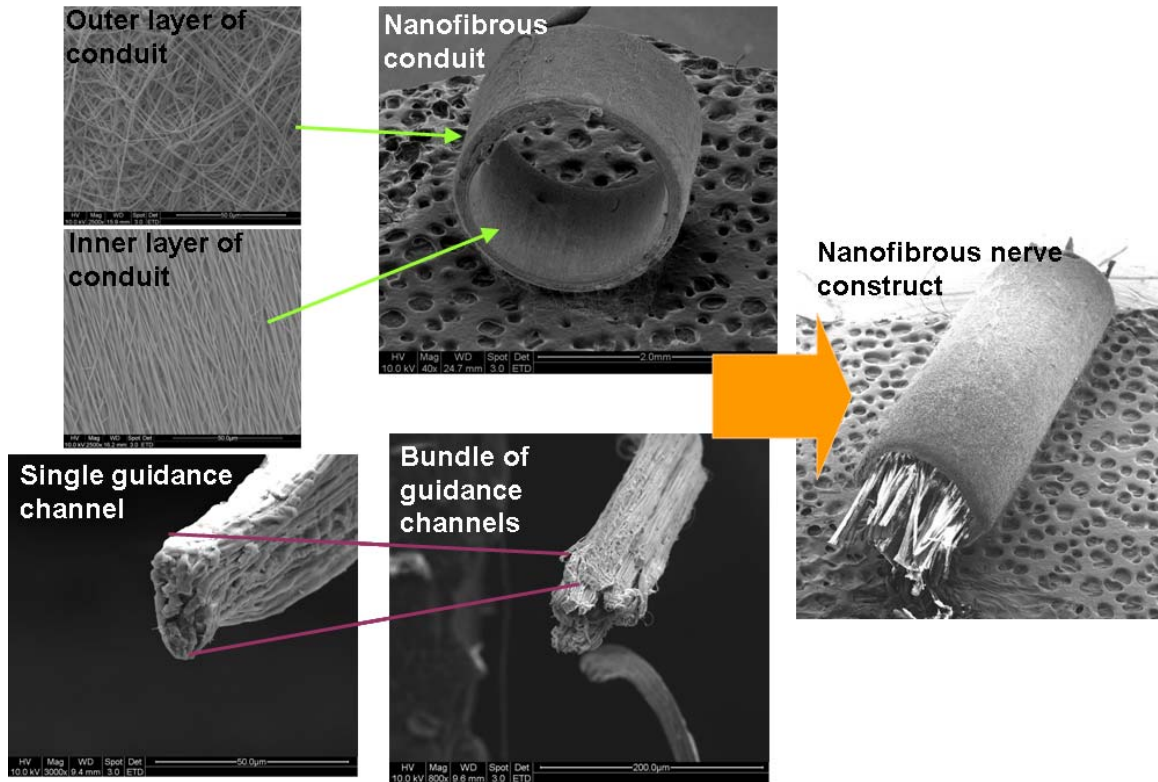
Figure 6.7. Scanning electron micrographs of nanofibrous nerve construct.

6.4.1.1 Nanofibrous nerve conduit

The fabricated conduits did not show significant swelling and no obvious *in vitro* degradation of the PLLA nanofibers was observed over 4 months macroscopically (Chapter 3). Besides evaluating PLLA nanofibrous conduit for bridging nerve gap injury, laminin-PLLA nanofibrous conduit was also fabricated using blended electrospinning to exploit the ECM molecule that can present a more natural interface and provide biochemical motifs for cell-matrix interactions to enhance nerve regeneration.

6.4.1.2 Nanofibrous intra-luminal guidance channels

Individual intra-luminal guidance channel was made up of nanofibers bundle (bundle had a diameter range of 25 ± 5 µm) (Fig. 6.7), consisting of PLGA fibers with diameter of 200-600 nm. Intra-luminal guidance channels were inserted into the lumen of the nanofibrous conduits, occupying approximately 10% of the lumen area. This amount was loaded to reduce any hindrance to axonal outgrowth, while providing sufficient substrates for guidance of axons and migration of Schwann cells along the intra-luminal guidance channels. To determine if the addition of neurite-promoting neurotrophins such as NGF would aid in nerve repair, NGF-PLGA intra-luminal guidance channels were fabricated using blended electrospinning and the unique electrospinning set-up described in Chapter 5. *In vitro* analysis of NGF release form the intra-luminal guidance channels were sustained for at least 2 months (Chapter 5). The combination of nanofibrous conduit and intra-luminal guidance channels was evaluated for its efficacy to aid in nerve repair. The devices were implanted into rat sciatic nerves using microsurgery procedure. No ripping of conduits was observed when they were sutured into the transected nerves.

6.4.2   Nerve explants and gross findings

Explantations of implants were performed 12 weeks after implantation. The implanted conduits were still present at the operated sites, with no obvious biodegradation of the PLLA or laminin-PLLA nanofibrous conduits. Minimal adhesion was observed between the nerve implants and the surrounding tissues, and no noticeable neuroma formation could be found at the proximal and distal suture

sites (Figs. 6.8 and 6.9). There were also no observable wound inflammations. The nanofibrous conduits did not show significant swelling when immersed in saline solution a period of 2 months, thus no compromise of the quality of nerve regeneration was expected [87] or seen in this study. Table 6.1 describes the occurrences of conduit collapse after 3-month implantation. Half of the experimental empty nanofibrous conduits (Group A) collapsed while most or all of the nanofibrous conduits that contained intra-luminal guidance channels maintained conduit patency. Tissue cables formation across the interstump gaps were observed in all the animals, except in two of the 10 rats in Group A (bilayered nerve conduit + saline). Observation of nerve tissue traversing across the interstump gap showed that the presence of intra-luminal guidance channels guided nerve regeneration that did not hamper the axonal extensions through the lumen of the conduit. It is noted that although 50% of the empty conduits collapse, there was still an 80% of the empty conduits (Group A) with regenerated tissue bridging across the gaps. The collapse of these conduits could have occurred after the formation of the new nerve tissue.
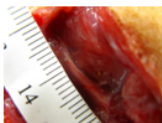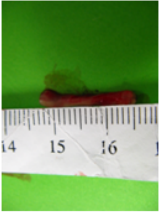
Nerve Construct						
Group	Nerve conduit	Nerve conduit + intra-luminal guidance channels	Nerve conduit coupled with laminin + intra-luminal guidance channels	Nerve conduit + intra-luminal guidance channels encapsulated with NGF	Nerve conduit coupled with laminin + intra-luminal guidance channels encapsulated with NGF	Autograft resected from the rat sciatic nerve
Explanted Nerve						

Figure 6.8. Images of regenerated nerve explants.
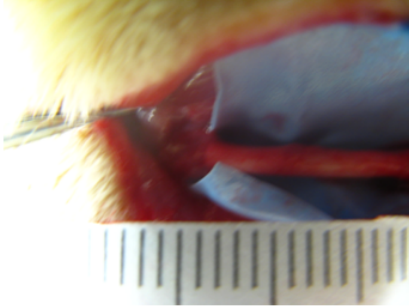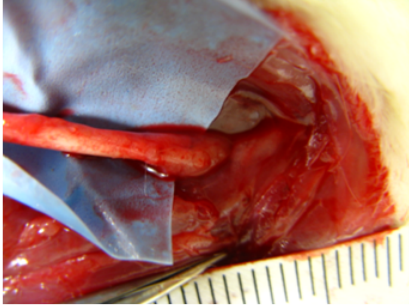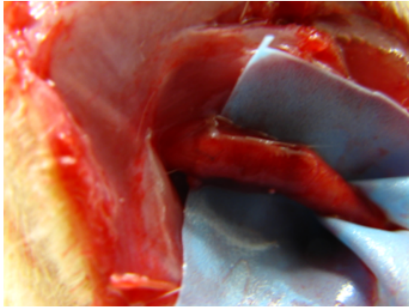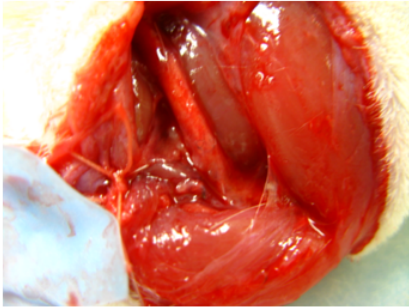
Position	Proximal	Distal
Nanofibrous conduit only (representative image)		
Nanofibrous conduit with intra-luminal guidance channels (representative image)		

Figure 6.9. Images of proximal and distal stumps of the nerve constructs after 3 months implantation.

Table 6.1. Description and results of *in vivo* experimental groups.

Group	Components	Number of animals	% of rats with regenerated nerve across the nerve gap	% of collapsing tubes
A	Nerve conduit	10	80	50
B	Nerve conduit + intra-luminal guidance channels	10	100	10
C	Nerve conduit coupled with laminin + intra-luminal guidance channels	10	100	0
D	Nerve conduit + intra-luminal guidance channels encapsulated with NGF	9	100	0
E	Nerve conduit coupled with laminin + intra-luminal guidance channels encapsulated with NGF	10	100	0
F	Autologous nerve graft	7	100	0

6.4.3 Sensory functional recovery analysis

Thermo-sensitivity was used to evaluate sensory functional recovery. The results are presented in Table 6.2. The experimental animals suffered sensory loss following sciatic nerve transections. Within six weeks after surgery, all animals implanted with intra-luminal guidance channels (Groups B-E) regained thermo-sensitivity and maintained reactivity till the end-point of the study. All rats with nerve implants containing intra-luminal guidance channels showed good recovery (100% recovery) as compared to the control groups (42.9% and 50% for autograft and empty nanofibrous conduit, respectively). This result indicated that intra-luminal channels could potentially aid nerve repair and sensory function repair. However, the addition of NGF in the guidance channels for sustained release did not show superior improvement on sensory functional recovery in this study. Some animals slowly developed thermo-sensitivity, but some also lost the reactivity to hotplate stimulation over the observation period. Similar gain and loss of sensory nerve recovery has also been described in another study [99] in which autologous nerve grafts and decellularized muscle grafts were implanted to repair 20 mm sciatic nerve gaps in rats for a period of 7 weeks. Studies have described that recovery of sensory nerve functions will start with the expansions of axons from the neighbouring tissue [182]. Collateral sprouts of axons from intact fibers in the skin around the denervated area may contribute to the return of sensory functions [183]. The sprouted sensory axons reconnected to the targets would be maintained if the targets were sensory synaptic origins, otherwise the regenerated axons would degenerate that could still result in the

loss of function [183]. In other cases, the sensory axons could regenerate at a slower speed to connect to the appropriate sensory targets for functional recovery.

Table 6.2. Sensory recovery test result.

		Nerve conduit (Group A)						Nerve conduit + intra-luminal guidance channels (Group B)						Nerve conduit coupled with laminin + intra-luminal guidance channels (Group C)						Nerve conduit + intra-luminal guidance channels encapsulated with NGF (Group D)						Nerve conduit coupled with laminin + intra-luminal guidance channels encapsulated with NGF (Group E)						Autologous nerve graft (Group F)					
Week		2	4	6	8	10	12	2	4	6	8	10	12	2	4	6	8	10	12	2	4	6	8	10	12	2	4	6	8	10	12	2	4	6	8	10	12
Animal	1	-	+	+	-	-	-	-	-	+	+	+	+	+	+	+	+	+	+	+	+	+	+	+	+	+	+	+	+	+	+	-	+	+	+	+	+
	2	-	+	+	-	-	+	-	-	+	+	+	+	+	+	+	+	+	+	+	+	+	+	+	-	+	+	+	+	+	+	-	+	+	+	+	+
	3	-	-	+	-	-	-	+	+	+	+	+	+	+	+	+	+	+	+	+	+	+	+	+	+	+	+	+	+	+	+	-	+	+	+	+	+
	4	-	+	-	+	+	+	-	-	+	-	+	+	+	+	+	+	+	+	+	+	+	+	+	+	+	+	+	+	+	+	-	-	-	-	-	-
	5	-	+	+	-	+	-	+	+	+	+	+	+	-	-	+	+	+	+	+	+	+	+	+	+	+	+	+	+	+	+	+	-	-	-	-	-
	6	-	+	+	-	-	-	-	+	+	+	+	+	+	+	+	+	+	+	+	+	+	+	+	+	+	+	+	+	+	+	+	+	+	+	+	-
	7	-	-	-	-	-	-	-	-	+	+	+	+	+	+	+	+	+	+	+	+	+	+	+	+	+	+	+	+	+	+	-	-	-	-	-	-
	8	-	-	-	-	-	+	+	+	+	+	+	+	+	+	+	+	+	+	+	+	+	+	+	+	+	+	+	+	+	+						
	9	-	+	-	+	+	+	-	-	+	+	+	+	-	+	+	+	+	+	+	+	+	+	+	+	+	+	+	+	+	+						
	10	-	-	-	-	-	+	+	+	+	+	+	+	+	+	+	+	+	+							+	+	+	+	+	+						

(-) no reaction at or after 12s

(+) reaction before 12s

6.4.4 Muscle reinnervation evaluation

Another assessment for evaluating nerve regeneration was achieved by analyzing the gastrocnemius muscles of the animals that provide information on the degree of muscle wasting or muscle reinnervation. Gastrocnemius muscle will start to atrophy when the sciatic nerve is transected because this muscle is supplied by the posterior tibial branch of the sciatic nerve. However if nerve regenerate into the muscle, it will result in a regain in the mass proportional to the amount of muscle reinnervation [85, 184, 185]. The gastrocnemius muscles were thus harvested from the experimental animals and weighed. Muscle reinnervation was indirectly determined by measuring the mass of the muscles in the experimental side as compared to the contra-lateral

intact muscles. There was obvious muscle atrophy in the experimental limbs in some of the animals. Figure 6.10 depicts the measurement and calculation of the experimental muscle and contra-lateral intact muscle mass ratio analysis. Significant improvement in muscle reinnervation was observed in nerve implants that contained intra-luminal guidance channels with biomolecules such as laminin (Group D) or laminin/NGF (Group E) that are compared to autologous nerve grafts and empty conduits. However, the addition of NGF did not significantly improve muscle reinnervation in implants that already contained laminin. There was no significant difference ($p > 0.05$) observed in terms of muscle reinnervation recovery when nerve constructs contained only NGF (Group D) was compared to empty nerve conduits and autologous nerve grafts (Groups A and F, respectively) (Fig. 6.10). NGF is known to positively affect sensory neurons [174], thus the addition of NGF might not be distinctively important for axonal reconnection to muscle synaptic targets. Although repairing with only intra-luminal guidance channels (Group B) did not show significant improvement in muscle reinnervation, the result was comparable to that of the autologous nerve grafts (Group F). Thus the result suggested that the introduction of intra-luminal guidance channels could nevertheless potentially encourage muscle regeneration.
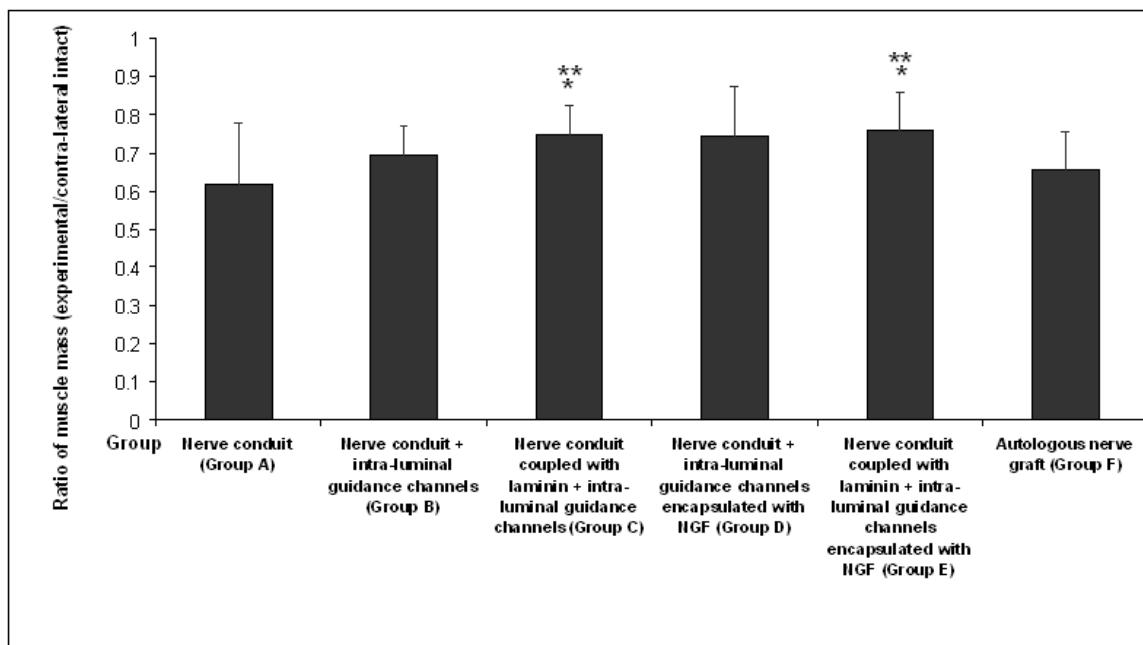
Figure 6.10. Comparison of muscle mass ratio to evaluate the degree of muscle reinnervation after nerve regeneration (* $p < 0.05$, as compared to autologous nerve graft group; ** $p < 0.05$, as compared to empty nerve conduit group).

6.4.5 Nerve conduction study of regenerated nerves

Neurophysiological analysis of the regenerated nerve can provide some information regarding the functional state of the nerves. Nerve conduction study of the regenerated nerves was performed under general anesthesia. To evaluate the recovery of the peripheral nerve segment, conduction velocity and action potential (i.e. amplitude) were obtained. Figures 6.11 and 6.12 compare the conduction velocity and amplitude among the experimental groups. All the experimental nanofibrous nerve constructs demonstrated comparable conduction velocities and amplitudes achieved as compared to the autologous nerve graft group.
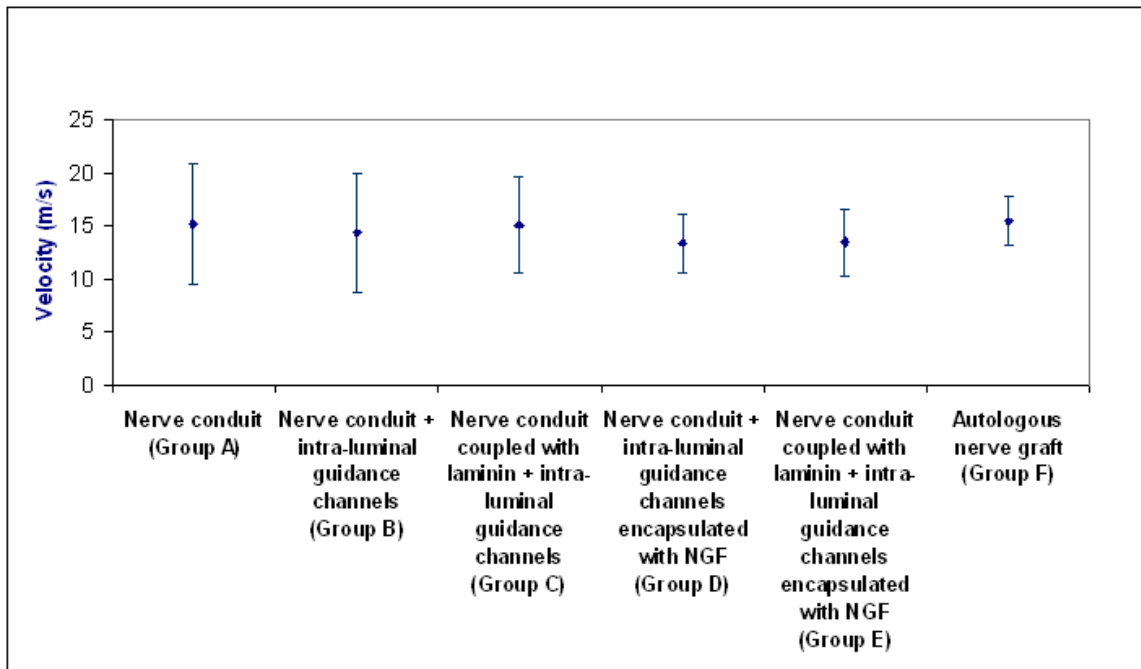
Figure 6.11. Conduction velocity of regenerated rat sciatic nerves at 12 weeks post-surgery.
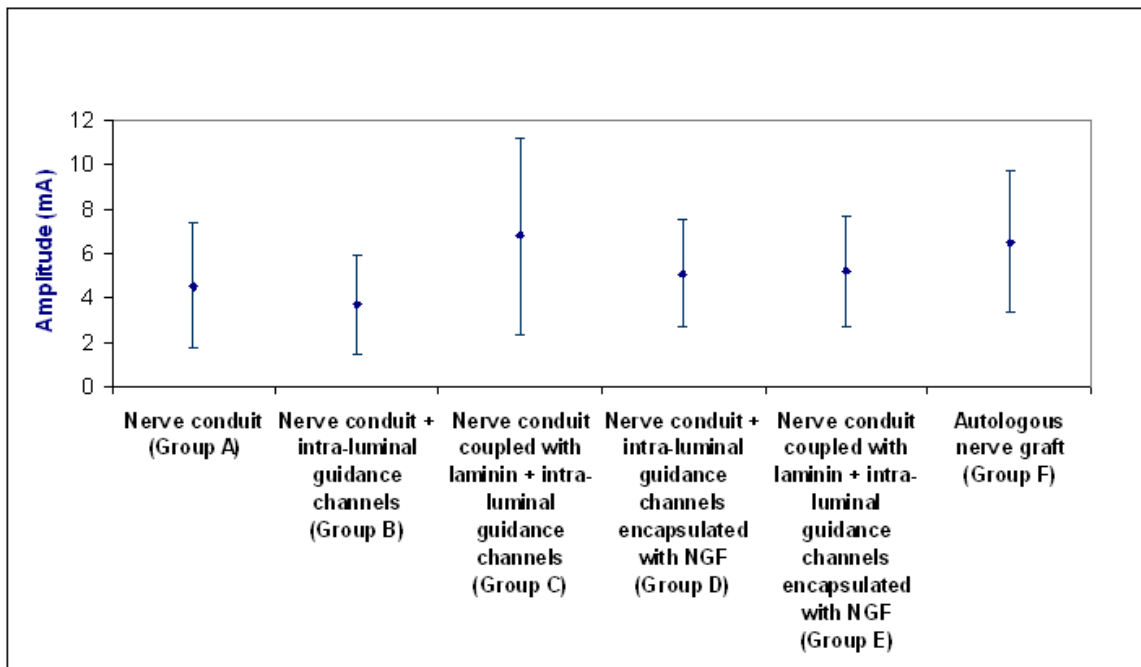
Figure 6.12. Amplitude of regenerated rat sciatic nerves at12 weeks post-surgery.

6.4.6   Immunohistochemistry for neurofilament and S-100 proteins

To visualize the degree of axonal extensions and Schwann cells migration in the regenerated nerve, immunohistochemistry analyses of neurofilament 200 kDa (NF200) and S-100 protein that is specific to Schwann cells were performed (Figs. 6.13-6.16) on the proximal and mid-graft transverse sections. Immunoreactivity to neurofilament 200 kDa was observed in the transverse regenerated nerve segments of the implants after 12 weeks of nerve repair. Neurofilament analysis of axons at the mid-graft sections provided information about the degree of regeneration in the nerve implants (Fig. 6.16). This suggested that myelinated and unmyelinated axons had extended across the gaps into the distal nerve stump.

Schwann cell marker, S-100 protein, staining was also observed throughout the regenerated tissues (Fig. 6.16). Migrated Schwann cells were found throughout all the nerve implants. In this study, there were more S-100 proteins present in the autologous nerve grafts (Group F) as compared to the other groups (Groups A-E) tested, indicating that autologous nerve grafts were superior in supporting Schwann cell proliferation and migration. Schwann cells were shown to ensheath and surround the regenerating axons. The transverse sections revealed that all regenerated axons were observed to co-localize with the Schwann cells. This highlighted that the aligned nanofibers potentially enhanced the migration and maturation of Schwann cells after nerve injury repair and aided axon elongation.
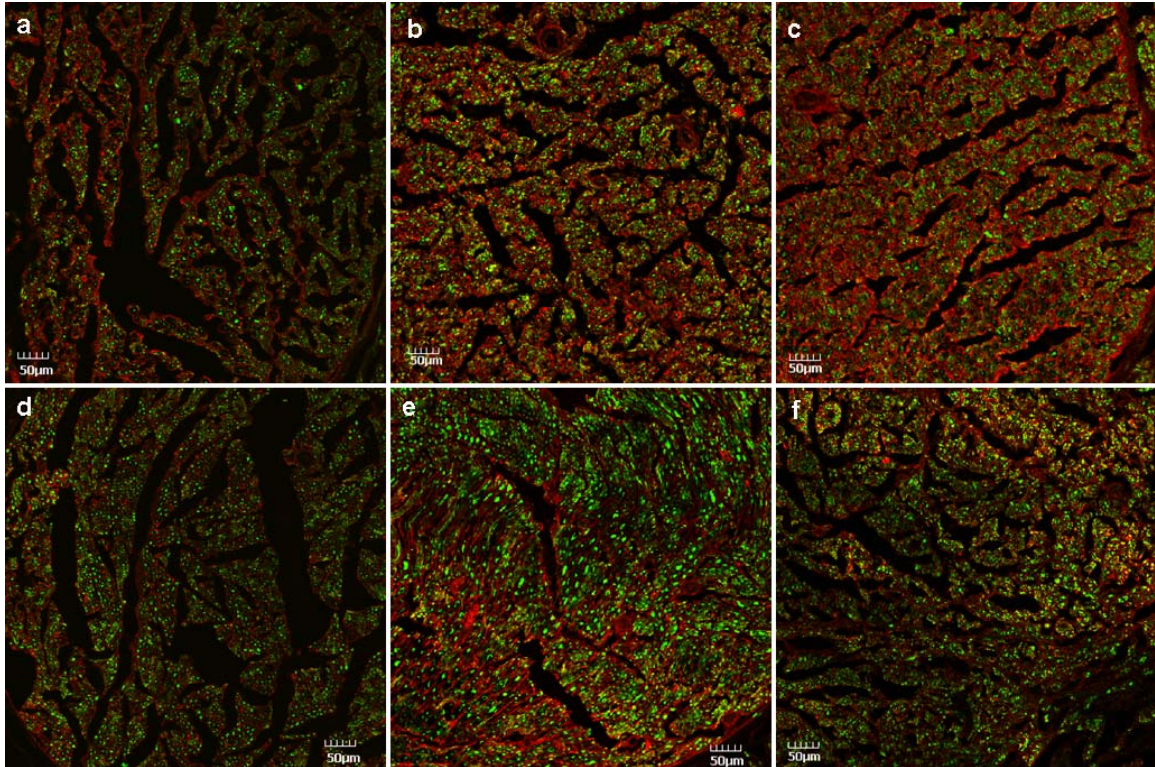
Figure 6.13. Immunohistochemical analysis of nerve regeneration in implants (20x magnification). Double immunostained of NF200 (green) and S-100 (red) (5 mm from proximal nerve stump, transverse cross-section). (a) bilayered nerve conduit with saline, (b) bilayered nerve conduit with intra-luminal channels, (c) bilayered nerve conduit with NGF incorporated intra-luminal channels, (d) bilayered nerve conduit coupled with laminin and intra-luminal channels, (e) bilayered nerve conduit coupled with laminin and NGF incorporated intra-luminal channels, and (f) autologous nerve graft.
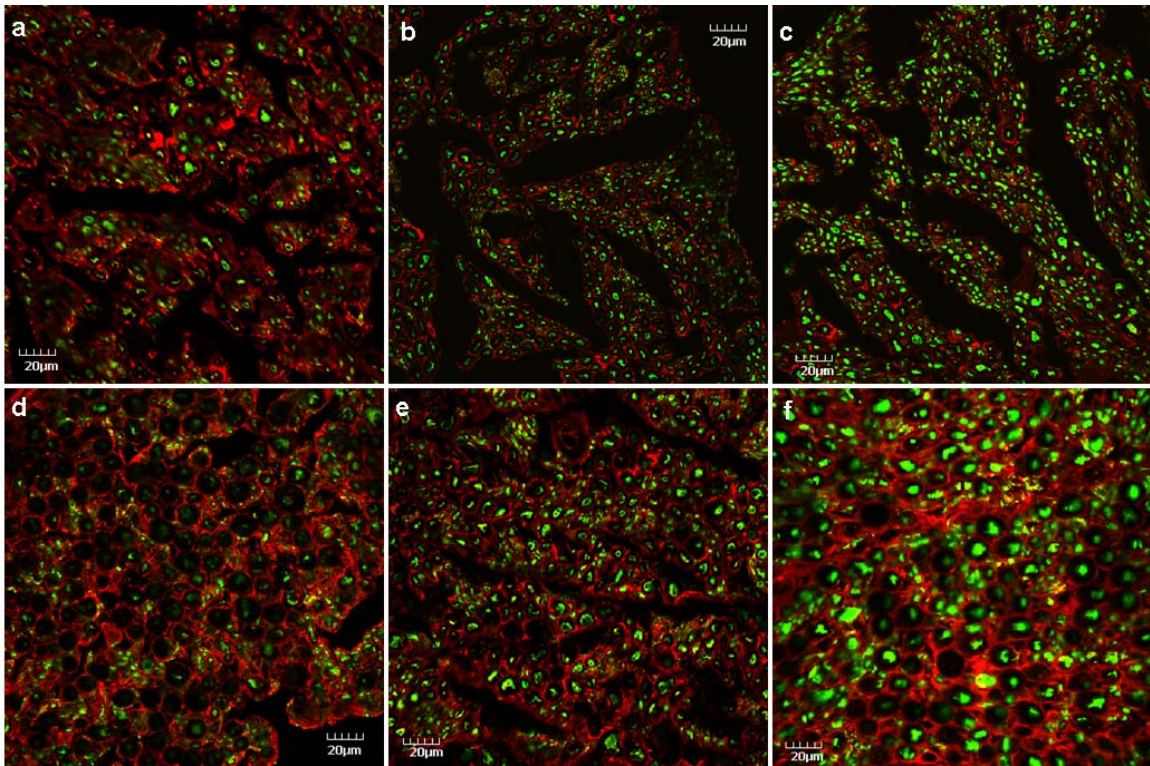
Figure 6.14. Immunohistochemical analysis of nerve regeneration in implants (60x magnification). Double immunostained of NF200 (green) and S-100 (red) (5 mm from proximal nerve stump, transverse cross-section). (a) bilayered nerve conduit with saline, (b) bilayered nerve conduit with intra-luminal channels, (c) bilayered nerve conduit with NGF incorporated intra-luminal channels, (d) bilayered nerve conduit coupled with laminin and intra-luminal channels, (e) bilayered nerve conduit coupled with laminin and NGF incorporated intra-luminal channels, and (f) autologous nerve graft.
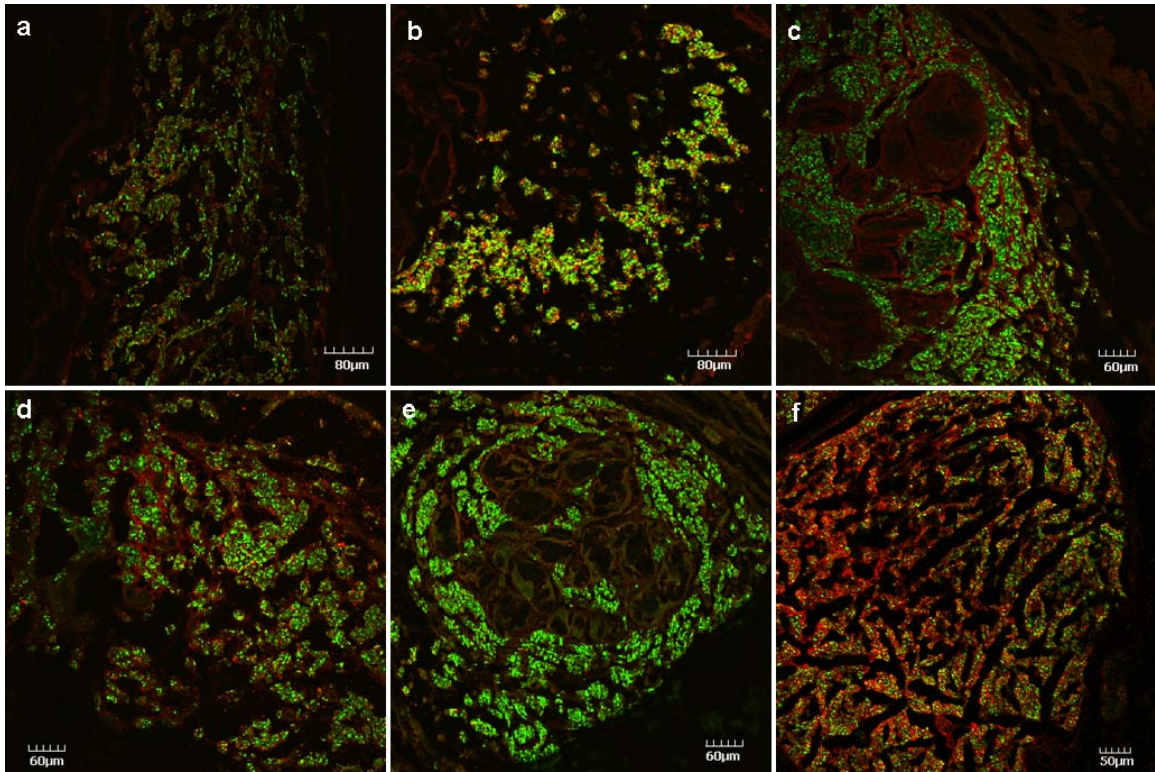
Figure 6.15. Immunohistochemical analysis of nerve regeneration in implants (20x magnification). Double immunostained of NF200 (green) and S-100 (red) (mid-graft, transverse cross-section). (a) bilayered nerve conduit with saline, (b) bilayered nerve conduit with intra-luminal channels, (c) bilayered nerve conduit with NGF incorporated intra-luminal channels, (d) bilayered nerve conduit coupled with laminin and intra-luminal channels, (e) bilayered nerve conduit coupled with laminin and NGF incorporated intra-luminal channels, and (f) autologous nerve graft.
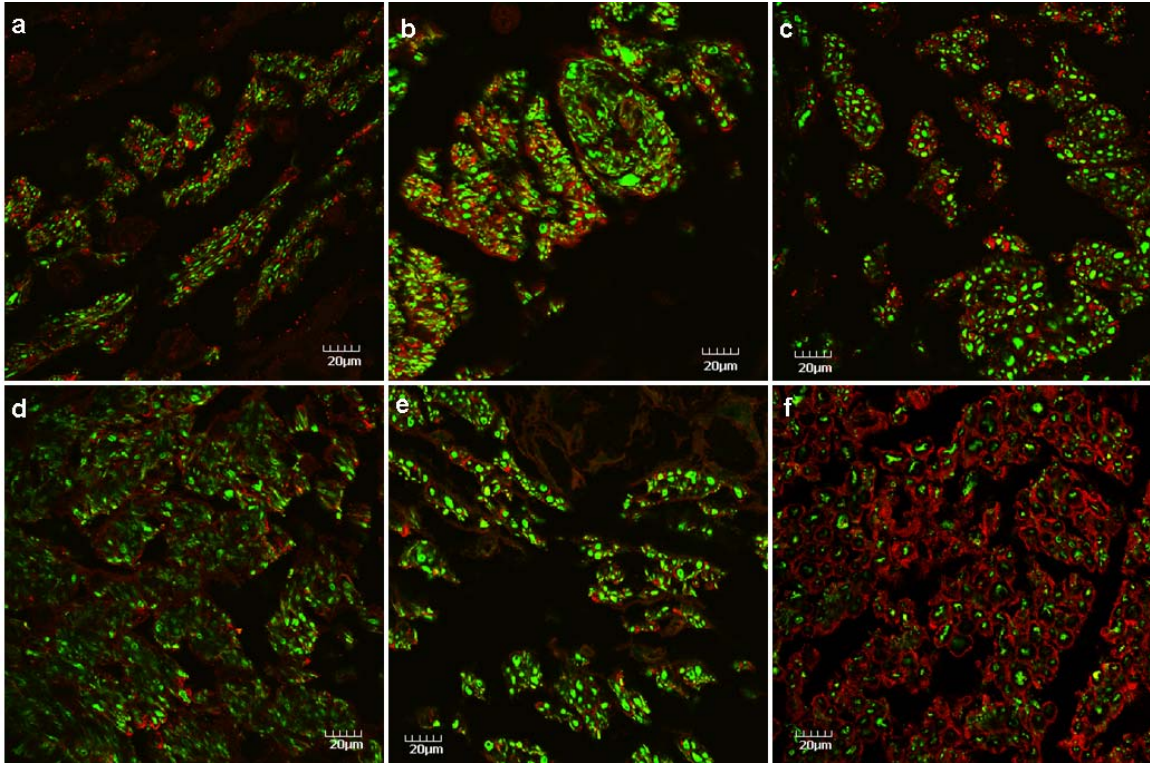
Figure 6.16. Immunohistochemical analysis of nerve regeneration in implants (60x magnification). Double immunostained of NF200 (green) and S-100 (red) (mid-graft, transverse cross-section). (a) bilayered nerve conduit with saline, (b) bilayered nerve conduit with intra-luminal channels, (c) bilayered nerve conduit with NGF incorporated intra-luminal channels, (d) bilayered nerve conduit coupled with laminin and intra-luminal channels, (e) bilayered nerve conduit coupled with laminin and NGF incorporated intra-luminal channels, and (f) autologous nerve graft.

These results showed that axons could be directed to bridge up the gap with the presence of nanofibrous guidance channels. It has been demonstrated that nanofibrous intra-luminal guidance channels can be effectively used to guide axonal extension and Schwann cells migration *in vivo*.

Also, immuno-staining for neurofilaments revealed that axon diameters at the proximal end of the autologous nerve graft group were generally larger as compared to the other experimental groups (Figs. 6.13 and 6.14). However, examining Figures 6.15 and 6.16 revealed that bigger axons were found in the groups that contains intra-luminal guidance channels at the mid-graft sections.

6.4.7   Quantification of regenerated axons

To evaluate the amount of axons that extended and bridged across the interstump nerve gap, analyses of the density of axons at the proximal and mid graft sections are shown in Figures 6.17 and 6.19, respectively. Additionally, the distribution of axons diameter at the proximal and mid graft sections are shown in Figures 6.18 and 6.20, respectively At the mid-graft sections, autologous nerve graft group (Group F) supported significantly more axon elongation across the nerve gap as compared to the other groups (Groups A-E) (Fig. 6.18).
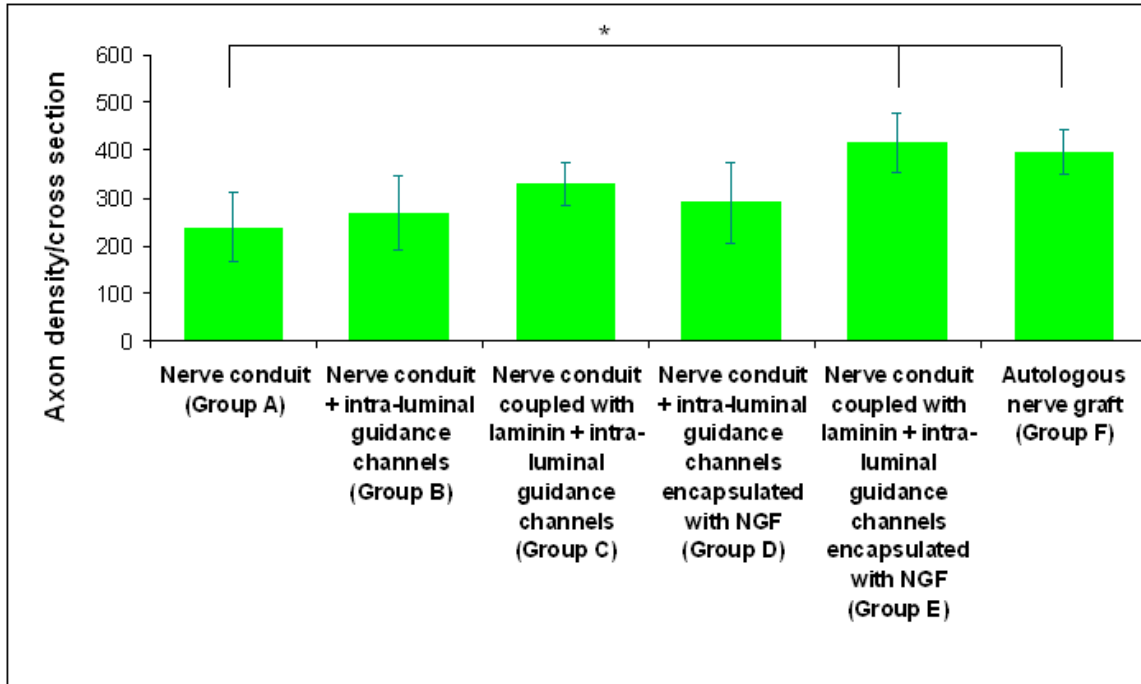
Figure 6.17. Comparison of the axon density at the proximal sections. Group F (autologous nerve grafts group) and Group E (nanofibrous conduit coupled with laminin + NGF incorporated intra-luminal guidance channels) showed significantly higher axon density compared to Group A (nerve conduit only) (* $p < 0.05$).
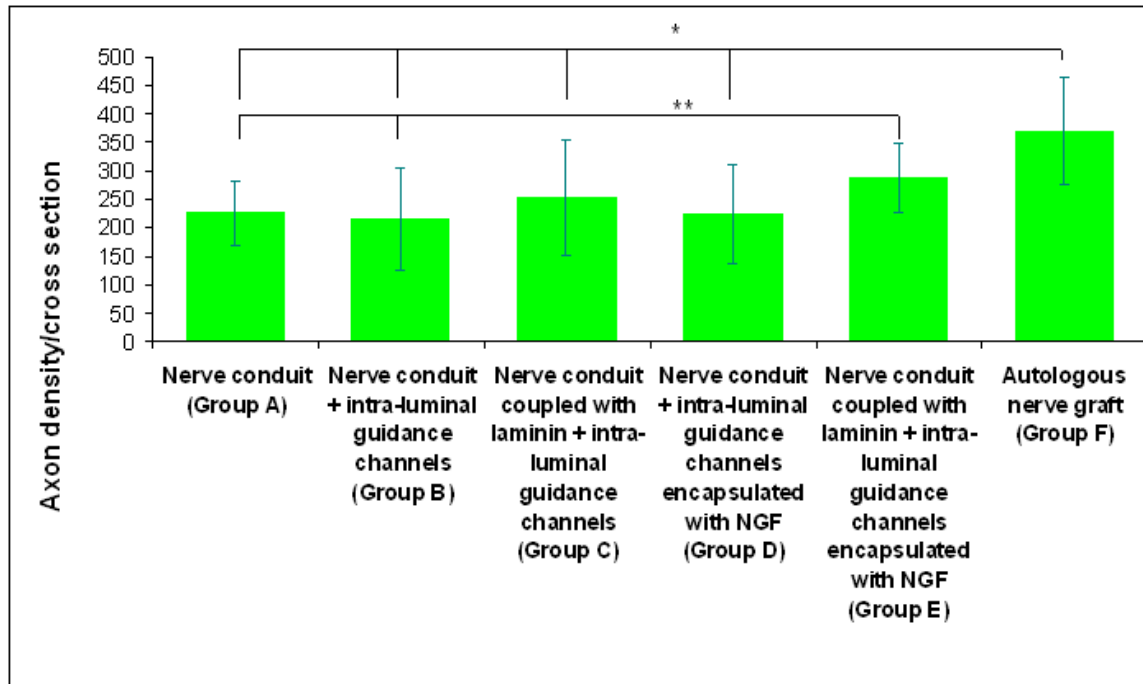
Figure 6.18. Comparison of the axon density at the mid-graft sections. Autologous nerve grafts group (Group F) showed significantly higher axon density compared to all the other experimental groups (* $p < 0.05$, except Group E). Group E (Nanofibrous conduit coupled with laminin + NGF incorporated intra-luminal guidance channels) demonstrated more regenerated axon density compared to Group A (Nanofibrous conduit + saline) and Group B (Nanofibrous conduit + intra-luminal guidance channels) (** $p < 0.05$).
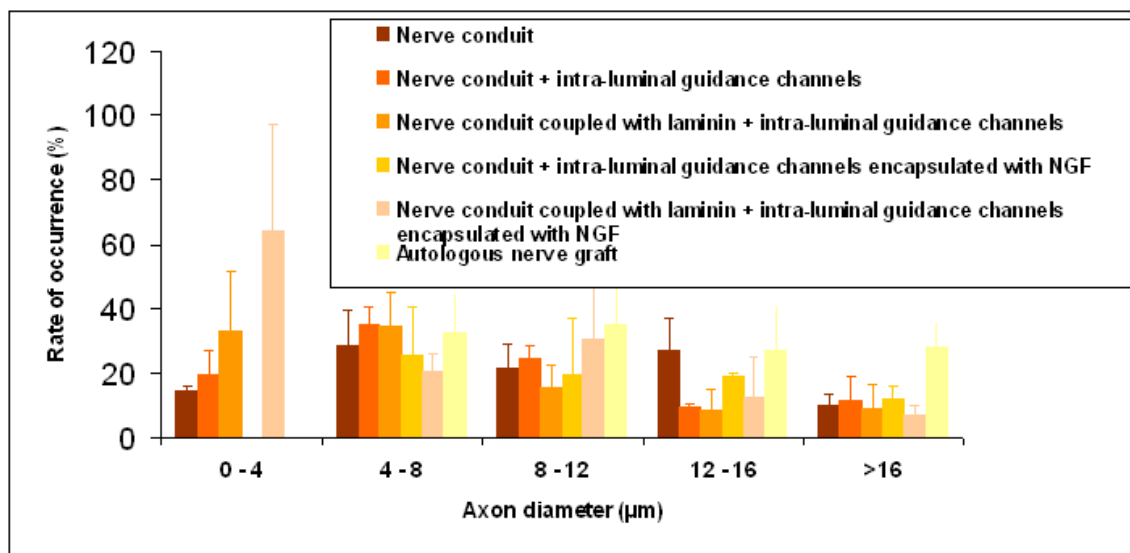
Figure 6.19. Distribution of regenerated axon diameter at the proximal sections.
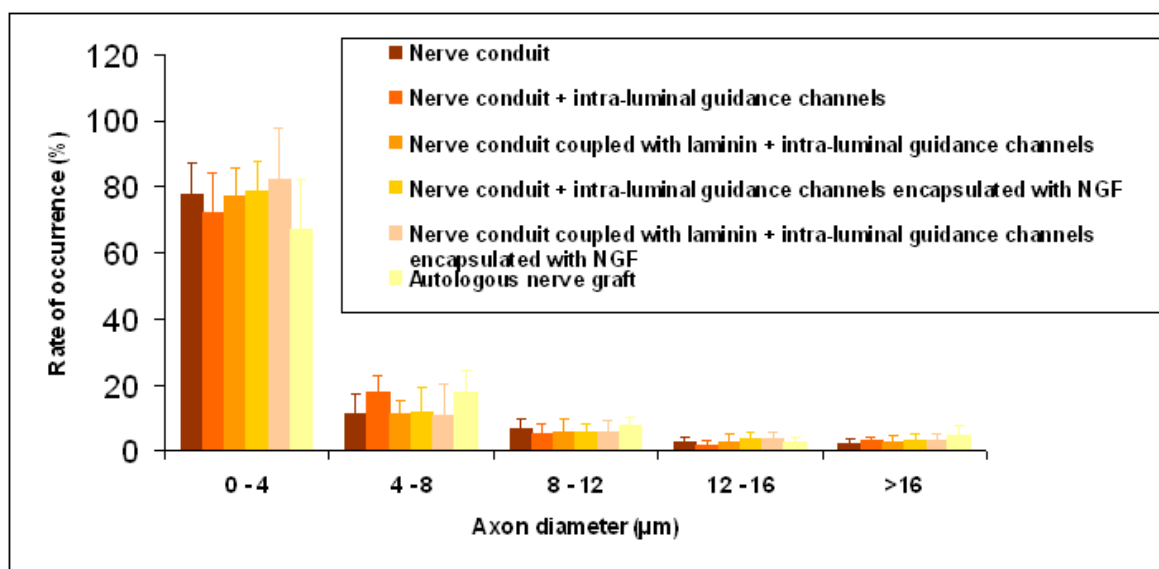
Figure 6.20. Distribution of regenerated axon diameter at the mid-graft sections.

Figure 6.21 illustrates the scanning electron micrographs of nerve tissue regeneration at the mid-sections of the artificial nerve grafts. The PLGA intra-luminal channels were still present and kept in bundles in the nerve constructs after 3-month post implantation.
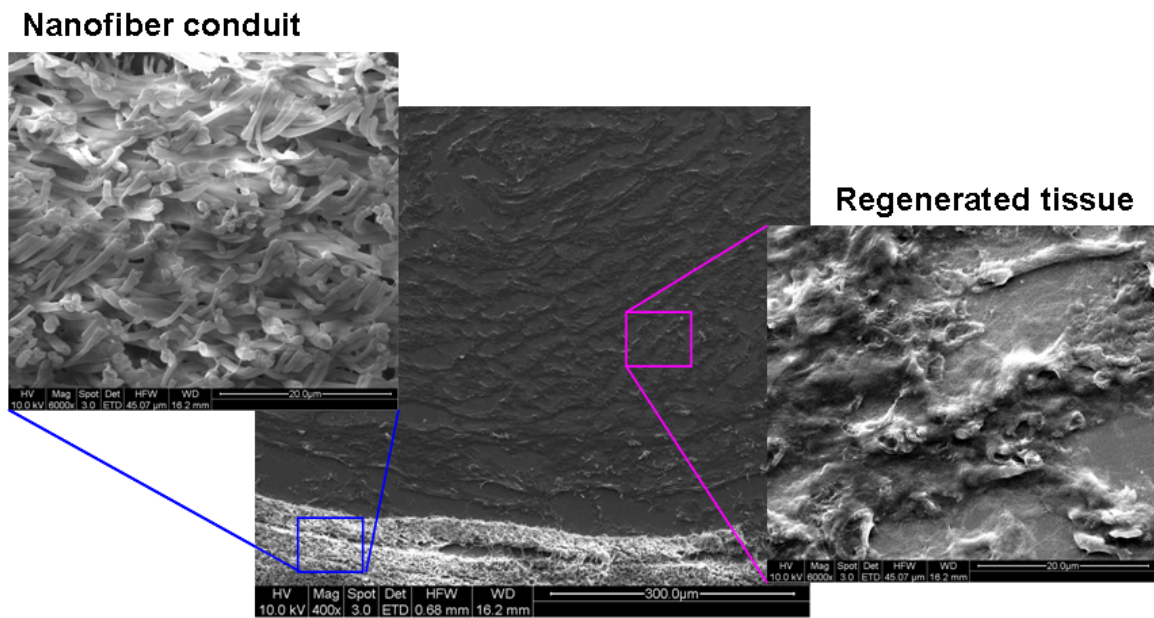
(a)
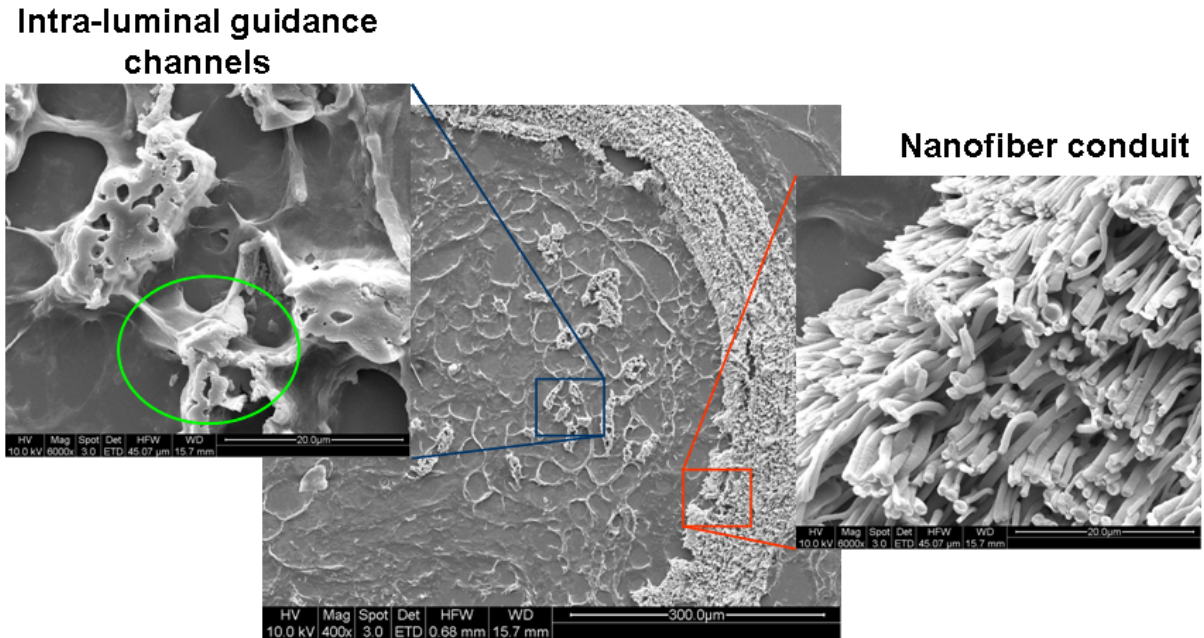
(b)

Figure 6.21. SEM images of the mid-section of nanofibrous nerve graft (a) bilayered nerve conduit only, and (b) bilayered nerve conduit with intra-luminal guidance channels.

6.5   Discussion

Patients with peripheral nerve injuries continue to get unsatisfactory outcomes due to the poor regenerative capacity of nerves. This creates a significant functional problem for patients, as well as social and economic burden for society. When direct repair of the transected nerves is possible, a functional outcome of 80% can be achieved in the best circumstances [2]. When there is a nerve gap that requires bridging with a graft, the results are invariably poor despite using the "gold standard" autologous nerve

grafts. Furthermore, use of autologous nerves grafts is complicated by donor site morbidity, lack of available nerves, and size mismatches. Electrospinning is a versatile technique that can produce nanofibers into highly controllable bioengineered tubular scaffolds and guidance channels that can be used as nerve construct to repair peripheral nerve injuries. An important feature of the nanofibrous nerve implants produced by electrospinning described in this study was the use of aligned nanofibers in the design of the conduit and the intra-luminal guidance channels. Aligned nanofibers have been shown to play pivotal role in promoting and guiding axon growth, and Schwann cells migration and maturation [43, 44]. The nano-texture and topography determine the extent of neurite outgrowth and direct Schwann cell migrations parallel to the aligned nanofibers [12, 43, 44]. In addition, several *in vivo* studies have shown that hollow conduit made up of aligned nanofibers improved nerve regeneration in rat sciatic nerve gap injury [130, 156]. In this study, electrospinning was successfully used to fabricate conduit and intra-luminal guidance channels that were made up of aligned nanofibers to guide nerve regeneration (Figure 6.13-6.20).

A common issue concerning the use of bioengineered conduit is the collapse of the construct when implanted *in vivo*. Collapse of the conduits may limit fibrin matrix formation, cellular infiltration and axonal outgrowth [141], thus affecting the nerve regeneration process. Therefore maintaining the patency of nerve conduit by creating and maintaining the lumen space during regeneration period is crucial for the success of peripheral regeneration within the nerve guidance construct [5, 87]. Despite

observing that 50% of the empty nanofibrous conduits collapsed in this study, the nanofibrous conduits fabricated generally possessed adequate mechanical properties to maintain a stable path for nerve regeneration across the injury site. The collapse of some of the empty conduits could be due to the weaker mechanical properties present at certain regions of each conduit, where less nanofibers were collected onto the region during fabrication that resulted in a smaller wall thickness. Furthermore introducing nanofibrous guidance channels in the lumen of the conduit would likely prevent conduit from collapsing, whilst not hindering nerve regeneration process (Table 6.1). Several researchers had also elegantly studied electrospun aligned nanofibrous conduits for nerve repair [35, 36]; however they had not described the patency of conduits after implantation. The bridging nerve conduit should be able to provide sufficient mechanical support to "withstand long-term *in vivo* forces" [5, 186]. It is also important to consider the probable weakening of the mechanical properties over time due to biodegradation process of the conduit; the degradation rate of nerve conduit must be designed to support the axonal outgrowth and prevent scar ingrowth [74]. In addition, PLLA has been shown to maintain its mechanical integrity for 4 months as described in Chapter 3.

Clinically, synthetic conduits have not functioned as well as autologous nerve grafts [78] for long nerve gap repair. It has been postulated that the basal lamina structures of autologous nerve graft act to provide guidance substrate for axonal outgrowth [9], thus displaying superior nerve regeneration outcome. Intra-luminal guidance channels used in this animal study aimed to mimic the basal lamina and the bands of Büngner

that could act as the initiate guidance scaffolds for axonal extensions towards the distal stump to form functional connections with the target organs. Intra-luminal guidance channels that were made up of aligned polymeric nanofibers were fabricated and a packing density of 10% of guidance channels was incorporated into the bilayered conduit to evaluate axonal regeneration in the transected sciatic nerve. A study performed by Ngo *et al.* [9] studied the effect of packing density of intra-luminal guidance channels in conduits and described that a 7.5% packing density would be optimal for bridging nerve gaps, even when a 3.5% packing density showed greater number of myelinated axons in an *in vivo* experiment. However, too low packing density of guidance channels would result in the tendency of the channels to settle to the bottom of the conduit [9]. In this project, a 10% packing density of intra-luminal guidance channels was used. Nanofibrous PLGA guidance channels (Groups B-E) were shown to enable better functional recovery as compared to autologous nerve graft (Group F). As no axons were found to be in immediate contact with the guidance channels, they did not directly act as scaffolds for axons regeneration. It is likely that these guidance channels aided in nerve regeneration through stabilizing the fibrin matrix that can be found in nerve regeneration process [8] and supporting Schwann cell migration to form bands of Büngner that laid the foundation for advancing axons.

To further enhance the performance of nanofibrous nerve implants, we incorporated laminin in the nerve construct. Laminin has been shown to improve *in vivo* nerve regeneration studies [119, 187-189]. Laminin can be easily electrospun with

biodegradable polymers to generate bioactive scaffolds. Laminin was blended with PLLA for the electrospinning of laminin-PLLA nanofiber conduit. This modification technique was chosen because higher amount of laminin can be coupled onto nanofibers as compared to physical adsorption or covalent binding methods that have been described in Chapter 4. Nerve conduit coupled with laminin was examined for the effect of laminin on *in vivo* nerve repairs. Successful coupling of laminin onto the nanofibers to create the nanofibrous conduit that provided robust regeneration was achieved (Groups C and E). In this experiment, improved muscle reinnervation and neurophysiology test results were observed in the rats that were implanted with constructs that contained laminin (Figs. 6.10-6.12), highlighting the beneficial effects of using laminin for transected nerve gap repair. Especially, laminin present in the nerve constructs was shown to promote muscle reinnervation as shown in Figure 6.10 (Groups C and E). Good muscle reinnervation was observed in the nanofibrous nerve constructs (especially Groups C and E) could be attributed to the presence of higher amount of ECM molecules (i.e. laminin) present in the constructs that can potentially promote better functional recovery. Although other ECM molecules such as collagen and fibronectin have been shown to influence and promote nerve regeneration [2], laminin was chosen as we have determined that laminin was more effective than collagen to promote neurite outgrowth *in vitro* (Chapter 4). A previous study also showed that laminin encouraged better attachment and proliferation of Schwann cells when compared to collagen and fibronectin [122].

Besides using ECM molecules to improve synthetic nerve devices, we also examined the possible additional effect on nerve regeneration if we included neurotrophins in nanofibrous nerve constructs. Encapsulation of neurotrophic factors into nanofibers to facilitate nerve regeneration was achieved in the present study by using blended electrospinning. Concerns regarding the use of blended electrospinning to couple of neurotrophins in nerve guides were low loading protein efficiency and loss of bioactivity of the biomolecules. Despite these limitations, blended electrospinning was chosen to encapsulate NGF in nanofibers because this method could allow uncomplicated fabrication of growth factor-nanofiber intra-luminal guidance channels (Fig. 5.1). In addition, blended electrospinning has been shown to produce nanofibers that contained even distribution of NGF within the fibers [128]. Bioactive NGF has been successfully coupled onto the nanofibrous intra-luminal guidance channels (Groups D and E) for sustained release to aid nerve regeneration in this study. Loading nerve constructs with neurotrophic factors can stimulate peripheral nerve regeneration [2]. These soluble factors play important roles in the differentiation, maintenance, and survival of neurons. NGF, the prototypical member of the neurotrophin family, protects neurons from injury-induced death in transected sciatic nerves [143]. Cell loss in the dorsal root ganglia or in the ventral horn of the spinal cord may be counteracted by administering NGF in the nerve implants. Previous studies have also shown that NGF-polymer nanofibers can be electrospun that maintain the bioactivity of the neurotrophins [128, 130] and electrospun GDNF-polymer nanofibrous conduit promoted rat sciatic nerve gap repair [130]. However, the release of NGF from the nanofibrous nerve constructs did not significantly benefit

functional recovery in terms of muscle reinnervation recovery. This could be due to the lower concentration of NGF released from the guidance channels or the absence of NGF receptors at the growth cones to exert its effects. An increase amount of NGF could be introduced during the fabrication of neurotrophin coupled nanofibers, but the increase in fabrication cost and the feasibility to improve degree of NGF bioactivity have to be examined and considered.

Combining haptotactic and chemotactic cues in the nerve constructs have shown better regeneration in terms of density of axons and functional recovery. Nerve constructs (Group E) that contained both laminin and NGF was shown to encourage axons extensions (Figs. 6.17 and 6.18) that were comparable to the autologous nerve grafts ($p > 0.05$). In terms of sensory recovery, incorporation of laminin or NGF alone in the nerve constructs allowed complete sensory recovery in the rats by week 6 post-implantation (Table 6.2). But the addition of NGF into laminin coupled nerve constructs encouraged early sensory recovery (i.e. by week 2 post-implantation, Table 6.2). Also, the combination of NGF and laminin in nerve constructs improved muscle reinnervation when compared to autologous nerve graft (Group A). A previous study has shown that synergistic combination of laminin and growth factor (i.e. FGF-2) in nanofibers could enhance *in vitro* nerve regeneration [158]. It would therefore be advantageous to incorporate haptotactic and chemotactic cues in the design of nerve constructs to encourage better axonal outgrowth across the interstump gaps.

Nerve conduction analysis of the regenerated nerve showed that the recovery of conduction velocity in the nanofiber constructs was lower than, but comparable to that of the autologous nerve grafts (Fig. 6.11) (non-operated nerve had a conduction velocity of 53 ± 6 m/s [182]). In order to obtain good recovery, proper reinnervation of the axons to the new target is required [182]. Increase in axons count is likely due to axonal sprouting. Several factors affect the quantity of axons such as the pruning of misdirected axons and loss of axons at the suture lines [184]. The number of nerve fibers and the size of the axons may account for the difference observed in nerve conduction study. In this study, more axons and larger axons were observed in autologous nerve graft that likely caused slightly better outcome observed in the nerve conduction velocity study (Figs. 6.17-6.20).

Despite more regenerated axons were found in the autologous nerve grafts (Group F, Figs. 6.17-6.20), functional recovery (in terms of sensory response and muscle reinnervation) was observed to be better in some of the nanofibrous nerve constructs (namely Group C-E). The presence of exogenous laminin and NGF in the nanofibrous constructs might have positive effects on functional recovery observed in the rats that has been discussed previously. In addition, studies have described that the higher degree of axon extensions does not always correlate to the functional recovery due to possible aberrant sprouting and establishment of incorrect synaptic connections with the organs [190, 191].

Synergistic effects of nanotopography and biochemical possessed by the nerve construct described herein present a novel substitute to repair peripheral nerve gap. As the regenerating axons extend towards the distal stump and make contact with Schwann cells, the speed of axonal regeneration may slow down because the axons will be myelinated [192]. Nerve tissue regeneration and functional recovery were shown in histological and animal behavior tests (e.g. nerve conduction, sensory and muscle wasting tests), respectively. Although regenerated axons (Figs. 6.13-6.20) were observed to be greater in the autologous nerve graft (Group F), the other experimental groups (Groups A-E) were able to support better sensory and motor functional recovery results (Table 6.2 and Fig. 6.10) when compared to autologous nerve graft group (Group F) in this study. Similar to the autologous nerve grafts, the conduits were packed with guidance channels could mimic the basal lamina, and the additional presence of inter-nanofiber space of the individual intra-luminal guidance channel could potentially provide axons and Schwann cells to be in adequate proximity to supporting scaffolds for adherence and migration across the interstump gap. Also, the presence of laminin and/or NGF that were added exogenously to the nerve constructs (Groups D-E) could have potentially provided a suitable environment for nerve regeneration that may explain the better functional recovery observed in these nerve constructs (especially Group E).

The observation in this study only lasted for 12 weeks when regeneration of the nerve was still incomplete. Longer observation might be necessary to further evaluate the effectiveness of the nanofibrous constructs for nerve repair. However, the current

results are satisfactory because nerve regeneration of nanofibrous constructs was comparable to that observed in the autologous nerve grafts. More importantly, sensory functional recovery and muscle reinnervation were observed to be even better in the nanofibrous constructs with intra-luminal guidance channels. Careful design of scaffolds in the lumen of the conduit needs to be considered as the presence of exogenous scaffolds in the lumen may impede the migration of cells or hinder the normal process of endogenous matrix formation [193]. In this study, the aligned nanofiber guidance channels were longitudinally arranged that could act to support cellular and axonal migration. This special nanofibrous feature of nerve construct with aligned nanofibrous intra-luminal guidance channels has not been examined in the synthetic nerve constructs up to now and our results suggested that nanofibrous intra-luminal guidance channels might be useful for nerve repair surgeries.

6.6   Conclusion

In this chapter, nerve constructs that combined physical nanotopography and biochemical signals to interpose nerve gaps for the enhancement of nerve regeneration and functional recovery were described. Herein, it has been shown that nanofibrous guidance channels made up of several longitudinally aligned nanofibers can effectively promote peripheral regeneration, evidenced by histological and functional recovery tests. Biochemical cues such as laminin and NGF were incorporated in the nerve constructs to evaluate their roles to improve nerve regeneration *in vivo*. It has been demonstrated that (1) nanofibrous conduit with longitudinally aligned fibrous intra-luminal guidance channels supported Schwann

cell migration and axon extensions *in vivo* (2) nerve enhancing molecules such as laminin could aid in nerve regeneration for bridging peripheral nerve gaps. In this study, nanofibrous nerve construct that combined synergistic effects of physical and biochemical cues described in this thesis could be further improved and potentially replace the use of autologous nerve grafts to repair injured peripheral nerves seen in the clinical situations.

Chapter 7

Conclusions and Recommendations

7.1   Conclusions

Bioengineered nerve construct is an attractive alternative method for clinicians to repair peripheral nerve injuries that might replace the use of autologous nerve grafts, thus eliminating some of the limitations encountered when autologous nerve grafts were to be used. The ECM of the peripheral nerve is made up of nano- and micro-fibers that present physical and biological cues for cell-matrix interactions, hence nanofibrous scaffolds have been fabricated and investigated to positively influence nerve regeneration. Nanofibrous bridging construct may thus produce better performance and enhance nerve regeneration and functional recovery in the repair of nerve gap injuries. This study aimed to fabricate and evaluate whether nanofibrous conduits containing intra-luminal guidance channels and combination with ECM proteins and neurotrophins would be suitable for repairing nerve transection injury.

Our assessment was performed on established rat sciatic nerve transection injury model and mainly focused on post-operative function recovery and histological parameters. It has been demonstrated that (1) nanofibrous conduit can provide physical guide for regeneration of nerve (2) intra-luminal guidance channels supported Schwann cell migration and axon extensions *in vivo* (3) laminin and neurotrophins such as NGF promoted nerve regeneration for bridging nerve gaps. Successful nerve regeneration requires the survival of neuron cell bodies after injury,

extension of axons to bridge the interstump gap, and functional reconnections of the axons with the appropriate synaptic targets. Axons and Schwann cells progressed longitudinally along the nanofibers as the intra-luminal guidance channels provided mechanical substrates for preferential adhesion and growth and the nanofibrous conduit served to prevent scar formation and entrap secreted beneficial biomolecules within the interstump gap to promote nerve regeneration. Although autologous nerve grafts are viewed as gold solution for repairing nerve gaps, mismatching of regenerated tissue and donor site mobility would need to be considered. Our initial results showed that intra-luminal channels resembled the bands of Büngner and the basal lamina, organized nerve cable formation, and aided in robust regeneration and functional recovery across the nerve gap. Although relatively good functional recovery and innervation was achieved to repair lesion in the sciatic nerve in this study, further comprehensive study should be performed. Larger gap lesions should be evaluated to determine if the novel nanofibrous construct can potentially replace the use of autologous nerve grafts and is useful for repair of transected nerve gaps often seen in the clinics.

7.2   Recommendations for future work

The nerve conduit and intra-luminal guidance channels described herein possessing longitudinally aligned nano-topograhical fibers have shown promising results in supporting directional neuronal growth across lesions *in vivo* to promote better functional recovery. However further comprehensive analysis can be done to investigate the spatial and temporal progression of axons from the proximal to the

distal ends when using this nanofibrous construct. These will provide important information on how the nanofibrous intra-luminal guidance channels acted as scaffolds to support nerve regeneration. Additionally, we observed the presence of relatively intact guidance channels within the conduit at the study end-point that revealed no complete biodegradation of the channels. Further studies can be performed to determine if faster degrading polymers of PLGA that have a lesser content of lactic acid would be more beneficial for supporting nerve regeneration, or vice versa.

Intra-luminal guidance channels can also be made with nanofiber architecture that is shown in Figure 7.1. The hollow inner structure will provide more surface area for regenerating axons and Schwann cells to adhere and extend that will limit the hindrance of nerve regeneration in the lumen of the conduit. Blended collagen-polymer intra-luminal guidance channels can also be fabricated that will provide cell recognition signals and faster degradation rate that may be beneficial for advancing growth cones and migrating Schwann cells in nerve regeneration.
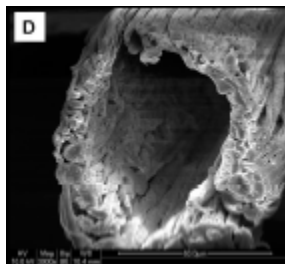
Figure 7.1 Intra-luminal guidance channels made up of hollow yarn.

Laminin presents cell recognition peptides to positively influence nerve regeneration. Laminin can be coupled onto intra-luminal guidance channels to determine if the outcome of nerve repair can be improved. Although laminin is an effective biological molecule to enable enhanced nerve regeneration, there are potential drawbacks of introducing these ECM molecules that originated from immunogenic proteins. We therefore propose to introduce bioactive laminin peptide analogs (e.g. IKVAV and YIGSR) into nanofibers to replace the use of natural biomolecules in the artificial nerve constructs, and that it is currently being investigated in the laboratory. Concerns regarding encapsulation of neurotrophins using conventional blended electrospinning could be minimized or circumvented by using co-axial electrospinning technique to introduce neurotrophins in the nanofibers to protect the neurotrophins during protein-nanofiber fabrication. In a co-axial electrospinning process, two polymer solutions can be concomitantly ejected in an electrostatic field through two co-axial capillaries. This will result in core-shell structured nanofiber. Solutions that are not easily electrospun (e.g. protein solution) can be encapsulated in the core of the core-shell nanofibers if the shell solution can be electrospun. This thus provides consideration protection to the core component from direct exposure to organic solvents, thus keeping maximum bioactivity of the biomolecules.

Peripheral nerve consists of a relative extensive network of blood vessels for maintaining the structural and functional integrity of peripheral axons [61]. For large nerve gap repair, providing sufficient adequate vascularization may be critical for the success of nerve repair so as to provide sufficient nutrients to proliferating Schwann

cells and possibly maintain survival of neurons. Poor vascularization may cause an increase in the formation of fibrosis that will decrease the speed of axonal extension. Angiogenesis can be induced by introducing vascular endothelia growth factor (VEGF) through recombinant protein delivery that will increase vascularity within the nerve construct. However, providing VEGF alone may not be sufficient because formation of dysfunctional, leaky and permanent immature blood vessels may occur [194-196]. Together with VEGF, platelet-derived growth factor-BB (PDGF-BB) may be required for formation of new matured blood vessels to aid in axon extension and maturation [194-196].

Functional nerve regeneration is a complex and delicate process. There is no single approach in the design of nerve construct that can be effective for use in clinical peripheral nerve repair. Better therapies may be required to improve the ability of the surviving neurons to regenerate and increase the speed of axonal outgrowth. For long gap repair, strategies could be devised to prevent the loss of basal laminae of the distal nerves because their maintenance is critical for regenerating axons to have a support to reinnervate and form synaptic contacts with the appropriate targets [197]. Further research in the areas of basic sciences such as developmental biology and applied sciences such as bioengineering is required to produce more suitable substitutes that can provide remarkable outcome of peripheral nerve repair and regeneration.

References

Bibliography

1. Belkas, J.S., Shoichet, M. S. and Midha, R., *Axonal Guidance Channels in Peripheral Nerve Regeneration.* Operative Techniques in Orthopaedic, 2004. **14**(3): p. 190-198.

2. Schmidt, C.E., and Leach, J. B., *Neural tissue engineering: Strategies for repair and regeneration.* Annual Review of Biomedical Engineering, 2003. **5**: p. 293-347.

3. Nichols, C.M., Brenner, M. J., Fox, I. K., Tung, T. H., Hunter, D. A., Rickman, S. R. and Mackinnon, S. E., *Effect of motor versus sensory nerve grafts on peripheral nerve regeneration.* Experimental Neurology, 2004. **190**(2): p. 347-355.

4. Dendunnen, W.F.A., Vanderlei, B., Robinson, P. H., Holwerda, A., Pennings, A. J. and Schakenraad, J. M., *Biological Performance of a Degradable Poly(Lactic Acid-Epsilon-Caprolactone) Nerve Guide - Influence of Tube Dimensions.* Journal of Biomedical Materials Research, 1995. **29**(6): p. 757-766.

5. Katayama, Y., Montenegro, R., Freier, T., Midha, R., Belkas, J. S. and Shoichet, M. S., *Coil-reinforced hydrogel tubes promote nerve regeneration equivalent to that of nerve autografts.* Biomaterials, 2006. **27**(3): p. 505-518.

6. Flemming, R.G., et al., *Effects of synthetic micro- and nano-structured surfaces on cell behavior.* Biomaterials, 1999. **20**(6): p. 573-588.

7. Laurencin, C.T., et al., *Tissue engineering: Orthopedic applications.* Annual Review of Biomedical Engineering, 1999. **1**: p. 19-46.

8. Arai, T., Lundborg, G. and Dahlin, L. B., *Bioartificial nerve graft for bridging extended nerve defects in rat sciatic nerve based on resorbable guiding filaments.* Scandinavian Journal of Plastic and Reconstructive Surgery and Hand Surgery, 2000. **34**(2): p. 101-108.

9. Ngo, T.T.B., Waggoner, P. J., Romero, A. A., Nelson, K. D., Eberhart, R. C. and Smith, G. M., *Poly(L-lactide) microfilaments enhance peripheral nerve*

regeneration across extended nerve lesions. Journal of Neuroscience Research, 2003. **72**(2): p. 227-238.

10. Ma, Z.W., Kotaki, M., Inai, R. and Ramakrishna, S., *Potential of nanofiber matrix as tissue-engineering scaffolds.* Tissue Engineering, 2005. **11**(1-2): p. 101-109.

11. Carbonetto, S., *The extracellular matrix of nervous system.* Trends in Neurosciences, 1984. **7**: p. 382-387.

12. Yang, F., Murugan, R., Wang, S. and Ramakrishna, S., *Electrospinning of nano/micro scale poly(L-lactic acid) aligned fibers and their potential in neural tissue engineering.* Biomaterials, 2005. **26**(15): p. 2603-2610.

13. Xu, C.Y., Inai, R., Kotaki, M. and Ramakrishna, S., *Aligned biodegradable nanofibrous structure: a potential scaffold for blood vessel engineering.* Biomaterials, 2004. **25**(5): p. 877-886.

14. Langer, R., Vacanti, J.P., *Tissue engineering.* Science, 1993. **260**(5110): p. 920-926.

15. Chen, R.R., Mooney, D.J., *Polymeric growth factor delivery strategies for tissue engineering.* Pharmaceutical Res., 2003. **20**(8): p. 1103-1112.

16. Hutmacher, D.W., *Scaffolds in tissue engineering bone and cartilage.* Biomaterials, 2000. **21**(24): p. 2529-2543.

17. Hubbell, J.A., *Biomaterials in Tissue Engineering.* Bio-Technology, 1995. **13**(6): p. 565-576.

18. Zuk, P.A., Zhu, M., Mizuno, H., Huang, J., Futrell, J. W., Katz, A. J., Benhaim, P., Lorenz, H. P. and Hedrick, M. H., *Multilineage cells from human adipose tissue: Implications for cell-based therapies.* Tissue Engineering, 2001. **7**(2): p. 211-228.

19. Ingber, D.E., Mow, V. C., Butler, D., Niklason, L., Huard, J., Mao, J., Yannas, I., Kaplan, D. and Vunjak-Novakovic, G., *Tissue engineering and developmental biology: Going biomimetic.* Tissue Engineering, 2006. **12**(12): p. 3265-3283.

20. Goldberg, M., Langer, R. and Jia, X. Q., *Nanostructured materials for applications in drug delivery and tissue engineering.* Journal of Biomaterials Science-Polymer Edition, 2007. **18**(3): p. 241-268.

21.   Stevens, M.M., and George, J. H., *Exploring and engineering the cell surface interface.* Science, 2005. **310**(5751): p. 1135-1138.

22.   Zhang, S.G., Gelain, F. and Zhao, X. J., *Designer self-assembling peptide nanofiber scaffolds for 3D tissue cell cultures.* Seminars in Cancer Biology, 2005. **15**(5): p. 413-420.

23.   Ellis-Behnke, R.G., et al., *Nano neuro knitting: Peptide nanofiber scaffold for brain repair and axon regeneration with functional return of vision.* Proceedings of the National Academy of Sciences of the United States of America, 2006. **103**(13): p. 5054-5059.

24.   Yang, F., Murugan, R., Ramakrishna, S., Wang, X., Ma, Y. X. and Wang, S., *Fabrication of nano-structured porous PLLA scaffold intended for nerve tissue engineering.* Biomaterials, 2004. **25**(10): p. 1891-1900.

25.   Zhang, Y.Z., Lim, C. T., Ramakrishna, S., Huang, Z. M., *Recent development of polymer nanofibers for biomedical and biotechnological applications.* Journal of Materials Science-Materials in Medicine, 2005. **16**(10): p. 933-946.

26.   Murugan, R. and S. Ramakrishna, *Design strategies of tissue engineering scaffolds with controlled fiber orientation.* Tissue Engineering, 2007. **13**(8): p. 1845-1866.

27.   Strehl, R., Schumacher, K., De Vries, U. and Minuth, W.W., *Proliferating cells versus differentiated cells in tissue engineering.* Tissue Engin., 2002. **8**(1): p. 37-42.

28.   Deister, C., and Schmidt, C. E., *Optimizing neurotrophic factor combinations for neurite outgrowth.* Journal of Neural Engineering, 2006. **3**(2): p. 172-179.

29.   Fine, E.G., Decosterd, I., Papaloizos, M., Zurn, A. D and Aebischer, P., *GDNF and NGF released by synthetic guidance channels support sciatic nerve regeneration across a long gap.* European Journal of Neuroscience, 2002. **15**(4): p. 589-601.

30.   Formhals, A., *Process and apparatus for preparing artificial threads.* US Patent No. 1,975,504., 1934.

31.   Yoshimoto, H., Shin, Y. M., Terai, H. and Vacanti, J. P., *A biodegradable nanofiber scaffold by electrospinning and its potential for bone tissue engineering.* Biomaterials, 2003. **24**(12): p. 2077-2082.

32.   Li, W.J., Cooper, J. A., Mauck, R. L. and Tuan, R. S., *Fabrication and characterization of six electrospun poly(alpha-hydroxy ester)-based fibrous scaffolds for tissue engineering applications.* Acta Biomaterialia, 2006. **2**(4): p. 377-385.

33.   Li, W.J., Laurencin, C. T., Caterson, E. J., Tuan, R. S. and Ko, F. K., *Electrospun nanofibrous structure: A novel scaffold for tissue engineering.* Journal of Biomedical Materials Research, 2002. **60**(4): p. 613-621.

34.   Matthews, J.A., Wnek, G. E., Simpson, D. G. and Bowlin, G. L., *Electrospinning of collagen nanofibers.* Biomacromolecules, 2002. **3**(2): p. 232-238.

35.   Zhang, Y.Z., Ouyang, H. W., Lim, C. T., Ramakrishna, S. and Huang, Z. M., *Electrospinning of gelatin fibers and gelatin/PCL composite fibrous scaffolds.* Journal of Biomedical Materials Research Part B-Applied Biomaterials, 2005. **72B**(1): p. 156-165.

36.   Rho, K.S., et al., *Electrospinning of collagen nanofibers: effects on the behavior of normal human keratinocytes and early-stage wound healing.* Biomaterials, 2006. **27**: p. 1452-1461.

37.   Fertala, A., W.B. Han, and F.K. Ko, *Mapping critical sites in collagen II for rational design of gene-engineered proteins for cell-supporting materials.* J. Biomed. Mater. Res., 2001. **57**: p. 48-58.

38.   Xu, C.Y., et al., *Aligned biodegradable nanofibrous structure: a potential scaffold for blood vessel engineering.* Biomaterials, 2004. **25**: p. 877-886.

39.   Zong, X., et al., *Electrospun fine-textured scaffolds for heart tissue constructs.* Biomaterials, 2005. **26**: p. 5330-5338.

40.   Bini, T.B., Gao, S. J., Tan, T. C., Wang, S., Lim, A., Lim, B. H. and Ramakrishna, S., *Electrospun poly(L-lactide-co-glycolide) biodegradable polymer nanofibre tubes for peripheral nerve regeneration.* Nanotechnology, 2004. **15**(11): p. 1459-1464.

41.   Reneker, D.H., et al., *Bending instability of electrically charged liquid jets of polymer solutions in electrospinning.* J Appl Phys, 2000. **87**: p. 4531-4547.

42.   He, W., Yong, T., Teo, W. E., Ma, Z. W. and Ramakrishna, S., *Fabrication and endothelialization of collagen-blended biodegradable polymer*

nanofibers: Potential vascular graft for blood vessel tissue engineering. Tissue Engineering, 2005. **11**(9-10): p. 1574-1588.

43.   Corey, J.M., et al., *Aligned electrospun nanofibers specify the direction of dorsal root ganglia neurite growth.* Journal of Biomedical Materials Research Part A, 2007. **83A**: p. 636-645.

44.   Chew, S.Y., et al., *The effect of the alignment of electrospun fibrous scaffolds on Schwann cell maturation.* Biomaterials, 2008. **29**: p. 653-661.

45.   Liang, D., Hsiao, B. S. and Chu, B., *Functional electrospun nanofibrous scaffolds for biomedical applications.* Advanced Drug Delivery Reviews, 2007. **59**: p. 1392-1412.

46.   Li, D., Wang, Y. L. and Xia, Y. N., *Electrospinning of polymeric and ceramic nanofibers as uniaxially aligned arrays.* Nano Letters, 2003. **3**(8): p. 1167-1171.

47.   Zhang, Y.Z., Huang, Z. M., Xu, X. J., Lim, C. T. and Ramakrishna, S., *Preparation of core-shell structured PCL-r-gelatin Bi-component nanofibers by coaxial electrospinning.* Chemistry of Materials, 2004. **16**(18): p. 3406-3409.

48.   Zhang, Y.Z., Venugopal, J., Huang, Z. M., Lim, C. T. and Ramakrishna, S., *Characterization of the surface biocompatibility of the electrospun PCL-collagen nanofibers using fibroblasts.* Biomacromolecules, 2005. **6**(5): p. 2583-2589.

49.   Yu, J.H., S.V. Fridrikh, and G.C. Rutledge, *Production of submicrometer diameter fibers by two-fluid electrospinning.* Adv Mater, 2004. **16**: p. 1562-1566.

50.   Jiang, H.L., et al., *A facile technique to prepare biodegradable coaxial electrospun nanofibers for controlled release of bioactive agents.* Journal of Controlled Release, 2005. **108**(2-3): p. 237-243.

51.   Huang, Z.M., et al., *Encapsulating drugs in biodegradable ultrafine fibers through co-axial electrospinning.* Journal of Biomedical Materials Research Part A, 2006. **77A**(1): p. 169-179.

52.   Zhang, Y.Z., Wang, X., Feng, Y., Li, J., Lim, C. T. and Ramakrishna, S., *Coaxial electrospinning of (fluorescein isothiocyanate-conjugated bovin*

serum albumin)-encapsulated poly(caprolactone) nanofibers for sustained release. Biomacromolecules 2006. **7**: p. 1049-1057.

53. Townsend-Nicholson, A.a.J., S. N., *Cell electrospinning: a unique biotechnique for encapsulating living organisms for generating active biological microthreads/scaffolds.* Biomacromolecules, 2006. **7**(12): p. 3364-3369.

54. He, W., et al., *Tubular nanofiber scaffolds for tissue engineered small-diameter vascular grafts.* Journal of Biomedical Materials Research Part A, 2008.

55. Teo, W.E., Gopal, R., Ramaseshan, R., Fujihara, K. and Ramakrishna, S., *A dynamic liquid support system for continuous electrospun yarn fabrication.* Polymer, 2007. **48**(12): p. 3400-3405.

56. Teo, W.E., et al., *Fiber structures and process for their preparation.* 2008.

57. Teo, W.E., and Ramakrishna, S., *Electrospun fibre bundle made of aligned nanofibres over two fixed points.* Nanotechnology, 2005. **16**(9): p. 1878-1884.

58. Elbert, D.L. and J.A. Hubbell, *Surface treatments of polymers for biocompatibility.* Annual Review of Materials Science, 1996. **26**: p. 365-394.

59. He, W., Ma, Z. W., Yong, T., Teo, W. E. and Ramakrishna, S., *Fabrication of collagen-coated biodegradable polymer nanofiber mesh and its potential for endothelial cells growth.* Biomaterials, 2005. **26**(36): p. 7606-7615.

60. Walsh, J.F., Manwaring, M. E. and Tresco, P. A., *Directional neurite outgrowth is enhanced by engineered meningeal cell-coated substrates.* Tissue Engineering, 2005. **11**(7-8): p. 1085-1094.

61. Sunderland, S., *Nerve injuries and their repair : a critical appraisal* 1991, Edinburgh ; New York Churchill Livingstone.

62. Lynch, S.E., Genco, R.J. and Marx, R.E., *Tissue Engineering: Applications in maxillofacial surgery and periodontics.* 1999, USA: Quintessence Publishing Co. Inc.

63. Topp, K.S., and Boyd, B. S., *Structure and biomechanics of peripheral nerves: Nerve responses to physical stresses and implications for physical therapist practice.* Physical Therapy, 2006. **86**(1): p. 92-109.

64. Collagen, Matrix, and Inc. *Neuroflex™ Flexible Collagen Nerve Cuff (http://www.collagenmatrix.com/products-neurological.htm)*. 2005 [cited 29 Sep 2008].

65. Stang, F., et al., *Structural parameters of collagen nerve grafts influence peripheral nerve regeneration.* Biomaterials, 2005. **26**(16): p. 3083-3091.

66. Longo, F.M., Hayman, E. G., Davis, G. E., Ruoslahti, E., Engvall, E., Manthorpe, M. and Varon, S., *Neurite-Promoting Factors and Extracellular-Matrix Components Accumulating Invivo within Nerve Regeneration Chambers.* Brain Research, 1984. **309**(1): p. 105-117.

67. Makwana, M., and Raivich, G., *Molecular mechanisms in successful peripheral regeneration.* Febs Journal, 2005. **272**(11): p. 2628-2638.

68. McDonald, D., Cheng, C., Chen, Y. Y. and Zochodne, D., *Early events of peripheral nerve regeneration.* Neuron Glia Biology, 2006. **2**: p. 139-147.

69. Frostick, S.P., Yin, Q. and Kemp, G. J., *Schwann cells, neurotrophic factors, and peripheral nerve regeneration.* Microsurgery, 1998. **18**(7): p. 397-405.

70. Fawcett, J.W., Rosser, A.E. and Dunnett, S.B., *Brain damage, brain repair.* 2001, New York: Oxford University Press.

71. Griffin, J.W., George, R., Lobato, C., Tyor, W. R., Li, C. Y. and Glass, J. D., *Macrophage Responses and Myelin Clearance During Wallerian Degeneration - Relevance to Immune-Mediated Demyelination.* Journal of Neuroimmunology, 1992. **40**(2-3): p. 153-166.

72. Belkas, J.S., Shoichet, M. S. and Midha, R., *Peripheral nerve regeneration through guidance tubes.* Neurological Research, 2004. **26**(2): p. 151-160.

73. Chaudhry, V., Glass, J. D. and Griffin, J. W., *Wallerian Degeneration in Peripheral-Nerve Disease.* Neurologic Clinics, 1992. **10**(3): p. 613-627.

74. Meek, M.F., Jansen, K., Steendam, R., van Oeveren, W., van Wachem, P. B. and van Luyn, M. J. A., *In vitro degradation and biocompatibility of poly(DL-lactide-epsilon-caprolactone) nerve guides.* Journal of Biomedical Materials Research Part A, 2004. **68A**(1): p. 43-51.

75. Brushart, T.M.E., *Motor Axons Preferentially Reinnervate Motor Pathways.* Journal of Neuroscience, 1993. **13**(6): p. 2730-2738.

76.   Madison, R.D., Archibald, S. J. and Brushart, T. M., *Reinnervation accuracy of the rat femoral nerve by motor and sensory neurons.* Journal of Neuroscience, 1996. **16**(18): p. 5698-5703.

77.   Martin, S., et al., *Deposition of the NG2 proteoglycan at nodes of Ranvier in the peripheral nervous system.* Journal of Neuroscience, 2001. **21**(20): p. 8119-8128.

78.   Schlosshauer, B., Dreesmann, L., Schaller, H. E. and Sinis, N., *Synthetic nerve guide implants in humans: A comprehensive survey.* Neurosurgery, 2006. **59**(4): p. 740-747.

79.   Meek, M.F., and Coert, J. H., *Clinical use of nerve conduits in peripheral-nerve repair: Review of the literature.* Journal of Reconstructive Microsurgery, 2002. **18**(2): p. 97-109.

80.   SaluMedical.   *SaluBridge (http://www.salumedica.com/salubridgeinfodoc.htm).*   2000   [cited 29 Sep 2008].

81.   Lundborg, G., *Nerve injury and repair*. 1988, Edinburgh: Churchill Livingstone.

82.   TessierLavigne, M., and Goodman, C. S., *The molecular biology of axon guidance.* Science, 1996. **274**(5290): p. 1123-1133.

83.   Yannas, I.V., Zhang, M. and Spilker, M. H., *Standardized criterion to analyze and directly compare various materials and models for peripheral nerve regeneration.* Journal of Biomaterials Science-Polymer Edition, 2007. **18**(8): p. 943-966.

84.   Evans, G.R.D., Brandt, K., Niederbichler, A. D., Chauvin, P., Hermann, S., Bogle, M., Otta, L., Wang, B. and Patrick, C. W., *Clinical long-term in vivo evaluation of poly(L-lactic acid) porous conduits for peripheral nerve regeneration.* Journal of Biomaterials Science-Polymer Edition, 2000. **11**(8): p. 869-878.

85.   Evans, G.R.D., Brandt, K., Widmer, M. S., Lu, L., Meszlenyi, R. K., Gupta, P. K., Mikos, A. G., Hodges, J., Williams, J., Gurlek, A., Nabawi, A., Lohman, R. and Patrick, C. W., *In vivo evaluation of poly(L-lactic acid) porous conduits for peripheral nerve regeneration.* Biomaterials, 1999. **20**(12): p. 1109-1115.

86.   Widmer, M.S., Gupta, P. K., Lu, L. C., Meszlenyi, R. K., Evans, G. R. D., Brandt, K., Savel, T., Gurlek, A., Patrick, C. W. and Mikos, A. G., *Manufacture of porous biodegradable polymer conduits by an extrusion process for guided tissue regeneration.* Biomaterials, 1998. **19**(21): p. 1945-1955.

87.   Den Dunnen, W.F.A., Meek, M. F., Robinson, P. H. and Schakernraad, J. M., *Peripheral nerve regeneration through P(DLLA-epsilon-CL) nerve guides.* Journal of Materials Science-Materials in Medicine, 1998. **9**(12): p. 811-814.

88.   Li, S.T., Archibald, S. J., Krarup, C. and Madison, R. D., *Peripheral Nerve Repair with Collagen Conduits.* Clinical Materials, 1992. **9**(3-4): p. 195-200.

89.   Matsumoto, K., Ohnishi, K., Kiyotani, T., Sekine, T., Ueda, H., Nakamura, T., Endo, K. and Shimizu, Y., *Peripheral nerve regeneration across an 80-mm gap bridged by a polyglycolic acid (PGA)-collagen tube filled with laminin-coated collagen fibers: a histological and electrophysiological evaluation of regenerated nerves.* Brain Research, 2000. **868**(2): p. 315-328.

90.   Thompson, D.M., and Buettner, H. M., *Neurite outgrowth is directed by Schwann cell alignment in the absence of other guidance cues.* Annals of Biomedical Engineering, 2006. **34**(4): p. 669-676.

91.   Chen, Y.Y., McDonald, D., Cheng, C., Magnowski, B., Durand, J. and Zochodne, D. W., *Axon and Schwann cell partnership during nerve regrowth.* Journal of Neuropathology and Experimental Neurology, 2005. **64**(7): p. 613-622.

92.   Schnell, E., Klinkhammer, K., Balzer, S., Brook, G., Klee, D., Dalton, P. and Mey, J., *Guidance of glial cell. migration and axonal growth on electrospun nanofibers of poly-epsilon-caprolactone and a collagen/poly-epsilon-caprolactone blend.* Biomaterials, 2007. **28**(19): p. 3012-3025.

93.   Vleggeert-Lankamp, C., et al., *Adhesion and proliferation of human Schwann cells on adhesive coatings.* Biomaterials, 2004. **25**(14): p. 2741-2751.

94.   Hadlock, T., Sundback, C., Hunter, D., Cheney, M. and Vacanti, J. P., *A polymer foam conduit seeded with Schwann cells promotes guided peripheral nerve regeneration.* Tissue Engineering, 2000. **6**(2): p. 119-127.

95.   Sinis, N., Schaller, H. E., Schulte-Eversum, C., Schlosshauer, B., Doser, M., Dietz, K., Rosner, H., Muller, H. W. and Haerle, M., *Nerve regeneration across a 2-cm gap in the rat median nerve using a resorbable nerve conduit*

filled with Schwann cells. Journal of Neurosurgery, 2005. **103**(6): p. 1067-1076.

96.   Miller, C., Jeftinija, S. and Mallapragada, S., *Synergistic effects of physical and chemical guidance cues on neurite alignment and outgrowth on biodegradable polymer substrates.* Tissue Engineering, 2002. **8**(3): p. 367-378.

97.   Heine, W., Conant, K., Griffin, J. W. and Hoke, A., *Transplanted neural stem cells promote axonal regeneration through chronically denervated peripheral nerves.* Experimental Neurology, 2004. **189**(2): p. 231-240.

98.   Lopes, F.R.P., Campos, L. C. D., Correa, J. D., Balduino, A., Lora, S., Langone, F., Borojevic, R. and Martinez, A. M. B., *Bone marrow stromal cells and resorbable collagen guidance tubes enhance sciatic nerve regeneration in mice.* Experimental Neurology, 2006. **198**(2): p. 457-468.

99.   Keilhoff, G., Goihl, A., Langnase, K., Fansa, H. and Wolf, G., *Transdifferentiation of mesenchymal stem cells into Schwann cell-like myelinating cells.* European Journal of Cell Biology, 2006. **85**(1): p. 11-24.

100.   Keilhoff, G., Goihl, A., Stang, F., Wolf, G. and Fansa, H., *Peripheral nerve tissue engineering: Autologous Schwann cells vs. transdifferentiated mesenchymal stem cells.* Tissue Engineering, 2006. **12**(6): p. 1-15.

101.   Verdu, E., Navarro, X., Gudino-Cabrera, G., Rodriguez, F. J., Ceballos, D., Valero, A. and Nieto-Sampedro, M., *Olfactory bulb ensheathing cells enhance peripheral nerve regeneration.* Neuroreport, 1999. **10**(5): p. 1097-1101.

102.   Li, Q.F., Ping, P., Jiang, H. and Liu, K., *Nerve conduit filled with GDNF gene-modified Schwann cells enhances regeneration of the peripheral nerve.* Microsurgery, 2006. **26**(2): p. 116-121.

103.   Ma, N., Wu, S. S., Ma, Y. X., Wang, X., Zeng, J. M., Tong, G. P., Huang, Y. and Wang, S., *Nerve growth factor receptor-mediated gene transfer.* Molecular Therapy, 2004. **9**(2): p. 270-281.

104.   Menei, P., Montero-Menei, C., Whittemore, S. R., Bunge, R. P. and Bunge, M. B., *Schwann cells genetically modified to secrete human BDNF promote enhanced axonal regrowth across transected adult rat spinal cord.* European Journal of Neuroscience, 1998. **10**(2): p. 607-621.

105.   Tuszynski, M.H., Weidner, N., McCormack, M., Miller, I., Powell, H. and Conner, J., *Grafts of genetically modified Schwann cells to the spinal cord: Survival, axon growth, and myelination.* Cell Transplantation, 1998. **7**(2): p. 187-196.

106.   Sayers, S.T., Khan, N., Ahmed, Y., Shahid, R. and Khan, T., *Preparation of brain-derived neurotrophic factor- and neurotrophin-3-secreting Schwann cells by infection with a retroviral vector.* Journal of Molecular Neuroscience, 1998. **10**(2): p. 143-160.

107.   Podratz, J.L., Rodriguez, E. and Windebank, A. J., *Role of the extracellular matrix in myelination of peripheral nerve.* Glia, 2001. **35**(1): p. 35-40.

108.   Vernon, R.B., Gooden, M. D., Lara, S. L. and Wight, T. N., *Native fibrillar collagen membranes of micron-scale and submicron thicknesses for cell support and perfusion.* Biomaterials, 2005. **26**(10): p. 1109-1117.

109.   Archibald, S.J., Krarup, C., Shefner, J., Li, S. T. and Madison, R. D., *A Collagen-Based Nerve Guide Conduit for Peripheral-Nerve Repair - an Electrophysiological Study of Nerve Regeneration in Rodents and Nonhuman-Primates.* Journal of Comparative Neurology, 1991. **306**(4): p. 685-696.

110.   Nakamura, T., Inada, Y., Fukuda, S., Yoshitani, M., Nakada, A., Itoi, S., Kanemaru, S., Endo, K. and Shimizu, Y., *Experimental study on the regeneration of peripheral nerve gaps through a polyglycolic acid-collagen (PGA-collagen) tube.* Brain Research, 2004. **1027**(1-2): p. 18-29.

111.   Dubey, N., Letourneau, P. C. and Tranquillo, R. T., *Guided neurite elongation and Schwann cell invasion into magnetically aligned collagen in simulated peripheral nerve regeneration.* Experimental Neurology, 1999. **158**(2): p. 338-350.

112.   Ceballos, D., Navarro, X., Dubey, N., Wendelschafer-Crabb, G., Kennedy, W. R. and Tranquillo, R. T., *Magnetically aligned collagen gel filling a collagen nerve guide improves peripheral nerve regeneration.* Experimental Neurology, 1999. **158**(2): p. 290-300.

113.   Yoshii, S., Oka, M., Shima, M., Taniguchi, A. and Akagi, M., *30 mm regeneration of rat sciatic nerve along collagen filaments.* Brain Research, 2002. **949**(1-2): p. 202-208.

114.   Rutka, J.T., Apodaca, G., Stern, R. and Rosenblum, M., *The Extracellular-Matrix of the Central and Peripheral Nervous Systems - Structure and Function.* Journal of Neurosurgery, 1988. **69**(2): p. 155-170.

115.   LuckenbillEdds, L., *Laminin and the mechanism of neuronal outgrowth.* Brain Research Reviews, 1997. **23**(1-2): p. 1-27.

116.   Timpl, R., Rohde, H., Robey, P. G., Rennard, S. I., Foidart, J. M. and Martin, G. R., *Laminin--a glycoprotein from basement membranes.* Journal of Biological Chemistry, 1979. **254**(19): p. 9933-9937.

117.   Yu, X.J., Dillon, G. P. and Bellamkonda, R. V., *A laminin and nerve growth factor-laden three-dimensional scaffold for enhanced neurite extension.* Tissue Engineering, 1999. **5**(4): p. 291-304.

118.   Rangappa, N., Romero, A., Nelson, K. D., Eberhart, R. C. and Smith, G. M., *Laminin-coated poly(L-lactide) filaments induce robust neurite growth while providing directional orientation.* Journal of Biomedical Materials Research, 2000. **51**(4): p. 625-634.

119.   Labrador, R.O., Buti, M. and Navarro, X., *Influence of collagen and laminin gels concentration on nerve regeneration after resection and tube repair.* Experimental Neurology, 1998. **149**(1): p. 243-252.

120.   Huber, M., Heiduschka, P., Kienle, S., Pavlidis, C., Mack, J., Walk, T., Jung, G. and Thanos, S., *Modification of glassy carbon surfaces with synthetic laminin-derived peptides for nerve cell attachment and neurite growth.* Journal of Biomedical Materials Research, 1998. **41**(2): p. 278-288.

121.   Luo, Y., and Shoichet, M. S., *A photolabile hydrogel for guided three-dimensional cell growth and migration.* Nature Materials, 2004. **3**(4): p. 249-253.

122.   Armstrong, S.J., Wiberg, M., Terenghi, G. and Kingham, P. J., *ECM molecules mediate both Schwann cell proliferation and activation to enhance neurite outgrowth.* Tissue Engineering, 2007. **13**: p. 2863-2870.

123.   Whitworth, I.H., Brown, R. A., Dore, C. J., Anand, P., Green, C. J. and Terenghi, G., *Nerve growth factor enhances nerve regeneration through fibronectin grafts.* Journal of Hand Surgery-British and European Volume, 1996. **21B**(4): p. 514-522.

124.   Sterne, G.D., Brown, R. A., Green, C. J. and Terenghi, G., *Neurotrophin-3 delivered locally via fibronectin mats enhances peripheral nerve regeneration.* European Journal of Neuroscience, 1997. **9**(7): p. 1388-1396.

125. Zhang, J., Lineaweaver, W. C., Oswald, T., Chen, Z. R., Chen, Z. W. and Zhang, F., *Ciliary neurotrophic factor for acceleration of peripheral nerve regeneration: An experimental study.* Journal of Reconstructive Microsurgery, 2004. **20**(4): p. 323-327.

126. Piotrowicz, A. and M.S. Shoichet, *Nerve guidance channels as drug delivery vehicles.* Biomaterials, 2006. **27**(9): p. 2018-2027.

127. Kapur, T.A.a.S., M. S., *Immobilized concentration gradients of nerve growth factor guide neurite outgrowth.* Journal of Biomedical Materials Research Part A, 2004. **68A**(2): p. 235-243.

128. Chew, S.Y., Wen, J., Yim, E. K. F. and Leong, K. W., *Sustained release of proteins from electrospun biodegradable fibers.* Biomacromolecules, 2005. **6**(4): p. 2017-2024.

129. Terris, D.J., Toft, K. M., Moir, M., Lum, J. and Wang, M., *Brain-derived neurotrophic factor-enriched collagen tubule as a substitute for autologous nerve grafts.* Archives of Otolaryngology-Head & Neck Surgery, 2001. **127**(3): p. 294-298.

130. Chew, S.Y., Mi, R. F., Hoke, A. and Leong, K. W., *Aligned protein-polymer composite fibers enhance nerve regeneration: A potential tissue-engineering platform.* Advanced Functional Materials, 2007. **17**(8): p. 1288-1296.

131. Aebischer, P., Salessiotis, A. N. and Winn, S. R., *Basic Fibroblast Growth-Factor Released from Synthetic Guidance Channels Facilitates Peripheral-Nerve Regeneration across Long Nerve Gaps.* Journal of Neuroscience Research, 1989. **23**(3): p. 282-289.

132. Sondell, M., Lundborg, G. and Kanje, M., *Vascular endothelial growth factor stimulates Schwann cell invasion and neovascularization of acellular nerve grafts.* Brain Research, 1999. **846**(2): p. 219-228.

133. Chen, M.H., Chen, P. R., Chen, M. H., Hsieh, S. T. and Lin, F. H., *Gelatin-tricalcium phosphate membranes immobilized with NGF, BDNF, or IGF-1 for peripheral nerve repair: An in vitro and in vivo study.* Journal of Biomedical Materials Research Part A, 2006. **79A**(4): p. 846-857.

134. Mohanna, P.N., Young, R. C., Wiberg, M. and Terenghi, G., *A composite poly-hydroxybutyrate-glial growth factor conduit for long nerve gap repairs.* Journal of Anatomy, 2003. **203**(6): p. 553-565.

135.   Chen, W.P., Chang, Y. C. and Hsieh, S. T., *Trophic interactions between sensory nerves and their targets.* Journal of Biomedical Science, 1999. **6**(2): p. 79-85.

136.   Vogelin, E., Baker, J. M., Gates, J., Dixit, V., Constantinescu, M. A. and Jones, N. F., *Effects of local continuous release of brain derived neurotrophic factor (BDNF) on peripheral nerve regeneration in a rat model.* Experimental Neurology, 2006. **199**(2): p. 348-353.

137.   Kingham, P.J., and Terenghi, G., *Bioengineered nerve regeneration and muscle reinnervation.* Journal of Anatomy, 2006. **209**(4): p. 511-526.

138.   Kelleher, M.O., Myles, L. M., Al-Abri, R. K. and Glasby, M. A., *The use of ciliary neurotrophic factor to promote recovery after peripheral nerve injury by delivering it at the site of the cell body.* Acta Neurochirurgica, 2006. **148**(1): p. 55-61.

139.   Pean, J.M., Venier-Julienne, M. C., Boury, F., Menei, P., Denizot, B. and Benoit, J. P., *NGF release from poly(D,L-lactide-co-glycolide) microspheres. Effect of some formulation parameters on encapsulated NGF stability.* Journal of Controlled Release, 1998. **56**(1-3): p. 175-187.

140.   Lee, A.C., Yu, V. M., Lowe, J. B., Brenner, M. J., Hunter, D. A., Mackinnon, S. E. and Sakiyama-Elbert, S. E., *Controlled release of nerve growth factor enhances sciatic nerve regeneration.* Experimental Neurology, 2003. **184**(1): p. 295-303.

141.   Yang, Y., De Laporte, L., Rives, C. B., Jang, J. H., Lin, W. C., Shull, K. R. and Shea, L. D., *Neurotrophin releasing single and multiple lumen nerve conduits.* Journal of Controlled Release, 2005. **104**(3): p. 433-446.

142.   Chew, S.Y., et al., *Sustained release of proteins from electrospun biodegradable fibers.* Biomacromolecules, 2005. **6**(4): p. 2017-2024.

143.   Chen, P.R., Chen, M. H., Lin, F. H. and Su, W. Y., *Release characteristics and bioactivity of gelatin-tricalcium phosphate membranes covalently immobilized with nerve growth factors.* Biomaterials, 2005. **26**(33): p. 6579-6587.

144.   Midha, R., Munro, C. A., Dalton, P. D., Tator, C. H. and Shoichet, M. S., *Growth factor enhancement of peripheral nerve regeneration through a novel synthetic hydrogel tube.* Journal of Neurosurgery, 2003. **99**(3): p. 555-565.

145. Kapur, T.A., and Shoichet, M. S., *Immobilized concentration gradients of nerve growth factor guide neurite outgrowth.* Journal of Biomedical Materials Research Part A, 2004. **68A**(2): p. 235-243.

146. Moore, K., Macsween, M. and Shoichet, M. S., *Immobilized concentration gradients of neurotrophic factors guide neurite outgrowth of primary neurons in macroporous scaffolds.* Tissue Engineering, 2006. **12**(2): p. 267-278.

147. Xu, X.Y., Yee, W. C., Hwang, P. Y. K., Yu, H., Wan, A. C. A., Gao, S. J., Boon, K. L., Mao, H. Q., Leong, K. W. and Wang, S., *Peripheral nerve regeneration with sustained release of poly(phosphoester) microencapsulated nerve growth factor within nerve guide conduits.* Biomaterials, 2003. **24**(13): p. 2405-2412.

148. Brandt, J., et al., *Spatiotemporal progress of nerve regeneration in a tendon autograft used for bridging a peripheral nerve defect.* Experimental Neurology, 1999. **160**(2): p. 386-393.

149. Lietz, M., Dreesmann, L., Hoss, M., Oberhoffner, S. and Schlosshauer, B., *Neuro tissue engineering of glial nerve guides and the impact of different cell types.* Biomaterials, 2006. **27**(8): p. 1425-1436.

150. Meek, M.F., Den Dunnen, W. F. A., Schakenraad, J. M. and Robinson, P. H., *Evaluation of functional nerve recovery after reconstruction with a poly (DL-lactide-epsilon-caprolactone) nerve guide, filled with modified denatured muscle tissue.* Microsurgery, 1996. **17**(10): p. 555-561.

151. Meek, M.F., Varejao, A. S. P. and Geuna, S., *Use of skeletal muscle tissue in peripheral nerve repair: Review of the literature.* Tissue Engineering, 2004. **10**(7-8): p. 1027-1036.

152. Cai, J., Peng, X. J., Nelson, K. D., Eberhart, R. and Smith, G. M., *Permeable guidance channels containing microfilament scaffolds enhance axon growth and maturation.* Journal of Biomedical Materials Research Part A, 2005. **75A**(2): p. 374-386.

153. Wen, X.J., and Tresco, P. A., *Effect of filament diameter and extracellular matrix molecule precoating on neurite outgrowth and Schwann cell behavior on multifilament entubulation bridging device in vitro.* Journal of Biomedical Materials Research Part A, 2006. **76A**(3): p. 626-637.

154. Liao, S., Li, B. J., Ma, Z. W., Wei, H., Chan, C. and Ramakrishna, S., *Biomimetic electrospun nanofibers for tissue regeneration.* Biomedical Materials, 2006. **1**: p. R45-R53.

155.   Yang, F., Xu, C. Y., Kotaki, M., Wang, S. and Ramakrishna, S., *Characterization of neural stem cells on electrospun poly(L-lactic acid) nanofibrous scaffold.* Journal of Biomaterials Science-Polymer Edition, 2004. **15**(12): p. 1483-1497.

156.   Kim, Y.T., et al., *The role of aligned polymer fiber-based constructs in the bridging of long peripheral nerve gaps.* Biomaterials, 2008. **29**(21): p. 3117-3127.

157.   Bini, T.B., Gao, S. J., Xu, X. Y., Wang, S., Ramakrishna, S. and Leong, K. W., *Peripheral nerve regeneration by microbraided poly(L-lactide-co-glycolide) biodegradable polymer fibers.* Journal of Biomedical Materials Research Part A, 2004. **68A**(2): p. 286-295.

158.   Patel, S., Kurpinski, K., Quigley, R., Gao, H. F., Hsiao, B. S., Poo, M. M. and Li, S., *Bioactive nanofibers: Synergistic effects of nanotopography and chemical signaling on cell guidance.* Nano Letters, 2007. **7**(7): p. 2122-2128.

159.   You, Y., Min, B. M., Lee, S. J., Lee, T. S. and Park, W. H., *In vitro degradation behavior of electrospun polyglycolide, polylactide, and poly(lactide-co-glycolide).* Journal of Applied Polymer Science, 2005. **95**(2): p. 193-200.

160.   Meek, M.F., et al., *Peripheral nerve regeneration and functional nerve recovery after reconstruction with a thin-walled biodegradable poly(DL-lactide-epsilon-caprolactone) nerve guide.* Cells and Materials, 1997. **7**(1): p. 53-62.

161.   Vleggeert-Lankamp, C.L.A.M., de Ruiter, G.C.W., Wolfs, J.F.C., Pego, A.P., van den Berg, R.J., Feirabend, H.K.P., Malessey, M.J.A. and Lakke, E.A.J.F. , *Pores in synthetic nerve conduits are beneficial to regeneration.* Journal of Biomedical Materials Research, 2006. **80A**: p. 965-982.

162.   Stankus, J.J., Guan, J. J., Fujimoto, K. and Wagner, W. R., *Microintegrating smooth muscle cells into a biodegradable, elastomeric fiber matrix.* Biomaterials, 2006. **27**(5): p. 735-744.

163.   Milner, R., Wilby, M., Nishimura, S., Boylen, K., Edwards, G., Fawcett, J., Streuli, C., Pytela, R. and ffrenchConstant, C., *Division of labor of Schwann cell integrins during migration on peripheral nerve extracellular matrix ligands.* Developmental Biology, 1997. **185**(2): p. 215-228.

164. Chen, Z.L.a.S., S., *Laminin gamma 1 is critical for Schwann cell differentiation, axon myelination, and regeneration in the peripheral nerve.* Journal of Cell Biology, 2003. **163**(4): p. 889-899.

165. Schmidt, C.E., Shastri, V. R., Vacanti, J. P. and Langer, R., *Stimulation of neurite outgrowth using an electrically conducting polymer.* Proceedings of the National Academy of Sciences of the United States of America, 1997. **94**(17): p. 8948-8953.

166. Attiah, D.G., Kopher, R. A. and Desai, T. A., *Characterization of PC12 cell proliferation and differentiation-stimulated by ECM adhesion proteins and neurotrophic factors.* Journal of Materials Science-Materials in Medicine, 2003. **14**(11): p. 1005-1009.

167. Villegas, G.M., Haustein, A. T. and Villegas, R., *Neuronal Differentiation of Pc12 and Chick-Embryo Ganglion-Cells Induced by a Sciatic-Nerve Conditioned Medium - Characterization of the Neurotrophic Activity.* Brain Research, 1995. **685**(1-2): p. 77-90.

168. Kinoshita, Y., Kuzuhara, T., Kirigakubo, M., Kobayashi, M., Shimura, K. and Ikada, Y., *Soft-Tissue Reaction to Collagen-Immobilized Porous Polyethylene - Subcutaneous Implantation in Rats for 20 Wk.* Biomaterials, 1993. **14**(3): p. 209-215.

169. Wang, K.K., Costas, P. D., Jones, D. S., Miller, R. A. and Seckel, B. R., *Sleeve Insertion and Collagen Coating Improve Nerve Regeneration through Vein Conduits.* Journal of Reconstructive Microsurgery, 1993. **9**(1): p. 39-48.

170. Matsuda, A., Kobayashi, H., Itoh, S., Kataoka, K. and Tanaka, J., *Immobilization of laminin peptide in molecularly aligned chitosan by covalent bonding.* Biomaterials, 2005. **26**(15): p. 2273-2279.

171. Yu, T.T.a.S., M. S., *Guided cell adhesion and outgrowth in peptide-modified channels for neural tissue engineering.* Biomaterials, 2005. **26**(13): p. 1507-1514.

172. Manthorpe, M., et al., *Laminin Promotes Neuritic Regeneration from Cultured Peripheral and Central Neurons.* Journal of Cell Biology, 1983. **97**(6): p. 1882-1890.

173. Keynes, R., and Cook, G. M. W., *Axon Guidance Molecules.* Cell, 1995. **83**(2): p. 161-169.

174. Terenghi, G., *Peripheral nerve regeneration and neurotrophic factors.* Journal of Anatomy, 1999. **194**: p. 1-14.

175. Raivich, G., Hellweg, R. and Kreutzberg, G. W., *Ngf Receptor Mediated Reduction in Axonal Ngf Uptake and Retrograde Transport Following Sciatic-Nerve Injury and During Regeneration.* Neuron, 1991. **7**(1): p. 151-164.

176. van de Weert, M., W.E. Hennink, and W. Jiskoot, *Protein instability in poly(lactic-co-glycolic acid) microparticles.* Pharmaceutical Research, 2000. **17**(10): p. 1159-1167.

177. Chernousov, M.A. and D.J. Carey, *Schwann cell extracellular matrix molecules and their receptors.* Histology and Histopathology, 2000. **15**(2): p. 593-601.

178. Zong, X.H., et al., *Structure and morphology changes during in vitro degradation of electrospun poly(glycolide-co-lactide) nanofiber membrane.* Biomacromolecules, 2003. **4**(2): p. 416-423.

179. Patist, C.M., et al., *Freeze-dried poly(D,L-lactic acid) macroporous guidance scaffolds impregnated with brain-derived neurotrophic factor in the transected adult rat thoracic spinal cord.* Biomaterials, 2004. **25**(9): p. 1569-1582.

180. De Bellard, M. and M.T. Filbin, *Myelin-associated glycoprotein, MAG, selectively binds several neuronal proteins.* Journal of Neuroscience Research, 1999. **56**(2): p. 213-218.

181. Schlosshauer, B., Muller, E., Schroder, B., Planck, H. and Muller, H. W., *Rat Schwann cells in bioresorbable nerve guides to promote and accelerate axonal regeneration.* Brain Research, 2003. **963**(1-2): p. 321-326.

182. Meek, M.F., van der Werff, J. F. A., Klok, F., Robinson, P. H., Nicolai, J. P. A. and Gramsbergen, A., *Functional nerve recovery after bridging a 15 mm gap in rat sciatic nerve with a biodegradable nerve guide.* Scandinavian Journal of Plastic and Reconstructive Surgery and Hand Surgery, 2003. **37**(5): p. 258-265.

183. Meek, M.F., Den Dunnen, W. F. A., Schakenraad, J. M. and Robinson, P. H., *Long-term evaluation of functional nerve recovery after reconstruction with a thin-walled biodegradable poly (DL-lactide-epsilon-caprolactone) nerve guide, using walking track analysis and electrostimulation tests.* Microsurgery, 1999. **19**(5): p. 247-253.

184. Belkas, J.S., Munro, C. A., Shoichet, M. S. and Midha, R. , *Peripheral Nerve Regeneration through a Synthetic Hydrogel Nerve Tube.* Restorative Neurology and Neuroscience, 2005. **23**(1): p. 19-29.

185. Yu, X.J. and R.V. Bellamkonda, *Tissue-engineered scaffolds are effective alternatives to autografts for bridging peripheral nerve gaps.* Tissue Engineering, 2003. **9**(3): p. 421-430.

186. Belkas, J.S., Munro, C. A., Shoichet, M. S., Johnston, M. and Midha, R., *Long-term in vivo biomechanical properties and biocompatibility of poly(2-hydroxyethyl methacrylate-co-methyl methacrylate) nerve conduits.* Biomaterials, 2005. **26**(14): p. 1741-1749.

187. Dodla, M.C. and R.V. Bellamkonda, *Differences between the effect of anisotropic and isotropic laminin and nerve growth factor presenting scaffolds on nerve regeneration across long peripheral nerve gaps.* Biomaterials, 2008. **29**: p. 33-46.

188. Itoh, S., et al., *Hydroxyapatite-coated tendon chitosan tubes with adsorbed laminin peptides facilitate nerve regeneration in vivo.* Brain Research, 2003. **993**(1-2): p. 111-123.

189. Suzuki, M., et al., *Tendon chitosan tubes covalently coupled with synthesized laminin peptides facilitate nerve regeneration in vivo.* Journal of Neuroscience Research, 2003. **72**(5): p. 646-659.

190. Tomita, K., et al., *Myelin-associated glycoprotein reduces axonal branching and enhances functional recovery after sciatic nerve transection in rats.* Glia, 2007. **55**: p. 1498-1507.

191. Priestley, J.V., *Promoting anatomical plasticity and recovery of function after traumatic injury to the central or peripheral nervous system.* Brain, 2007. **130**: p. 895-897.

192. Scott, J.J., *The functional recovery of muscle proprioceptors after peripheral nerve lesions.* Journal of Peripheral Nervous System, 1996. **1**: p. 19-27.

193. Meek, M.F., et al., *Electronmicroscopical evaluation of short-term nerve regeneration through a thin-walled biodegradable poly(DLLA-epsilon-CL) nerve guide filled with modified denatured muscle tissue.* Biomaterials, 2001. **22**(10): p. 1177-1185.

194.   Benjamin, L.E., I. Hemo, and E. Keshet, *A plasticity window for blood vessel remodelling is defined by pericyte coverage of the preformed endothelial network and is regulated by PDGF-B and VEGF.* Development, 1998. **125**(9): p. 1591-1598.

195.   Richardson, T.P., et al., *Polymeric system for dual growth factor delivery.* Nature Biotechnology, 2001. **19**(11): p. 1029-1034.

196.   Tsai, J.C., C.K. Goldman, and G.Y. Gillespie, *Vascular Endothelial Growth-Factor in Human Glioma Cell-Lines - Induced Secretion by Egf, Pdgf-Bb, and Bfgf.* Journal of Neurosurgery, 1995. **82**(5): p. 864-873.

197.   Hoke, A., *Mechanisms of disease: what factors limit the success of peripheral nerve regeneration in humans?* Nature Clinical Practice Neurology, 2006. **2**(8): p. 448-454.
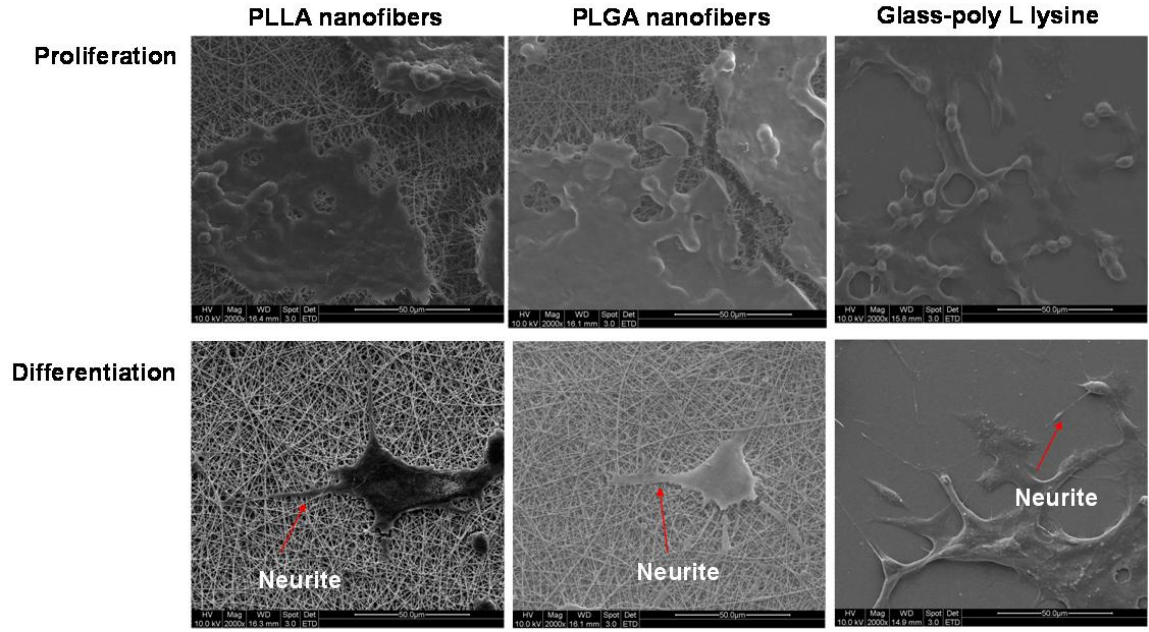
Appendix A

Cell viability assay of PC12 cells cultured on different polymeric nanofibers
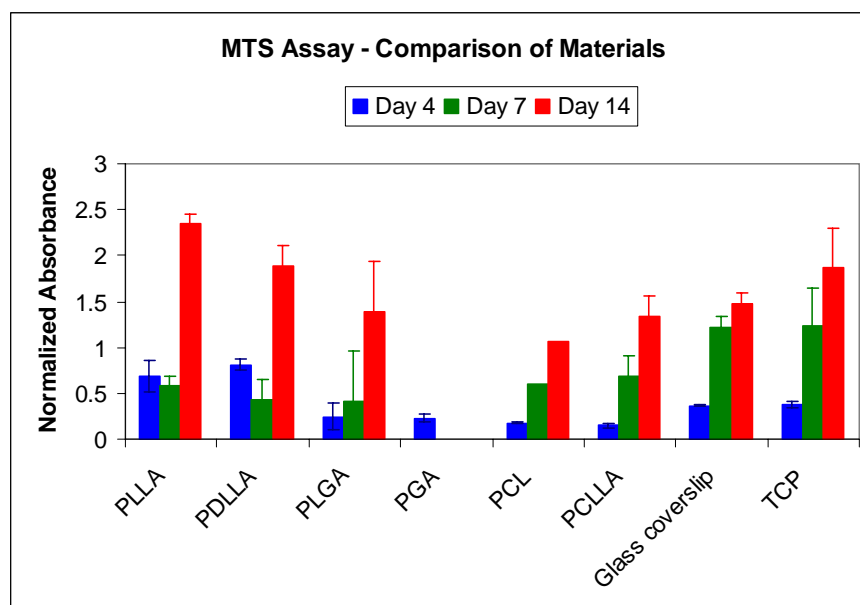
*No data is obtained for PGA nanofibers on Day 7 and 14 as the scaffolds had fragmented totally.

Scanning electron micrographs of PC12 cell proliferation and differentiation on nanofibers

Appendix B

Sample preparation for scanning electron microscopy observation

Scanning electron microscopy is used to image cell-matrix composite.

1. Wash the samples 3 times with PBS (5 min each wash).
2. Immerse samples in 2.5% glutaraldehyde (300uL each well). Incubate for 1-2 hours.
3. Wash 3 times with DI water (5 min each wash).
4. Immerse samples in 50% ethanol (500 uL each well) incubate for 15 min.
5. Repeat step 4 with 75% ethanol.
6. Repeat step 4 twice with 95% ethanol.
7. Repeat step 4 twice with 100% ethanol, incubating for 30 min each time.
8. Cover samples with HMDS (hexamethyldisilizane) (200uL each sample) allow to dry overnight.
9. Gold-coat samples prior to SEM.

Appendix C

Covalent coupling with EDC/NHS method

1. Preparation of 2-4(-Morpholino)ethanesulfonic acid hydrate,
   (MES hydrate) buffer solution (Sigma, M2933)
   To prepare 0.1 M buffer solution (pH = 5.0), Mw = 195.24 g/mol
   For example, to prepare a **20 mL** of 0.1 M MES buffer solution

   Mass required = volume x concentration
   = 20 mL x 0.1 mol/L x 1L/1000mL x 195.24 g/mol
   = **0.390 g** of MES hydrate required

   Volume of DI water to be added = 20 mL (1 M = 1 Molarity (1 mol/L))

2. Preparation of *N*-(3-Dimethylaminopropyl)-*N'*-ethylcarbodiimide hydrochloride
   solution (Sigma, E1769) MW=191.7
   To prepare 5 mg/mL of EDC in MES buffer (i.e. ~26.1mM)

   Mass required = 5 mg/mL x 5 mL = 25 mg or **0.025 g**
       *** EDC is unstable in solution. Mix immediately before using and discard
   excess. Use the solution within 10min of mixing.**

3. Preparation of *N*-Hydroxysuccinimide solution (Sigma, 130672) MW=115.09
   To prepare 5 mg/mL of 5mL NHS in MES buffer (~43.4 mM)

   Mass required = **0.025 g**

   If it is required to quench the EDC, addition of of 2-mercaptoethanol should be
   done.

   - Plasma treat the samples for desired time. Immediately immerse the
     polymer with glass coverslip with freshly prepared 1mL each EDC/NHS
     (molar ratio=0.6, recommended by Pierce is 0.4) in MES buffer at 4 ^{o}C for
     2 hour.

   - Rinse material PBS at pH 7.4.

   - Immerse material in protein (e.g. collagen or laminin) solution for 24
     hours at 4 ^{o}C.

   - Rinse protein-grafted material in deionized water for 3 times with PBS to
     remove the physically adsorbed protein (e.g. gelatin) and sterilize in 75%
     ethanol for 24 hours. Rinse thoroughly with sterile PBS thereafter.

Appendix D

Physical coating of proteins on nanofibers

1. Place the nanofiber coverslips on a rectangle glass-slide. Each slide can carry 3 coverslips at one time. Put the slide in plasma cleaner/sterilizer (Harrick Scientific Corp. PDC-001).
2. Tightly close the door and open the pump to vacuum the chamber for 5 mins.
3. Adjust the RF level to low level and turn on the power button. Please ensure that there is red light. If there is no light, loosen the door a little until red light appears. Adjust the RF level to high level for 5 mins.
4. Quickly take the coverslips out and put them in a 24-well plate (Plasma treatment will lose effect if nanofiber is placed outside for too long).
5. Add 500 uL protein (e.g. collagen or laminin) solution in the well and put the plate in 4 $^{\circ}$C to incubate overnight.
6. Rinse modified material in deionized water for 3 times with PBS to remove the physically adsorbed protein (e.g. gelatin) and sterilize in 75% ethanol for 24 hours. Rinse thoroughly with sterile PBS thereafter.

Appendix E

Immunohistochemical staining protocol for nerve tissue

Mainly for *neurofilament and S-100 protein* observation on the explanted rat nerve.

Solutions
1x PBS, Goat serum (20%) in PBS

Primary antibodies
1. Mouse anti-rat neurofilament 200 kDa phosphorylated and non-phosphorylated forms (1:100)

2. Rabbit anti-rat S-100 protein (1:100)

Secondary antibody
1. Goat anti-mouse IgG (H+L) FITC (1:50)

2. Goat anti-rabbit IgG (H+L) RBITC (1:50)

Procedure

1. Fix harvested proximal nerve in 4% paraformaldehyde at 4 ^{o}C overnight.

2. Wash the specimen with cacodylate buffer and cryo-protect in 20% buffer sucrose solution overnight at 4 ^{o}C.

3. Quickly freeze specimen in Tissue-Tek O.C.T compound and stored at -80 ^{o}C.

4. Cut longitudinal sections using a cryostat, thickness = **10 μm.**

5. Collect sections on poly-L-lysine coated slides and stored at -20 ^{o}C.

6. Non-specific antibody adhesion is blocked with 20% goat serum for 2 hours.

7. Using monoclonal anti-200 kDa neurofilament to identify regenerating axons, visualized with FTIC conjugated anti-mouse IgG.

8. Using anti-S-100 protein to identify Schwann cells protein, visualized with RBITC conjugated anti-mouse IgG.

9. Incubate primary antibody (1:100) overnight at 4 ^{o}C.

10. Wash with PBS solution and incubate secondary body (1:50) at room temperature for 30 min.

11. Add mounting media for laser confocal scanning microscopy observation.

Appendix F

Sensory recovery test

*WRL is used as an assessment of the nociception recovery of the rat.*

Procedure

(Handle the rat with care and minimize stress for the rat.)

1. Warp the rat with a surgical towel above its waist and position it to stand with the affected hind paw on a hot plate of 56 $^{\circ}$C.
2. WRL is defined as the time elapsed from the onset of hotplate contact and the withdrawal of the hind paw. Measure the time with a stopwatch.
3. Normal rats withdraw their paws from the hotplate within 4.3 s or less.
4. If no paw withdrawal after 12s, remove the heat stimulus IMMEDIATELY to prevent tissue damage; assign the maximal WRL of 12 s to the rat.
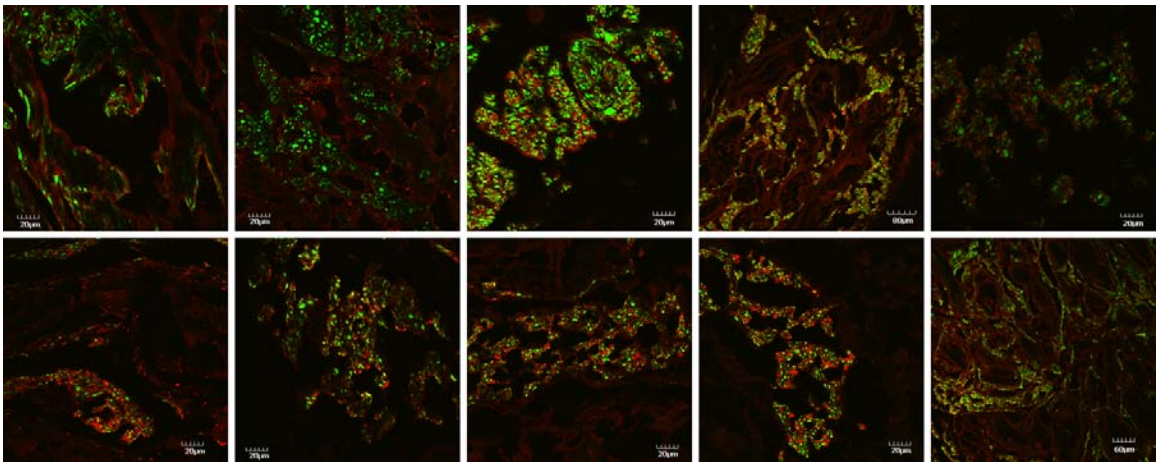
Appendix G

Immuno-staining of neurofilament 200 kDa and S-100 protein of regenerated nerve at the mid-graft section
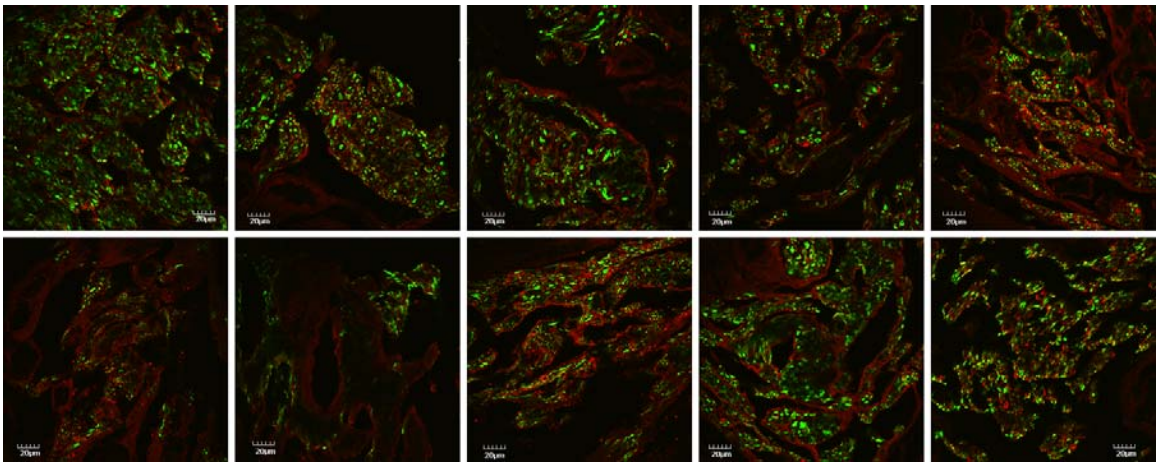
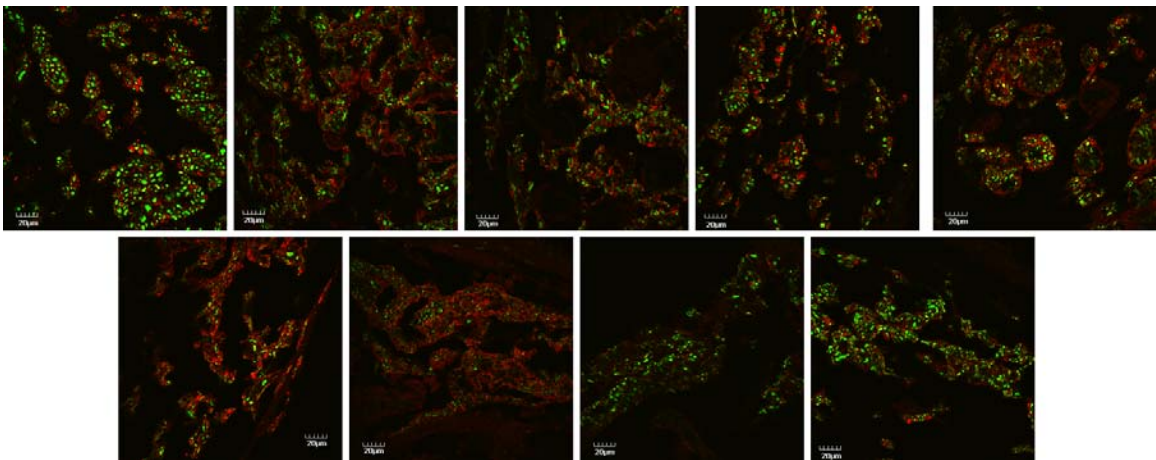(A)   Bilayered nerve conduit and saline (20x magification).
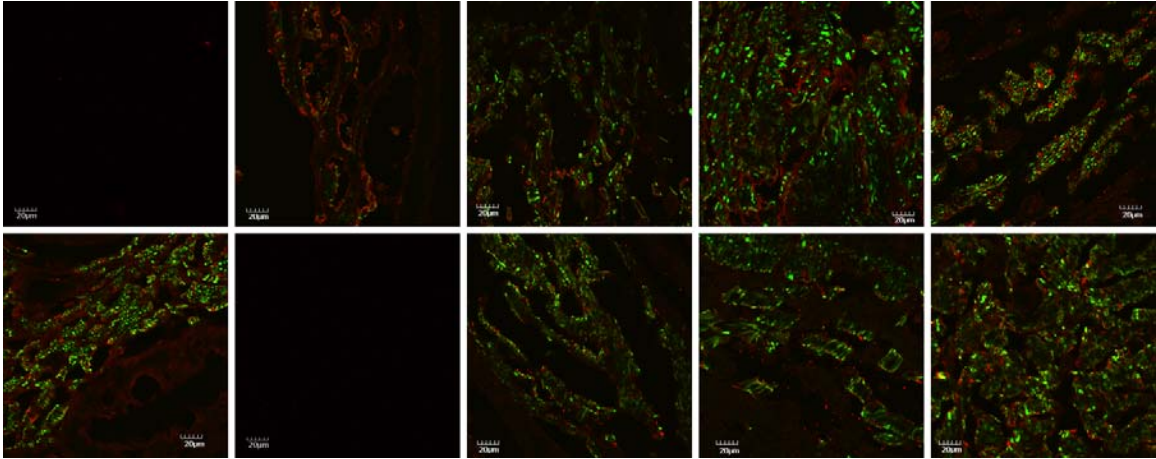
(B)   Bilayered nerve conduit and intra-luminal guidance channels (20x magification).

(C)   Bilayered nerve conduit coupled with laminin and intra-luminal guidance channels (20x magification).

(D)   Bilayered nerve conduit and and NGF incorporated intra-luminal guidance channels (20x magification).

(E)   Bilayered nerve conduit coupled with laminin and and NGF incorporated
intra-   luminal guidance channels (20x magification).
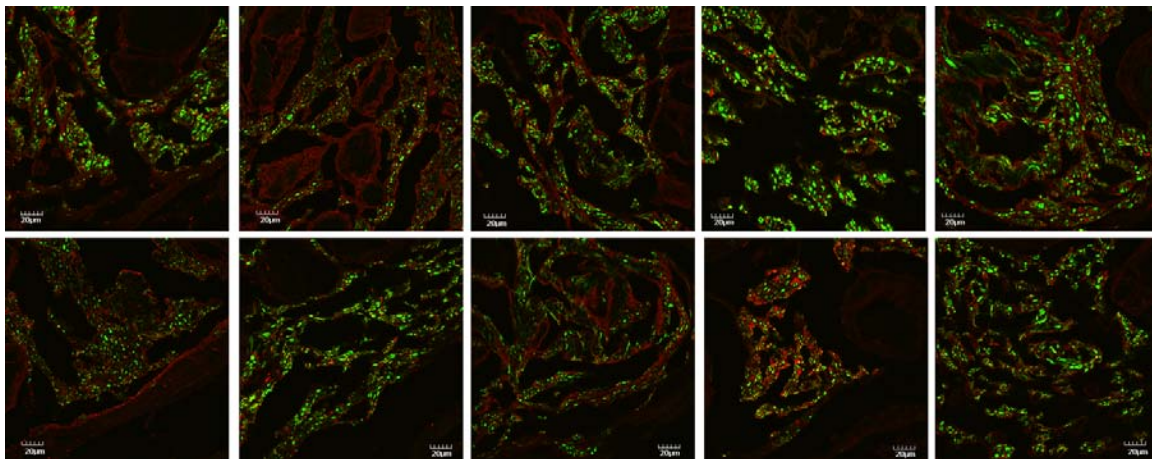
(F)   Autologous nerve graft (20x magification).